

University of Bradford eThesis

This thesis is hosted in [Bradford Scholars](#) – The University of Bradford Open Access repository. Visit the repository for full metadata or to contact the repository team



© University of Bradford. This work is licenced for reuse under a [Creative Commons Licence](#).

**STUDY OF CONTINUOUS-PHASE FOUR-
STATE MODULATION FOR CORDLESS
TELECOMMUNICATIONS**

M. A. BOMHARA

PhD

UNIVERSITY OF BRADFORD

2010

STUDY OF CONTINUOUS-PHASE FOUR- STATE MODULATION FOR CORDLESS TELECOMMUNICATIONS

Assessment by simulation of CP-QFSK as an alternative
modulation scheme for TDMA digital cordless
telecommunications systems operating in indoor applications

Mohamed Ali BOMHARA

BSc, MSc

Submitted for the degree of

Doctor of Philosophy

Faculty of Engineering and Informatics

University of Bradford

2010

Abstract

STUDY OF CONTINUOUS-PHASE FOUR-STATE MODULATION FOR CORDLESS TELECOMMUNICATIONS

Study of Continuous-Phase Four-State Modulation for Cordless Telecommunications
Assessment by simulation of CP-QFSK as an alternative modulation scheme for TDMA
Digital Cordless Telecommunications Systems operating in indoor applications

Keywords

TDMA; PCS; DECT; Coding; CPM; CP-QFSK; Modulation; OFDM; GMSK; WiFi;
Femtocells;

One of the major driving elements behind the explosive boom in wireless revolution is the advances in the field of modulation which plays a fundamental role in any communication system, and especially in cellular radio systems. Hence, the elaborate choice of an efficient modulation scheme is of paramount importance in the design and employment of any communications system. Work presented in this thesis is an investigation (study) of the feasibility of whether multilevel FSK modulation scheme would provide a viable alternative modem that can be employed in TDMA cordless communications systems. In the thesis the design and performance analysis of a non-coherent multi-level modem that offers a great deal of bandwidth efficiency and hardware simplicity is studied in detail. Simulation results demonstrate that 2RC pre-modulation filter pulse shaping with a modulation index of 0.3, and pre-detection filter normalized equivalent noise bandwidth of 1.5 are optimum system parameter values. Results reported in chapter 5 signify that an adjacent channel rejection factor of around 40 dB has been achieved at channel spacing of 1.5 times the symbol rate while the DECT system standards stipulated a much lower rejection limit criterion (25-30dB), implying that CP-QFSK modulation out-performs the conventional GMSK as it causes significantly less ACI, thus it is more spectrally efficient in a multi-channel system. However, measured system performance in terms of BER indicates that this system does not coexist well with other interferers as at delay spreads between 100ns to 200ns, which are commonly encountered in such indoor environment, a severe degradation in system performance apparently caused by multi-path fading has been noticed, and there exists a noise floor of about 40 dB, i.e. high irreducible error rate of less than $5 \cdot 10^{-3}$. Implementing MRC diversity combiner and BCH codec has brought in a good gain.

Acknowledgement

I would like to thank my supervisors: Professor J. G. Gardiner and Dr. T. L. Doumi for their support and extremely valuable guidance and discussions throughout the period of this research work.

I am most thankful to my parents and my family who have supported and encouraged me throughout my study. I would also like to thank my sponsor, the Higher Education Ministry for giving me the opportunity to pursue my higher education for MSc. and PhD.

I would also like to thank Professor A. Raed for the many valuable comments and discussions. I would also like to express my gratitude to Dr. L. David, the Departmental Computer System Administrator, for his help with computer software and IT support.

It has been a great pleasure to work as part of the Telecommunications Research Group at the University of Bradford along with Dr. A. Jones, Dr. A. Alkahtani, Mr. O. Pena, R. Gonzalo, M. Ismael and C. Dimitris. The exchange of knowledge and research ideas and friendship is highly appreciated.

.

Contents

CHAPTER 1

Introduction	1
1.1 Literature review	1
1.2 Aims and objectives	5
1.3 Thesis Outline	6
References	8

CHAPTER 2

Mobile and Personal Communications Systems Overview	10
2.1 Evolution of Mobile and Personal Communications Systems	10
2.2 First Generation Mobile Systems	11
2.3 Second Generation Mobile Systems	13
2.3.1 Global System for Mobile Communications.....	15
2.3.2 Code Division Multiple Access.....	17
2.3.3 Cellular Digital Packet Data	19
2.4 2.5 G Networks	20
2.4.1 General Packet Radio Services	20
2.4.2 High Speed Circuit Switched Data	24
2.4.3 Enhanced Data Rates for GSM Evolution	25
2.5 Third Generation Wireless Networks	27
2.5.1 Wideband Code Division Multiple Access	30
2.5.2 Code Division Multiple Access 2000	32
2.5.2.1 Cdma2000 1x EV-DO and Cdma2000 3x	32
2.5.2.2 CDMA2000 1x for Voice and Data	33
2.5.2.3 CDMA2000 1xEV-DO for Faster Data	33
2.5.3 Universal Mobile Telecommunications System	34
2.6 Indoor Wireless Base Stations	35
2.6.1 Emergence of Femtocells	38

2.6.2	Femtocell Network Architecture	41
2.6.2.1	Legacy lub IP	44
2.6.2.2	IMS and SIP	45
2.6.2.3	Generic Access Network	46
2.6.3	Interference Management in Femtocells	48
2.6.3.1	Co-Channel Femtocell Senarios	49
2.6.3.2	Interference Mitigstion	51
2.6.4	Air Interface	53
2.6.5	WCDMA Evolution Towards HSDPA	57
	References	61

CHAPTER 3

Simulation of the DECT system	66
3.1 Personal Communications Systems	66
3.1.1 An Overview of the DECT System	68
3.1.2 The Physical Layer	70
3.1.3 The DECT Cordless Office	74
3.2 Simulation Background	76
3.2.1 Monte Carlo Simulation	78
3.2.2 Complex low pass representation of bandpasss signal	81
3.2.3 Factors affecting Simulation Accuracy	85
3.2.4 Software programs for simulating comm. Systems	86
3.2.4.1 MATLAB and Simulink	86
3.2.4.2 Description of the simulation software	88
3.3 DECT Simulation Model	90
3.4 Simulstion of the DECT System in static channel	99
Summary	102
References	104

CHAPTER 4

Continuous phase quaternary frequency shift keying system	109
4.1 Grounds of suitability of CP-QFSK	109
4.2 Theoretical background of CP-QFSK	114

4.2.1	CPFSK signal space diagram	119
4.2.2	Power density spectrum of CP-QFSK	119
4.2.3	Bandwidth occupancy comparison	124
4.3	CP-QFSK baseband system simulation model	125
4.4	Optimization of CP-QFSK system parameters.....	130
4.4.1	Gaussian pulse shaping	132
4.4.2	Spectrally raised cosine pulse shaping	137
4.4.3	Raised cosine pulse shaping	140
Summary		143
References		145

CHAPTER 5

Performance of CP-QFSK under different channel conditions		148
5.1	CP-QFSK system performance in non-fading environment	148
5.1.1	Adjacent channel interference	148
5.1.2	Co-channel interference	150
5.2	CP-FSK system performance in fading dispersive channel.....	154
5.2.1	The Multipath fading channel.....	155
5.2.1.1	Delay spread	157
5.2.1.2	Rayleigh fading	157
5.2.1.3	Rician fading	158
5.3	Characterisation of the multipath fading channel.....	158
5.4	The Multipath Fading channel modeling and simulation.....	161
5.4.1	Rayleigh fading simulator.....	162
5.4.2	Performance of CP-QFSK in Rayleigh fading channel.....	163
Summary		164
References		166

CHAPTER 6

Adaptive and non-adaptive techniques		169
6.1	The need for adaptive techniques	169
6.1.1	Diversity reception Techniques.....	170
6.1.2	Diversity combining methods.....	173

6.1.2.1	Maximum ratio diversity receiver.....	174
6.2	The need for non-adaptive techniques.....	179
6.2.1	Error control coding in communications systems.....	184
6.2.2	Simulation of BCH-encoded CP-QFSK system	185
Summary	189
References	190
 CHAPTER 7		
Conclusions and further work		194
7.1	Conclusions	194
7.1.1	Rationale	194
7.1.2	Methodology	195
7.2	Further observations	197
7.3	Further work	198
References	200
 Appendix A: BER Computations Program for CP-QFSK		
		203
Appendix B: List of Possible BCH Codes Parameters		
		209
Appendix C: BCH CODEC		
		211
Appendix D: Author's list of publication		
		213

List of Abbreviations

ACI	Adjacent Channel Interference
ADC	Analogue to Digital Converter
ADPCM	Adaptive Differential Pulse Code Modulation
AMPS	Advanced Mobile Telephone System
AWGN	Additive White Gaussian Noise
BER	Bit Error Rate
BSCs	Base Station Controllers
BSH	Bose-Chaudhuri-Hocquengham
BOSS	Block Oriented Systems Simulator
BT	3dB Bandwidth
CAPEX	Capital Expenditure
CB	Citizen Band
CCI	Co-Channel Interference
CDMA	Code Division Multiple Access
CDPD	Cellular Digital Packet Data
CEPT	Conference of European Posts and Telecommunications
CN	Core Network
CPM	Continuous Phase Modulation
CPP	Cordless Portable Part
CPQFSK	Continuous Phase Quaternary Frequency Shift Keying
CDT	Cordless Data Terminal
CS	Circuit Switched
DAC	Digital to Analogue Converter
D-AMPS	Digital Advanced Mobile Phone Service
DECT	Digital European Cordless Telephone
DS	Double Slot
ECSD	Enhanced Circuit Switched Data
EDGE	Enhanced Data rates for GSM Evolution
EGC	Equal Gain Combining

ETACS	Extended Total Access Communication System
ETSI	European Telecommunications Standards Institute
FAP	Femtocell Access Point
FCC	Federal Communications Commission
FCS	Femtocell Convergence Server
FDMA	Frequency Division Multiple Access
FMC	Fixed Mobile Convergence
FMS	Femtocell Device Management System
FNG	Femtocell Network Gateway
FS	Full Slot
GMSK	Gaussian Minimum Shift Keying
GPRS	General Packet Radio System
GSM	Global System for Mobile communication
HARQ	Hybrid Automatic Repeat Request
HNB	Home Node
HPA	High Power Amplifiers
HSCSD	High-Speed Circuit Switched Data
IMTS	Improved Mobile Telephone Service System
ICIC	Inter-cell Interference Coordinator
ISI	Inter Symbol Interference
ITU	International Telecommunications Union
LANs	Local Area Networks
LOS	Line-of-Sight
LPF	Low Pass Filter
LRC	Raised Cosine (in time domain)
LTE	Long-Term Evolution Network
MAC	Medium Access Control
MDT	Mobile Data Terminal
MNO	Mobile Network Operator
MRC	Maximum Ratio Combining
MSK	Minimum Shift Keying
MU	Mobile Unit
N-CDMA	Narrow-band Code Division Multiple Access
NMT	Nordic Mobile telephone

NRZ	Non Return to Zero (bit stream)
NSC	Mobile Switching Center
OPEX	Operational Expenenditure
OSI	Open Systems Interconnection
PCS	Personal Communication Systems
PDF	Probability Density Function
PHL	Physical Layer
PLL	Phase Locked Loop
PRBS	Psudo Random Binary Source
PS	Packet Switched
PSDF	Power Spectral Density Function
PDP	Power Delay Profile
QAM	Quadrature Amplitude modulation
QFSK	Quaternary Frequency Shift Keying
QoS	Quality of Service
RAB	Radio Access Bearer
RFP	Radio Fixed Part
RNC	Radio network Controller
SAP	Service Access Point
SAE	System Architecture Evolution
SeGW	Security Gateway
SIP	Session Initiated Protocol
SIR	Signal to Interference Ratio
SME	Small/Medium Enterprise
SMS	Short Message Service
SNR	Signal to Noise Ratio
SRS	Spectral Raised Cosine (frequency domain)
STR	Symbol Timing Recovery
TDMA	Time Division Multiple Access
UMTS	Universal Mobile Telecommunication System
UMTS	Universal Mobile Telecommunications System
UTRAN	UMTS Terrestrial Radio Access Network
Wi-Fi	Wireless Fidelity

List of Figures

2.1 GSM network elements	16
2.2 CDMA network	18
2.3 Architecture of GSM GPRS	23
2.4 Femtocell network architecture components	42
2.5 GAN-based femtocell access network architecture	46
2.6 UMTS femcell network based on lu-over-IP architecture	54
2.7 FDD and TDD operation Principle	56
3.1 DECT protocol layers	70
3.2 DECT frame and slot structure	73
3.3 The DECT cordless office	76
3.4 Probability density function	79
3.5 Functional structure of the BOSS software	90
3.6 Block diagram of DECT simulated system	93
3.7 Generated user data	97
3.8 Eye diagram of the Gaussian filtered data	98
3.9 Power spectrum of DECT GMSK signal	98
3.10 Transmitter Structure	99
3.11 Simulated BER performance of DECT static channel	102
3.12 Theoretical BER of DECT static channel	103
3.13 Simulated BER performance of DECT in Rayleigh fading channels ...	105
4.1 Phase trajectories of CP-QFSK	121
4.2 Signal-space diagram for CP-FSK	122

4.3	Normalised one-sided power spectral density of CP-QFSK	126
4.4	Power density spectra of CP-QFSK, MSK, and QPSK	127
4.5	Block diagram of Simulate CPQFSK system	129
4.6	User binary data of twice the DECT rate	130
4.7	The baseband quaternary data	131
4.8	Modulated signal amplitude	131
4.9	Signal space diagram of CP-QFSK	132
4.10	Phase trajectory of the generated quaternary signal for 10 symbols	132
4.11	Impulse response of Gaussian filter	136
4.12	Power spectrum of Gaussian shaped CP-QFSK signal	137
4.13	Eye diagram of the received signal	138
4.14	Required E_b/N_0 for $P_e = 10^{-3}$ vs. filter bandwidth	139
4.15	CP-QFSK performance with Gaussian-type modulation	140
4.16	Power spectrum of SRC-shaped CP-QFSK signal	141
4.17	Eye diagram of SRC-shaped quaternary data	142
4.18	Measured BER performance for SRC-shaped CP-QFSK	142
4.19	Power spectrum of 2RC modulation type	143
4.20	Eye diagram of the received signal	144
4.21	Measured BER performance for 2RC-shaped CP-QFSK	146
4.22	Theoretical BER performance for CP-QFSK	147
5.1	Relative ACI vs channel spacing	155
5.2	Block diagram of the simulated CCI	157
5.3	CP-QFSK system Performance under co-channel interference	159
5.4	Rayleigh fading generator	168
5.5	Rayleigh fading with AWGN	169

5.6 Measured Rayleigh PDF	169
5.7 Q-CP-FSK performance in static and Rayleigh fading channels	171
6.1 Block diagram of post detection MRC combiner	182
6.2 Block diagram of post-detection MRC receiver	184
6.3 Block diagram of the 2-branch MRC implementation	185
6.4 Performance of MRC diversity CP-QFSK receiver	186
6.5 Block diagram of a coding system	191
6.6 Block diagram of an Encoder	193
6.7 BCH encoder input data stream	195
6.8 BCH encoder output data stream	196
6.9 Detected data	198
6.10 Decoded data	196
6.11 BCH-encoded-CP-QFSK performance	197

List of Tables

2.1 Cellular mobile radio standards	18
2.2 Main WCDMA air interfaces parameters	32
2.3 Comparison between Femtocells and Picosells	38
3.1 Personal Communication Systems standards	68
3.2 DECT Air-Interface Parameters	75
3.3 User bite rate for DECT slot types	77
4.1 Symbol mapping for QFSK	130
4.2 Optimization of system parameters having fixed $P_e = 10^{-3}$	138
4.3 Simulation Parameters	145

CHAPTER 1

INTRODUCTION

1.1 Literature Review

In the developed and industrialized countries, the number of wireless access connections between the user terminals of a telecommunication network such as mobile phones and the fixed, high-capacity transport network has already exceeded the number of wired ones. Communications and computing have become sort of a lifestyle, and the trend will undoubtedly grow further in the near future, with the development of wireless fidelity (Wi-Fi) hot spots and the commercialization of low-cost wireless local area networks (LANs) for the home. The driving elements behind this wireless revolution are the advances in the fields of modulation, coding, equalisation and multiple access schemes. At the heart of all these is modulation which plays a fundamental role in any communication system, and perhaps especially in a wireless or radio system that enables information to be transmitted over the radio channel [1].

In any communication system, the two primary resources that are of paramount importance are the transmitted power and channel bandwidth, hence communication channels can be classified primarily as power-limited or band-limited, and a general system design objective priority would be to use these two resources as efficiently as possible since government regulatory bodies, such as the UK Radio communications Agency, define limits on spectrum occupancy for a given transmitted data rate, hence it is highly desirable to operate a digital communications system with narrow band signalling [2]. As far as band-limited channels are concerned, spectrally efficient

modulation techniques would be used to maximize the spectrum efficiency in these channels such as the mobile radio channel. Thus the choice of modulation technique has a direct impact on the capacity of a digital mobile communication system as it determines the bandwidth efficiency of a single physical channel in terms of the number of bits per second per Hertz (b/s/Hz). In selecting a suitable modulation scheme for a mobile radio system, careful consideration must be given to achieving the following [3, 4]:

- High bandwidth efficiency.
- High power efficiency.
- Low carrier-to-cochannel interference power ratio (C/I).
- Low out-of-band radiation.
- Low sensitivity to multipath fading.
- Constant or near constant envelope.
- Ease and cost of system implementation.

Optimising all these features at the same time is not possible as each has its practical limitation and also is related to others. For instance, to achieve high bandwidth efficiency one may choose to use high-level modulation. However, the power efficiency of the system would be reduced consequently. Moreover, the band-limited high-level modulated signal will have a large envelope variation which results in a large out-of-band radiation. Accordingly if this signal is to be passed through a power efficient nonlinear amplifier that in turn introduces interference to adjacent channels, and although this can be circumvented by using linear power amplifiers, these have poor power efficiency. Hence, it is necessary to look for a good compromise among these criteria, depending on the precise nature of the anticipated utilisation of the system in question [5].

Digital modulation techniques are broadly classified in two groups: linear and nonlinear schemes, each one being thought to be more appropriate for the two channels types mentioned earlier on. Linear schemes are generally non-constant envelope after band-limiting and the information is carried in both the amplitude and phase of the carrier, whereas nonlinear modulation has a constant envelope property and the information is solely contained in the excess phase function of the carrier. The modulation techniques more used in the present systems belong to the group of continuous phase modulations or, equivalently, constant envelope modulations, which are inherently power efficient. However, further improvements in related systems, like amplification devices, permit the increasing use of linear modulations, leading to a more bandwidth efficient systems.

The use of multilevel modulation schemes instead of binary ones results in an increase of the bit transmission rate for a given bandwidth. So, for a given bit rate, they imply a reduction of the required channel bandwidth and an increase in the spectrum efficiency, thus achieving a significant increase in the number of accommodated users. However, a consequence of transmitting more than one bit per symbol is that the signal power must be commensurately increased for the same channel noise if the symbol error is not to increase. This implies an increase in the cluster size in cellular radio, leading to a reduction of the number of channels per cell. The result is that the teletraffic throughput is not modified, but the complexity is significantly increased. This situation is very frequently encountered in conventional cellular systems i.e., where macro cells are deployed which also requires a low SNR (Signal to Noise Ratio) to avoid co-channel interference, it is not surprising therefore, that multilevel modulation schemes were not deployed. However, in a micro cell environment, as in the case of an indoor environment, the situation is completely different due to the close proximity of the base station and the mobile. High values of SNR can be achieved within the coverage area

with considerably lower power, thus increasing the power efficiency of the unit. Furthermore, because of the extremely fast fall off in signal level, the signal to interference ratio (SIR) is significantly higher. A research study performed in such minimum cluster sizes showed that multilevel modulation schemes can be introduced without cluster size penalties [6].

Returning to further general issues in the evolution of advanced personal communications systems, much research effort has focused on increasing the system capacity in terms of both enhancing data rate and user numbers. Given the constraints imposed by the limitations of spectrum availability it is becoming increasingly necessary to evolve new strategies to meet present and projected user requirements. Proposed approaches include both reducing cell sizes even further and finding strategies for managing co-channel interference [7, 8].

Over the past two decades or so, there has been a large amount of research done on continuous phase- constant envelope digital modulation systems (CPM) on account of their promising potential merits if employed in applications where efficient spectrum utilisation is required and/or some immunity to nonlinear distortion produced by the power amplifiers in transmitters are obtained. This constraint of phase continuity affects the signal in two important ways. Firstly, the transient effects are lessened at the symbol transitions, thereby offering spectral bandwidth advantages. Secondly, memory imposed upon the waveform by continuous phase transitions, improves performance by providing for the use of several symbols to make a decision. This property of introducing memory into the modulated carrier while maintaining a constant envelope allows for the received signal to be detected non-coherently, and since fast acquisition of the reference carrier phase is one of the crucial technical problems encountered in the rapid fading conditions of mobile radio channels when coherent detection is used, non-

coherent demodulation techniques are beneficial as carrier recovery circuit is not needed and that reduces the complexity of the handset which in turn reduces its cost [9-15]. A detailed account of the suitability and rationale behind the choice of a sub-class of the CPM signalling called quaternary frequency shift keying (QFSK) in which the instantaneous frequency is constant over each symbol interval and the phase is constrained to be continuous is given in chapter 4.

Again in the context of the deployment of CP-QFSK in cellular and pico-cell environments, it is worthy of note that the success of Orthogonal Frequency Division Multiple Access (OFDMA) suggests application of CP-QFSK in this access scheme. In OFDMA the transmitted frame contains many sub-carriers which are independently modulated whilst each sub-carrier remains orthogonal to every other.

In the intervening years since continuous phase modulation schemes were first investigated, the personal communications environment has changed out of all recognition as new services have emerged and user demand has far exceeded all earlier projections for growth. This means that not only are new strategies in multiple access required but also earlier schemes need to be re-evaluated in the light of the changing circumstances.

From the aforementioned accounts, the CP-QFSK modulation scheme is a case in point and merits consideration as a viable promising alternative modulation scheme that could be employed for cordless telephony with telepoint facility and in other applications such as systems employing femtocell technology.

1.2 Aims and objectives

This research work aims to investigate the feasibility of employing Continuous Phase Quaternary Frequency Shift Keying (CP-QFSK) modem in short-range cordless systems

such as DECT and other applications such as femtocells systems to enhance their data transmission capacity in a dual data rate system with a common air interface for the same allocated spectrum, and keeping the introduced changes to the standard system to a minimum thereby allowing a significant increase in the number of the accommodated users. To this end, the following objectives are sought:

- 1- To justify the choice of a bandwidth-efficient modulation scheme as an optimum candidate for short range digital telephony systems.
- 2- To design a simulation model and test bed with interrelated system design parameters carefully defined and optimised.
- 3- Assess the overall system performance in different radio propagation channel media.
- 4- To evaluate the utilisation of adaptive and non-adaptive techniques in sustaining system quality and robustness.
- 5- To highlight some important aspects proposed for future work.

1.3 Thesis Outline

Following this introductory chapter, an overview of cellular mobile and femtocell communications systems reviewing their background information is presented in chapter 2.

Chapter 3 starts off by an overview of the DECT system with main focus placed on its physical layer structure as it is to be used as a base line reference. Then, a concise treatment of computer simulation techniques highlighting their significance in the system design and in particular it gives an insight of the simulation software being used

in the design and optimisation of the current and proposed systems is presented. It also explores the DECT system design and its performance characterisation.

Chapter 4 outlines a rationale of the grounds justifying CP-QFSK scheme as a candidate proposed to improve DECT data throughput. It includes a detailed account of the modem design along with its parameter optimisation. Measured system performance under static channel conditions is reported at the end of this chapter.

Chapter 5 is devoted for investigating the system behaviour in different propagation media. It is divided into two main areas: the evaluation of system performance in indoor channel under the effects of non-fading conditions and under fading conditions and in turn evaluating the system quality in both environment scenarios.

Chapter 6 examines a number of countermeasures against the aforementioned adverse propagation effects through the use of adaptive and non-adaptive techniques so as to maintain an acceptable system quality. The overall system performance is evaluated and presented herein.

Chapter 7 concludes the outcomes from this project work and recommends some further research work to be conducted.

REFERENCES

- [1] IBNKAHLA MOHAMED; "Signal Processing for Mobile Communications Handbook". CRC Press LLC, 2005.
- [2] PROAKIS J. G.; "Digital Communications". Fourth Edition, McGraw Hill, New York, 2001.
- [3] BURR A. G.; "Application of High Rate Coded Modulation Systems to Radio LANs". IEE Colloquium on Radio LANs", pp. 5/1-5/6, London 7th May 1992.
- [4] STEEL R.; "Deploying Personal Communications Networks". IEEE Communications Magazine, Vol. 28, No. 9, pp. 12-15, September 1990.
- [5] AGHVAMI A. H.; "Digital Modulation Techniques for Mobile and Personal Communication Systems". Electronics and Communication Engineering Journal, Vol. 5, No. 3, June 1993.
- [6] WEBB W. T.; "QAM: The Modulation Scheme for Future Mobile Radio Communications?". IEE Electronics & Communication Engineering Journal, Vol. 4, No. 4, pp. 167-176, August 1992.
- [7] CICCONETI C, de la OLIVA A, CHIENG D & ZUNIGA J C; "Extremely Dense Wireless Networks", IEEE Communications Magazine, Vol. 53, No 1, pp88-89, January 2015.
- [8] SORET B, PEDERSON K I, JORGENSEN N T K, & FERNANDEZ-LOPEZ V; "Interference Co-ordination for Dense Wireless Networks", ibid pp 102-109, January 2015.

- [9] JOSEPH BOCCUZZI; "Signal Processing for Wireless Communications".
The McGraw-Hill Companies, Inc., 2008.
- [10] ANDRISANO O., CORAZZA G., and IMMOVILLI G.; "Effects of the Interferences in Cellular Digital Mobile Radio Systems using Full Response CPM with Limiter-Discriminator Detection.". *Alta Frequenza, Focus on Mobile Radio Systems*, No. 2, pp. 109-117, 1988.
- [11] PHOEL W. G.; "Improved Performance of Multiple-Symbol Differential Detection of Offset QPSK". *IEEE Wireless Communications and Networking Conference*, Vol. 1, pp. 548-553, 2004.
- [12] SUN J. and REED I. S.; "Performance of MDPSK, MPSK, and Noncoherent MFSK in Wireless Rician Fading Channels". *IEEE Transactions on Communications*, Vol. 47, No. 6, pp. 813-816, June 1999.
- [13] CHO M. and KIM S. C.; "Non-Coherent Detection of FQPSK signals using MLDD". *Proceedings of the 7th Korea-Russia Symposium*, Vol.2, pp. 314-318, KORUS 6-6 July 2003.
- [14] ANDERSON J. B. and SUNDBERG C. E.; "Advances in Constant Envelope Coded Modulation". *IEEE Communications Magazine*, Vol. 29, No. 12, pp. 36-45, December 1991.
- [15] PARK H. C., LEE K and FEHER K.; "Continuous Phase Modulation for F-QPSK-B Signals". *IEEE Transactions on Vehicular Technology*, Vol. 56, No. 1, pp. 157-172, January 2007.

CHAPTER 2

Mobile and Personal Communications Systems Overview

2.1 Evolution of mobile and personal communications systems

The cellular radio business has expanded explosively over the last two decades or so and continues to expand rapidly. Mobile radio has been used for over 70 years. Even though the cellular concept, spread spectrum techniques, digital modulation, trunking techniques, and other modern radio technologies were known more than 50 years ago, mobile telephone service did not appear in useful forms until the early 1960's, and then only as elaborate adaptations of simple dispatching systems. Wireless communications have become very pervasive. The first cellular systems were analog voice transmission, and some 'data transmission' modulated into the voice channel for signaling the occasionally handover or power control command [1].

Some of the most used standards were/are AMPS, D-AMPS, TACS, PCS, CDMA, NMT, GSM, DCS and UMTS (WCDMA). The number of mobile phones and Wireless Internet users has increased significantly in recent years to the extent that in some countries there exist more mobile phones than fixed phones. Mobile communications technology has evolved along a logical path, from the simple first-generation analogue products designed for business use to second-generation digital wireless telecommunications systems for residential and business environments to the third-generation aimed at bringing together the wireless and the Internet worlds together along the real-time video and multimedia graphics over the wireless medium [2]. These technologies took their own logical evolutionary process and the following sections briefly discuss that.

2.2 First Generation Mobile Systems (1G)

Although commercial mobile telephone networks existed as early as the 1960s, many consider the analogue networks of the late 1970s and early 1980s to be the first generation (1G) wireless networks when mobile phones came about into the market. The technology was designed for specific business purposes of voice communications and created to putting the telephones on the move (hence the term mobile phones). Various analogue techniques came into the market.

In the 1960's, Bell Systems developed the Improved Mobile Telephone Service System (IMTS), which was to form the basis of the first generation mobile communications system. With the invention of microprocessors and the cellular communications concept in the 1970's – 1980's, the first generation mobile communication system was born [3]. In the early 1970's Motorola designed and manufactured low, mid and high tier private land mobile radios having few competitors for the mid and high tier product lines (50 and 100 watt radios). However, in the low tier, less than 25 watt radio category, there were numerous contenders, mostly from European manufacturers with a “Nordic Mobile Telephone” heritage. In Europe, TACS was introduced with 1000 channels and a data rate of 8 kbps. AMPS and TACS use the frequency modulation technique for radio transmission. Traffic is multiplexed onto an FDMA (Frequency Division Multiple Access) system.

AMPS, which was made available in 1983 had a total of 40MHz of spectrum allocated from the 800MHz band by the Federal Communications Commission (FCC) and offered 832 channels with a data rate of 10 kbps [4].

In the late 1970's the American public got their first taste of mobile communications when Citizen Band (CB) radio became popular. It was an unlicensed, short range,

“party-line” experience. Those skilled in the art knew that something better was needed.

And the American communications industry responded. The Federal Communications Commission and major industry players, like AT&T and Motorola, specified America’s first public mobile radio telephone system, AMPS (Advanced Mobile Telephone System). By the mid 19980’s AMPS was a proven technology and cellular subscriber growth was constantly exceeding forecasts. The most prominent 1G systems are [5]:

- ETACS (Extended Total Access Communication System) in the UK
- AMPS (Advanced Mobile Phone System) in North America and Asia
- NMT (Nordic Mobile telephone) in Norway, Sweden and Finland
- NTT (Nippon Telegraph and Telephone) in Japan

These mobile systems worked on the concept of cells where, the mobile system's total coverage area is divided into a number of smaller interlocking regions called cells, whose radii are 5 to 10 miles only rather than 100 miles as in earlier mobile radio systems. Each cell is assigned its own base station and a fixed number of radio channels for duplex communications with the mobile units within its cell boundary. Furthermore, the base station's radio coverage is deliberately limited to within one cell size so that the frequency channels allocated to one cell can be safely reused in cells that are sufficiently remote. This "frequency reuse" capability of the cellular network is the key feature that allows more users to be accommodated in the network without requiring any additional channel allocation, and consequently, the system capacity is improved. A further desirable feature of the cellular concept is its ability to expand the traffic handling capacity gracefully with "cell splitting". When traffic builds up in a busy cell and traffic blockage begins to occur, that cell is subdivided into a number of smaller units called split cells. By careful frequency planning and appropriate reduction of the transmit power in these new split cells, it is again possible to increase the total

number of mobile users serviceable within the original cell boundary. Cell splitting thus provides an attractive expansion strategy for upgrading the cellular mobile system capacity [6].

With 1G introduction, the mobile market showed annual growth rates of 30 to 50 percent, rising to nearly 20 million subscribers by 1990. However, all these systems, based on analogue modulation techniques, had their inherent practical limitations in terms of the number of channels, proliferation of incompatible standards in different countries and regions, and one big challenge faced these systems was the inability to handle the growing capacity needs in a cost-efficient manner. Also different bandwidths and protocols made it difficult to enlarge the network for digital processing. This restricted the expansion plans of these technologies and thus, was costly to implement. Most of the users of the first generation mobile phones were restricted to big corporate and business users only. All of these limitations were the key forces behind the emergence and development of a new generation of digital systems [7].

2.3 Second Generation Mobile Systems (2G)

By the end of the 1980's, it became clear that the first generation analog cellular systems would not be able to meet continuing demand into the next century unless something was done about four inherent limitations of these systems; (1) severely confined spectrum allocations; (2) a perception among more sophisticated users, the chief revenue generators, that the systems were limited in usefulness because of annoying sounds and interference as the mobiles moved about in a multipath fading environment, as well as their having only trivial access to a growing catalog of attractive network features; (3) inability to substantially lower the cost of mobile terminals and infrastructure, and (4) incompatibility among the various analog systems,

especially in Europe, thus preventing the subscriber from using his or her phone abroad, coupled with the trend towards globalization of the world's economy it is desirable that communications take place globally providing 'communications anywhere – any time'. What is the solution? Spectrum space is probably the most limited and precious resource available in the industrialized world [8]. Continued allocation of additional spectrum to meet the cellular services' growing demand is simply out of the question. The solution is to further multiplex traffic (e.g., in the time domain) into a radio system on top of the conventional frequency and spatial domains. Such time multiplexing requires that all the traffic and signaling functions be realized with digital techniques [2].

Digital radio hides the effects of fading and interference from the user. Moreover, digital modulation and all its logical extensions make access to network features much easier. Half-duplex digital radios are theoretically cheaper to produce than full-duplex analog radios. These practical considerations together with political pressure in Europe have led to the rise of the second generation (2G) digital systems, most prominent of which are [9]:

- GSM system (Global System for Mobile communication, the European 200 KHz TDMA standard): The most successful family of cellular standards and the first digital cellular system developed for compatibility throughout Europe operating at 900MHz range. Data rates vary according to switching type.
- D-AMPS (Digital Advanced Mobile Phone Service, also known as IS-45), operates at 800MHz, and uses TDMA standard. Used mainly in USA.
- N-CDMA (Narrow-band Code Division Multiple Access, also known as IS-95): operates at 800MHz and characterized by high capacity and small cell radius and uses spread spectrum technology. It is used mainly in USA

- Digital European Cordless Telephone (DECT) in the late 1980's and early 1990's in which specific features were included to allow international roaming and a wide variety of auxiliary services.

A new design was introduced into the mobile switching center of 2G systems. In particular, the use of base station controllers (BSCs) lightens the load placed on the NSC (Mobile Switching Center) found in the 1G systems. This design allows the interface between the MSC and BSC to be standardized. Hence, considerable attention was devoted to interoperability and standardization in 2G systems so that carriers could employ different manufacturers for the MSC and BSCs. In addition to enhancements in MSC design, mobile-assisted handoff mechanism was introduced by sensing signals received from adjacent base stations, a mobile unit can trigger a handoff by performing explicit signaling with the network. Currently there are three prevalent 2G networks. These are: GSM, CDMA, and CDPD [10].

2.3.1 Global System for Mobile Communications (GSM)

GSM was launched in the early 1990's, and was one of the first truly digital systems for mobile telephony. It was specified by ETSI and originally intended to be used only in the European countries. However GSM proved to be a very attractive technology for mobile communications and, since the launch in Europe, GSM has evolved to more or less a global standard [7].

GSM networks are by far the most popular and widespread wireless communication media across the world, having a wide customer base in Europe and Asia-Pacific and command more than 50 percent of mobile customers. It is based on narrow-band TDMA technology, where available frequency bands are divided into time slots. Each user is given access to one particular time slot separated by regular intervals. It allows

eight simultaneous communications on a single 200 KHz carrier and is designed to support 16 half-rate channels. GSM supports data services where users can send and receive data at rates up to 9600bps. A unique feature of GSM, not found in older analog systems, is the Short Message Service (SMS). SMS allows GSM users to exchange text-based messages up to a length of 160 characters over the wireless network [11]. A GSM network, as shown in figure 2.1, typically consists of three major components: mobile stations, base station sub-system, and primary network.

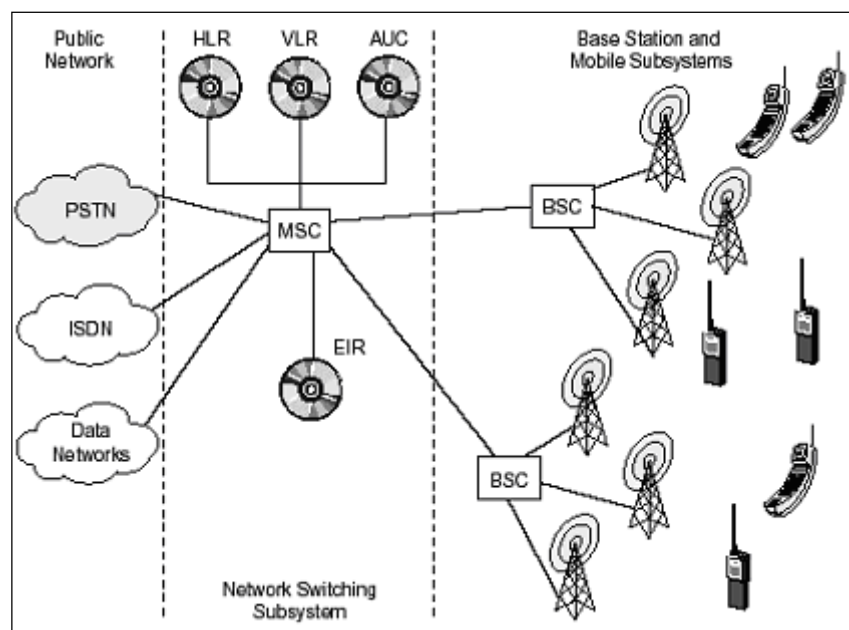


Fig. 2.1. GSM network elements

GSM network architecture, as shown above, comprises several transceiver stations (BTS), which are clustered and connected to a base station controller (BSC). Several BSCs are then connected to an MSC which in turn has access to several databases, including the visiting location register (VLR), home location register (HLR), and equipment identity register (EIR). It is responsible for establishing, managing, and clearing connections, as well as routing calls to the proper radio cell. It supports call routing at times of mobility. A gateway MSC provides an interface to the public telephone network. The HLR provides identity information about a GSM user, its home

subscription base, and service profile. It also keeps track of mobile users registered within its home area. The VLR stores information about subscriptions visiting a particular area within the control of a specific MSC. The EIR is used for equipment registration so that the hardware in use can be identified. If a device is stolen, service access can be denied by the network or if a device has not been previously approved by the network vendor, EIR checks can prevent the device from accessing the network. In GSM, each mobile device is uniquely identified by International Mobile Subscription Identity (IMSI). It identifies the country in which the mobile system resides, the mobile network, and the mobile subscriber. The IMSI is stored on a Subscriber Identity Module (SIM) that can exist in the form of a plug-in module or an insertable card. With a SIM, a user can practically use any mobile phone to access network services. The protocols behind 2G networks support voice and some limited data communications, such as Fax and short messaging service (SMS), and most 2G protocols offer different levels of encryption and security. While first-generation systems support primarily voice traffic, second-generation systems support voice, paging, data, and fax services [10].

2.3.2 Code Division Multiple Access (CDMA)

CDMA (Code Division Multiple Access) was the first digital standard implemented in North America, USA, by Qualcomm. CDMA uses the spread spectrum concept of sharing a larger spectrum with multiple users, at the same time as assigning them unique digital codes. CDMA uses a spread spectrum in the 824-849 and 869-894 MHz bands. There is a channel spacing of 1.23 MHz, and a total of 10 radio channels with 118 users per channel. Main advantage of operating in these bands is its ability to provide higher bandwidth while preventing interference due to the digital coding. CDMA's ability to allow more calls to occupy the same space in the channel increases its capacity, hence,

provides a cost-effective solution to its users. It can provide higher data rates of more than 64 kbps due to frequency reuse and soft handoffs. Additionally, the cell planning is simpler. It is promoted in a big way as a step towards 3G high bandwidth networks [5].

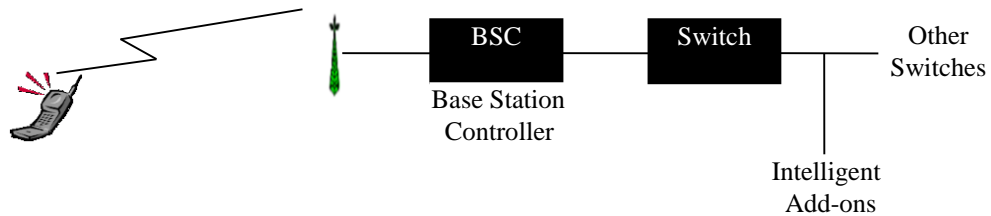


Fig. 2.2. CDMA network

Table 2.1 [6] summarizes some essential characteristics of the cellular mobile standards:

System	IS-54	GSM	CDMA
Multiple access	TDMA/FDMA	TDMA/FDMA	CDMA/FDMA (DS)
Up link (MHz)	869-894	935-960	869-894
Down link (MHz)	824-849	890-91.5	824-849
Duplexing	FDD	FDD	FDD
Ch. spacing (kHz)	30	200	1250
Modulation	P /4QPSK	GMSK.	BPSK/QPSK
Tx power (Peak)	600 mW	1 W	600 mW
Tx power (avg.)	200 mW	125 mW	600 mW
Speech coding	VSELP	RPE-LTP	QCELP
Codec rate (kb/s)	7.95	13	8 (var.)
Speech/RF Ch.	3	8	None
Ch. bit rate (kb/s)	48.6	270.833	
Ch. coding	1/2 rate conv.	1/2 rate conv.	1/2 rate fwd, 1/3 rate
Frame dur. (ms)	40	4.615	20

Table 2.1. Cellular mobile radio standards

2.3.3 Cellular Digital Packet Data (CDPD)

While the above technologies were advancing, there was a concern amongst certain organizations that had already invested substantially in analog networks. There was a need to have a technology that could be put as an overlay over these existing networks and at the same time provide some digital services to their customers. Cellular Digital Packet Data (CDPD) is the solution more popular in North America [5]. It uses unused bandwidth normally used by AMPS mobile phones between 800 and 900 MHz to transfer data. Speeds up to 19.2 kbit/s are possible. It is a packet data overlay that works on idle time in-between calls to transmit and receive information. It uses the concept that cell phones are not always used for voice communication, and hence the time slot can be exploited to provide a low-cost data transmission facility to consumers. Its popularity comes mainly from its cost-effectiveness, as it uses existing networks, thus reducing the risk of technology obsolescence.

In the early 1990's, CDPD was large on the horizon as a future technology. However, it had difficulty competing against existing slower but less expensive Mobitex and Data Tac systems, and never quite gained widespread acceptance before newer, faster standards such as GPRS became dominant.

These technologies are still voice-centric. Digitization of signals was aimed at improving channel capacity and voice clarity rather than transmission of data. However, the very fact that digitized information could be transmitted over these channels gave rise to the idea of exchanging information on top of voice over the same networks. This gave rise to the concept of Personal Communication Systems (PCS) that could shift the focus to data communications as well, although the prime focus remains voice. PCS operates in the frequency band of 1800-1900MHz and thus can

accommodate a higher number of channels. More bandwidth was made available, hence a higher subscriber base could be achieved. Also, the focus slowly started shifting towards data communications over wireless, leading to protocols such as SMS, WAP, Wi-Fi, and Bluetooth, among others. As of the year 2004, major carriers in the United States are threatening to shut down CDPD service. As of July 2005, the former AT&T Wireless CDPD network is no longer active, and singular Wireless CDPD customers have been informed that as of the end of the year, it will be down as well [11].

2.4 2.5G Networks – A Step towards 3G

The evolution of GSM to 3G is about gradually adding more functionality, possibilities and value to the existing GSM network and business. The evolution begins with an upgrade of the GSM network to 2.5G by introducing the general packet radio system (GPRS) technology. GPRS provides GSM with a packet data air interface and IP based core network. Before going ahead full-fledged into 3G mobile systems, there are a few crucial technologies, popularly known as 2.5G networks, that are taken to gradually migrate existing networks towards 3G [4]. Some of these network technologies such as GPRS, HSCSD, and EDGE that aim to implement packet data services and increase the data rates over the existing GSM and TDMA networks, will be discussed in the sub-sections to follow.

2.4.1 General Packet Radio Service (GPRS)

The move into the 2.5G world began with GPRS aiming at extending 2G networks to have the capability of launching packet-based services while enhancing the data rates supported by these networks, hence, it is essentially an overlay on top of existing GSM

and TDMA networks, which provides a telecom operator with the facility of reusing the radio spectrum across multiple users and thereby enhancing the capacity of the network. Soon after the first GSM networks became operational in the early 1990s and the use of the GSM data services started, it became evident that the circuit switched bearer services were not particularly well suited for certain types of applications with a bursty nature. The circuit switched connection has a long access time to the network and the call charging is based on the connection time.

In packet switched networks, the connections do not reserve resources permanently, but make use of the common pool, which is highly efficient in particular for applications with a bursty nature. The GPRS system has a very short access time to the network and the call charging is solely based on the amount of transmitted data compared to circuit-switched data that always requires at least one time slot to be allocated during an entire data session, regardless of how much data is actually transmitted and the user has to establish a new connection when he or she wants to get some information. This connection establishment process sometimes takes as much as 20-40 seconds [12].

The idea of packet data solution is to reuse frequencies across multiple users and hence optimize the use of frequency spectrum at all times. Thus, users can have the advantage of being connected all the time but paying only for the data exchanged between the mobile device and the network. This facilitates the convergence of cellular and Internet service providers, leading to a very exciting new business model.

The GPRS system brings the packet switched bearer services to the existing GSM system, i.e. it is not a completely new system; rather, it is an upgrade or data overlay over the voice-based existing GSM cellular networks, meaning, it is still having the same functionality for voice calls, and it is even possible to have simultaneous voice and data on some handsets. This smooth migration also means that users enjoy the same

coverage for GPRS as for present cellular networks, as opposed to building a completely new network from scratch. This situation is possible because GPRS is introduced as a simple software upgrade for the majority of the operator's equipment: the base station, and being able to reuse the same base stations saves lots of money and trouble. In the GPRS system a user can access the public data networks directly using their standard protocol addresses (IP, X.25), which can be activated when the MS is attached to the GPRS network.

The GPRS MS can use between one and eight channels over the air interface depending on the MS capabilities, and those channels are reserved separately making it possible to have multi-slot MSs with various uplink and downlink capabilities. The resource allocation in the GPRS network is dynamic and dependent on demand and resource availability. Packets can also be sent on idle time between speech calls. With the GPRS system it is possible to communicate point-to-point or point-to-multipoint, it also supports the SMS and anonymous access to the network. The theoretical maximum throughput in the GPRS system is 160 kbps per MS using all eight channels without error correction.

The network architecture of GPRS is shown in figure 2.3. It consists of a packet wireless access network and an IP-based backbone. It brings a few new network elements and a software upgrade to the GSM network. The most important ones are the Serving GPRS Support Node (SGSN) and Gateway GPRS Support Node (GGSN), to perform the tracking of packet-based mobile terminals, security and access control, interfacing with external packet data networks for exchange of packet-based data. As shown in Fig.2.3, base stations (BSSs) are connected to SGSNs, which are subsequently connected to the backbone network. SGSNs interact with MSCs and various databases to support mobility management functions. The BSSs provide wireless access through a

TDMA MAC protocol. Both the mobile station (MS) and SGSNs execute the Sub-network-Dependent Convergence protocol (SNDCP), which is responsible for compression / decompression and segmentation and reassembly of traffic. The SGSNs and GGSNs execute the GRPS tunneling Protocol (GTP), which allows the forwarding of packets between an external public data networks (PDN) and mobile unit (MU). It also allows multiprotocol packets to be tunneled through the GPRS backbone.

The application developer can access the advanced features of GPRS by using Attention (AT) commands, and GPRS turns the handset into an IP-based device on which just about any Internet Application can run. However, it is worth mentioning that GPRS has difficulties guaranteeing any quality of service (QoS) because of a lack of support in the base station controller, and the Packet Control Unit (PCU) is limiting the functionality by not being capable of handling different data streams differently, and that's why one of the most important additions to GPRS in the second release of the core network (3GPP release 1999) is the extensive QoS functionality. This standard is the same for EDGE and UMTS. Another important part of this standard is the possibility to use several services for one MS and have different qualities of service for them [10].

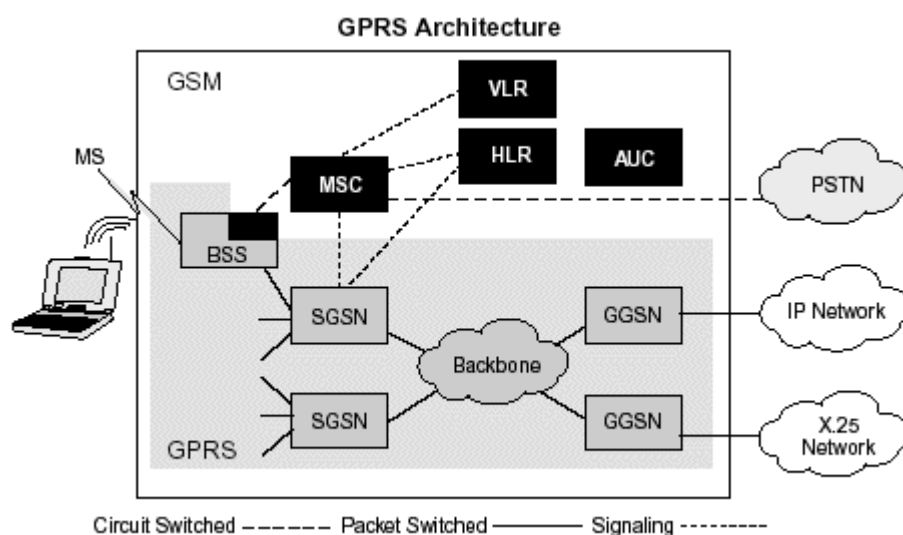


Fig. 2.3 Architecture of GSM GPRS

2.4.2 High-Speed Circuit Switched Data (HSCSD)

The first phase GSM specifications provided only basic transmission capabilities for the support of data services, with the maximum data rate in these early networks being limited to 9.6 kbps on one timeslot. HSCSD specified in rel'96, was the first GSM phase 2 + work item that clearly increased the achievable data rates in the GSM system. The maximum data rate of a HSCSD configuration with 14.4 kbps channel coding is 115.2 kbps, i.e. up to eight times the bit rate on the single slot full-rate traffic channel (TCH/F). In practice, the maximum data rate is limited to 64 kbps due to core network and interface limitations. The main benefit of the HSCSD feature compared to other data enhancement schemes is that it is an inexpensive way to implement higher data rates in GSM networks due to relatively small incremental modifications needed to the network equipment. Terminals, however, need to be upgraded to support multislot capabilities. Two types of HSCSD configurations exist, symmetric and asymmetric. For both types of configurations the channels may be allocated on either consecutive or non-consecutive timeslots taking into account the restrictions defined by the mobile station's multislot classes, described in detail in [13].

With HSCSD, the same circuit-switched technology is used as regular GSM, but multiple timeslots can be used for one connection. The first HSCSD systems appeared in 2000, and the first batch of terminals was in the form of PC cards. This format enables users who are already frequently checking their mail and using the Internet / intranet on the go to achieve higher speeds. The network implementation suits best applications that have continuous streaming of data since the network continues to be circuit-switched. The problem with this implementation consists of its complex

handover mechanism while roaming and its potential conflict with GPRS. Hence, the solution may be seen implemented mostly in isolated packets [5].

2.4.3 Enhanced Data Rates for GSM Evolution (EDGE)

EDGE, is a cost-effective upgrade to existing GSM / GPRS and TDMA networks providing users with data speeds as high as 384 kbps. GSM networks, as mentioned above, have already offered advanced data services, like HSCSD, with multislot capability and the simultaneous introduction of 14.4 kbps per time slot data, and GPRS are both major improvements, increasing the available data rates from 9.6 kbps up to 64 kbps (HSCSD) and 160 kbps (GPRS). Now that these two services are available, there is a need for even higher speeds for both of them. This feature is exactly what EDGE provides, making it possible to transfer more data in each time slot. While a GPRS upgrade mainly consists of new nodes in the core network, EDGE accelerates speeds over the air.

EDGE is specified in a way that enhances the throughput per time slot for both HSCSD and GPRS. The enhancement of HSCSD is called Enhanced Circuit Switched Data (ECSD), whereas the enhancement of GPRS is called Enhanced General Packet Radio Service (EGPRS). In ECSD, the maximum data rate does not increase from 64 kbps due to the restrictions in the A-interface, but the data rate per time slot triples. Similarly, in EGPRS, the data rate per time slot triples and the peak throughput, with all 8 time slots in the radio interface, reaches 473 kbps.

The enhancement behind tripling the data rates is the introduction of Octagonal Phase Shift Keying (8-PSK) modulation in addition to the existing Gaussian Minimum Shift Keying (GMSK). An 8-PSK signal is able to carry 3 bits per modulated symbol over the radio path, while a GMSK signal carries only 1 bit per symbol. The carrier symbol rate

(270.833 kbps) of standard GSM is kept the same for 8-PSK and the same pulse shape as used in GMSK is applied to 8-PSK. The increase in data throughput does not come for free, the price being paid in the decreased sensitivity of the 8-PSK signal as it makes the reception and decoding trickier. This affects, e.g. the radio network planning, and the highest data rates can only be provided with limited coverage. As a result, the receiver must be more advanced, and the signal quality must be higher. This situation is a bit of a problem, however, because the signal quality for wireless systems often varies greatly as users move around (especially as they move further from the base stations). To remedy this problem, EDGE provides nine different coding schemes compared to the four that GPRS uses, and a connection can be switched between different schemes. The choice of coding scheme is dynamic and depends on the current Channel to Interference (C/I). As the signal quality goes down, EDGE switches to a coding scheme that is more robust but that also gives a lower throughput. The GMSK spectrum mask was the starting point for the spectrum mask of the 8-PSK signal but along the standardization process, the 8-PSK spectrum mask was relaxed with a few dB in the 400 kHz offset from the center frequency [14]. This was found to be a good compromise between the linearity requirements of the 8-PSK signal and the overall radio network performance.

In order to facilitate the convergence between GSM and TDMA, EDGE also has access to an upgrade for TDMA networks. One obstacle here is that TDMA channels are 30 kHz while GSM channels are 200 kHz. An EDGE version that remedies this situation is called Compact EDGE, as opposed to the standard classic EDGE. The compact version is for data only and uses a time-divided control for its 200 kHz channel using less spectrum than classic (6 MHz compared to 2.4 MHz required by classic). A TDMA operator can either choose to deploy compact EDGE in its existing channel structure or

free up some frequencies in order to implement classic EDGE. One major benefit of this convergence is the emergence of handsets that support both systems in the future [3].

2.5. Third Generation (3G) Wireless networks

It is now obvious that the 2.5G systems such as GPRS can provide a large host of new possibilities when developing applications. Also, new needs now exist and that people in general want fancier handsets and more network capabilities. However, the quality of service for applications was clearly not prioritized in 2.5G, and the bit rates are not all that high in reality. By the late 1990's the Internet was pervasive and the wireless industry looked to mobile data as the growth opportunity, and hence a greater demand to remove the distinction between fixed and mobile networks became apparent. Access to internet and Intranets, Teleworking, and the advent of the Virtual Office, were concepts that became more commonplace, and once again the industry undertook the task of defining new wireless systems commonly known thereafter as third generation (3G) which to be based on packet data. 3G systems are therefore designed for multimedia communications: with them person-to-person communication can be enabled with high quality images and video, and access to information and services on public and private networks is enabled by the higher data rates and new flexible communication capabilities of third generation systems. This, together with the continuing evolution of the second generation systems is creating new business opportunities not only for manufacturers and operators, but also for the providers of content and applications using these networks [15]. For 3G, the challenge is globalization and convergence of office and home applications and services with the help of new communications tools.

The International Telecommunications Union (ITU) has made a recommendation (ITU-R M687-2) on what the 3G systems, or International Mobile Telecommunications 2000(IMT-2000), should bring. This recommendation includes the following items [3]:

- A QoS that is comparable to fixed voice networks
- A Phased development, with the first phase supporting bit rates of up to 2Mbps
- The capability to build terminals that have many different form factors ranging in size from what 2G phones offer to what you can carry in vehicles
- A flexible architecture where you can easily add additional applications

The involved companies agreed that things such as flexible multimedia management, Internet access, flexible bearer services, and cost-effective packet access for best-effort services were of high importance. Because the Internet has become a global force and a daily tool for people (both professionally and privately), it is important to define a wide-area wireless system that is capable of utilizing all of those services. The challenge was to migrate toward an architecture where all of the benefits of the Internet remained while still preserving the high QoS of 2G systems (with low down times and guaranteed bit rates in 2G via circuit switching). The vision of a mobile Internet where not only Internet services but also a whole new range of tailored services would emerge started to form. This vision included the capability to access the services any time, anywhere, and on any device.

During the late 1990s, there was an intriguing race between a number of camps in order to convince the world that their idea of the 3G was the best. The different contestants in this race all had reasons for liking some proposals better than others (such as patents, in-house competence, similarity, compatibility with legacy systems, and so on). At the same time, everyone had the feeling that things needed to work better than in the 2G

systems, where the different and incompatible standards made international roaming difficult and expensive.

In 1997, this standardization was driven separately in the United States, Japan, and Europe, although the participating companies often were present in all of the standardization bodies. In the first half of 1998, Europe made several decisions in the direction of WCDMA while the United States supported EDGE and cdma2000. Japan was also working toward standardizing WCDMA, but there were some key differences between its work and the European standard. In 1998, the ITU called for proposals for IMT-2000, and 10 proposals were submitted for the terrestrial part. These proposals spurred several standards to work toward harmonization and the Japanese standardization body, ARIB/TTC, and the European counterpart, ETSI, T1P1 (United States), and TTA (Korea) to join forces in the strive toward a global standard. The result was one WCDMA standard, and the Third Generation Partnership Project (3GPP) formed. U.S. standardization bodies then created 3GPP2, which standardizes the cdma2000 system. Also in 2000, GERAN (GSM EDGE Radio Air Interface) was added to 3GPP.

After additional harmonization work resulted in compromises between the different CDMA standards, they became closer to each other but still had three modes of the CDMA standard. In addition, EDGE is also part of the IMT 2000 Family of 3G standards. The work toward making the different standards compatible is an ongoing process, and it will probably take some time. Not only does it involve technical issues, but it also involves the business aspects for operators who have customers who have legacy handsets to consider. The good part is that most applications will run on top of the Internet Protocol (IP) over any of these bearers, making it easy for developers to produce products that work anywhere. With the advent of 3G networks, the wireless

and the Internet worlds are being brought together along with more real-time video and multimedia graphics, also made available over the wireless medium [16]. The following sub-sections serve a brief overview of some emerged 3G systems such as WCDMA, CDMA2000, UMTS.

2.5.1 Wideband Code Division Multiple Access (WCDMA)

After the big global success with the second generation (2G) GSM and the increased need for spectrum efficiency and data transmission, it was evident that there was a need for a third-generation mobile system. UMTS was selected as the first 3G system for many reasons, mainly because it is a very efficient way to utilize the radio resources – the RF spectrum. Wideband Code-Division Multiple-Access (WCDMA) is a wideband Direct-Sequence Code Division Multiple Access (DS-SS) system, i.e. user information bits are spread over a wide bandwidth by multiplying the user data with quasi-random bits (called chips) derived from CDMA spreading codes. In order to support very high bit rates (up to 2 Mbps), the use of a variable spreading factor and multicode connections is supported. WCDMA was adopted as a standard by the ITU under the name "IMT-2000 direct spread". Its specification has been created in 3GPP (the 3rd Generation Partnership project), which is the joint standardisation project of the standardisation bodies from Europe, Japan, Korea, the USA and China. Within 3GPP, WCDMA is called UTRA (Universal Terrestrial Radio Access) FDD and TDD, the name WCDMA being used to cover both FDD and TDD operation. WCDMA is a technology for wideband digital radio communications of Internet, multimedia, video and other capacity-demanding applications.

WCDMA has been selected for the third generation of mobile telephone systems in Europe, Japan and the United States. It is based on radio access technique proposed by

ETSI Alpha group and the first full specifications was completed at the end of 1999.

However, commercial networks were scheduled to open in Europe and elsewhere in Asia at the beginning of 2002. UMTS is all about noise and power control. Strict power control is a necessity to make sure that transmitted signals are kept to a level that ensures they all reach the base station at the same power level, hence the inter-cell interference needs to be minimized since all cells are operating on the same frequency; this is a challenge.

Voice, images, data, and video are first converted to a narrowband digital radio signal. The signal is assigned a spreading code to distinguish it from the signal of other users. WCDMA uses variable rate techniques in digital processing and it can achieve multi-rate transmissions. UMTS networks need to support all current second generation services and numerous new applications and services [17]. UMTS has now become the global standard and has been accepted throughout the world. Several upgrades that accommodate higher data speed HSDPA (High Speed Downlink Packet Access) and HSUPA (High Speed Uplink Data Access) and service the users with data speeds in excess of 10Mbps. There are several current consideration about converting the current GSM900 spectrum into UMTS900, giving a much higher spectrum efficiency, and better indoor RF penetration. The main system design parameters of the WCDMA air interface are summarized in table 2.2 [15]

Mutiple access method	DS-CDMA
Duplexing method	Frequency division duplex/time division duplex
Base station synchronization	Asynchronous operation
Chip rate	3.84 Mbps
Frame length	10 ms
Service multiplexing	Multiple services with different quality of service requirements multiplexed on one connection
Multirate concept	Variable spreading factor and multicode
Detection	Coherent using pilots symbols or common pilot
Multiuser detection, smart antennas	Supported by the standard, optional in the implementation

Fig. 2.2 Main WCDMA air interfaces parameters

2.5.2 Code Division Multiple Access 2000 (CDMA 2000)

Cdma2000 specification was developed by the 3GPP2, a partnership consisting of five telecommunications standards bodies: ARIB and TTC in Japan, CWTS in China, TTA in Korea and TTA in North America. Cdma2000 has already been implemented to several networks as an evolutionary step from cdmaOne as cdma2000 provides full backward compatibility with IS-95B, and is not constrained to only the IMT-2000 band, but operators can also overlay acdma2000 1x system, which supports 144 kbps now and data rates up to 307 kbps in the future, on top of their existing cdmaOne network [15].

2.5.2.1 Cdma2000 1x EV-DO and cdma2000 3x

Cdma2000 1x EV-DO and cdma2000 3x are an ITU-approved, IMT-2000 (3G) standards. Cdma2000 3x is part of what the ITU has termed IMT-2000 CDMA MC

(Multi Carrier). It uses less than 5 MHz spectrum to give speeds of over 2 Mbps. Cdma2000 1x with lower data speed is considered to be a 2.5G technology. Commercially introduced in 1995, CDMA quickly became one of the world's fastest-growing wireless technologies. In 1999, the International Telecommunications Union selected CDMA as the industry standard for new "third-generation" (3G) wireless systems. Many leading wireless carriers are now building or upgrading to 3G CDMA networks in order to provide more capacity for voice traffic, along with high-speed data capabilities. Today, over 100 million consumers worldwide rely on CDMA for clear, reliable voice communications and leading-edge data services [15, 18].

2.5.2.2 CDMA2000 1X for Voice and Data

CDMA2000 1X technology supports both voice and data services over a standard (1X) CDMA channel, and provides many performance advantages over other technologies. First, it provides up to twice the capacity of earlier CDMA systems (with even bigger gains over TDMA and GSM), helping to accommodate the continuing growth of voice services as well as new wireless Internet services. Second, it provides peak data rates of up to 153 kbps (and up to 307 kbps in the future), without sacrificing voice capacity for data capabilities. CDMA2000 1X phones also feature longer standby times. And because it's backwards-compatible with earlier CDMA technology, CDMA2000 1X provides an easy and affordable upgrade path for both carriers and consumers [15, 18].

2.5.2.3 CDMA2000 1xEV-DO for Faster Data

For users who want higher-speed or higher capacity data services, a data-optimized version of CDMA2000 called 1xEV-DO provides peak rates of over 2 Mbps, with an average throughput of over 700 kbps, comparable to wireline DSL services, and fast

enough to support even demanding applications such as streaming video and large file downloads. CDMA2000 1xEV-DO also delivers data for the lowest cost per megabyte, an increasingly important factor as wireless Internet use grows in popularity. 1xEV-DO devices will provide "always-on" packet data connections, helping to make wireless access simpler, faster and more useful than ever [15].

2.5.3 Universal Mobile Telecommunications System (UMTS)

UMTS is a 3G broadband, packet-based transmission of text, digitized voice, video, and multimedia at data rates up to and possibly higher than 2 Mbps, offering a consistent set of services to mobile computer and phone users no matter where they are located in the world. Based on the GSM communication standard, UMTS, endorsed by major standards bodies and manufacturers, is the planned standard for mobile users around the world. Once UMTS is fully implemented, computer and phone users can be constantly attached to the Internet as they travel and, as they roaming service, have the same set of capabilities no matter where they travel to. Users will have access through a combination of terrestrial wireless and satellite transmissions. The higher bandwidth of UMTS also promises new services, such as video conferencing. UMTS promises to realize the Virtual Home Environment in which a roaming user can have the same services to which the user is accustomed when at home or in the office, through a combination of transparent terrestrial and satellite connections. UMTS is a network consisting of two main elements connected over a standard interface, called Iu. These two elements are:

- UTRAN (UMTS Terrestrial Radio Access Network). This is composed of Node B which is equivalent to the GSM BTS and the Radio Network Controller (RNC) which is equivalent to the GSM BSC. A novelty with the UTRAN

concept is the existence of a new modulation scheme: the Frequency Division Duplex (FDD) and W-CDMA. This mode offers the highest efficiency within a single system whatever the conditions. One carrier uses 5 MHz.

- The Core Network: This is the equivalent of the GSM NSS. There are two options for the implementation of 3G and the evolution of the GSM Core Network:
 - ATM based architecture: this R'99 architecture may reuse in some cases the two-domain architecture of GSM/GPRS, with:
 - Iu-PS: Packet Switched instead of Gb on the packet domain.
 - Iu-CS: Circuit Switched instead of A on the circuit domain.
 - Transport Independent and multimedia architecture: this R'00 architecture is in line with the Next Generation Networks architecture and introduces separation of control and user planes. It also integrates multimedia capabilities [19].

2.6 Indoor Wireless Base Stations (Small Cells)

Indoor base stations commonly known as picocells and femtocells are one of the fastest growing areas of mobile communications addressing the problem of achieving high quality indoor coverage. They represent a massive business opportunity and many analysts view it as a key for unlocking the Small/Medium Enterprise (SME) revenue stream for all kinds of operators. Basically, these are small indoor access points that are designed to provide dedicated mobile network coverage within a limited area, such as a house or an office. Unlike larger macrocells, these units are relatively low-power devices and are designed to be as 'plug and play' as broadband modems have become. Another key difference between traditional base stations and these scaled-down

versions is that they link back to the service provider via a broadband line, usually any variant of the Digital Subscriber Line (xDSL) to provide network backhaul, rather than using a leased line or microwave link [20].

Picocells and femtocells not only employ the same base technology, they have much more in common such as:

- Low hardware costs: Femtocells cost under \$100. Picocells cost slightly more as they contain additional functionality.
- Internet connectivity: Femtocells and picocells are designed to plug into any home/office network that is connected to the internet which connects them to the rest of the mobile operator's network.
- Plug and play installation: Femtocells and picocells are designed to be plugged into a router or DSL modem, the power to be turned on and for the devices to automatically configure themselves with no customer intervention.
- Low cost operation: Both technologies are designed to have very low operational costs for the operator. They offer in most cases fully automated installation as well as fully automated remote management capabilities.

Although the architecture and technology platforms employed for femtocells and picocells are identical, significant differences still exist between them [21] such as:

- Enhanced capacity: Individual picocells are likely to be able to support a greater number of simultaneous users than a femtocell.
- Expandability: Picocells can be intelligently chained together to increase capacity as well as connected to distributed antenna systems to improve coverage further.

- More complex IT environment: Picocells operate inside company IT networks.
Consequently, installation is essentially plug and play, and there exists a need to tailor the installation in many cases to the business so as to fit the IT policies of.
- Picocells are normally installed and maintained directly by the network operator who pays for site rental, power and fixed network connections back their switching centre. However, femtocells are intended to be much more autonomous. They are self-installed by the end user in their home or office.
- Femtocells automatically determine which frequency and power levels to operate at, rather than being directed from a central network element. This allows the network to adapt automatically as new femtocells are added or moved. Hence femtocell would not normally broadcast a list of nearby neighbouring cells. Mobile phones would thus maintain the connection on the femtocell as much as possible, but risk dropping the call or having a short outage if the call needs to be switched across to an external macro or microcell.
- Femtocell capacity is somewhere between 4 and 32 users, depending on applications, whereas picocell is thought to support 16 to 64 users or more.

The cell radii of femtocells are about 10% – 30% of those of picocells. Therefore, by using a large number of femtocells, the total indoor capacity can be increased by a factor of 10–100 compared to the case of using a few picocells.

Femtocell's highest in-building capacity, easiness of deployment and maintenance (plug-and-play), Wi-Fi offloading, and convenience of broadband backhaul make it more attractive than picocell for indoor deployment [22]. Table 2.3 summarizes key traits of picocells and femtocells:

Aspect	Picocell	Femtocell
Installation	Operator	User
Capacity	10-50 users	3-5 users
Connection to the core network	Coaxial or fiber optic	ADSL, Cable
Coverage range	<100m	<30m
Price	Cheap	Very cheap
Frequency/radio parameters	Centrally planned	Locally determined
Site rental	Operator	Customer

Table 2.3 Comparison between femtocells and picocells

In-building coverage options are not limited to picocells and femtocells. Also used are repeaters, distributed antennas, radiating cable and in-building microcells, however, the focus would be herein solely on femtocells.

2.6.1 Emergence of Femtocells

Femtocells have emerged in the last few years as an alternative solution for operators to improve coverage and throughput in indoor environments. Recently they have gained momentum in the mobile industry due to their unique characteristics and capabilities that resolve the problems existing macrocell-based systems have. Some of those problems and technological factors behind the emergence of femtocells as a viable compelling solution are:

Long-Term Evolution networks (LTE) promise to change the mobile broadband landscape with peak data rates of over 100 Mbps, high-speed mobility, reduced latency, and the support of a variety of real-time applications. However, simply providing LTE

coverage is not enough to fulfill indoor service requirements. Therefore, operators need to complement macro network with femtocell deployments more tailored to residential and workplace use [23]. Traditionally, mobile operators' mission is to deliver services to mobile users constantly on the move who use their mobile phones mainly for voice services. With the emergence of technologies such as UMTS and the Fixed Mobile Convergence (FMC), mobile services usage are changing and new trends are appearing leveraging indoor importance. In such context, high data rates and coverage are the two main ingredients that each operator should offer to remain competitive. However, operators usually fail to provide high quality of services to home users and 45% of home and 30% of business subscribers experience problems with poor indoor coverage [24]. With macro cellular network, it is very difficult for operators to provide high-quality services and cell coverage to indoor users. It is nearly impossible for operators to deploy a huge number of outdoor base stations in areas densely populated in order to improve indoor coverage.

Recent studies show that voice revenues are declining in favour to data volumes and revenues. This is partly due to the convergence between mobile and Internet since the introduction of 3G mobile services. With fast and reliable access to the Internet, data volumes have increased far faster than the revenues and this trend is expected to accelerate in the future. In order to be competitive, operators need to find ways to substantially decrease the cost per bit of delivering this data, while not placing limits on customers' appetites for consuming the data. This emphasizes the need of femtocells as indoor solutions. From a business perspective, femtocell saves Operational Expenditure (OPEX) on the macro backhaul network due to traffic offload from macrocell network. Capital Expenditure (CAPEX) is also saved since no new base stations or capacity expansions are needed [25].

Besides voice revenues diminishing, a new trend appears regarding wireless usage. Roughly 66% of calls initiated from mobile handset and 90% of data services are occurring indoor [26]. Voice networks are designed to tolerate low signal quality, since the required data rate for voice signals is very low, on the order of 10 kbps or less, whereas data networks, require much higher signal quality in order to provide the higher data rates, and as the signal from the macrocell attenuates and deteriorates quicker once it reaches indoors due to high frequency range commonly used in 3G system, the operators need to improve indoor coverage without additional macrocell deployment. Femtocell constitutes a promising solution to address indoor coverage with limited cost impact. Femtocell satisfies both the subscriber, who is happy with the higher data rates and reliability, and the operators, who increase revenues with no additional deployment of macrocell networks [27].

In addition, one of the fundamental characteristics of WCDMA as a radio multiplexing access technology is that the effective cell capacity is interference-limited. This implies that 3G service, which requires high-bandwidth capacity, is available to end users only when the user is located near the cell, and the number of simultaneous users in the cell is small. This is almost contradictory to the macrocell environment, leading to a situation in which the effective data rate in the macrocell environment is only a fraction of the theoretical maximum data rate. The solution to this problem necessitates the provision for good indoor signal quality and low number of simultaneous users per cell. These are both met by a femtocell as a device that is specifically intended for small-scale indoor coverage to solve exactly these very issues.

2.6.2 Femtocell Network Architectures

Femtocell network is an extension of the Mobile Network Operator (MNO) macro network, and connecting it to existing operator networks requires a network architecture that addresses the security needs of operators and mobile users, while supporting the scalable deployment of millions of femtocells. In addition, it must allow ordinary customers to install them with plug-and-play simplicity ensuring that critical services such as emergency calling are also supported with the same reliability and accuracy as fixed-line emergency calling [28] (in this publication, simulation work was carried out and results were reported, so there is no point in repeating such simulations herein). The femtocell network architecture describes the major nodes and connections in a femtocell network. As shown in Fig.2.4, there are three network elements that are common to any femtocell network architecture [29]. These are:

- Femtocell Access Point (FAP)
- Security Gateway (SeGW)
- Femtocell Device Management System (FMS)

Two other elements that are in all femtocell network architectures are entities that enable connectivity to the mobile operator core. Depending on the specific architecture used for circuit switched calls, there can be either a Femtocell Convergence Server (FCS) or a Femtocell Network Gateway (FNG). For packet calls, depending on the air link technology, there can be either a PDSN or xGSN (GGSN/SGSN) in the core. In most cases, the PDSN / xGSN are the same as those used for macro networks.

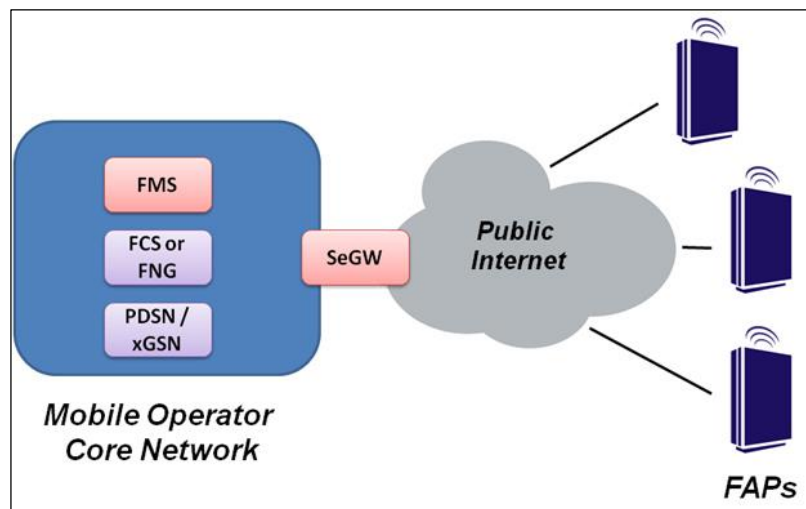


Fig. 2.4 Femtocell network architecture components

➤ Femtocell Access Point (FAP)

Femtocell Access Point is the primary node in a femtocell network that resides in the user premises to implement the functions of the base station and base station controller and connects to the operator network over a secure tunnel via the Internet. A FAP can be introduced into a home in multiple ways. A standalone FAP can be directly connected to the home router. In some applications, FAP may also include a built-in router, which is useful in prioritizing FAP voice traffic over other Internet traffic in the home network. More advanced FAP's include an Analog Terminal Adapter (ATA) to connect a fixed line phone. In some cases, FAPs are full-blown residential gateways with built-in Wi-Fi and a broadband modem (xDSL, cable).

➤ Security Gateway

The security gateway is a network node that secures the internet connection between femtocell users and the mobile operator core network. It uses standard Internet security protocols such as IPSec to authenticate and authorize femtocells and provide encryption support for all signaling and user traffic. It supports a large number of femtocells

connecting to the operator's network and is designed for use in carrier networks, thus meets requirements such as scalability, high availability, and network management.

➤ **Femtocell Device Management System**

The femtocell management system, also located in the operator network, plays a critical role in the provisioning, activation and operational management of femtocells using industry standards such as TR-069. It is perhaps the most critical node in ensuring the scalability of a femtocell network to millions of devices. To ensure low-cost deployment and easy setup for subscribers, the activation and provisioning of the femtocell must be plug-and-play with no on-site assistance required from the mobile operator. Various standards bodies specify the use of the TR-069 family of standards as the base device management framework for femtocells. TR-069 uses a proven web-based architecture that can scale to support millions of devices.

- **FCS or FNG**

FCS or FNG enables femtocells to connect to the operator core network. This is important for the operation of femtocells as this is what allows it to communicate with the core elements in the operator's networks and allow seamless service for mobiles. Depending on the specific architectural model used to support Circuit-Switched Services the FCS /FNG can be used.

- **PDSN / xGSN**

The PDSN / xGSN enable femtocell users to receive packet data services over the mobile operator's core. In most cases, these will be the same as those used by the mobile operator's macro network.

Latest technological progress allowed powerful processing capabilities to be applied to low cost home base stations, and the network protocol stacks can now be substantially collapsed. The P protocol has rapidly replaced hierarchic telecom-specific transmission

protocols. This enabled femtocells to utilize flat networks, such as the Internet, as a backhaul transport to operator core networks. At the 3GPP RAN plenary meeting held on May 2008 a feasibility study was compiled and the reference architecture for the Home NodeB was agreed on. The agreed architecture is based on a UMA/GAN. The feasibility study is described in the 3GPP Technical Report (TR) 25.820 [30] which is a part of UMTS release 8 defined the HNB feasibility and to outlined possible obstacles, and defined the basic architecture and characterizes the different RF and interference issue. It also listed the mobility and access control scenarios. In the same meeting two work items were set. Stage 2 specifies the architecture and Stage 3 specifies the protocols. The stage 2 UTRAN architecture is specified in the 3GPP release 8 Technical Specification (TS) 25.467 [31]. Three different 3G femtocell architectures have been proposed [32]. The following sub-sections discuss these models with more focus on the GAN-based RAN architecture.

2.6.2.1 Legacy Iub IP

The first way is to change as little as possible and to use the existing standard Circuit Switched (CS) and Packet Switched (PS) interfaces tunneled over the internet to connect the femtocell and the RNC. This is called the Iu-b over IP [33]. This saves expenses due to less extra hardware is needed on the operator side. Handovers are also possible between femtocells and macrocells, just like between the current macro NodeBs. These solutions looked to exert leverage on the existing 3GPP defined Iub interface that exists between 3G Radio Network Controllers (RNCs) and 3G base stations (NodeBs). Primarily proposed by RNC vendors, these approaches allowed operators to influence the same RNC to support Home NodeBs in addition to macro network NodeBs. Each femtocell is connected to the RNC over the standard 3GPP Iub

interface (TS 25.434) [34]. The Iub protocol stack is encapsulated within the IP signalling, also called a tunnelling Iub. Network security is handled by the Internet Protocol Security (IPsec) protocol. As Iub over IP solutions enable operators to operate their existing core networks through standard interfaces (Iu-CS and Iu-PS), they meet the operator requirement for full service transparency, as well as the requirement for low initial deployment cost and network disruption. The main concern with this approach is the ability of the RNC to scale up to serving hundreds of thousands of Home NodeBs (HNBs). The challenge with scaling this approach is in the basic design of RNCs, which are typically optimized to support a relatively low number of very high-capacity macro NodeBs. The fact that Iub typically has vendor-specific features, makes this approach only suitable for equipment manufacturers with an installed RNC base. The RNC's lack of scalability in accommodating a large number of HNBs resulted in this alternative architecture no longer being considered after an initial feasibility study carried out in 3GPP standardization.

2.6.2.2 IMS and SIP

One alternative approach to femtocells integrated into core network connectivity is to use a new SIP-based protocol between the mobile core network and the Home NodeB. These include Voice-over IP (VoIP) using the Session Initiated Protocol (SIP), with the RNC function now fully integrated into the FAP. Operators would deploy a new SIP-based core network that operates in parallel with their existing circuit and packet-based core network. When a handset is connected to a femtocell, it receives all of its services from the new SIP core network. This architecture is more aligned with the Wireless Interoperability for Microwave Access (WiMAX) architecture, which is IP-based. SIP-based approaches also hold the promise of cost-effective support for large-scale

deployments. As handsets are served by different core network when connected to femtocells as compared with when they are connected to macrocell network, service continuity between the indoor and outdoor base stations becomes potentially more complex due to different technologies being involved. As SIP-based approach requires operators to acquire and integrate a new core service network, the initial deployment costs are much higher than with other approaches. From Release-8 onwards, 3GPP started standardizing integration of femtocell access network into IMS infrastructure.

2.6.2.3 Generic Access Network (GAN)-Based RAN Gateway

Generic Access Network as defined in 3GPP TS 43.318 [35] and TS 44.318 [36] is a current 3GPP standard that may be used to support Home NodeB. The most recent proposals for femtocells integrating to core network are generally referred to as RAN Gateway solutions. As illustrated in Fig. 2.5, the RAN Gateway approach is based on a new, purpose-built, RAN Gateway that resides between an operator's existing core network and the IP access network, akin to an RNC.

On its Internet side, the RAN Gateway aggregates traffic from a large number of femtocells over the new Iu-over-IP interface. The RAN Gateway then integrates the traffic into the existing mobile core network through standard Iu-CS and Iu-PS interfaces on the core network side. As the RAN Gateway solutions influence an operator's existing core network through standard interfaces, they allow for full-service continuity as well as a low initial cost of deployment.

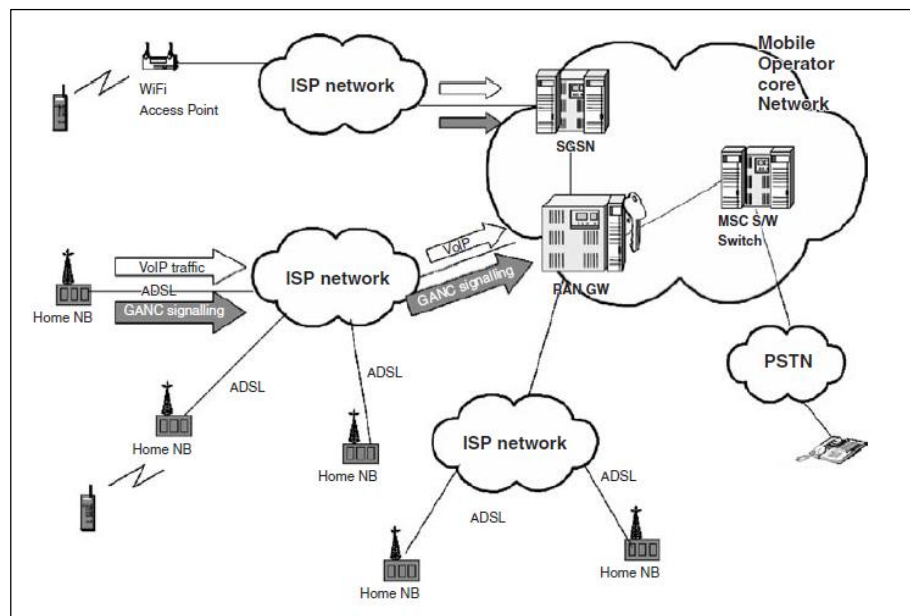


Fig. 2.5 GAN-based femtocell access network architecture

The RAN Gateway approach employs ‘Flat IP’ architecture, in which a number of functions of a standard RNC are moved to the femtocell itself, and the scaling issues associated with the Iub over IP approach are avoided. Since this architecture removes the RNC, the functionality associated with this is moved into the Home NodeBs, as such, the Home NodeB is now more intelligent or autonomous and is often renamed as an ‘Access Point’. These tasks are significantly simpler than those required in a traditional RNC; for example, given the constrained environment of a femtocell, support for mobility is simpler, there is no need for soft-handoff, etc. This architecture is often referred to as ‘flattened’, ‘collapsed stack’ or ‘Base Station Router’. GAN-based Home NodeB architecture has been considered in 3GPP, and the defined standard femtocell interface between HNB and HNB Gateway, Iuh, is likely to evolve from GAN-based Home NodeB architecture.

2.6.3 Interference Management in Co-channel Femtocell

The introduction of femtocells fundamentally alters the cellular topology by creating an underlay of small cells, with largely random placements and possible restrictions on access to certain BSs, such that the femtocell and macrocell are located in two different layers, hence the network is known as a two-tier network, and consequently two types of interferences are distinguished; cross- and co-tier interferences. The cross-tier interference is caused by an element of the femtocell tier to the macrocell tier and vice versa. The co-tier interference takes place between elements of the same tier.

To facilitate the integration and co-existence of these two tiers, several technical challenges such as network architecture, handover control, and interference management need to be tackled, of which interference management is perhaps the most significant one that occurs predominantly when femtocells are deployed in the same spectrum as the wireless network [20]. The interference of femtocell networks cannot be fully eliminated but it is possible to mitigate its effects through frequency allocation and power control as key factors among other techniques. The deployable femtocell zones are classified according to the density of femtocells, and co-existence of femtocells and macrocell to mitigate different sources of interferences and to ensure the best utilization of the spectrum [37].

Precise characterizations of the interference conditions in such heterogeneous and multi-tier networks have been the subject of extensive study [38, 39]. One of the important results reported in [40] is that, with open access and strongest cell selection, heterogeneous, multi-tier deployments do not worsen the overall interference conditions or even change the SINR statistics. This “invariance property” has also been observed in real-world systems by Nokia Siemens [41] and Qualcomm [42], and provides

optimism that femtocell deployments need not compromise the integrity of the existing macrocell network. However, in practice, at least two aspects of femtocell networks can increase the interference significantly. First, under closed access, unregistered mobiles cannot connect to a femtocell even if they are close by. This can cause significant degradation to the femtocell (in the uplink) or the cell-edge macrocell user in the downlink, which is near to a femtocell [43]. Second, the signalling for coordinating cross-tier interference may be logistically difficult in both open and closed access. Over-the-air control signaling for interference coordination can be difficult due to the large disparities in power. Recognizing these challenges, standards bodies have initiated several study efforts on femtocell interference management including those by the Femto Forum [44] and 3GPP [45, 46]. In addition, advanced methods for intercell interference coordination (ICIC) specifically for femtocell networks has been a major motivation for the 3GPP LTE-Advanced standardization effort [47].

For 3G CDMA femtocells, the dominant method for interference coordination has been power control strategies [48–50] and/or reserving a “femtofree” band where macrocell users can go to escape cross-tier interference when it arises [51]. It is noteworthy that there has been a lot of experimental and simulation work undertaken in most of the above published references, so it is deemed herein that there is no point in repeating simulations of that kind.

2.6.3.1 Co-Channel Femtocell Scenarios

In indoor environment where femtocell is within the house and where losses due to walls and floors are fairly small, femtocell can provide coverage throughout a wide area with low power. Its users are protected from interference from the macrocell network by the exterior walls of the building which also cause the femtocell power to diminish

rapidly outside and consequently protect nearby macrocell users. Even when some interference increase does occur it is only felt when in close proximity, in which case the macrocell will simply allocate a little more power to affected users, thereby maintaining their signal quality with little impact on other users. Femtocell power is only high enough to just serve internal users, thus causing minimal degradation to macrocell user having a strong macrocell signal to access in most cases. In worst case scenario, where the macrocell user may be operating at the limit of macrocell coverage with a weak signal and low tolerance to additional interference and also where the femtocell is near the edge of the house and close to the window, thereby delivering its highest levels of interference to the user. Without special mitigation techniques being applied, the femtocell can create a ‘dead zone’ around it, where the service available to the macrocell user is degraded. As well as the general downlink dead-zone instance, a number of other extreme interference situations could arise such as [52]:

- Downlink power from femtocells with closed subscriber group causes interference to macrocell user that impacts on macrocell user experiences degraded service and potential loss of service.
- Femtocell user at edge of femto coverage transmits at high power, causing noise rise to nearby macrocells yielding service degradation experienced by macrocell users at edge of coverage.
- Macrocell user close to femtocell but far from macrocell operates at high power, causing interference and potentially receiver blocking to femtocell whereby Femtocell users experience degraded coverage and service.
- Femtocell user at edge of coverage of femtocell 1 but close to femtocell 2, whereby the user experiences degraded downlink service due to interference from

femtocell 1 and transmits at high power, degrading uplink service for users of femtocell 2.

2.6.3.2 Interference Mitigation in Co-Channel Femtocell Deployments

The above cases have been thoroughly studied by a variety of organisations particularly, the 3GPP [28] and the Femto Forum [53]. Overall these studies demonstrated that there is a clear need for femtocells to implement interference mitigation techniques in order to avoid the occasional interference extreme cases. Some of these interference mitigation techniques are:

- Channel assignment: The network assigns users who are not part of the femtocell subscriber group to the most appropriate channel. Users who are on the macrocell can avoid femtocell dead zones. Femtocell users can be assigned different channels to avoid interference in overlapping coverage areas.
- Downlink power management: Femtocell transmit power is adjusted to give an appropriate trade-off between coverage and interference at a given location. This may be done using direct measurements of both the uplink and downlink channels and using measurements taken by both femtocells and user equipment to provide enhanced accuracy.
- Power capping of user maximum transmit power: The Femtocell sends a broadcast message to mobiles in its coverage to ensure a given maximum transmit power is never exceeded. As users leave the femtocell coverage, they are thus prevented from causing excessive uplink interference to macrocells.
- Dynamic receiver gain management: An adaptive attenuation level is included in the femtocell receiver to reduce its gain when a strong co-channel mobile is nearby, keeping the receiver operating within its linear dynamic range and

avoiding blocking while still providing sufficient sensitivity to detect mobile at the edge of femtocell coverage

- Broad dynamic range specification and testing: Since mobiles can approach very close to femtocells, the strong signal-handling ability of the femtocell should be verified in conformance testing

Numerous studies and increasing numbers of practical measurements have demonstrated that, if the interference mitigation techniques are appropriately implemented, they deliver performance within the network which improves overall performance for all users, including those on both the macrocell and femtocell networks, while significantly increasing overall network capacity and spectrum efficiency for the mobile network as a whole.

Extensive user trials and measurements carried out on a system model mimic the real-world potential co-channel interference between individual femtocells case proved that femtocells using the same interference mitigation techniques are capable of adapting well to deliver coverage over the desired areas with good performance delivering a full carrier of HSDPA capacity, resulting in very high traffic density and spectrum efficiency [52].

A number of techniques have been proposed to overcome interference in femtocell, some of which are hardware-based approaches such as cancellation techniques or the use of sectorial antennas. However, these techniques usually expensive to implement and imply an increase in the HeNB cost which is contrary to the femtocell essence. Even in WCDMA networks, where they are supposed to perform best, the tendency now is to drop their use, mainly due to errors in the cancellation process and therefore, interference avoidance is being considered as an approach with higher chances of success [54, 55]. Efficient alternatives are represented by strategies based on

interference avoidance and sub-channel management. These techniques are often used to mitigate interference in cellular networks and are of a great importance in femtocell due to cross-tier interference [27]. Interference avoidance strategies for two-tier CDMA network are proposed in [56] and for WiMAX OFDMA femtocell networks in [57] and [58]. Interference management and performance analysis in UMTS/HSPA+ femtocells is shown in [49]. Power control issues are investigated in [59]. UMTS macrocell and femtocell co-existence performance is evaluated also in [60].

2.6.4 Air Interface

The femtocell concept can be based upon a wide variety of wireless technologies. Wideband Code Division Multiple Access (WCDMA) is the main radio access technology that is used by the UMTS network which is currently the dominating technology for radio access in femtocell development due to the fact that the interference averaging makes WCDMA receivers capable of separating UMTS signals at very low levels of SINR, and for its capability of delivering much high data rates, hence from the point of view of the air interface, UMTS is better suited than bearer technologies to cope with the high interference levels of two-layer networks and well suited for the deployment of femtocells.

UMTS is a set of radio technologies specified by the 3GPP RAN group. The name given to its air interface is UMTS Terrestrial Radio Access (UTRA), which is specified for functioning in FDD and TDD modes. The main 3GPP Technical Specifications (TS) of the UMTS air interface consists of two parts: TS 25.101, which can be found in [61]; specifies the minimum RF features that the FDD mode of UTRA must provide in the UE. Then, TS 25.102, can be found in [62] which specifies the requirements of the TDD variant. Although the two options exist, most of the UMTS networks deployed worldwide use UMTS in FDD mode, mainly due to interference issues rising between

adjacent NodeBs that transmit in the same frequency band. Figure 2.6 shows the UMTS Release 4 femtocell network based on an Iu-over-IP architecture [33]. The main parts of the UMTS network are explained in the following sub-section.

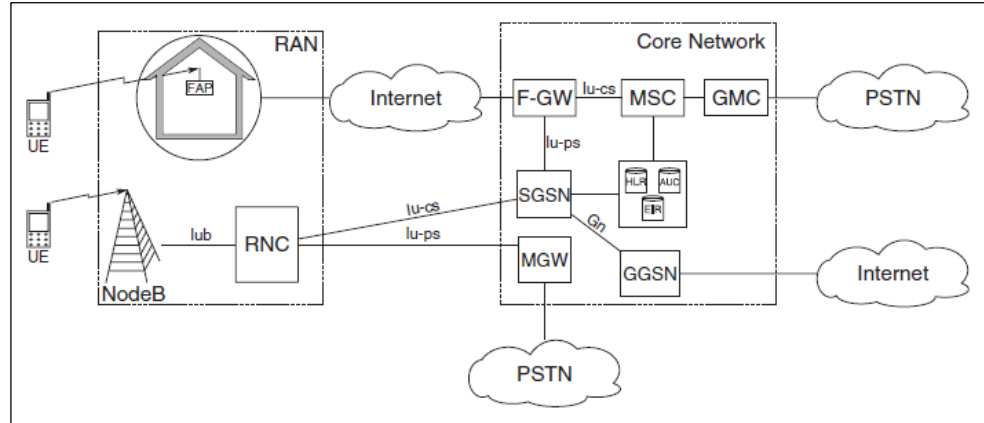


Fig. 2.6 UMTS femtocell network based on an Iu-over-IP architecture

- **The Radio Access Network (RAN)**

RAN in UMTS is called UTRAN, it connects the UEs with the core network and is responsible for handling the air interface, and it connects the UEs with the core network and is responsible for handling the air interface. The only part of UTRAN visible to the mobile user is the NodeB, which handles a single cell throughout the WCDMA air-interface. RNC controls several NodeBs, performs Radio Resource Management (RRM) and is capable of directly communicating with other RNCs through the Iur interface. Furthermore, the RNC communicates with the core network by means of a logical interface called Iu. It also assigns CDMA codes to the UEs and determines the power control limits to avoid near-far problems.

It is possible for the RAN to be fully integrated into the FAP device. However, there are different approaches where this could be done. If the RNC functionality is to be performed by the femtocell, then Iu messages to the core network need to be

encapsulated into IP packets in order to be transmitted through the Internet. This configuration is called an Iu-tunnel or Iu-over-IP and it seems an appropriate architecture for small and medium businesses [63], where several users simultaneously access the femtocell. The elevated number of users in this case with respect to the home environment, introduces the need for bringing the RNC functionality closer to the HNB. Since the number of UEs in a SOHO environment is reduced, other approaches are needed to remove the RNC from the femtocell and introduce it into the core network. This implies that Iub communications between the FAP and the RNC need to be encapsulated on IP packets. This architecture is thus called Iub-over-IP.

- **The Core Network (CN)**

UTRAN uses ATM for transporting speech at a different rate and hence RNCs cannot talk directly to old MSCs. Due to this, a new network element called the Media Gateway (MGW) was introduced to interface between UTRAN and MSCs. The SGSN is a network element inherited from the GPRS network that deals with data communications. It routes incoming packets to/from the appropriate RNC and it authenticates users into the network of the operator. The GGSN is nothing other than the entry point of the SGSN to the Internet.

The air interface of UMTS is based on CDMA with a chip rate of 3.84 Mcps for a bandwidth of 5 MHz. A total of 12 channels are available. The radio frame has a time duration of 10 ms that is subdivided in 15 time slots of duration 0.667 ms, each containing 2560 chips. However, the number of bits carried by each time slot depends on the CDMA Spreading Factor (SF) and the digital modulation being used. UMTS employs QPSK modulation scheme, with each symbol is carrying 2 bits. Fig. 2.7 illustrates the modes of operation of FDD and TDD operation

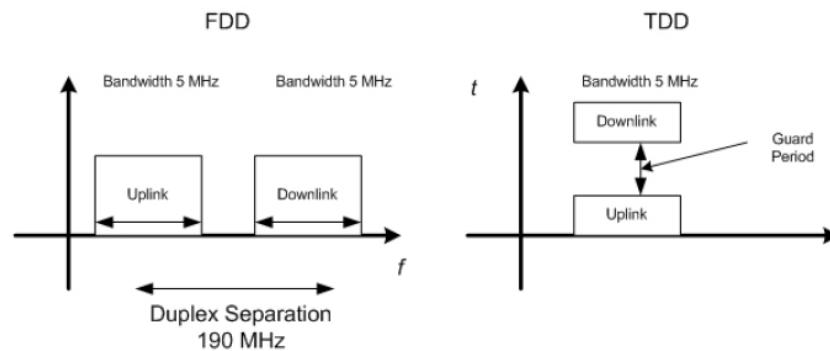


Fig. 2.7 FDD and TDD operation principle

The UMTS protocol stack has two well defined parts:

- The Access Stratum (AS) comprises the layers that make up UTRAN plus lower layers that implement the ATM transport functionality.
- The Non-Access Stratum (NAS) includes the upper layers that communicate the UE with the CN.

Another key concept is that of the Radio Access Bearer (RAB) which is the means for transmitting information that the AS provides to the NAS. Basically it is the Service Access Point (SAP) that the RLC layer provides to the upper layers in the UTRA protocol stack. RABs are continuously established and released in order to provide transmission capabilities with different QoS to UMTS channels. UTRA is thus one of the fundamental parts of the AS because it communicates the UE with the NodeB and it is the entry point of users into the UMTS network. The UMTS air-interface channels are SAPs provided by the lower layers and are classified into three categories:

- Logical channels are provided by the MAC layer to the RLC layer for the transmission of user information.
- Transport channels are provided by the Physical (PHY) layer.

- Physical channels are transmitted over the air and communicate the PHY layers of different UTRA elements.

In UMTS, channels are often transmitted by mapping several upper-layer channels into one lower-layer sub-channel. One upper-layer channel might be split across several lower-layer channels. Among other tasks, it is the responsibility of each layer to multiplex and segment channels received through its SAPs into the appropriate sub-channels of the layer beneath. A more in-depth study of UMTS can be found in [64].

2.6.5 WCDMA Evolution Towards HSDPA

The vision for further development in mobile communications is gradually shifting towards improved network coverage and capacity, higher data rates to users and progressive business model for the operators. To achieve these targets, there is ongoing research to identify the elements which require enhancements and changes to cope with the vision of the forthcoming 4G telecommunication system.

According to the 3GPP framework, the further development of the UMTS network is based on an 'All IP' solution. This concept also introduces the IP traffic handling in the UMTS core network (CN). In order to make a full UMTS system capable of handling IP traffic, it is also necessary to evolve the UTRAN and introduce an IP based solution especially for its air interfaces.

3GPP has introduced the concept of High Speed Downlink Packet Access (HSDPA) for WCDMA in Release 5 specification [65, 66]. According to this specification, functions of RNC are implemented into BS and therefore, a separate RNC is not needed. These functions include scheduling and retransmission of packets, etc. HSDPA enables base stations to schedule downlink packet operations and packet retransmission control. In order to increase the performance of packet base transmission, HSDPA uses Hybrid

Automatic Repeat Request (HARQ) and Adaptive Modulation and Coding (AMC) techniques. These techniques provide backward compatibility with Release 4, and are also used as building blocks for HSDPA evolution especially for the enhancement of the UTRAN air interface. The introduction of HSDPA in the UMTS increases packet data performance up to 100% compared to earlier releases. HSDPA used TDM to transfer data packets in a single shared channel. In HSDPA over-the-air efficient scheduling, modulation, and encoding is done with the help of certain functions and some set of procedures. The HSDPA main functional entities comprise of cell change procedures, AMC, Fast Packet Scheduling (FPS) and HARQ [66]. With the help of the above mentioned functional entities, HSDPA provides higher data throughput up to 10 Mbps, mainly this much data rates on the radio link are usually obtained with the help of a modulation mechanism that is used for resource configuration. Along with the variety of benefits, HSDPA also comes with some drawbacks. HSDPA uses adaptive modulation and coding methods which require modifications in the physical layer architecture. These modifications in the physical layer require significant changes in channel structure, multiplexing and a timing mechanism during HSDPA operation. HSDPA introduces three different types of channels [65], namely; HS-DSCH (high speed downlink shared channel), HS-SCCH (high speed shared control channel is a logical uplink channel, and HS-DPCCH (high speed shared control channel is a logical uplink channel).

For the evaluation of 4G systems, major research emphasis is put on achieving higher data rates, to improve the coverage and capacity of the radio link and to find a good business model for operators. UMTS networks transformed to packet-switched technology architecture. 3GPP Release 7 and beyond specifications outlines the future development, enhancement and migration of the existing telecommunications network

architecture and radio interfaces. In the 3GPP vision, the evolution of telecommunication system is explained under High Speed Packet Access Evolution (HSPA+), System Architecture Evolution (SAE) and LTE [67]. HSPA+ is considered as a framework to improve UMTS network performance for further mobile communication development towards LTE and SAE. HSPA evolution brings advancement only in the packet-switched elements of the UMTS system, and intended to provide full backward compatibility to evolved UMTS systems.

Along the path of communication system evolution, LTE has emerged to provide a packet-switched solution which uses OFDMA as an access technology [68]. LTE is used to provide an all-IP solution with flat network architecture, and has the capability to operate in both FDD and TDD modes. Unlike UMTS, LTE does not support soft handover. The LTE core network is based on an all-IP solution. According to the LTE forum, the evolution of HSPA will provide three to four times more efficient downlink rates and two to three times more efficient uplink rates. The trend of achieving a higher data rate is still continuous in 3GPP and it is known as HSPA+. One step towards the further development of LTE has already been taken and it is known as International Mobile Telecommunications Advanced (IMT-Advanced). For each LTE architectural design there is a shift of the capacity bottleneck between the air interface and the core network. LTE promises to give downlink transmission capacity of at least 100 Mbps, but it is quite evident that today's broadband link which is mainly comprised of DSL and cable modems cannot simply provide data rate support with sufficient capacity up to 100+ Mbps. Hence operators have to think about the deployment of new solutions with fiber/Ethernet and WiMAX solutions.

The use of LIPA in the HNB and HeNBs makes the femtocell an attractive solution for the users, because LIPA enables users to maintain simultaneous access with both their

LAN and with the operator's networks. LIPA functionality will remain the main point of focus in femtocell. LTE is likely to be the dominant cellular data platform for the foreseeable future, and the smooth integration of femtocells into LTE would follow suit. It is noteworthy that regardless of how air interfaces are configured, e.g., in OFDMA the subcarriers carry modulated and coded information, it still matters if the modulation process is investigated, so as a tractable example, the DECT system modulation scheme is investigated in the next chapter.

REFERENCES

- [1] Calhoun, G., "Introduction in Digital Cellular Radio", Boston: Artech house, 1988.
- [2] Siegmund, M., Matthias K., and Malcolm W.; "An Introduction to GSM" Artech House Publishers, Boston, London 1995.
- [3] Christoffer A.; "GPRS and 3G Wireless Applications" John Wiley & Sons, Inc., Canada, 2001.
- [4] Rappaport, T. "The Wireless Revolution"; IEEE Communications Magazine, pp. 52-71 Nov. 1991.
- [5] "Information – Anyone, Anywhere, Anything: Evolution of mobile Network Systems", http://www.tcs.com/0_whitepapers/htdocs/MCG-6.pdf
- [6] Cox, D. "Wireless Network Access For Personal Communications"; IEEE Communication Magazine, pp. 96-115, December 1992.
- [7] MORTEN T; "Indoor Radio Planning; Practical Guide for GSM, DCS, UMTS and HSPA". First Edition, John Wiley & Sons, Ltd, 2008.
- [8] David J. Goodman, "Wireless Personal Communications Systems", Addison Wesley Longman, Inc., 1997.
- [9] Viterbi, A., Padovani, R. "Implications of Mobile Cellular CDMA"; IEEE Communication Magazine, pp. 38-41, December 1992.
- [10] The Wireless Network Evolution, By C. K. Toh, [http:// www. informit. com/ articles/article.asp?p=26330](http://www.informit.com/articles/article.asp?p=26330). Apr 2002.
- [11] Rogier Noldus; "CAMEL, Intelligent Networks for the GSM, GPRS and UMTS Networks", John Wiley & Sons Ltd, 2006.
- [12] Timo Halonen, Javier Romero, and Juan Melero,"GSM, GPRS and EDGE Performance, Evolution towards 3G / UMTS"; John Wiley & Sons, Ltd, 2002.
- [13] Pirhonen R., Rautava T., Penttinen J., "TDMA Convergence for Packet Data Services", IEEE Personal Communications., Vol. 6, No. 3, pp. 68-73, June 1999.
- [14] 3GPP TS 45.005, Radio transmission and reception 3rd Generation Partnership Project; Technical Specification Group GERAN.
- [15] Harri Holma and Antti Toskala; "WCDMA FOR UMTS, Radio Access For Third Generation Mobile Communications", John Wiley & Sons, Ltd 2000.
- [16] <http://learning.ericsson.net/>.

-
- [17] “WCDMA (UMTS)”; <http://www.umtsworld.com/technology/wcdma.htm>.
 - [18] <http://www.cellular.co.za/cdma.htm>.
 - [19] <http://www.3g-generation.com/>
 - [20] V. Chandrasekhar and J. G. Andrews, “Femtocell Networks: A Survey”, IEEE Communication Magazine, vol. 46, no. 9, pp. 59-67, September 2008.
 - [21] <http://www.thinksmall.com/FAQ.html>.
 - [22] <http://www.fujitsu.com/downloads/TEL/fnc/whitepapers/High-Capacity-Indoor-Wireless.pdf>.
 - [23] Lester T. W. Ho, Holger Claussen, “Effects of User-Deployed, Co-channel Femtocells on the Call Drop Probability in a Residential Scenario”, The 18th Annual International Symposium on Personal, Indoor and Radio Communications, 2007.
 - [24] Internet World Statistics, <http://www.internetworldstats.com/>
 - [25] Douglas N. Knisely, Airvana, Inc. , Takahito Yoshizawa, Thomson Telecom, Frank Favichia, Alcatel-Lucent, “Standarization of Femtocells in 3GPP”, IEEE Communications magazine, September 2009.
 - [26] GSM Association, “Mobile Data Statistics 2008,” November 2008.
 - [27] Tara A. Yahiya, Kaldom Al (FRW), “Understanding LTE and its performance”, Engelsenka, Springer Science and Business Media, LLC, 2011.
 - [28] Elias Chavarria Reyes, David M. Gutierrez-Estevez and Ian F. Akyildiz“, A Complete Femtocell Network Modeling and Development Platform”, Globecom Wireless Networking symposium 2012.
 - [29] <http://www.airvana.com/technology/femtocell-network-architecture>.
 - [30] 3GPP Technical Report 25.820 v.8.2.: “3G Home NodeB Study Item Technical Repot”, Release 8 09/2008, available online at www.3gpp.org.
 - [31] 3GPP Technical Specification 25.467 v.8.0.0: “UTRAN architecture for 3G Home NodeB”, Release 8 12/2008, available online at www.3gpp.org.
 - [32] Vikran Chandrasekhar and Andrews, “Femtocell Networks: A Survey”, IEEE Communications Magazine, September 2008.
 - [33] Jie Zhang, Guillaume de la Roche, “Femtocell: Technologies and Developments”, John Wiley and Sons Ltd., 2010.
 - [34] TS 25.434 UTRAN Iub Interface Data Transport and Tansport Signalling for Common Transport Channel Data Streams, Rel-7.

-
- [35] TS 43.318, Generic Access Network (GAN) Stage 2, Rel-5.
 - [36] TS 44.318, Generic Access Network (GAN); Mobile GAN Interface Layer 3 Specification, Rel-5.
 - [37] Mostafa Zaman Chowdhury, Yeong Min, and Zygmunt J. Haas, “Interference Mitigation Using Dynamic Frequency Re-use for Dense Femtocell Network Architectures”, IEEE Communications society International Conference on ubiquitous and future networks, 2010.
 - [38] M. Haenggi and R. Ganti,. “Interference in Large Wireless Networks,” Foundations and Trends in Networking, vol. 3, no. 2, pp. 127–248, 2008.
 - [39] S. Kishore, L. J. Greenstein, H. V. Poor, and S. C. Schwartz, “Soft handoff and uplink capacity in a two-tier CDMA system,” IEEE Trans. Wireless Commun., vol. 4, no. 4, pp. 1297–1301, Jul. 2005.
 - [40] H. S. Dhillon, R. K. Ganti, F. Baccelli, and J. G. Andrews, “Modeling and Analysis of K-Tier Downlink Heterogeneous Cellular Networks,” IEEE J. Sel. Areas Commun., Apr. 2012.
 - [41] A. Ghosh, J. G. Andrews, N. Mangalvedhe, R. Ratasuk, B. Mondal, M. Cudak, E. Visotsky, T. A. Thomas, P. Xia, H. S. Jo, H. S. Dhillon, and T. D. Novlan, “Heterogeneous cellular networks: From theory to practice,” IEEE Commun. Mag., Jun. 2012.
 - [42] A. Damnjanovic, J. Montojo, Y. Wei, T. Ji, T. Luo, M. Vajapeyam, T. Yoo, O. Song, and D. Malladi, “A survey on 3GPP heterogeneous networks,” IEEE Wireless Commun., vol. 18, no. 3, pp. 10 –21, Jun. 2011.
 - [43] H. S. Jo, P. Xia, , and J. G. Andrews, “Downlink femtocell networks: Open or closed?” IEEE International Conference on Communications, Jun. 2011.
 - [44] Femto Forum, “Interference Management in OFDMA Femtocells,” Whitepaper available at www.femtoforum.org, Mar. 2010.
 - [45] 3GPP, “3G Home NodeB Study Item Technical Report,” TR 25.820 (release 11), 2011.
 - [46] “UTRAN Architecture for Home NodeB Stage 2,” TS 25.467 (release 11), 2011.
 - [47] “New Work Item Proposal: Enhanced ICIC for non-CA based deployments of heterogeneous networks for LTE,” RP-100372, 2010.

-
- [48] V. Chandrasekhar, J. Andrews, Z. Shen, T. Muharemovic, and A. Gatherer, "Power control in two-tier femtocell networks," *IEEE Trans. Wireless Commun.*, vol. 8, no. 8, pp. 4316–28, August 2009.
- [49] M. Yavuz, F. Meshkati, S. Nanda, A. Pokhariyal, N. Johnson, B. Raghothaman, and A. Richardson, "Interference management and performance analysis of UMTS/HSPA+ femtocells," *IEEE Commun. Mag.*, vol. 47, no. 9, pp. 102–109, Sep. 2009.
- [50] H.-S. Jo, C. Mun, J. Moon, and J.-G. Yook, "Interference mitigation using uplink power control for two-tier femtocell networks," *IEEE Trans. Wireless Commun.*, vol. 8, no. 10, pp. 4906–4910, Oct. 2009.
- [51] Jeffrey G. Andrews, Holger Claussen, Mischa Dohler, Sundeep Rangan, Marc C. Reed, "Femtocells: Past, Present, and Future", *IEEE journal on selected areas in communications*, vol. 30, No. 3, April 2012.
- [52] Simon R. Saunders, Stuart Carlaw, Andrea Giustina, Ravi Raj Bhat, V. Srinivasa Rao, and Rasa Siegborg, "Femtocells: Oportunities and Challenges for Business and Technology". John Wiley & Sons Ltd, Publication, 2009.
- [53] Femto Forum. Interference management in UMTS femtocells. www.femtoforum.org, 2008.
- [54] W. Webb, *Wireless Communications: The Future*. John Wiley & Sons, 2007, ch. 6, pp. 73–74.
- [55] S. P. Weber, J. Andrews, X. Yang, and G. de Veciana, "Transmission capacity of wireless ad hoc networks with successive interference cancellation," *IEEE Transactions on Information Theory*, vol. 53, no. 8, pp. 2799–2814, Aug. 2007.
- [56] V. Chandrasekhar and J.G Andrews "Uplink capacity and interference avoidance for two-tier femtocell networks," *IEEE Trans. Wireless Commun.*, vol. 8, pp. 3498–3509, July 2009.
- [57] D. L'opez-P'erez, A. Valcarce, G. de la Roche, and J. Zhang, "OFDMA femtocells: a roadmap on interference avoidance," *IEEE Commun. Mag.* vol. 47, pp. 41–48, Sept. 2009.
- [58] D. L'opez-P'erez, G. D. L. Roche, A. Valcarce, A. J'uttner, and J. Zhang, "Interference avoidance and dynamic frequency planning for WiWAX femtocell networks," in *Proc. IEEE International Conference on Communication Systems*, Guangzhou, China, Nov. 2008, pp. 1579–1584.

-
- [59] V. Chandrasekhar, J. G. Andrews, T. Muharemovic, Z. Shen, and A. Gatherer, "Power control in two-tier femtocell networks," *IEEE Trans. Wireless Commun.*, vol. 8, pp. 4316–4328, Aug. 2009.
- [60] H. Claussen, "Performance of macro- and co-channel femtocells in a hierarchical cell structure," in *Proc. IEEE International Symposium on Personal, Indoor and Mobile Radio Communications (PIMRC'07)*, Athens, Greece, Sept. 2007, p. 5.
- [61] 'User Equipment (UE) radio transmission and reception (FDD),' Feb. 1999. [Online]. Available: <http://www.3gpp.org/ftp/Specs/html-info/25101.htm>.
- [62] 'User Equipment (UE) radio transmission and reception (TDD),' Feb. 1999. [Online]. Available: <http://www.3gpp.org/ftp/Specs/html-info/25102.htm>.
- [63] S. Rao and R. R. Bhat, 'Assessing Femtocell Network Architecture and Signaling Protocol alternatives,' <http://www.embedded.com>, Feb. 2008.
- [64] H. Holma and A. Toskala, Eds., "WCDMA for UMTS", 3rd ed. John Wiley & Sons, Chichester, 2004.
- [65] 3GPP, 'Technical Specification Group Radio Access Network; High Speed Downlink Packet Access (HSDPA); Overall description', Stage 2, Release 5, TS 25.308; <http://www.3gpp.org/>
- [66] H. Holma and A. Toskala; "WCDMA FOR UMTS - HSPA Evolution and LTE", Fourth Edition, John Wiley & Sons Ltd 2009.
- [67] 3GPP, 'Technical Specification Group Radio Access Network; Requirements for Evolved UTRA (E-UTRA) and Evolved UTRAN (E-UTRAN)"; Release 7, Release 8 and Release 9, TR 25.913; <http://www.3gpp.org/>
- [68] X. Wang, "OFDM and its application to 4G Wireless and Optical Communications", IEEE 2005, December 2005.

CHAPTER 3

SIMULATION OF THE DECT SYSTEM

3.1 Personal communications systems

The explosive growth in demand for personal mobility in recent years has led to the development of Personal Communication Systems (PCS) that allow people to communicate anywhere, anytime [1,2]. In contrast to cellular mobile, PCS employ micro-cell technology with low power base stations and small cell sizes. This allows PCS to handle a significantly higher traffic density than its cellular counterpart. Currently, standards for the emerging PCS are the Cordless Telephone (CT-2) [3, 4], and the Digital European Telecommunications (DECT) [5]. CT-2 is designed mainly for telepoint services. It maps one telephone conversation onto a single frequency channel and operates in the 800 MHz band with 100 kHz channel spacing and 72 kb/s system bit rate.

A third standard is the DCS1800 developed by the European Telecommunications Standards Institute (ETSI) to operate at the 1.8 GHz band [6]. It differs from GSM standard in operating frequency band, allowable transmitted power, and roaming capability. Table 3.1 summarises the basic technical characteristics of these PCS standards [7].

System	<i>DECT</i>	CT-2	DCS-1800
Multiple access	TDMA/FDMA	FDMA	TDMA/FDMA (SD)
Freq. band (MHz)	1800-1900	864-868	1710-1785
Duplexing	TDD	TDD	FDD
Ch. spacing (kHz)	1728	100	200
Modulation	GMSK	GMSK	GMSK
Tx power (peak)	250 mW	10 mW	1 MW
Tx power (avg.)	10 mW	5 mW	125 mW
Speech coding	ADPCM	ADPCM	RPE-LPP
Codec rate (kb/s)	32	32	13
Speech/Rf Ch.	12	1	8
Ch. bit rate (kb/s)	1152	72	270.833
Ch. coding	CRC		1/2 rate conv.
Frame dur. (ms)	10	2	4.615

Table 3.1 Personal Communication Systems standards

It is noted from this brief survey that all three PCS standards employ GMSK digital modulation as part of their air interface specifications.

Cordless business communications span a range of potential applications and uses from a simple cordless telephone up to high capacity cordless business communications systems providing services for speech and high speed data. To meet requirements in large buildings, cordless office communications systems must adopt a channel re-use strategy to cover the entire building with the available resources. When frequency re-use is considered, the entire building needs to be divided into smaller cells varying from one-cell-per floor-to one-cell-per-room. The smaller cells, in the case of one-cell-per-

room, can be referred to as picocells, which is employed when a line-of-sight (LOS) between the transmitter and the receiver is strictly necessary [8, 9].

A semi-isotropic or omni-horizontal centrally placed antenna can be used in order to illuminate each room by a single antenna with satisfactory SNR levels throughout the room. Each room must have its own antenna so that, whenever possible, a line-of-sight will be provided to all receivers in the vicinity of the centrally placed transmitter antenna [10].

3.1.1 An overview of the DECT system

The real merit of cordless technology is the provision of in-building cordless communication with high traffic density and a wide variety of both voice and data services. Because these requirements were not met by any of the analogue cordless telephone specifications that have been in use in Europe, the Conference of European Posts and Telecommunications (CEPT) decided to develop a new standard for digital cordless telephony that would address the problems of incompatibility, cost and service quality. A new European standard was formally initiated in 1988, built upon the earlier work (e.g. CT-2) which was originally called CT3, but has been known as DECT [4]. The DECT standard has grown out of the need to provide for cordless communication, primarily for voice traffic, but also to provide support for a range of wireless data traffic requirements at a cost that encourages wide adoption. It is particularly targeted to support the following integrated telecommunications applications:

- VOICE
 1. Business telephone exchange (single and multi-cell).
 2. Residential telephony with intercom facility.
 3. Public telephone services (Telepoint).

- DATA
 1. ISDN connections such as telefax, teletext, and videophone.
 2. Patch transfer
 3. Remote terminal services
 4. Real time file access

DECT is based on a micro-cellular radio communication system that provides low-power radio (cordless) access between portable parts and fixed parts at ranges up to a few hundred metres. DECT is also able to support a number of alternative system configurations ranging from single cell equipment (e.g. domestic fixed parts) to large multiple cell installations (e.g. large business cordless PBX) [10]. The DECT specifications are fully described in the European Telecommunication Standard (ETS) draft (a series of 11 parts) proposed by the Radio Equipment and Standards (RES) Technical Committee of the ETSI. The structure of this standard is based on the layered principles used in the Open Systems Interconnection (OSI) model as shown in Fig.3.1

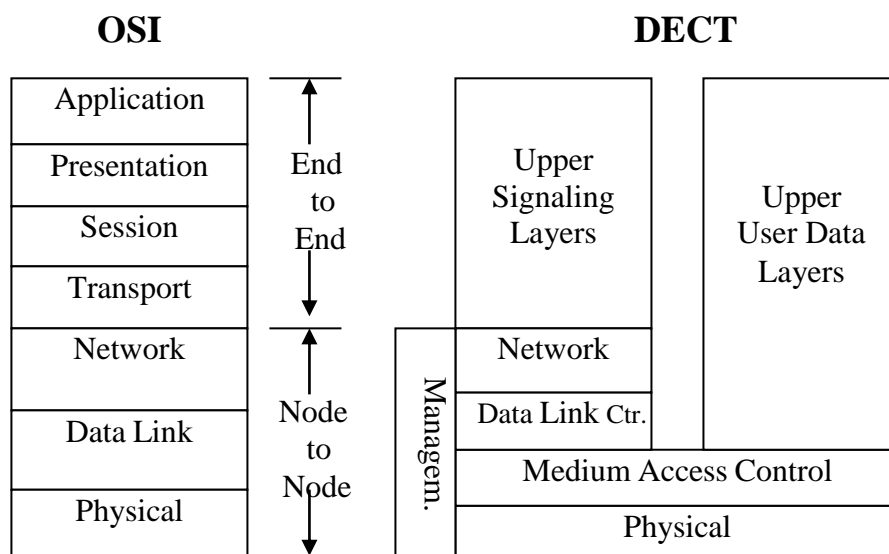


Fig. 3.1 DECT protocol layers

The complete interface corresponds to the lower three layers of the OSI model, however DECT defines four layers of protocol for the node-to-node communication. The additional layer is the Medium Access Control (MAC) layer, which exists in most of the mobile radio specifications having multiple access schemes (DECT, GSM, DCS1800, etc.).

The Physical Layer (PHL) and the MAC layer are common to both user data and signalling data. The PHL layer modulates and demodulates radio carriers with a bit stream of a defined rate to create a radio frequency channel, and the MAC layer is responsible for effective allocation of radio resources and for multiplexing and demultiplexing user and signalling data into slot-sized packets.

The Data Link Control (DLC) layer maintains secure data link for signalling even when the base station has to be changed during the call (i.e. hand over process). The Network Layer (NWL) is responsible for routing calls from the portable wishing to make a call to the fixed network and vice versa.

The PHL is discussed in more detail in the next sub-section, as the following chapters will be dealing with the assessment of a multi-level digital modulation scheme for DECT system.

3.1.2 The Physical Layer

The PHL as mentioned earlier is responsible for segmenting the radio transmission medium into physical channels. This is done using a TDMA scheme on multiple carriers. Presently ten RF carriers are provided in the allocated frequency band between 1800 MHz and 1900 MHz. The standard also provides for possible extension of the band down to 1850 MHz to meet future demand [11]. On each carrier the TDMA structure defines 24 timeslots in a time frame of 10 ms which results in timeslots of

approximately 416.7 μ s, that are used to transmit oneself contained packet of data per slot. As seen from Fig.3.2 [4], the burst contains two fields, a synchronisation field of 32 bits, and a data field of 388 bits (together with control information and error control). The synchronisation data allows the receiver to demodulate a single packet immediately, so as to enable very fast call set-up and unnoticeable handovers. The data field is received from the MAC layer.

The total 420 bits are modulated onto the carrier using a two-level FSK modulation with Gaussian prefiltering at a relative bandwidth (BT product) of 0.5. If the modulation were coherent it would be GMSK; coherence is, however, not necessary. The chosen modulation scheme permits the use of a simple receiver with non-coherent demodulation, bit-by-bit decision, and easily-implementable IF filters.

The modulated data rate is 1152 kbit/s. The complete packet therefore has a length of 420 bit/1152 kbit/s, i.e. 364.6 μ s. When these packets are transmitted within a timeslot, there remains a guard space of 52 μ s which is needed to allow for propagation delays, smooth ramp-up and ramp-down of the transmitter, and synthesiser switching between packets. A physical channel is created by transmitting one packet every frame during a particular timeslot on a particular carrier. The throughput of a physical channel available to the MAC layer is therefore 388bit/10ms, i.e. 38.8kbit/s. The average transmitted power per physical channel is 10 mW. The PHL is instructed by the MAC layer to transmit on which timeslot and carrier.

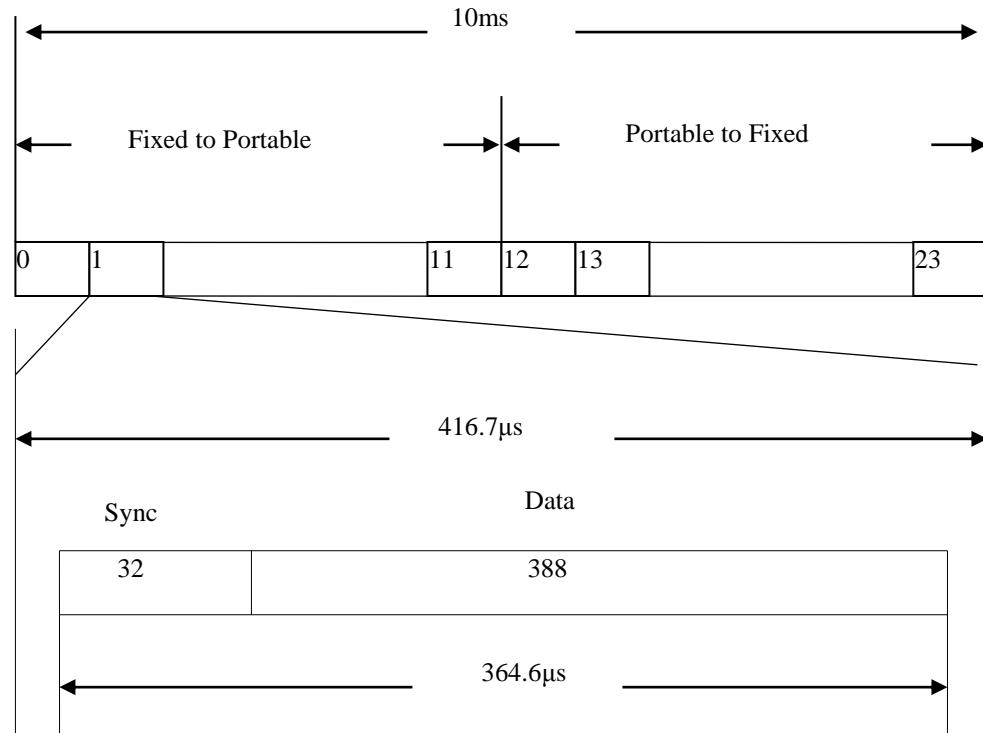


Fig. 3.2 DECT frame and slot structure

As indicated in Fig. 3.2, the first 12 slots are normally used for transmission to the portable (down-link), and the second 12 slots for transmission in the opposite direction (up-link). The PHIL does not know that there is a Time Division Duplex (TDD) transmission mode, but is simply told by the MAC layer to transmit for instance on timeslot 5 and to receive on timeslot 17 [4].

In DECT, an Adaptive Differential Pulse Code Modulation (ADPCM) voice connection requires a pair of 32kbit/s TDD physical channels, whilst data services require various bandwidths. Data connections for those services with data rates greater than 32kbit/s duplex are provided by using multiple duplex channels. Those requiring less are provided by intermittent packet access of a single physical channel. Since data connections are rarely symmetrical in their information transfer rate at any given moment, DECT allows the Mobile Data Terminal (MDT) or the base station (whichever

is sending more data) to transmit in both halves of the frame in one direction rather than to allow one frame half for the duplex reply as happens in voice connections. This maintains a paired slot structure to all users but allows considerable asymmetric data transfer without allocating underused duplex bandwidth. This enhances the spectral efficiency.

With data communications on a cordless interface it is necessary to be able to allocate a variable number of physical channels to a connection, dependent on the required data rate, and to provide asymmetric radio channels to maintain spectral efficiency. During a call the number of physical channels required and the level of asymmetry may vary due to changes in network demand or radio link quality. Low bit rate services are serviced efficiently by packet access and by making use of any half slot provision whenever available.

The MAC layer controls the transmission and/or reception of data for every half, full, or double slot by issuing primitives to the physical layer. Each primitive specifies the operation for one slot position. Continuous operation on a given physical channel requires a regular series of primitives. Table 3.2 summarises the main parameters of the DECT air interface.

Access Scheme	TDMA / FDMA
Duplexing	TDD
Band of Operation (MHz)	1800 – 1900
Channel Bit Rate (Mb/s)	1.152
Number of Carriers	10
Number of Channels	12
Modulation Scheme	GMSK
Channel Spacing (MHz)	1.728
Tx Power (mW)	250 (Peak), 10 (Average)
Frame Duration (ms)	10
Number of Slots in a Frame	24 (12 uplink, 12 down link)
Speech Coding	ADPCM
Codec Rate (Kb/s)	32
Channel Coding	CRC

Table 3.2 DECT Air-Interface Parameters

3.1.3 The DECT Cordless Office

An office scenario is shown in Fig. 3.3 [12]. The handsets (Cordless Portable Part, CPP) establish radio links with the base stations (Radio Fixed Part, RFP). The fixed network connections from the RFPs run to the Cordless Control Fixed Part (CCFP) and from there to the ISDN and PSTN connections. With data, rather than speech calls the CPP becomes a Cordless Data Terminal (CDT) which communicates via the RFPs to the Cordless Data Control Fixed Part (CDCFP) located in the CCFP. A voice connection, using ADPCM, simply requires a single 32 kbit/s TDD radio channel, while

data services may require much more bandwidth. These data connections are provided by using more than one duplex 32 kbit/s radio channel [13, 14].

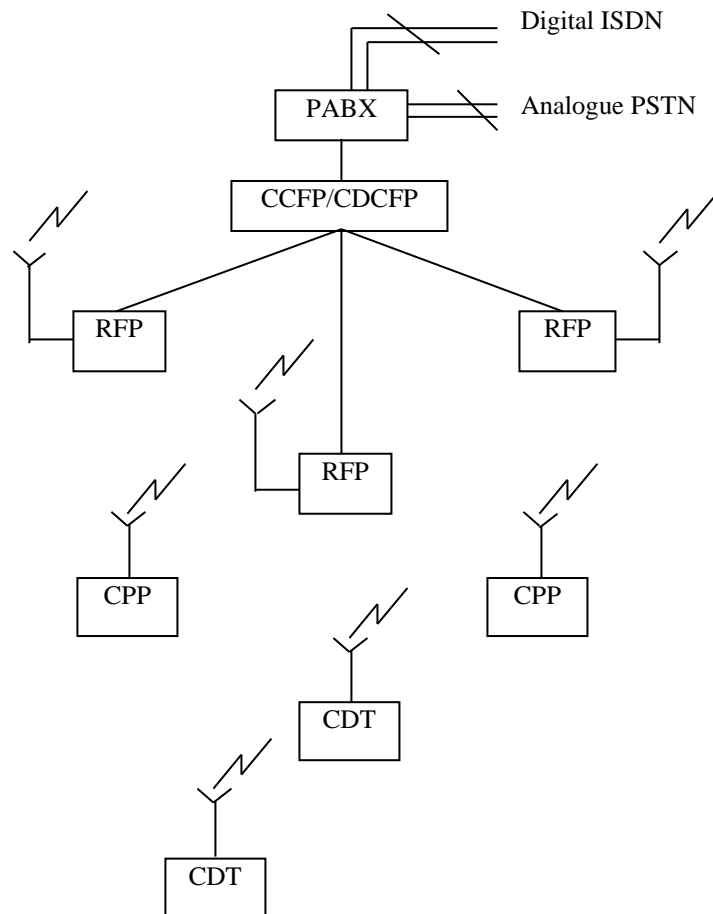


Fig.3.3 The DECT Cordless Office

Data links are established between the CDCFP and the CDT and the information data is transferred in a numbered packets with some error protection. The RFP's may just transfer information on to the CDT or CDCFP for them to correct errors, request retransmission of erroneous data, and to perform re-sequencing of packets. As an RFP does not interfere with the data, wideband multi-slot calls may use several RFP's. Data connections are rarely symmetrical in their information transfer rate, e.g. file transfer in one direction at 64 kbit/s with only acknowledgements in the return direction. If this asymmetry is not considered the channels will be under used with a corresponding

decrease in spectral efficiency. Low bit rate services are supported by dividing a full 32 kbit/s slot in two to provide shorter sub slots. These full and half rate slots can coexist in the same DECT system. The half rate slots contain the same synchronisation and control channel bandwidth as the full rate slot. These three slot types are outlined in table 3.3 [13]

Slot	Protected user rate (kbite/s)	Unprotected user rate (kbite/s)
DS (P80)	64.0	80
FS (P32)	25.6	32
HS (P08)	6.4	8

Table 3.3 User bite rate for DECT slot types (DS=double slot, FS=full slot)

3.2 Simulation Background

Computer simulation has grown to become an integral part of the digital communication system design. In order to efficiently design an effective and reliable communication system, it is necessary to assess the system to select the optimum operating parameters. Often, performance evaluation and trade-off considerations need to be undertaken. To predict the performance of a communication system, three methods are generally used, an analytical approach, computer simulation, or direct measurement. At the system design level, direct measurement is not applicable leaving either an analytical or computer simulation approach. Analytical evaluation of performance can be carried out if the effects of system impairments can be represented correctly by analytical formula. In practice, it is extremely difficult to directly analyse the performance of complex systems for factors such as interference effects, multipath fading etc. without some form of simulation being involved. Due to these reasons, system design engineers are becoming increasingly dependent on the use of simulation techniques as an essential aid

to the design and understanding of such systems. Computer-aided techniques provide a useful and effective adjunct to direct analytical evaluation of system performance, some advantages of which are listed below:

1. Experimental results can be reproduced effortlessly provided the system model remains unchanged.
2. Seeing the effect of different system parameters on the system performance can easily be achieved simply by changing a model parameter.
3. Different system scenarios can be evaluated prior to the procurement of the hardware.

Also, driven by the rising cost of process equipment, computer modelling has replaced time-consuming, trial and error equipment design in industry. Not only has computer modelling proven extremely advantageous in design, but also in process optimisation and process control.

Computer-aided techniques for systems analysis and design fall into two categories: formula-based approaches where the computer is used to evaluate complex formulas, thus freeing the designer from the repetitive work involved in substituting numbers into formulas, and simulation-based approaches where the computer is used to simulate the voltage and current waveforms or signals that flow through the system. The second approach which involves waveform level simulations as the primary analysis tool is very flexible and can be used to model and analyse complex systems with any desired level of detail. Waveform level simulation of communication and signal processing systems consist of the following steps:

1. Representing the system in the form of a signal flow block diagram.
2. Generating samples of all input signals (waveforms).

3. Performing discrete-time signal processing operations according to the functional model of each block.
4. Storing the simulated waveforms and analysing the stored waveforms to extract performance measures.

Monte Carlo techniques are used to handle random variations in signals and system parameters, and the simulations are run until enough samples have been accumulated to obtain statistical valid estimates of performance measures [15].

3.2.1 Monte Carlo Simulation

For any simulation technique to be accurate, reasonable assumptions must be made on the statistical properties of the random sources and the communication system model. One common assumption in all is the Gaussian distribution for the channel noise and statistical independence of the random sources representing information bits and noise. BER estimation is performed at the decision device which can be either adaptive or fixed depending on the receiver used. In the simple threshold sensing device an error will occur whenever the received signal exceeds the threshold into the opposite side e.g. when a zero is sent and the received voltage v_r exceeds threshold voltage V_T . Fig. 3.4 shows the probability density function

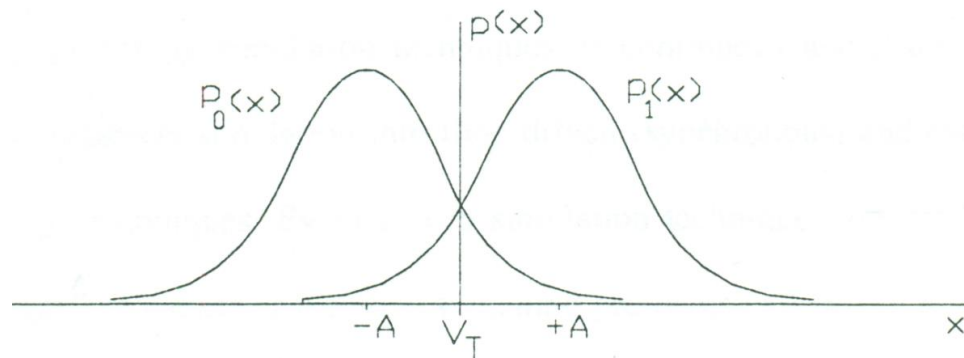


Fig. 3.4 Probability density function

The probability of exceeding V_T when a zero is sent is given by

$$P_0 = \int_{V_T}^{\infty} P_0(V) dV = 1 - F_0(V_T) \quad (3.1)$$

Where $P(x)$ is the PDF, and $F(x)$ is the CDF of the random variable x . Similarly, when a one is sent, the probability of making an error and receiving a zero is given by

$$P_1 = \int_{-\infty}^{V_T} P_1(V) dV = F_1(V_T) \quad (3.2)$$

Making the reasonable assumptions that transmission of 0's and 1's are equally probable, the average probability of error, P , will be

$$P = \frac{1}{2}P_0 + \frac{1}{2}P_1 = \frac{1}{2}(P_0 + P_1) \quad (3.3)$$

Simulation techniques differ from each other in the way the density functions are handled. Assumptions should be made in order to propose a method of relating the tail of the density function to the probability of symbol error. However, only in the Monte Carlo simulation technique no prior assumption is required for handling the tail function. Instead, empirical determination of the distribution function is employed [16-18]. The Monte Carlo simulation technique is the most general error estimation technique. The price paid for generality and high accuracy is the high computational cost related to the number of observations that must be made in order to obtain a given probability. The number of samples N_s required for simulation is related to the target probability of error P_e by [19, 20]

$$N_s = \frac{n_e}{P_e} \quad (3.4)$$

Where N_s is the total number of samples observed, n_e is the number of errors observed. That is, if one error is expected at every 10^6 samples, the total number of samples required for simulation will be at least

$$N_s = \frac{n_e}{P_e} = \frac{1}{10^{-6}} = 10^6$$

Using 10 samples per symbol, the minimum number of samples required will be

$$N_s = \frac{10}{P_e} = \frac{10}{10^{-6}} = 10^7$$

To observe at least 10 errors, the minimum number of samples required for simulation would be $10 \times 10^7 = 10^8$. In a sophisticated system, simulation would mean several days of simulation time even with the advent of high speed workstations.

The accuracy of the estimation depends on the number of samples in the simulation, probability of error, and the correlation between samples. In general, the variance of the estimated error probability is inversely proportional to the number of samples, decrease with decreasing probability, and increase when there is correlation between the samples [21]. The dependence of the variance on the correlation between samples is complicated. Davis has a fairly easy way of tackling the problem [22]. For a stationary ergodic sequence of random variables $V_{ij} = 1, 2, 3, \dots, N$, the estimate of the mean η and the variance are given by

$$E \left\{ \hat{\eta} \right\} = \eta \quad (3.5)$$

And

$$V \left\{ \hat{\eta} \right\} = \frac{P_e}{N_s} \quad (3.6)$$

It is clear that if the variance is zero, the pdf of the estimator \hat{p} would be equal to the true error probability P , and the estimator is strongly dependent on its variance. Despite the superior accuracy of this method over all other simulation techniques, it has the demerit of extremely long simulation times due to the large number of samples required. In order to reduce the sampling rate requirements, bandpass signals and systems are usually represented by their equivalent lowpass complex envelopes for simulation purposes as will be highlighted in the following subsection.

3.2.2 Complex Lowpass Representation of Bandpass Signals

One of the primary problems of all simulation techniques is the large number of samples required during a simulation run. Large number of samples implies very large memory requirement and enormous computational power. To clarify this, the concept of simulation in the context of sampling follows:

From Nyquist theory, the minimum sampling rate f_s for a bandpass system is given by

$$f_s = n_s \cdot f_{max} \quad (3.7)$$

Where $n_s = 2$ and f_{max} is the maximum frequency content in the signal given by

$$f_{max} = f_c + f_m \quad (3.8)$$

With f_c is the carrier frequency, and f_m is the single sided message bandwidth. The step time (or clocking time) Δt is related to f_s by

$$\Delta t = \frac{1}{f_s} \quad (3.9)$$

When a channel is represented by a tapped-delay-line FIR filter, this step time must be smaller than the separation between taps, otherwise, taps may overlap and distort the shape of the power delay profile. If f_s is smaller than the coherence bandwidth of the channel W_{ch} , the f_s must be represented by W_{ch} and the step time becomes $\Delta t = 1/W_{ch}$. The duration of the simulation is determined from the minimum number of symbols required to achieve an accurate estimate of the probability of error. With N_s symbols required for a simulation run, and n_s samples per symbols, the simulation duration will be

$$\text{stop time} = \text{symbol time} * \text{number of symbols}$$

$$T_{stop} = T_s N_s n_s$$

The total number of samples used for simulation, N_T , is given by

$$N_T = \frac{T_{stop}}{\Delta t} = \frac{T_s N_s n_s}{\Delta t} = (T_s N_s) n_s (f_c + f_m) \quad (3.10)$$

Hence it is apparent from (3.7) that the number of samples required is proportional to the maximum frequency content in the signal. For a microwave or millimetre wave system the carrier frequency is of the order of GHz, and therefore the number of samples required is substantially large and will result in enormous computational power requirements. One way of reducing the number of samples required for the simulation is to use complex lowpass representation for bandpass signals [23, 24]. A bandpass signal $x(t)$ can be represented as

$$x(t) = \text{Re} \left\{ \hat{x}(t) e^{j2\pi f_0 t} \right\} \quad (3.11)$$

Where $\hat{x}(t)$ is the complex envelope of $x(t)$ given by

$$\hat{x}(t) = X_c(t) - jX_s(t)$$

and f_0 is the centre (or carrier) frequency. $\hat{x}(t)$ is a straightforward extension of the conventional phasor representation of a lowpass signal referred to the arbitrary centre frequency f_0 .

Bandpass operations such as filtering can be represented in the same manner as the signal itself by its complex envelope [25, 26]. The impulse response $h(t)$ of a bandpass filter can be written as

$$h(t) = 2\text{Re} \left\{ \hat{h}(t) e^{j2\pi f_0 t} \right\} \quad (3.12)$$

Where $\hat{h}(t) = h_c(t) - jh_s(t)$ represents the baseband equivalent impulse response. Here $h_c(t)$ and $h_s(t)$ are real lowpass functions representing the inphase (I) and quadrature (Q) filtering effects respectively. The complex envelope of the filter output $\hat{y}(t)$ will then be given by

$$\hat{y}(t) = \hat{x}(t) \otimes \hat{h}(t) \quad (3.13)$$

in which \otimes represents convolution and

$$\hat{y}(t) = y_c(t) - jy_s(t) \quad (3.14)$$

Where

$$y_c(t) = X_c(t) \otimes h_c(t) - X_s(t) \otimes h_s(t) \quad (3.15)$$

And

$$y_s(t) = X_c(t) \otimes h_s(t) + X_s(t) \otimes h_c(t) \quad (3.16)$$

Hence the bandpass signals as well as bandpass filtering operations can be reduced to complex lowpass signals and complex lowpass filtering operations respectively. Recalling that the complex envelope is a lowpass signal, a sampled representation needs only to have a bandwidth corresponding to the bandwidth of the signal. In other words, since the complex envelope carries all the information necessary to estimate the

behaviour of a bandpass signal, there is no need to represent the carrier frequency f_c in the sampled domain. Thus, the carrier frequency can be dropped from (3.7) and the number of samples required for a simulation would be reduced to

$$N_T = (T_s N_s)(n_s f_m) \quad (3.17)$$

Comparing (3.7) and (3.14), one can easily see the reduction in the number of samples required for simulation. This is the technique commonly employed in transmission systems simulations.

3.2.3 Factors Affecting Simulation Accuracy

A simulation model can be a very close replica of the actual system if all of the individual models constituting the simulation model are carefully designed. But, like any other techniques, computer simulation techniques are not without short falls. However close the simulation model stands to the actual system, there will still remain some sources causing errors in the final simulation results [27]. Some of these error sources are:

- a) Round off and amplitude errors will result due to the finite word length of computers being used.
- b) Drifts in the sampling clock will cause time jitter errors.
- c) When the continuous signals are not strictly bandlimited aliasing errors will occur.
- d) Due to the representation of continuous time signals over a limited time period, truncation errors will result.
- e) Because bit error estimation is a statistical process, the outcome of the simulation is therefore subject to statistical uncertainties caused by:

- i) Finite rather than infinite data observation time
- ii) Imperfect randomness properties of the random number generators used to represent the transmitted data and system noise contributions.

Despite the deviation from a practical system, a simulation model can still reveal the relative differences in the performance of communication protocols, channel allocation, handover, frequency management strategies, modulation techniques, coding, interleaving etc. It is of great importance to check the simulation against analysis for specific simple cases in order to verify the simulation. This would enable to detect, if there is any, systematic errors in the systems simulator. A typical case is to compare simulation against analysis for the systems performance in an AWGN channel.

3.2.4 Software programs for Simulating Communication Systems

The outstanding contribution of computer simulation to system performance prediction has strengthened the need to develop a number of software packages for simulating communication systems. Simulation based approaches have been studied by a large number of people starting in the 1950's with block oriented languages such as MIDAS, SCADS, CSMP etc. [28]. These packages imitate the behaviour of analogue systems on a component by component basis based on the analogue block diagram as a convenient way of describing continuous systems. By the new developments in digital signal processing, software packages based on transform domain techniques began to appear in the early 1970's. Two examples of such software packages are described next.

3.2.4.1 MATLAB and Simulink

MATLAB is both a computer programming language and a software environment for using that language effectively. It is maintained by the MathWorks, Inc., of Natick,

Massachusetts, and is available for MS Windows and other computer systems. The MATLAB interactive environment allows the user to manage variables, import and export data, perform calculations, generate plots, and develop and manage files for use with MATLAB. The language was originally developed in the 1970s for applications involving matrices, linear algebra, and numerical analysis (the name MATLAB stands for “Matrix Laboratory”). Thus the language’s numerical routines have been well-selected and improved through many years of use, and its capabilities have been greatly examined.

MATLAB has a number of add-on software modules, called toolboxes that perform more specialized computations. They can be purchased separately, but all run under the core MATLAB program. Toolboxes deal with applications such image and signal processing, financial analysis, control systems design, and fuzzy logic. And up-to-date list can be found at the MathWorks website. Simulink is built on top of MATLAB, so the user must have MATLAB to use Simulink. It is included in the Student Edition of MATLAB, and is also available separately from The MathWorks Inc. Simulink provides a graphical user interface that uses various types of elements called blocks, which are located in “libraries”, to create a simulation of a dynamic system, that is, a system that can be modelled with differential or difference equations whose independent variable is time. The Simulink graphical interface enables the user to position the blocks, resize them, label them, specify block parameters, and interconnect the blocks to describe complicated systems for simulation. Simulink models are developed by constructing a diagram showing the elements of the problem to be solved. Such diagrams are called simulation diagrams or block diagrams [29].

3.2.4.2 Description of the simulation software package (BOSS)

Shanmugan [30] described a very powerful simulation package, the Block Oriented System Simulator (BOSS) designed to benefit from the integrated hardware/software environment offered by workstations. A brief description is presented in this section for one of the most popular packages, namely, BOSS, which is the package to be used by the author.

Block Oriented Systems Simulator (BOSS) is an excellent example of an innovative framework for time-driven computer aided modelling, analysis, and design of communication systems [30-31]. It may be considered as an operating system for simulation as it makes all software requirements to build models and run simulations transparent to the user. BOSS provides an intelligent, flexible and user-friendly simulation environment that employs the latest advances in the hardware, software, CAD/CAM technology and expert systems whereby it can perform a time-domain (waveform level) simulation of any system.

The functional structure of the BOSS software is shown in Fig. 3.5. A simulation in BOSS is performed in four stages; module construction, system configuration, simulation, and presentation of results; by means of six stand-alone software packages. These are, the window manager, the block diagram editor, database manager, code generator, simulation manager, and the post processor.

A system in BOSS is constructed by using the block diagram editor from the library blocks or user defined modules in a hierarchical manner allowing highly complex systems to be modelled. In the event that a new model can not be constructed from existing models using the block diagram approach, a so called custom coded block can be created whose function is specified by a subroutine, and once this programmed and

tested it could be linked to the existing set of BOSS library blocks, thus, new applications can be handled within the BOSS environment.

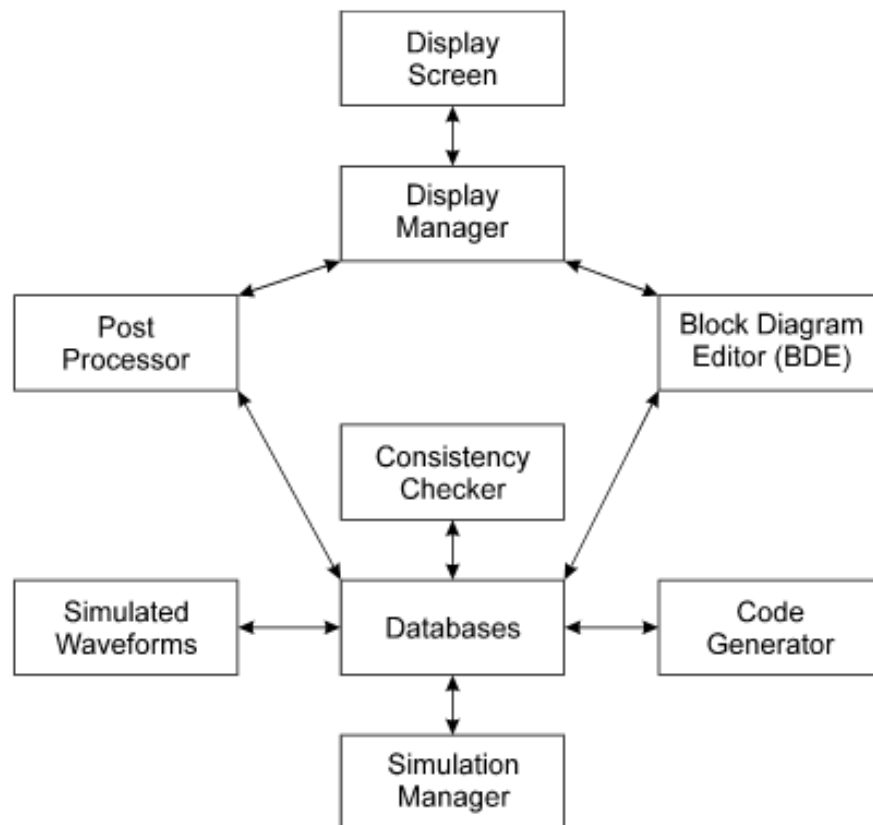


Fig. 3.5 Functional structure of the BOSS software.

Once a module is constructed it can be stored into a user created database where in a subsequent BOSS session, this module can be accessed by opening this database. BOSS also performs a variety of error and consistency checks as the models are being created. This coupled with the visual interface and on-line help to minimise the bookkeeping problem, minimises errors considerably and permits the user to concentrate on problem definition and analysis rather than on the mechanics of simulation.

The code generator produces the code. The simulation manager checks for validity of simulation and system parameters, then compiles the code, producing the executable file and runs it. The user has to choose the simulation duration and the step time. Probes can be attached to desired points in the system to observe the signals behaviour at that point. During a simulation execution, selected signal values can be saved in a data file. The post processor displays the simulation results on a high resolution screen using a variety of signal processing and plotting techniques. The simulation system block diagram and the run time parameters are also presented along with the simulation results. Simulation results can be presented in a various forms of plots including time domain plots (time plots, eye diagrams, scatter diagrams etc.), frequency domain plots (amplitude, phase, and power spectral plots), and other displays (histograms, correlation, probability density functions, cumulative distribution functions etc.).

Due to the fact that Monte Carlo simulation technique is the most accurate and general error estimation technique [19, 20], and also due to the aforementioned advantages and merits of BOSS over MATLAB coupled with the author is acquainted with the coding language of the BOSS software, should a primitive (custom coded block) need be constructed, hence, BOSS has been adopted herein as a simulation tool.

3.3 DECT Simulation Model

Since the DECT system is to be used as a baseline reference in the proposed dual rate mobile data system having a common air interface, and to establish a frame of reference, the simulation of the DECT system is considered first.

The simulation was implemented on a Sun Sparc workstation using the software package BOSS (Block Oriented Systems Simulator) systems simulator from Comdisco Systems, Inc. which runs under the UNIX operating system using X-windows. Boss

program acts as a translator which converts block diagrams into simulation programs.

The simulation of the DECT communications system was performed using the equivalent complex baseband lowpass representation as depicted in Fig.3.6.

In the transmitter, the PRBS (Pseudo Random Binary Source) generates a series of random binary NRZ (non-return-to-zero) square pulses of rate normalised with the DECT data rate equal to 1 bit/s, and have probability of 0 or 1 set to 0.5 with an initial seed set to a large odd number. This data was first applied to a Gaussian pre-modulation filter having bandwidth bit period product, BT of 0.5, function of which is to bandlimit and smooth out the baseband data stream, and consequently control the shape of the signal power spectrum (the design of this filter type will be outlined in next chapter). The smoothed data was then driven into an FM transmitter via a VCO (voltage controlled oscillator) having a modulation index of 0.5. At the receiver, a non-coherent demodulation process of GMSK received signal was performed.

Here, the received signal was passed through a pre-detection 6th order Butterworth lowpass filter before detection in order to remove noise and interference from adjacent channels. Its bandwidth was made a bit larger than the signalling bandwidth (normalised signalling bandwidth is 1.5), thereby preventing unnecessary degradation from intersymbol interference, in such case this filter has a normalised bandwidth of 1.51. The signal is then limited so that unwanted envelope fluctuations can be eliminated before demodulation by the frequency discriminator. Consequently, the output of the limiter is a constant envelope signal.

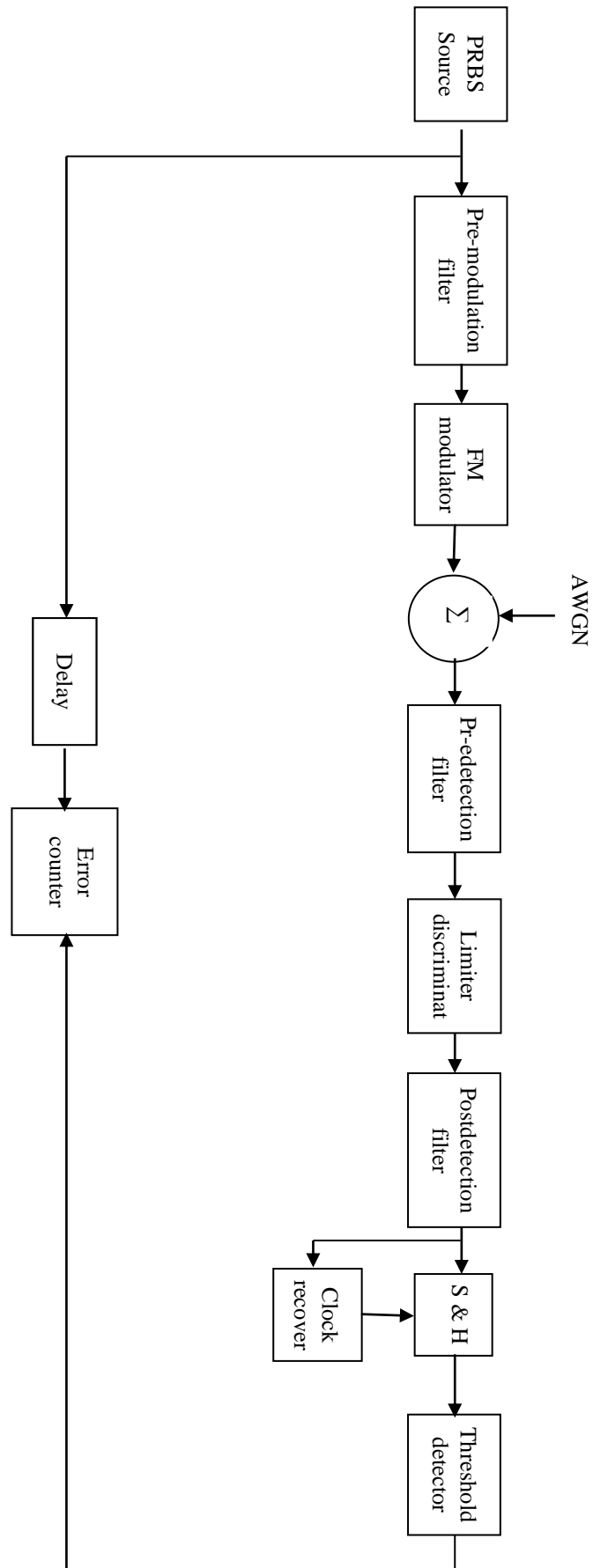


Fig. 3.6 Block diagram of simulated DECT system

When this signal is input to the demodulator, a baseband signal proportional to the instantaneous frequency of the received signal is produced, i.e. the limiter discriminator gives a response proportional to the time derivative of the received signal phase. That is, if the received signal is represented by

$$y(t) = A(\cos \omega_c t + \phi(t)) \quad (3.18)$$

the response of the limiter discriminator [32] is

$$\omega_i(t) = \omega_c + \frac{d\phi(t)}{dt} \quad (3.19)$$

where ω_i is the instantaneous frequency. In terms of in-phase ($i(t)$) and quadrature ($q(t)$) components, the output of the demodulator is given by

$$\omega_i'(t) = \frac{d}{dt} \left\{ \tan^{-1} \left[\frac{q(t)}{i(t)} \right] \right\} \quad (3.20)$$

Using the identity

$$\frac{d}{dt} (\tan^{-1} u) = \left(\frac{1}{1+u^2} \right) \frac{du}{dt} \quad (3.21)$$

and letting

$$u = \frac{q(t)}{i(t)}$$

Equation (3.17) becomes

$$\omega_i'(t) = \left(1 + \frac{q^2(t)}{i^2(t)}\right)^{-1} \left[\frac{i(t) \frac{dq(t)}{dt} - q(t) \frac{di(t)}{dt}}{i^2(t)} \right] \quad (3.22)$$

which can be rewritten as

$$\omega_i'(t) = \frac{i(t) \frac{dq(t)}{dt} - q(t) \frac{di(t)}{dt}}{i^2(t) + q^2(t)} \quad (3.23)$$

from equation 3.23, it is clear that when the received signal is a GMSK modulated signal, the output of the demodulator is given by

$$\omega_i'(t) = 2\pi f_a(a(t) * h(t)) \quad (3.24)$$

which are the original Gaussian filtered pulses that drive the modulator in the transmitter. Based on equation 3.23, the BOSS model for the frequency discriminator was designed. The output of the discriminator was passed through a post-detection 4th order Butterworth lowpass filter having a normalised bandwidth, larger than the restored signal, of 0.7 for minimum intersymbol interference, it removes noise and unwanted frequency components which may result from the demodulation process. The effect of pre and post-detection filtering on the performance of GMSK has been covered extensively by Lopes [33]. To achieve optimum performance at the demodulator, the timing clock should be recovered from the incoming data by means of a clock recovery circuit. This circuit is composed of two stages; the symbol timing recovery circuit, and

the clock generator circuit. In the symbol timing recovery, a timing sine wave having frequency equal to the symbol rate was extracted from the filtered data as follows:

The pre-detection filter was tuned to $f_1 = \frac{1}{2T}$, thus producing a spectral line at this frequency. This filter is followed by a nonlinear device (squarer), used to obtain the sampling frequency which is subsequently filtered by means of a phase locked loop (PLL) tuned to $f_o = \frac{1}{T}$ to achieve closer tracking of this frequency and to suppress the phase jitter contribution from the recovered signal and consequently reducing the number of occurring errors [34, 35]. Squaring the signal at the output of the pre-detection filter yields

$$\cos^2(2\pi f_1 t) = \frac{1}{2}(1 + \cos 2(2\pi f_1 t)) \quad (3.25)$$

Since $f_1 = \frac{f_o}{2}$ from equation 2.22

$$\cos^2(2\pi f_1 t) = \frac{1}{2} + \frac{1}{2} \cos(2\pi f_o t) \quad (3.26)$$

Thus extracting a frequency f_o aligned to the incoming data. A more detailed analysis is presented in [36, 37]. The second stage of the clock recovery is the clock generator that extracts the sampling instances from the zeros of the "timing wave". This generated sequence of impulses is used to clock the sample and hold circuit every T_s seconds at the centre of each symbol, as this is the optimum sampling point. Initially, the sign wave is delayed in order to be aligned with the lowpass filtered data. This delay for the alignment of the clock is related to the filter used at the demodulator. The

exact value of the delay is extracted from the filtered eye diagram. The output of the sample and hold is applied to a threshold detector whose output is decided by

$$\omega_i/(nT) > 0: \text{output} = +1$$

$$\omega_i/(nT) < 0: \text{output} = -1$$

The simulation of the described system model of Fig. 3.6 was executed on BOSS which generates samples of all input waveforms and then performs discrete-time signal processing operations according to the functional model of each block. In Fig.3.7, the generated user data that have a normalised bit rate of 1 is shown.

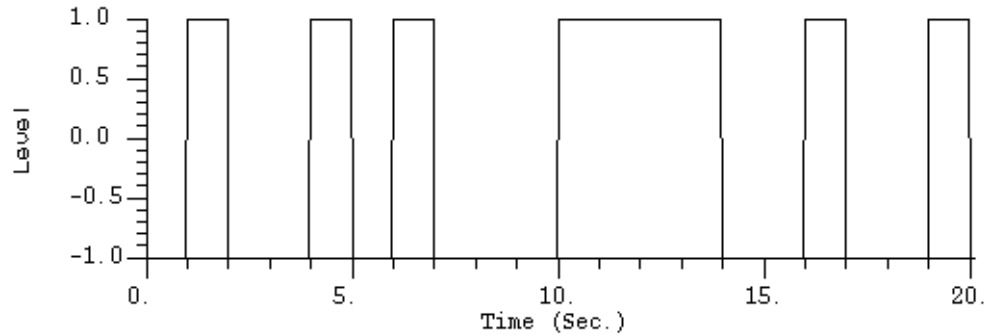


Fig. 3.6 Generated user data

Figure 3.8 below shows the eye diagram of the Gaussian pre-modulation filter having a normalised bandwidth of 0.5.

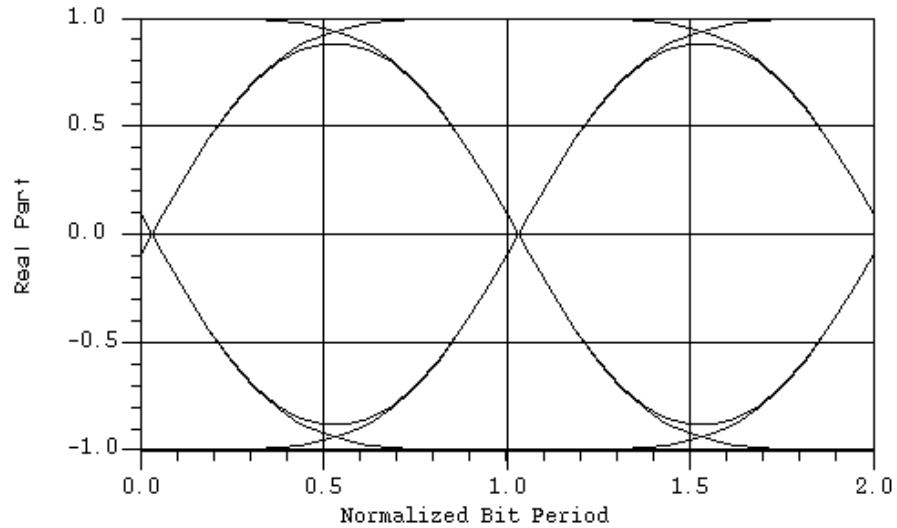


Fig.3.8 Eye diagram of the Gaussian filtered data

The small eye closure in figure 3.7 signifies that a small amount of ISI has been introduced by the Gaussian filter. Figure 3.9 shows the power spectrum of the transmitted GMSK baseband signal. From this figure it can be seen that the main lobe width is approximately 1.728MHz, also each sidelobe is around 30 dB down with respect to the main lobe, so they will not create a critical amount of interference.

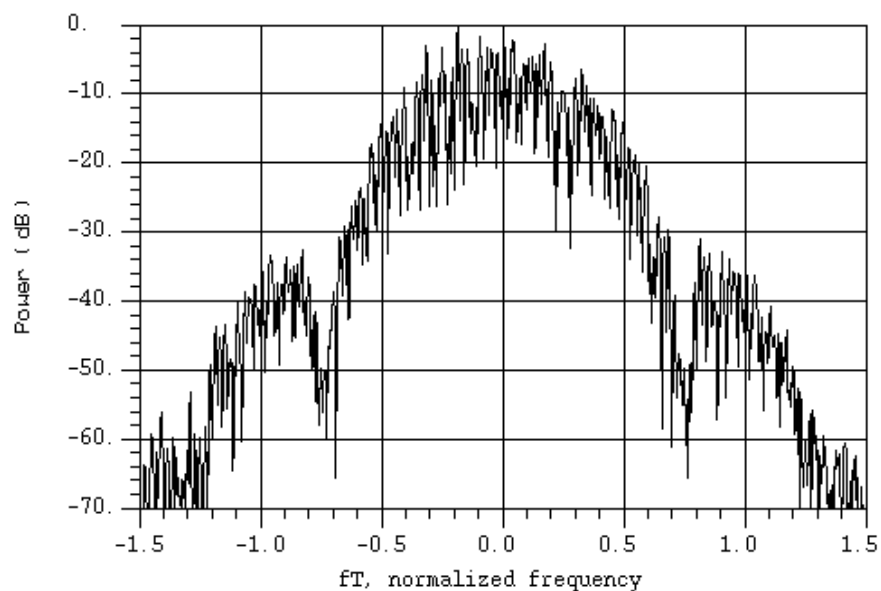


Fig.3.9 Power spectrum of DECT GMSK signal.

Using MATLAB software some computations were carried out to assess the amount of power contained by the main lobe and the sidelobes. The main lobe retains 99.89% of the total power which is the percentage of the transmitted power in each DECT channel. Each sidelobe retains $41.25 \cdot 10^{-3}$ % of the total power. Assuming that the transmitted power per base station is 250mW (24dBm) is transmitted within the actual channel, and the remaining 274 μ W are spread outside the channel. This interference power is measured in 1 MHz bandwidth centred around the adjacent channel carrier, giving a value of 118.38 μ W (-9.27dB) or 33dB below the transmitted power inside the channel. If the GMSK signal were to be filtered to remove these sidelobes, an AM modulation would be generated which would in turn make the GMSK signal lose one of its advantages, i.e., the constant envelope property. When this filtered signal is amplified in the final stages before transmission, the non-linearities of the amplifiers will generate back those lobes [38, 39]. In order to maximize the transmitted output power an amplitude limiter device has instead been used in the transmitter as shown in Fig. 3.10 below.

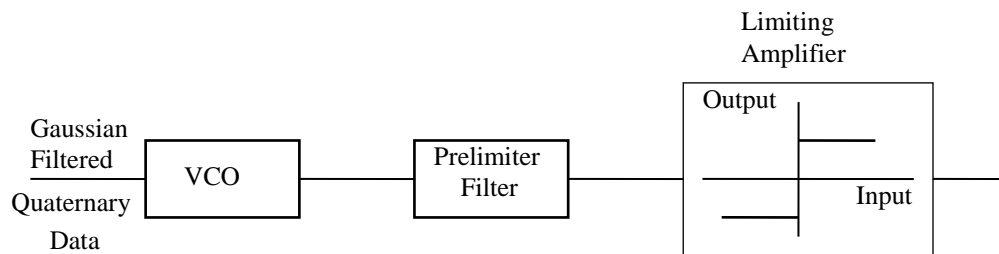


Fig.3.10 Transmitter Structure.

3.4 Simulation of the DECT system in static channel

Transmissions in a static channel are only affected by Additive White Gaussian Noise (AWGN). The DECT system performance in the AWGN channel and in the multipath fading environment has been evaluated by means of simulation in terms of the BER. Monte Carlo estimation technique was used. In the following sections, the obtained computer simulation results are presented.

In any communication system, when the signal voltage impressed on the communication channel at the transmitter arrives at the demodulator, it will be accompanied by a voltage waveform which varies with time in an entirely unpredictable manner. This unpredictable voltage waveform is a random process called noise. A signal accompanied by such a waveform is described as being contaminated or corrupted by noise. The communication of the signal may take several forms. The noise may be added to the signal, in which case it is called additive noise, or the noise may multiply the signal, in which case the effect is called fading. The term white is used in analogy with white light, which is a superposition of all visible spectral components over the band of optical frequencies [40]. The noise frequency components in a band limited system are expected to possess equal power in the passband, thus white by definition. AWGN is a measure of the noise generated in a receiver when the transmission path is ideal. The noise is assumed to have a constant power spectrum density over the channel bandwidth, and a Gaussian amplitude probability density function (pdf). Generally, this type of channel is unrealistic in digital mobile radio, except in the case of microcells environment where there exists a line of sight transmission path with essentially no multipath. The main use of the Gaussian channel is to give an upper bound on system's performance. The Gaussian channel represents a

means of modelling the minimum possible SNR that can be achieved in a communication system, and improvements to that system can be assessed in terms of how close the BER approaches that of the Gaussian channel.

Gaussian noise effects were simulated by a block which measures the input signal power. The user specifies the desired SNR together with the receiver filter's equivalent noise bandwidth. The output of this block is a complex white Gaussian noise with zero mean and variance adjusted to provide the desired signal to noise ratio. The AWGN signal was directly added to the output signal from the transmitter, and its value corresponds to a given noise bandwidth such that the SNR is expressed in terms of bit energy to noise spectral density (E_b/N_o).

The BER was being measured in a block called error counter applying Monte Carlo technique. Whilst BOSS library includes a simple error counter block, it was adapted to make it compatible with the system under investigation. First, every received bit is compared with a delayed version of the transmitted bit to take account of the system and filters delay. One hundred erroneous bits are accumulated by the error counter before the simulation was halted, so that the variance on the error probability estimate could be reduced to some reasonable value, thus the obtained BER would be a reliable measure. Finally the ratio of the number of bits in error to the number of the bits received is computed in the error counter block. The number of samples, number of errors, and the bit error rate are written to a file which can be accessed through the post processor. In Fig. 3.11 the simulated BER performance versus E_b/N_o for the AWGN channel is plotted. As can be seen from this plot that at E_b/N_o of 12 dB, a bit error rate of 10^{-3} can be attained, and these results are in broad agreement with those presented in [41].

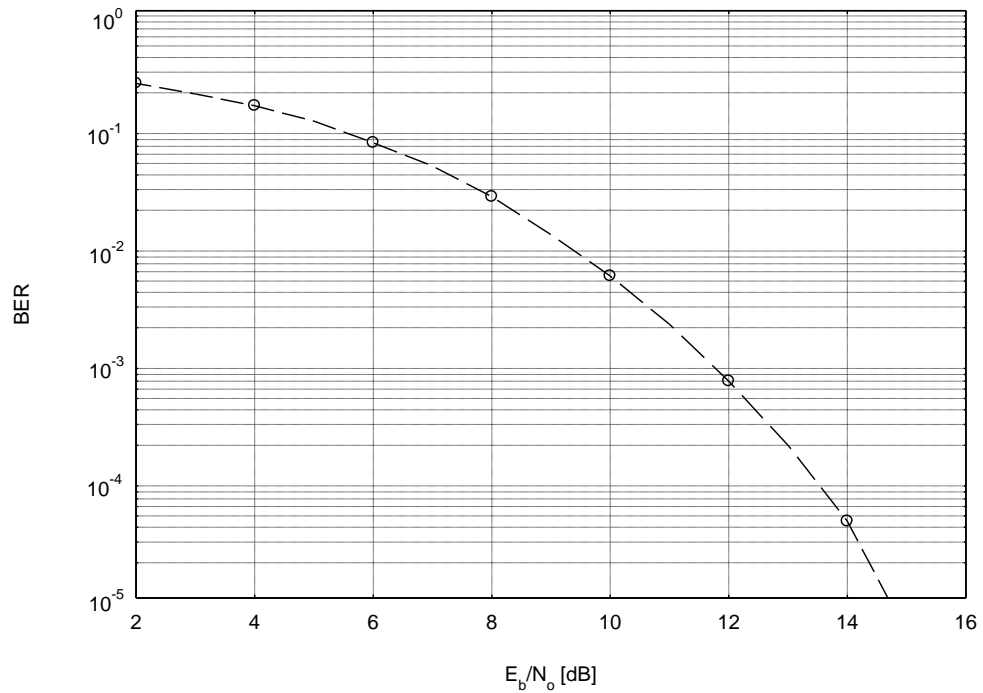


Fig. 3.11 Simulated BER performance of DECT static channel

Using a closed form expression for the probability of error of digital FM perturbed by AWGN with discriminator detection found in [42, 43], a theoretical bit error rate was computed by means of MATLAB software and plotted against E_b/N_0 as shown in figure 3.12 below. These calculated results agree with that obtained by computer simulation presented in Fig.3.11 (from Fig. 3.12, to obtain BER performance of 10^{-4} , E_b/N_0 has to be about 12dB. For the same BER criteria, from Fig. 3.11, E_b/N_0 should be about 13dB. On average, there is about 1dB difference. This level of disparity is acceptable considering the inevitable factors affecting simulation results outlined paragraph 3.2.3 of this chapter). It follows from the close coincidence of the theoretical and measured performance results that the modelled system adequately simulates the real scenario.

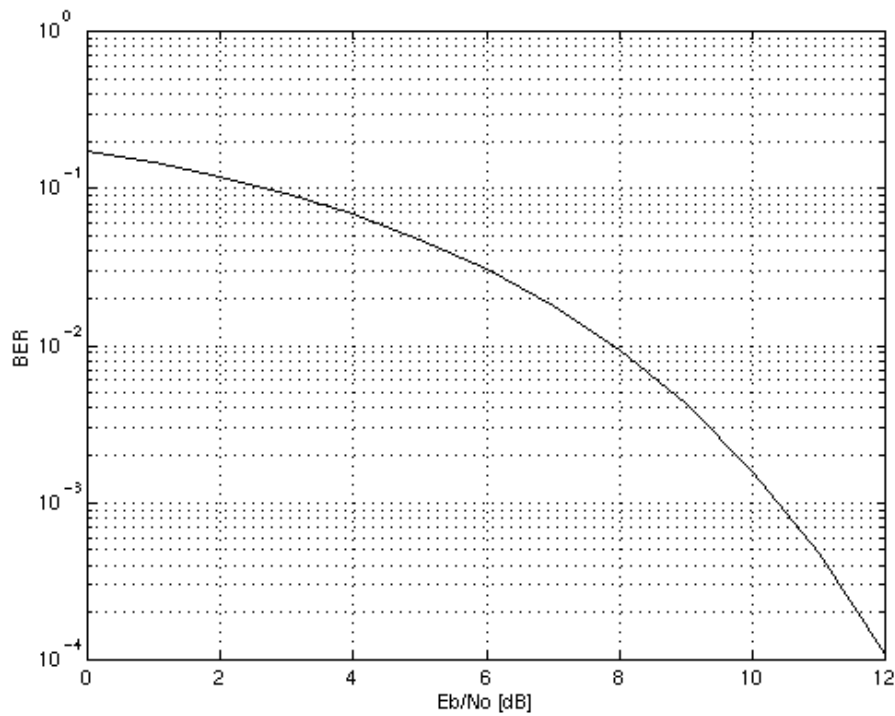


Fig. 3.12 Theoretical BER of DECT static channel

Summary

In this chapter, an overview of the simulation principles and the simulation package to be used have been presented.

A DECT system model program has been created to serve as a baseline reference in the proposed dual rate data system to be designed in the later chapters to be having common air interface. The results generated from the simulation tests of the DECT system have revealed that the small amount of ISI appears to have an insignificant impact on the signal quality. Also, examining the generated GMSK power spectrum graph reveals that the simulated signal bandwidth is typical to the actual one i.e. 1.728MHz, and that each sidelobe is around 30dB down with respect to the main lobe which results in no critical amount of interference to the adjacent channel occurs.

The theoretical and simulation results of the BER performance results in a multipath-free channel conditions showed a close coincidence, which proves that the modelled system adequately simulates the real scenario.

Building on this binary system, a 4-Level (quaternary) modulation system would be designed, simulated and evaluated in the next chapter aiming to double the current data throughput.

REFERENCES

- [1] Rappaport, T. "The Wireless Revolution"; IEEE Communications Magazine, pp. 52-71 Nov. 1991.
- [2] Ginn, S.; "Personal Communications Services: Expanding The Freedom to Communicate"; IEEE Communication Magazine, vol. 29, No. 2, pp. 30-39.
- [3] Goodman, D. "Trends in Cellular and Cordless Communications"; IEEE Communication Magazine, pp. 31-40, June 1991.
- [4] Tuttlebee, W. "Cordless Personal Communications"; IEEE Communication Magazine, pp. 42-53, December 1992.
- [5] Ochsner, H.; "DECT-Digital European Cordless Telecommunications"; IEEE Proc. Veh. Tech. Conf. pp. 718-721, San Francisco, May 1989.
- [6] Potter, A. "Implementation of PCNs Using DCS 1800"; IEEE Communication Magazine, pp. 32-36, December 1992.
- [7] Cox, D. "Wireless Network Access For Personal Communications"; IEEE Communication Magazine, pp. 96-115, December 1992.
- [8] Alexander, S.E. "radio propagation within buildings at 900MHz", Electronic letters, Vol. 18,, No. 21, pp. 913-914, 14th October 1982.
- [9] Parsons, J. D. and Ibrahim, M. F. "Signal strength prediction in built up areas, Part2, signal variety". Proc. IEE Part F 130 (5), pp. 385-391, 1983.
- [10] European Telecommunications Standard Institute (ETSI), "Digital European Cordless Telecommunications Common Interface, Part1; Overview"; Aug. 1991.
- [11] ETSI, "Digital European Cordless Telecommunications Common Interface Part 2: Physical Layer", July 1992.

-
- [12] OWEN, F.C., PUDNEY, C.D.; "DECT - Integrated Services For Cordless Telecommunications". 5th IEE International Conference on Mobile Radio and Personal Communications, 11-14 September 1989.
- [13] HALLS, G. A. and DAVIS, G. C.; "The Application of the Digital European Cordless Telecommunications (DECT) to Local Area Networks (LAN); Roke Manor Research Limited, Romsey, Hampshire, UK."
- [14] DOUMI, T. L., KANAROPOULOS, and GARDINER J. G.; "Teletraffic Performance of indoor Cordless Communications with Co-existing Voice and Data Services."; The IEEE 44th Vehicular Technology Conference, pp. 659-663; Stockholm, Sweden, June 1994.
- [15] JERUCHIM M. C., BALABAN P. and SHANMUGAN S.; "Simulation of Communication Systems". Plenum, New York, 1992.
- [16] AMCA, H., and SERIFF, R. E.; "Computer Simulation of Digital Communication Systems: A Beginner's Guide". University of Bradford, Department of Electrical Engineering, Report No. 467, January 1992.
- [17] PENT, M.; PRESTI, L. L.; ARIA, G.D. and LUCA, G.D., "Semi-Analytic BER evaluation by simulation for noisy bandpass channels". IEEE Journal on Selected Areas in Communication, Vol. 6, No. 1, pp. 34-41. January 1988.
- [18] MARSAN, N. A. ; BENEDETTO, S. ; BIGLIERI, E. ; CASTELLANI, V. ; ELIA, M. ; PRESTI, L. L. and PENT, M. "Digital simulation of communication systems with TOPSIM III". IEEE Journal on Selected Areas in communication, Vol. 2, No. 1, pp. 29-41. January 1984.

-
- [19] COATES, R. F. W., JANACEK, G. J. and LEVER, K. V. "Monte Carlo Simulation And Random Number Generation". IEEE Journal on Selected Areas in communication, Vol. 6, No. 1, January 1988.
- [20] KUROSE, J. F. MOUFTAH, H. T. "Computer-aided modelling, analysis, and design of communication networks". IEEE SAC, Vol. 6, No. 1, pp. 130-145. January 1988.
- [21] SHANMUGAN, K. S. and BALABAN, P. "A Modified Monte Carlo Simulation Technique for Evaluation of Error Rate In Digital Communication Systems". IEEE Transactions on Communication, Vol. COM-28, No. 11, November 1980.
- [22] DAVIS, B. R. "The effect of correlation on probability of error estimation in Monte Carlo simulations". Journal of Electrical and Electronic Engineering, Australia IE Aust IREE Aust, Vol. 8, No. 24, December 1988.
- [23] McNAIR, E. A. and SAUER, C. H. "Elements of practical performance modelling". Englewood Cliffs, NJ, Prentice Hall 1985.
- [24] PROAKIS, J. G. "Digital Communications", 4th. edition. McGraw Hill, New York 2001.
- [25] JOSEPH BOCCUZZI, "Signal Processing for Wireless Communications". The McGraw-Hill Companies, 2008.
- [26] MODESTINO, J. W. and MATIS, K. R. (1984). Interactive Simulation of digital communication systems. IEEE Journal on Selected Areas in Communication, Vol. 2, pp. 51-76, 1969.
- [27] SARGENT, R. G. "A tutorial on validation and verification of simulation models". Proceedings of the 1988 winter simulation conf. San Diego, CA, USA, 1988.

-
- [28] SHANMUGAN, K. S. "An update on software packages for simulation of communication systems (links)". IEEE Journal on Selected Areas in communication, Vol. 6, No. 1, January 1988.
- [29] William J. Palm, "Introduction to Matlab 7 For Engineers", McGraw-Hill International Edition, 2005.
- [30] SHANMUGAN, K. S. ; MINDER, G. J. and KOMP, E. "Block Oriented Systems Simulator (BOSS)". University of Kansas, Telecommunications lab. Technical Report, 1986.
- [31] COMDISCO, "Block Oriented Systems Simulator (BOSS) User's Guide and Systems Administrator's Guide", version 2.7. COMDISCO INC. USA, 1991.
- [32] Roger L. FREEMAN; "Fundamentals of Telecommunications". Second Edition, John Wiley & Sons, Inc, 2005.
- [33] Lopes B. L, "On the radio link performance of the Digital European Cordless Telecommunications (DECT) System.", IEEE Global Telecommunications Conference and Exhibition, Vol. 1-3 pp. 1013-1017, San Diego, California, 2nd – 5th Dec. 1990.
- [34] WILKINSON, T. A., "Channel Modelling and Link Simulation Studies for the DECT Test Bed Program. ", IEE 6th. International Conference on Mobile Radio and Personal Communications, pp. 293-299, December 1991.
- [35] GARDNER,F.M.; "Phase lock Techniques", John Willey & Sons, New York, 1st ed., 1966.
- [36] STIFFLER, J.J. "Theory of Synchronous Communications". New Jersey, Prentice-Hall Inc., 1971.
- [37] FEHER, K. "Digital Communication Satellite/Earth Station Engineering". New Jersey, Prentice-Hall Inc., 1983.

- [38] FRANKS, L.E. Bubrouski, J. P.; "Statistical Properties of Timing Jitter in a PAM Timing Recovery Scheme". IEEE Transactions on Communications, Vol. 22, No. 7, pp. 913-920, July 1974.
- [39] DOUGLAS H. M., FEHER K.; "The Effects of Filtering and Limiting on the Performance of QPSK, Offset QPSK, and MSK Systems", IEEE Transactions on Communications, Vol. COM 28, NO. 12, December 1980.
- [40] BERNARD SKLAR, "Digital Communications, Fundamentals and Applications", Second edition, Prentice Hall PTR, 2001.
- [41] EUCO-COST, European Cooperation In The Field of Scientific and Technical Research, COST 231 TD, Copenhagen, 14-18 May 1990.
- [42] STREMLER, F. G.; "Introduction to Comm. Systems"; Addison-Welsley, 1982.
- [43] BENNET, W. R., and SALZ, J.; "Binary Data Transmission by FM over a Real Channel". Bell Technical Journal, pp. 2387-2426, April 1963.

CHAPTER 4

Continuous Phase-Quaternary Frequency Shift Keying System

4.1 Grounds of suitability of CP-QFSK

The two primary communication resources in any communication system are the transmitted power and channel bandwidth. A general system-design objective priority would be to use these two resources as efficiently as possible. Many communication channels can be classified primarily as power-limited or band-limited [1]. Different strategies are taken to optimize the use of the resources in each case:

- 1- Power-limited channels: Such channels are often characterised by the power efficiency which is a measure of how much received power is required to achieve a specified BER performance. This efficiency is also defined in terms of the required average received bit energy-to-noise density ratio (E_b/N_o) for a given f_d . In these channels, coding schemes would generally be used to save power at the expense of bandwidth. The typical example is a satellite mobile channel.
- 2- Band-limited channels: Spectrally efficient modulation techniques would be used to maximise the spectrum efficiency in these channels frequently expressed in terms of the number of transmitted bits per second per Hertz (b/s/Hz). A common example is the urban cellular radio channel.

Apart from spectrally efficient modulation techniques, other approaches or strategies are used to reduce the required bandwidth such as:

- Low-bit-rate speech and channel coding.
- Multiple access techniques.
- Deployment of microcells.
- Increase in network intelligence.

The choice of modulation technique has a direct impact on the capacity of a digital mobile communication system. It determines the bandwidth efficiency of a single physical channel in terms of the number of bits per second per Hertz (b/s/Hz) [2, 3].

Multilevel modulation schemes can be divided into three main categories according to the varying parameter:

- M-ary Phase Shift Keying (PSK) in which the phase variations contain the transmitted information.
- M-ary Frequency Shift Keying (FSK) where the information modulated in the frequency variations of the carrier.
- M-ary Quadrature Amplitude modulation (QAM) where the transmitted information is contained in both the amplitude and phase variations.

In selecting a suitable modulation scheme for a mobile radio system, consideration must be given to achieving the following:

- High bandwidth efficiency.
- High power efficiency.
- Low carrier-to-cochannel interference power ratio (C/I).
- Low out-of-band radiation.
- Low sensitivity to multipath fading.
- Constant or near constant envelope.
- Ease and cost of system implementation.

Optimising all these features at the same time is not possible as each has its practical limitation and also is related to others. For instance, to achieve high bandwidth efficiency one may choose to use high-level modulation. However, the power efficiency of the system would be reduced consequently. Moreover, the bandlimited high-level modulated signal will have a large envelope variation which results in a large out-of-band radiation accordingly if this signal is to be passed through a power efficient nonlinear amplifier that in turn introduces interference to adjacent channels, and although this can be circumvented by using linear power amplifiers, but these have poor

power efficiency. Hence, it is necessary to look for a good compromise among these criteria, depending on the precise nature of the anticipated utilisation of the system in question [4].

Regarding the digital modulation techniques, these can be broadly classified in two groups, each one being thought to be more appropriate for the two kinds of channels mentioned at the beginning. The modulation techniques more used in the present systems belong to the group of continuous phase modulations or, equivalently, constant envelope modulations, which are inherently power efficient. However, further improvements in related systems, like amplification devices, permit the increasing use of linear modulations, leading to a more bandwidth efficient systems.

At this point it is worth pointing out the following issues:

1. Amplification problem:

Obviously, a highly efficient method of amplification should be searched for. In a mobile environment, the power supply problem is quite important and a maximum duration of battery use without recharging is desired. Also, the power amplifier in the handset is constrained to operate in its saturated nonlinear region in order to maximise the dc efficiency of the battery powered handset. Owing to this imposed nonlinearity, linear modulation schemes such as QAM and QPSK would be unsuitable for mobile radio telephony [5]. The high power amplifiers (HPA) used in many systems, for example, in mobile radio handsets, are usually highly non-linear, because of the requirement for power efficiency. These amplifiers give rise to amplitude modulation-amplitude modulation (AM-AM) and amplitude modulation-phase modulation (AM-PM) conversion, which may result in an irreducible BER floor. The optimum solution is to use a constant envelope modulation scheme, which does not give rise to these effects. For this reason, it is favourable if the signalling scheme can be of constant envelope and continuous phase type such as multilevel CP-FSK which falls under digital FM. This is not the case for a modulation system with any kind of amplitude modulation or even for a system which in principle has a constant envelope but a non-continuous phase. This is due to the fact that this discontinuity introduces a high level

of side lobes which need be suppressed. By doing this with the appropriate filtering, envelope variations are introduced. If these variations are suppressed by hard limiting, the side lobes are introduced again resulting in severe adjacent channel interference, and in digital systems that transmit voice (GSM, DCS 1800, DECT), the bandwidth of the signal relative to the carrier is usually narrow, and filter implementation would be extremely difficult. It has been found that the amplification of linear signals with high power non-linear amplifiers introduces a penalty of 2 to 3 dB, in terms of power efficiency [6].

2. Detection problem:

An optimum receiver is usually a coherent one which requires the recovery of the frequency and phase of the carrier. Non-coherent receivers such as the differential (when possible) or the limiter-discriminator type are suboptimum in the sense that they require an increase in the E_b/N_0 to achieve a given BER with respect to the optimum (typical values range from 1 to 3 dB), leading to not very power efficient systems. This is true in an AWGN channel, but things are quite different in a phase-noisy channel, with multipath (fast Rayleigh fading), Doppler effect, and random FM. As this is the case in the mobile radio channel, the possibility of non-coherent demodulation schemes such as discriminator detection due to its immunity against fast fading, centre frequency drift, and its applicability to arbitrary values of modulation index, should be valued positively [7]. It has been established in [8] that a small price is paid in using noncoherent FSK instead of coherent FSK for the decidedly large advantage of not having to establish M-coherent references at the receiver.

3. System Complexity:

Modulation schemes as mentioned earlier can be classified as either linear or nonlinear. Linear schemes are generally non-constant envelope after bandlimiting and the information is carried in both the amplitude and phase of the carrier, whereas nonlinear modulation has a constant envelope property and the information is solely contained in the excess phase function of the carrier. If linear techniques are demodulated coherently, this requires carrier recovery using phase-locked techniques which greatly

increase the level of complexity of the demodulator [1]. Nonlinear schemes such as GMSK can be realised as direct modulation of a VCO, where the data sequence is applied directly to the tuning port. Besides, nonlinear schemes can be demodulated noncoherently with limiter discriminator detection in which case the carrier reference required in a coherent system need not be generated at the demodulator. With mobile telephony, where the requirement of a light handheld radio, imposed by the personal communication scenario in which everybody has fast access to all services through a personal handheld mobile unit, would mean a great decrease in size and weight of the handset and associated circuitry and this in turn reduces dramatically the cost. Therefore, modulation schemes that can be detected non-coherently offer a great deal of hardware simplicity and hence are much more desirable.

4. Binary versus Multilevel schemes:

The use of multilevel modulation schemes instead of binary ones produces an increase of the bit transmission rate for a given bandwidth. So, for a given bit rate, they imply a reduction of the required channel bandwidth and an increase in the spectrum efficiency, thus achieving a significant increase in the number of the accommodated users. However, a consequence of transmitting more than one bit per symbol is that the signal power must be commensurately increased for the same channel noise if the symbol error is not to increase. This implies an increase in the cluster size in cellular radio, leading to a reduction of the number of channels per cell. The result is that the teletraffic throughput is not modified, but the complexity is significantly increased. This situation is very frequently encountered in conventional cellular systems, but if we consider microcells, e.g. in an indoor environment the situation is completely different due to the close proximity of the base station and the mobile, a high values of SNR can be achieved within the coverage area with considerably lower power, thus increasing the power efficiency of the unit. Furthermore, because of the extremely fast fall off in signal level, the signal to interference ratio (SIR) is significantly higher. Based on these principles, a research study performed in such minimum cluster sizes showed that multilevel modulation schemes can be introduced without cluster size penalties [9, 10].

To sum up, the immunity to transmitter amplifier nonlinearity overweighs the use of constant envelope modulations, and the fading conditions and random phase and applicability to arbitrary values of modulation index lead to employing noncoherent detection methods (the severe fading conditions make carrier recovery quite difficult) which positively impacts on complexity and cost. Based on the above considerations and given that the objective of this research is to accommodate the B-band ISDN services by the DECT system maintaining the spectral properties and keeping the introduced changes to the standard system to a minimum, it thus follows from all this that the multilevel FSK modulation scheme is a viable and promising alternative option and hence proposed for the aforementioned accounts. The subsequent subsections explore this modulation scheme in more detail.

4.2 Theoretical background of CP-QFSK

Over the past two decades or so, there has been a large amount of research done on continuous phase- constant envelope digital modulation systems (CPM) on account of their promising possibilities if employed in applications where efficient spectrum utilisation is required and/or some immunity to nonlinear distortion produced by the power amplifiers in transmitters are obtained [11-16]. In this sub-section a sub-class of the CPM signalling scheme called quaternary frequency shift keying (QFSK) in which the instantaneous frequency is constant over each symbol interval and the phase is constrained to be continuous will be discussed. This constraint of phase continuity results in affecting the signal in two important ways: Firstly, the transient effects are lessened at the symbol transitions, thereby offering spectral bandwidth advantages. Secondly, memory imposed upon the waveform by continuous phase transitions, improves performance by providing for the use of several symbols to make a decision [17].

An FSK signal can be generated by shifting the carrier signal by an amount equal to:

$$A_n(f) = \frac{\sin \pi [fT - (2n - 1 - M)h/2]}{n[fT - (2n - 1 - M)h/2]}$$

Where $I_n = \pm 1, \pm 3, \dots, \pm(M-1)$ represents the sequence of symbols that results from mapping k -bit blocks $= \log_2 M$ of binary digits from the information sequence $\{a_n\}$ into $M=2^k$ possible levels, to reflect the digital information that is being transmitted [1].

The switching from one frequency to another may be accomplished by having M separate oscillators tuned to the desired frequencies and selecting one of the M frequencies according to the particular k -bit symbol that is to be transmitted in a signal interval of duration $T = k/R_b$ seconds, with R_b being the bit rate. However, such abrupt switching from one oscillator output to another in successive signalling intervals results in relatively large spectral side lobes outside of the main spectral band of the signal, and consequently this method requires a large frequency band for transmission of the signal. To avoid this happening, the information-bearing signal frequency modulates a single carrier whose frequency is changed continuously. The resulting frequency-modulated signal is phase continuous i.e. the phase is a continuous function of time, and hence it is called Continuous-Phase Frequency Shift Keying (CP-FSK).

In order to represent a CPFSK signal, we begin with a PAM signal. The baseband data signal may be represented as

$$d(t) = \sum_n I_n g(t - nT) \quad (4.1)$$

Where $g(t)$ is a rectangular pulse of amplitude $1/2T$ and duration T seconds. The signal $d(t)$ is used to frequency-modulate the carrier. Consequently, the equivalent complex lowpass waveform $v(t)$ is expressed as

$$v(t) = A \exp \left\{ j \left[4\pi T f_d \int_{-\infty}^t d(\tau) d\tau + \Phi_0 \right] \right\} \quad (4.2)$$

In the foregoing representation A is a real amplitude and f_d is the peak frequency deviation which relates frequency displacement to baseband signal voltage, and Φ_0 is an initial phase of the carrier. The carrier modulated signal corresponding to (4.2) may be expressed as

$$s(t) = A \cos[2\pi f_c t + \Phi(t, I) + \Phi_0] \quad (4.3)$$

Where Φ_0 is an arbitrary starting phase, and $\Phi(t, I)$ represents the time-varying phase of the carrier, which is defined as

$$\Phi(t, I) = 4\pi T f_d \int_{-\infty}^t d(\tau) d\tau$$

Which by means of equation (4.1) becomes

$$\Phi(t, I) = 4\pi T f_d \int_{-\infty}^t \left[\sum I_n g(\tau - nT) \right] d\tau \quad (4.4)$$

Although the signal $d(t)$ contains discontinuities, the integral of $d(t)$ is continuous which implies continuous-phase signal $s(t)$. The phase of the carrier in the interval $nT \leq t \leq (n+1)T$ is determined by integrating (4.4), thus

$$\begin{aligned} \Phi(t, I) &= 2\pi f_d T \sum_{k=-\infty}^{n-1} I_k + 2\pi f_d (t - nT) I_n \\ &= \theta_n + 2\pi h I_n q(t - nT) \end{aligned} \quad (4.5)$$

Where h , θ_n , and $q(t)$ are defined respectively as

$$h = 2f_d T \quad (4.6)$$

$$\theta_n = \pi h \sum_{k=-\infty}^{n-1} I_k \quad (4.7)$$

$$q(t) = \begin{cases} 0 & t < 0 \\ \frac{t}{2T} & 0 \leq t \leq T \\ \frac{1}{2} & t > T \end{cases} \quad (4.8)$$

θ_n represents the accumulation (memory) of all symbols up to time $(n-1)T$. The deviation ratio parameter h is called the modulation index. Equation 4.8 represents a full response CPFSK modulation scheme which corresponds to linear phase trajectories over each symbol interval [18]. The set of phase trajectories $\Phi(t, I)$ generated by the information sequence $\{I_n\}$ for the CP-QFSK with $\Phi_0 = 0$ is sketched in Fig.(4.1) for two symbol intervals. As can be seen, the phase trajectories have a tree-like quality that corresponds to linear phase trajectories over each symbol interval in this case as a consequence of the fact that the pulse $g(t)$ is rectangular. Smoother phase trajectories and phase trees can be obtained using pulses that do not contain discontinuities such as the class of raised cosine pulses as will be shown later. Furthermore, if h is a rational number, the tree will eventually fold upon itself modulus 2π , producing a trellis-like depiction.

When expressed in the form of (4.5), CP-FSK becomes a special case of a general class of continuous-phase modulated (CPM) signalling scheme in which the carrier phase is given by

$$\Phi(t, I) = 2\pi \sum_{k=-\infty}^n I_k h q(t - kT); \quad nT \leq t \leq (n+1)T \quad (4.9)$$

Where $q(t)$ is some normalized waveform shape (phase response function) that may be represented in general as the integral of some frequency pulse $g(t)$, i.e.

$$q(t) = \int_0^t g(\tau) d\tau \quad (4.10)$$

If $g(t)=0$ for $t>T$, the CPM signal is called full response CPM. Otherwise, if $g(t) \neq 0$ for $t>T$, the modulated signal is called partial response CPM, and in this case the pulse shape $g(t)$ is smoother and the corresponding spectral occupancy of the signal is reduced. An infinite variety of CPM signals can be generated by choosing different pulse shapes $g(t)$ and varying the modulation index h and the alphabet size M [22].

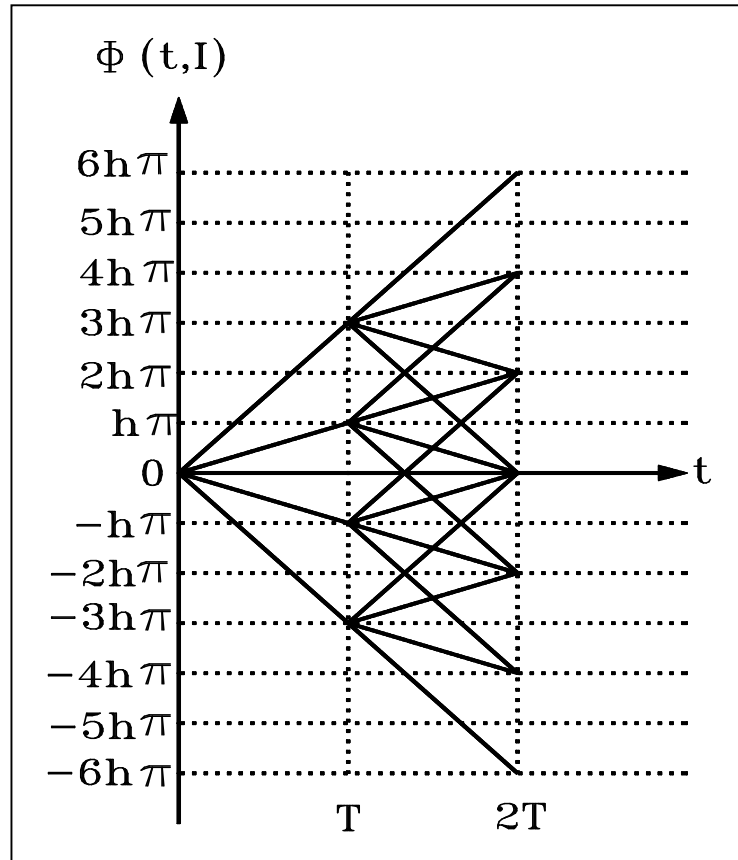


Fig. 4.1 Phase trajectories of CP-QFSK

4.2.1 CPFSK Signal space diagram

Continuous-phase signals cannot be represented by discrete points in signal space as in the case of PAM, PSK, and QAM due to the fact that the phase of the carrier is time-variant. Instead, a continuous-phase signal is described by the various paths or trajectories from one phase to another. A constant amplitude CPM signal trajectories form a circle. As an example, the signal space diagram for CP-FSK signals with $h=1/2$ and $h=1/4$ is illustrated in Fig.(4.2). The beginning and ending points of these phase trajectories are marked in the figure by a dot. It is noted that the length of the phase trajectory increases with an increase in h and this in turn increases the signal bandwidth accordingly as will be demonstrated in the following sub-section.

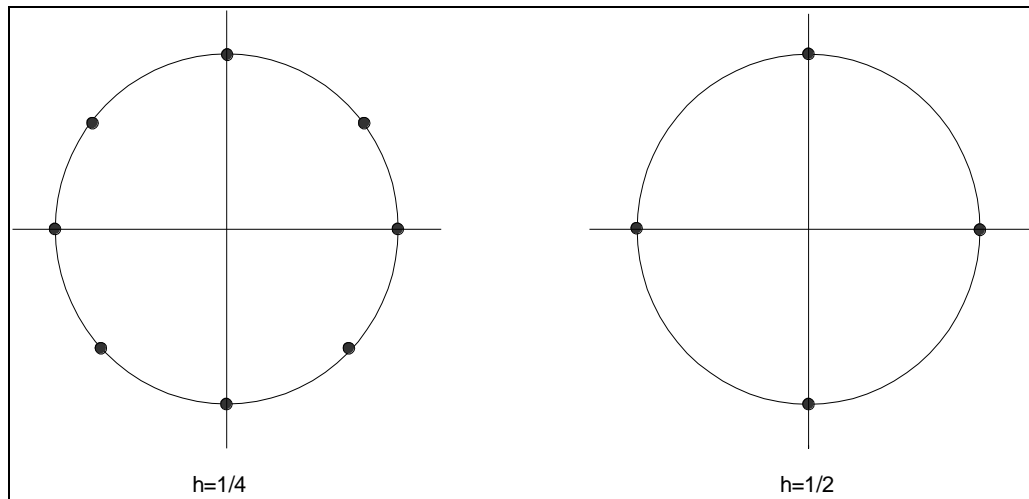


Fig.4.2 Signal-space diagram for CP-FSK

4.2.2 Power density spectrum of CP-QFSK

An important descriptive feature of any information-carrying system is the power spectral density function (psdf) that results from the combination of the characteristics of the information signal and the technique of modulation. Estimates of bandwidth occupancy, interference to or from flanking carrier channels, and relative comparisons of different modulation techniques all exemplify situations where a knowledge of the psdf is imperative [20]. In most digital communications systems, the available channel

bandwidth is limited. It is of great importance to consider the constraints imposed by the channel bandwidth limitation in the selection of the modulation technique to be used to transmit the information. Hence, the spectral content of the CP-QFSK modulation scheme described in section 4.1 needs to be derived from the general equation representing CPM. Since the information sequence is random, a digitally modulated signal is a stochastic process. We are interested in determining the power density spectrum of such a process, from which the channel bandwidth required to transmit the information-bearing signal can be determined. We begin by computing the autocorrelation function and its Fourier transform. The constant amplitude CPM signal previously defined by equation (3.3) is

$$s(t, I) = A \cos[2\pi f_c t + \Phi(t, I)] \quad (4.11)$$

In the above equation the term Φ_0 has been omitted (set to zero) without any loss of generality, and the information carrying phase function $\Phi(t, I)$ is given by

$$\Phi(t, I) = 2\pi h \sum_{k=-\infty}^{\infty} I_k q(t - kT) \quad (4.12)$$

The symbols in the sequence I_k are statistically independent, identically distributed, and each symbol can take one of the four levels; $\{\pm 1, \pm 3, \dots, \pm (M-1)\}$. The autocorrelation function of the equivalent lowpass signal

$$V(t) = e^{j\Phi(t, I)}$$

Is

$$\Phi_{vv}(t + \tau, t) = E \left\{ \exp \left(j2\pi h \sum_{k=-\infty}^{\infty} I_k [q(t + \tau - kT) - q(t - kT)] \right) \right\} \quad (4.13)$$

Performing expectation over the data symbol $\{I_k\}$, and since these symbols are statistically independent, yielding; $\Phi_{vv}(t+\tau; t) =$

$$\prod_{k=-\infty}^{\infty} \sum_{n=-(M-1)}^{M-1} P_n \exp(j2\pi hn[q(t+\tau-kT) - q(t-kT)])$$

The average autocorrelation function is

$$\Phi_{vv}^-(\tau) = \frac{1}{T} \int_0^T \Phi_{vv}(t+\tau, t) dt \quad (4.14)$$

If we let $\tau = \xi + mT$ where $0 \leq \xi < T$ and $m=0,1,\dots$, then (3.14) reduces to

$$\begin{aligned} & \Phi_{vv}^-(\xi + mT) \\ &= \frac{1}{T} \int_0^T \prod_{k=1-L}^{m+1} \left\{ \sum_{n=-(M-1)}^{M-1} P_n \exp(j2\pi hn[q(t+\xi - (k-m)T) - q(t-kT)]) \right\} \end{aligned} \quad (4.15)$$

P_n stands for the probability that the level being considered is n with $n = \pm 1, \pm 3, \dots, \pm(M-1)$. When $\xi + mT \geq LT$, where LT denotes the pulse length, in this case

$$\Phi_{vv}^-(\xi + mT) = [\psi(jh)]^{m-N} \lambda(\xi); \quad m \geq L, 0 \leq \xi < T \quad (4.16)$$

Where $\psi(jh)$ is the characteristic function of the random sequence $\{I_n\}$, defined as

$$\psi(jh) = E[e^{j\pi h I_n}] = \sum_{n=-(M-1)}^{M-1} P_n e^{j\pi h n} \quad (4.17)$$

The Fourier transform of $\Phi_{VV}^-(\tau)$ yields the average power density spectrum of CPM signal as $S(f) =$

$$2\text{Re} \left\{ \int_0^{LT} \Phi_{vv}^-(\tau) e^{-j2\pi f\tau} d\tau + \frac{1}{1-\psi(jh)e^{-j2\pi fT}} \int_{LT}^{(L+1)T} \Phi_{vv}^-(\tau) e^{-j2\pi f\tau} d\tau \right\} \quad (4.18)$$

A closed form expression for the power density spectrum can be obtained from the above equation (4.18) when the pulse shape $g(t)$ is rectangular and zero outside the interval $[0, T]$. In this case $q(t)$ is linear for $0 \leq t \leq T$. The resulting power spectrum may be expressed as

$$S(f) = T \left[\frac{1}{M} \sum_{n=1}^M A_n^2(f) + \frac{2}{M^2} \sum_{n=1}^M \sum_{m=1}^M B_{nm}(f) A_n(f) A_m(f) \right] \quad (4.19)$$

Where

$$A_n(f) = \frac{\sin \pi [fT - (2n - 1 - M)h/2]}{\pi [fT - (2n - 1 - M)h/2]}$$

And

$$B_{nm}(f) = \frac{\cos(2\pi fT - \alpha_{nm}) - \psi \cos \alpha_{nm}}{1 + \psi^2 - 2\psi \cos 2\pi fT}$$

$$\alpha_{nm} = \pi h(m + n - 1 - M)$$

$$\psi = \psi(jh) = \frac{\sin M\pi h}{M \sin \pi h}$$

This is a formidable looking set of expressions, but they are relatively straight forward to calculate by means of MATLAB software on a computer. Results of the power density spectra computation of CP-QFSK ($M=4$) are plotted in Fig.(4.3) as a function of

the normalized frequency fT , with the modulation index h as a parameter. The modulation index is a function of the transmission rate, T , and the frequency deviation (f_d), $h=2f_dT$. Only one half of the bandwidth occupancy is shown in the graph and the origin corresponds to the carrier f_c . The graph illustrates that the spectrum of CP-QFSK is relatively smooth and well confined for $h<1$. As h approaches unity, the spectrum becomes very peaked and for $h=1$ where $|\psi|=1$, it is found that impulses occur at M frequencies. When $h>1$ the spectrum becomes much broader.

In communication systems where CP-QFSK is used, the modulation index is designed to conserve bandwidth so that $h<1$. Therefore it is concluded that the bandwidth occupancy of CP-FSK depends on the choice of the modulation index h , the pulse shape $g(t)$, and the number of the signal levels M .

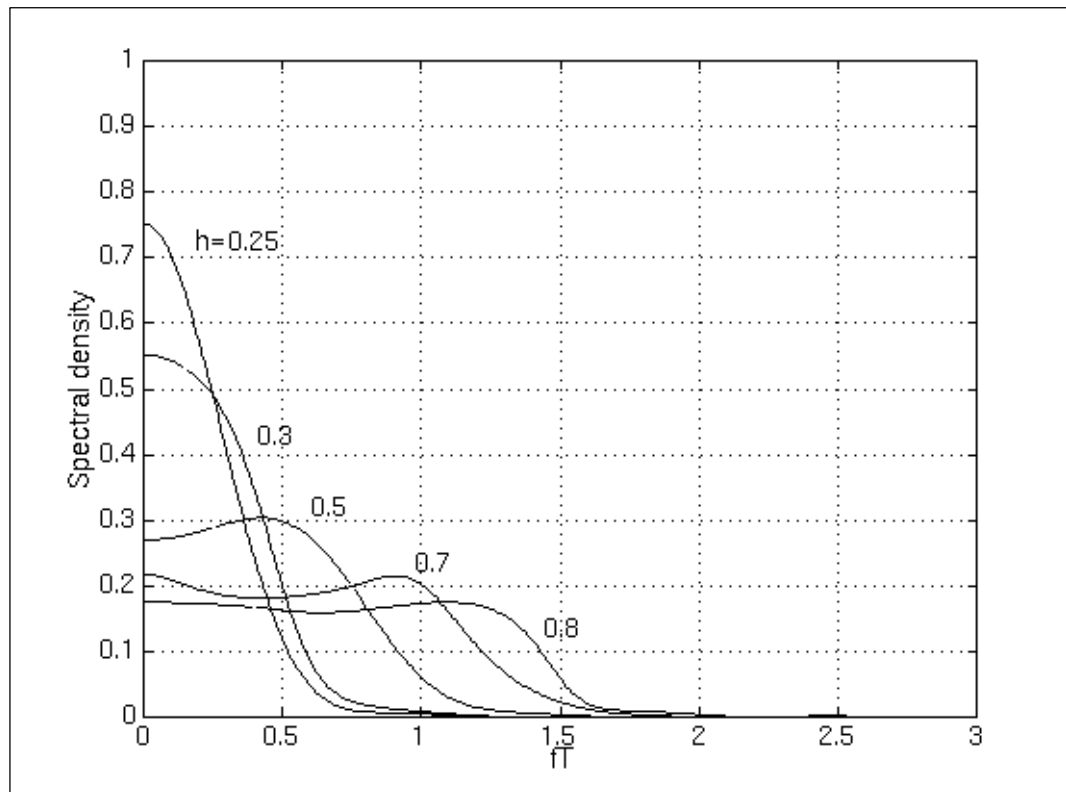


Fig. 4.3 Normalised one-sided power spectral density of CP-QFSK

4.2.3 Bandwidth occupancy of CP-QFSK, MSK, and QPSK

The special case of binary CPFSK with $h=1/2$ ($f_d=1/4T$) and $\psi=0$ corresponds to minimum shift keying (MSK), spectrum of which is [21]

$$S(f) = \frac{16T}{\pi^2} \left[\frac{\cos 2\pi fT}{1 - 16f^2T^2} \right]^2 \quad (4.20)$$

whereas the spectrum of the quadrature phase shift keying (QPSK) is [22]

$$S(f) = 2T_b \left[\frac{\sin 2\pi fT_b}{2\pi fT_b} \right]^2 \quad (4.21)$$

Comparing these three spectral characteristics, the frequency variable was normalized by the bit interval T_b and these spectra are illustrated in Fig.4.4 below.

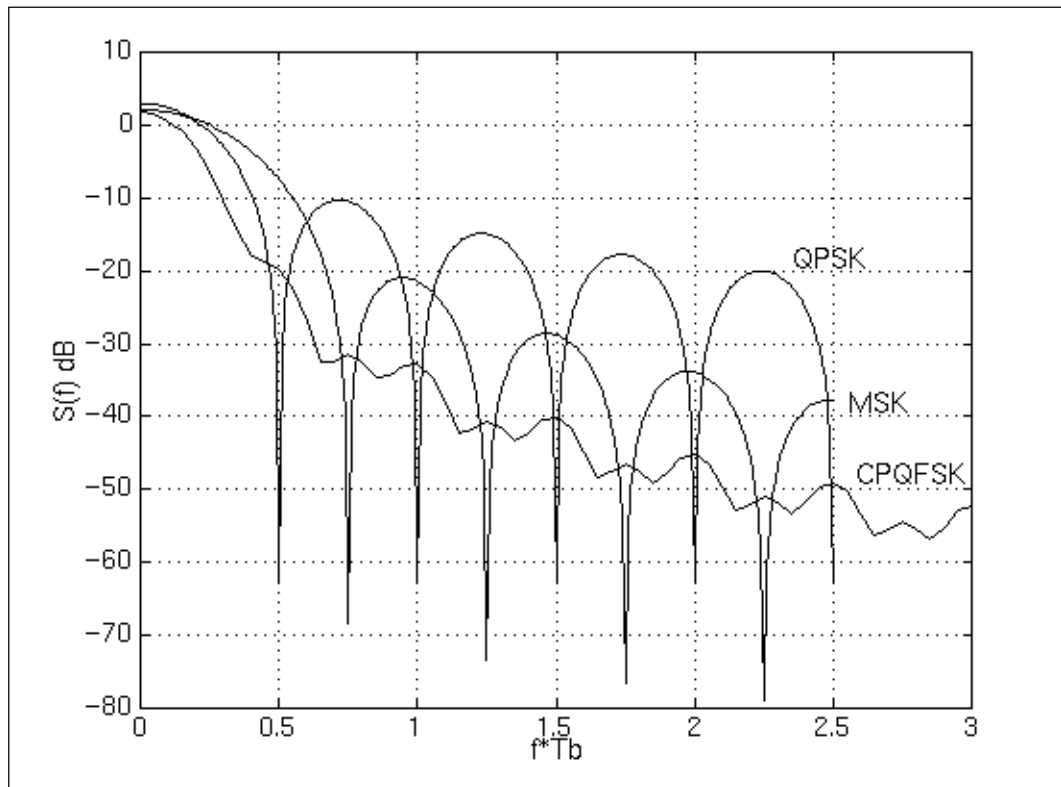


Fig.4.4 Power density spectra of CP-QFSK, MSK, and QPSK.

From the above graph, it is clearly seen that the CP-QFSK signal has the narrowest main lobe among the three spectra and its side lobes fall off considerably faster than the MSK and QPSK do. Consequently CP-QFSK has the narrowest spectral occupancy and hence is more bandwidth efficient than QPSK and MSK allowing more channels to be accommodated in a given bandwidth. It has been proven in [23] that M-ary CPFSK has significantly less fractional-out-of-band power compared to PSK. Thus, in bandlimited situations, CP-QFSK is superior to MSK and PSK.

4.3 CP-QFSK baseband system simulation model

Based on the theoretical basis presented in the previous section, a CP-QFSK system model has been designed. In QFSK system the modulated signal has four distinct level states that are generated by a unique mapping scheme of consecutive dibits (pairs of bits) into symbols, i.e. each two consecutive bits in the TDMA signal are formed into a symbol having four possible levels depending on the logical levels of the two-bits. Obviously, the quaternary system would differ from the standard 2-level DECT system, previously shown in chapter 3 (Fig.3.6), in three circuit units, namely, the 2-4 level converter, the threshold comparator (decision circuit), and the 4-2 converter. The global functional block diagram of the baseband equivalent model of the CP-QFSK is shown in Fig.4.5.

The transmitter configuration consists of a PRBS data source which generates a serial NRZ binary data stream at a rate twice that of the DECT bit rate ($f_b=2b/s$ normalised value) as shown in figure 4.5. This unipolar binary bit stream was then converted by a serial-to-parallel (s-p) block, contained in the 2-4 level converter, into two separate NRZ bit streams one of which is delayed by a single bit duration creating an in phase, $I(t)$, and quadrature phase, $Q(t)$, sets having a symbol rate equal to half that of the incoming bit rate $\{\pm 1, \pm 3\}=1b/s$, i.e., the baud (symbol) rate is equal to the DECT symbol rate. These two bi-polar bit streams are combined together after the most significant stream is multiplied by a constant to form the four level states.

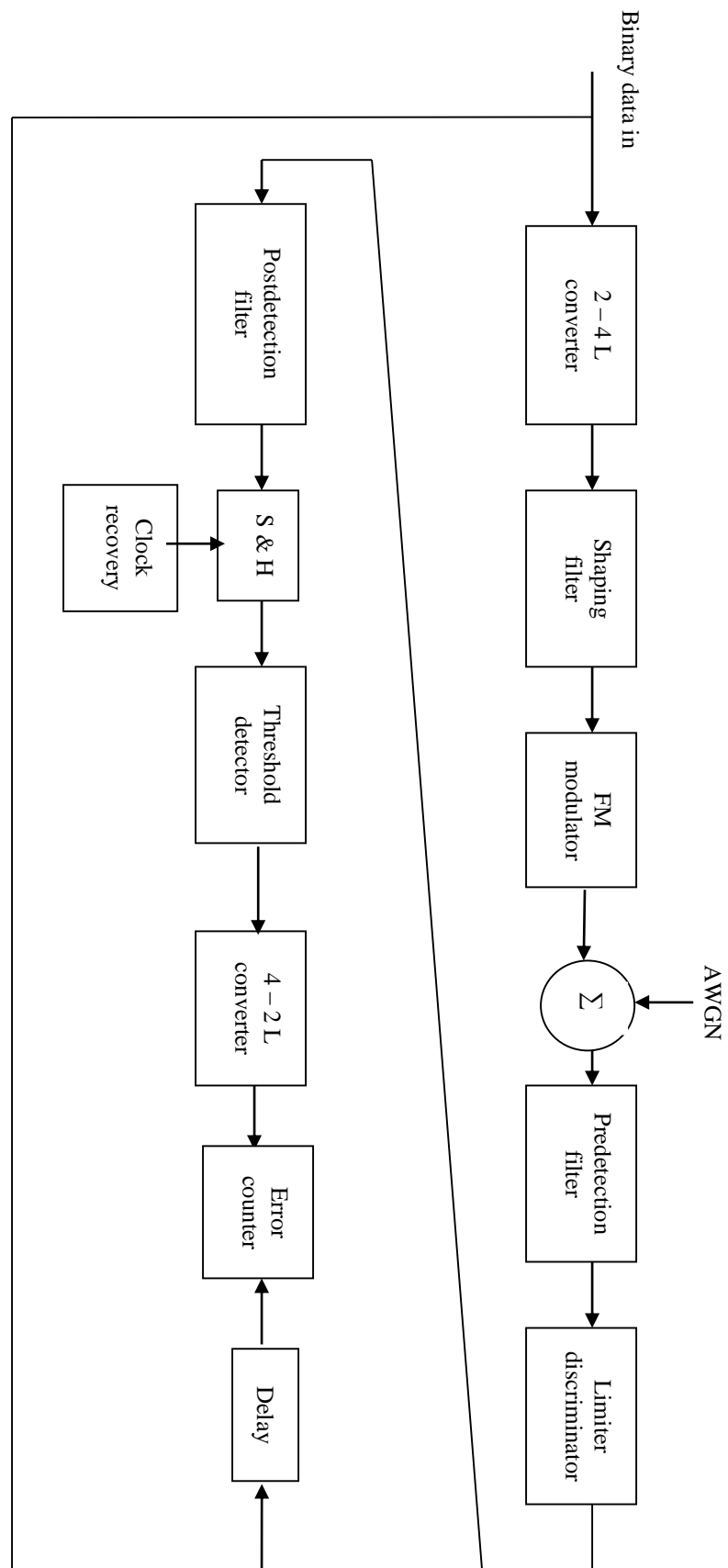


Fig 4.5 Block diagram of simulated CPQFSK system

The mapping of the bits into symbols was done in accordance with Gray code, so that adjacent symbols differ by only one bit, and as noise and interference tend to cause decision errors mostly between adjacent symbols, any single symbol error will correspond to a single bit error. Since the BOSS simulator library does not have a quaternary data generator, a custom coded look-up table created and incorporated into the BOSS module library. The generated user data which is double that currently accommodated by DECT is shown in Fig. 4.6 below

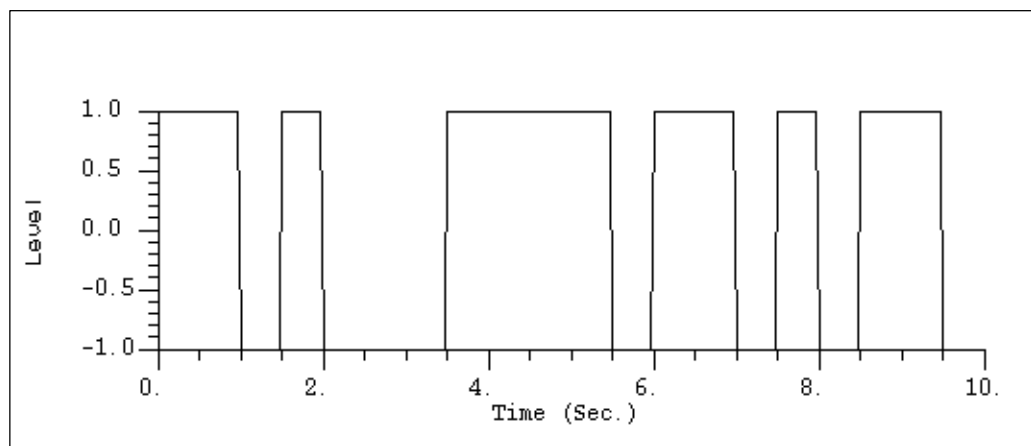


Fig.4.6. User binary data of twice the DECT rate.

Eventually, each particular voltage level was associated with each symbol as shown in table 4.1.

Quaternary Symbols		Transmitted Signal
Binary	Dibits	State (level)
0 0	0 0	-3
0 1	0 1	-1
1 0	1 1	1
1 1	1 0	3

Table 4.1 Symbol mapping for QFSK

With this correspondence, each consecutive two bits in the TDMA signal are formed into a symbol having four possible levels depending on the logical levels of the two-bits, thus a quaternary baseband data was created. Figure 4.7. below shows a generated set of 10 consecutive arbitrary symbols.

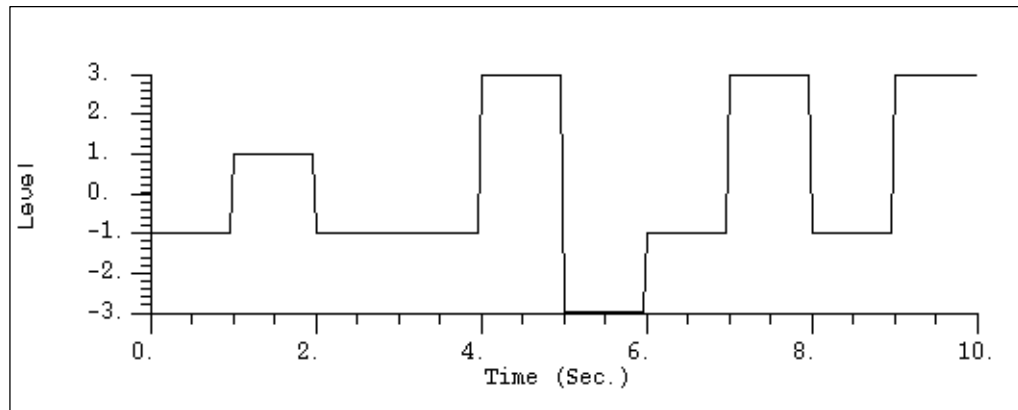


Fig.4.7 The baseband quaternary data.

The generated quaternary signal was then applied to a premodulation filter with pulse shape $g(t)$, to smooth out the sudden variations in the baseband signal, and consequently control the shape of the signal power spectrum. The smoothed data is then applied to an FM modulator, the output of which is a constant amplitude signals as can be seen from figure 4.8 below

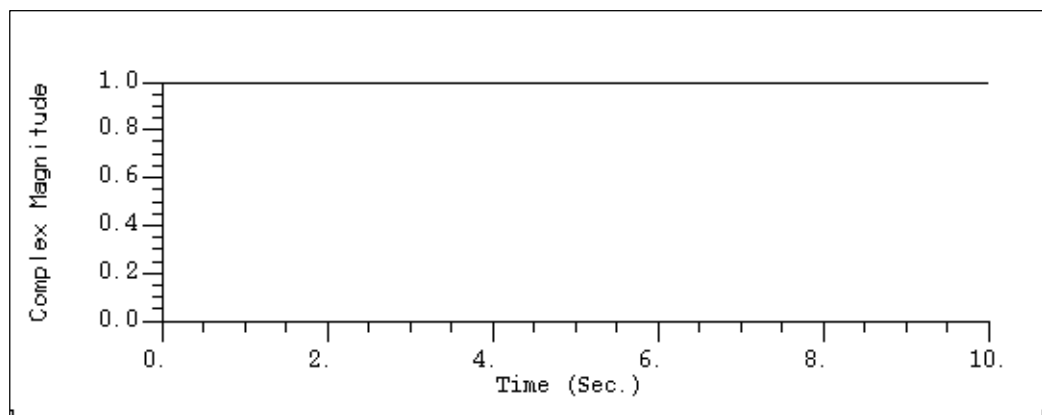


Fig.4.8 Modulated signal amplitude.

Figures 4.9 through 4.10 show the signal space diagram and phase trajectories

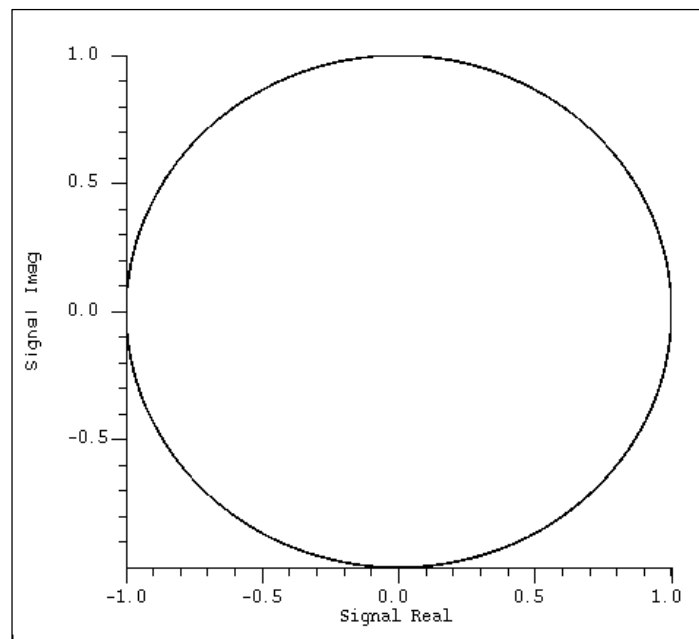


Fig. 4.9 Signal space diagram of CP-QFSK

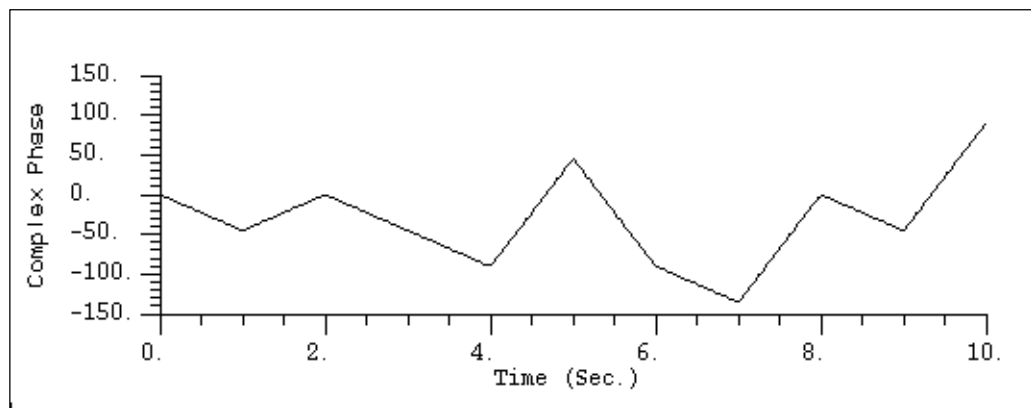


Fig.4.10 Phase trajectory of the generated quaternary signal for 10 symbols.

The input to the receiver consists of the transmitted signal plus additive white Gaussian noise with single sided spectral density, N_0 . The predetection lowpass filter at the front end of the receiver suppresses noise and interference power in the signal band. The output of the pre-detection filter is then limited before being passed on to the discriminator which converts the frequency variations, i.e., the derivative of the phase of the incoming signal, into voltage variations to yield the quaternary signal plus noise. After passing through a post-detection filter (LPF), the noise and unwanted components

are removed. The output of the post-detection filter is then fed to a threshold comparator which converts the recovered baseband modulation signal into a sequence of di-bit symbols. The threshold comparator is gated by the recovery clock that is generated by the symbol timing-recovery (STR) block at the baud rate enabling to sample the demodulated signal right in the middle of each symbol duration time. The threshold voltage comparator has at its disposal three decision levels (rather than one in the standard system) corresponding to angular frequency deviations 0, η ; $\eta > 0$ to regenerate the symbols and are set at the centre of the eye openings of the output signal of the post-detection filter, and the binary data is recovered back by means of the 4-2 level converter. Finally, the regenerated output is fed into the error rate counter for BER measurement. In what follows, the parameters of the CP-QFSK system will be specified and optimised.

4.4 Optimization of CP-QFSK System Parameters

An important parameter in the specification of multi-level CPFSK is the modulation index h which determines the signal bandwidth. Correct selection of h is critical not only in terms of the power spectral density but also in terms of the error rate performance of the modulation scheme [24]. However, the increase in the number of levels or the decrease in modulation index results in a narrower signal bandwidth and hence a higher spectrum efficiency. But such strategy causes degradation in receiver sensitivity or bit error rate performance. Therefore, a higher E_b/N_0 or otherwise an improvement in the BER performance is required for the increased level if to maintain the same system performance quality. This can be attained through higher modulation index at the expense of increasing the degradation in the interference power in the adjacent channels due to spreading in the transmitted signal spectrum. However, this increase in the signal bandwidth can be controlled by introducing pre-modulation filtering of the baseband waveform of the input to the FM modulator using proper pulse shaping. The degree to which the spectrum of the modulated signal is compacted can be controlled by changing the bandwidth of the pre-modulation filter. Correct selection

of modulation index is critical not only in terms of the power spectral density but also in terms of the error rate performance. The optimum value of modulation index is 0.5 which is the minimum value that produces orthogonality in the signaling waveforms. That is, the signaling waveforms can be detected independently with no cross-correlation between other signaling states. For binary signaling this is generally referred to as minimum shift keying. In CPQFSK orthogonal signaling ($h=0.5$) will result in a broad spectrum. In addition, only two distinct signaling states would exist due to the phase wrap-around nature of the modulation scheme, and consequently, an ambiguity would arise in the demodulation process ($270^\circ=-90^\circ$, $-270^\circ=90^\circ$).

In order to reduce the spectral occupancy the modulation index has to be reduced. Therefore, there is a trade-off between the modulation index and the baseband filtering (pulse shaping) necessary to get a power spectrum that fits within the DECT spectral mask. Thus, it follows from the above qualitative considerations that an optimum pulse shape which has good characteristics in both the time and frequency domain and a modulation index which will serve as system simulation parameters or system design criteria need to be found, i.e. there are three issues of concern: How does the system performance degrade in the presence of noise when varying the RF spectrum through baseband modulation pulse shaping? What is the role of channel filtering in the obtainable performance? What are the optimum values of the system parameters with different baseband shaping?

Different types of pulse shaping functions for CPM are available to control the modulation signal power spectrum [19]. For the purpose of this work we shall restrict ourselves to investigate three particular pulse shaping functions:

- i) Raised Cosine shaping in the time domain (LRC), where L refers to the length in symbol intervals of the pulse. Raised Cosine pulse shaped CPQFSK (LRC-CPQFSK) can be either full or partial response signalling, such that when $L > 1$ the modulation scheme is termed partial response.

- ii) Raised Cosine shaping in the frequency domain or spectral RC (SRC).
- iii) Gaussian pulse shaping.

In what follows, the interrelated system parameters in the presence of an AWGN channel having varied the transmitted spectrum through modulation pulse shaping, modulation index, and the IF filter bandwidth will be investigated and these interrelated system factors or parameters will be optimised accordingly. For this purpose, since there is no unique definition of the M-ary CPFSK bandwidth [19], we will consider here the energy percentage bandwidth criterion provided that this bandwidth confines within the DECT bandwidth. So, the 99.85%, 99.90%, 99.95%, and 99.99% energy bandwidths were examined to satisfy the above conditions. At this point, it is worth mentioning that it is meant here by 99.95% energy bandwidth, the modulation frequency band containing 99.95% of the signal power.

4.4.1 Gaussian Pulse Shaping

BOSS library does not contain Gaussian type filters within its library. However, it does include a convolutional filter, capable of implementing a time domain filtering by reading a time domain description of the transfer function file created by means of MATLAB software using Gaussian frequency pulse function [19] below in order to generate the respective time domain impulse response.

$$g(t) = \frac{1}{2T} \left[Q \left(2\pi B \frac{t - \frac{T}{2}}{\sqrt{\ln 2}} \right) - Q \left(2\pi B \frac{t + \frac{T}{2}}{\sqrt{\ln 2}} \right) \right] \quad (4.22)$$

Where $0 \leq BT < \infty$ is the 3dB bandwidth of the Gaussian filter and Q is the error function that is given by

$$Q(t) = \int_t^{\infty} \frac{1}{\sqrt{2\pi}} e^{-\tau^2/2} d\tau$$

Fig.4.11 shows the generated Gaussian impulse responses for various bandwidth bit period product, BT, one of which then to be convolved in the time domain with the input quaternary signal sequence to produce the CP-QFSK signal.

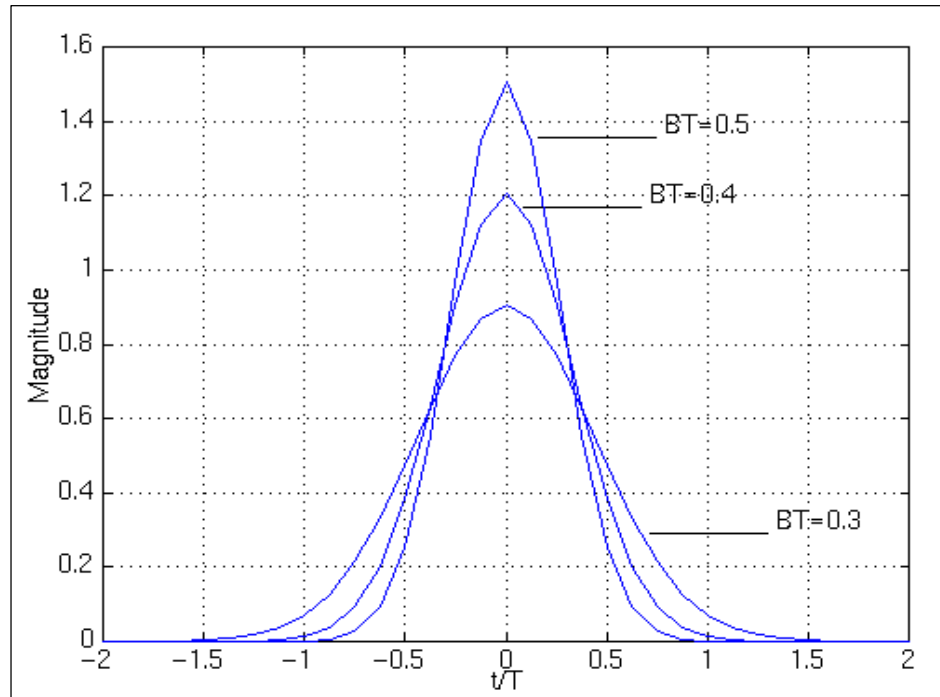


Fig.4.11. Impulse response of Gaussian filter.

The generated power spectrum of the CP-QFSK signal in this case is shown in Fig.4.12. It can clearly be seen that the spectral occupancy is still within the DECT bandwidth shown in chapter 3 (Fig. 3.5). The power spectrum also shows that the first side lobe is at about 30 dB below the main lobe, and the other side lobes diminish off in a fairly fast rate and this is reflected in eye opening of the eye diagram shown in Fig. 4.13.

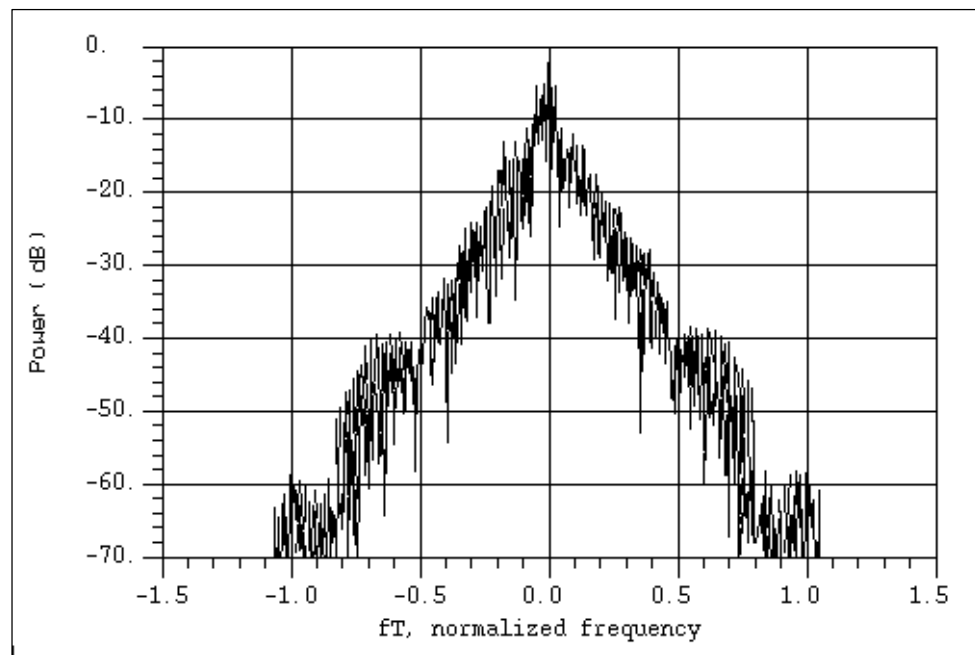


Fig.4.12 Power spectrum of Gaussian shaped CP-QFSK signal

Pre-detected received signal eye diagram is shown in Fig. 4.13. Narrow eye opening signifies a considerable amount of ISI is being generated.

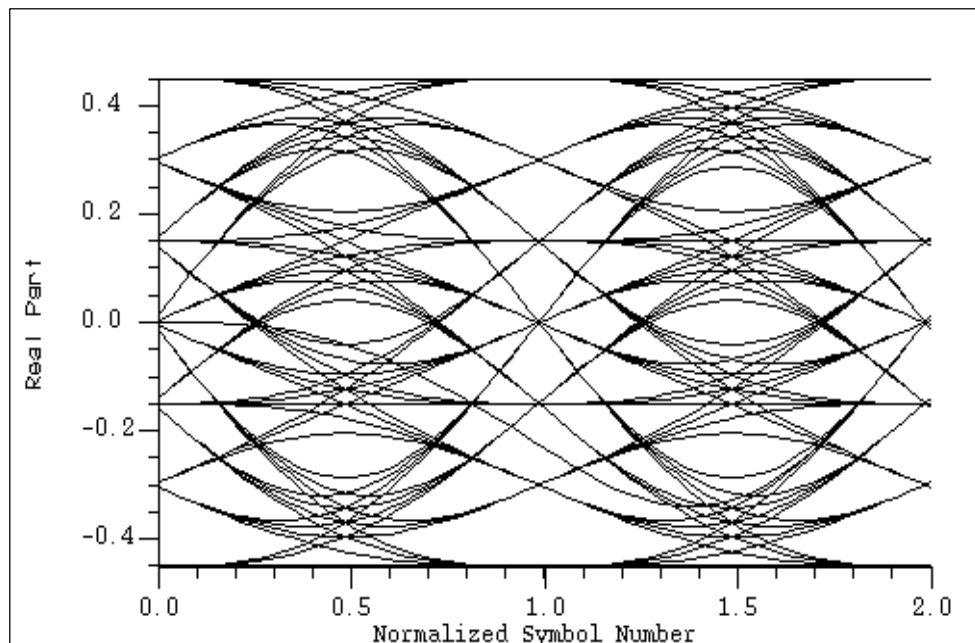


Fig.4.13 Eye diagram of the received signal

The simulation was run to evaluate BER performance for a range of IF filter bandwidths, h , and receiver pre-detection filter normalized equivalent-noise bandwidth (B) which is dependent of the energy percentage bandwidth. The output of the simulation is tabulated in table 4.2 having fixed the system performance quality at $P_e = 10^{-3}$ which is denoted in the table by W .

h	B	W [dB]
0.25	1.15	20.3
0.3	1.2	19.2
0.35	1.25	18.3
0.4	1.3	17.6
0.45	1.35	18.2
0.5	1.4	18.9

Table 4.2. Optimization of system parameters having fixed $P_e = 10^{-3}$.

The above table has the aim of exhibiting the optimum performance which refers to the choice of $h=0.4$, and $B=1.3$ for 6th order Butterworth receiver filter (a six-pole Butterworth filter requires less E_b/N_o than other types to attain the same BER performance quality), yielding a minimum value of E_b/N_o ratio, i.e. smallest degradation, required to assure $P_e = 10^{-3}$, that can be further seen quite clearly in the comparison between Butterworth and Gaussian filters reported in Fig.4.14 below. The total noise power is proportional to the bandwidth of the transmission channel, and $N_o = N_T/B$, apparently, as the IF bandwidth, B , decreases, less E_b/N_o is needed due to more noise rejection. However, a point is finally reached below which any further decrease in B , i.e. below optimality, will eventually lead to P_e being escalated. Thus, to minimise the noise at the demodulator input the IF bandwidth has to be reasonably narrow. In Fig.4.14, narrow bandwidth errors are due to inter-symbol interference predomination; whereas for wider bandwidths, the error increases owing to noise.

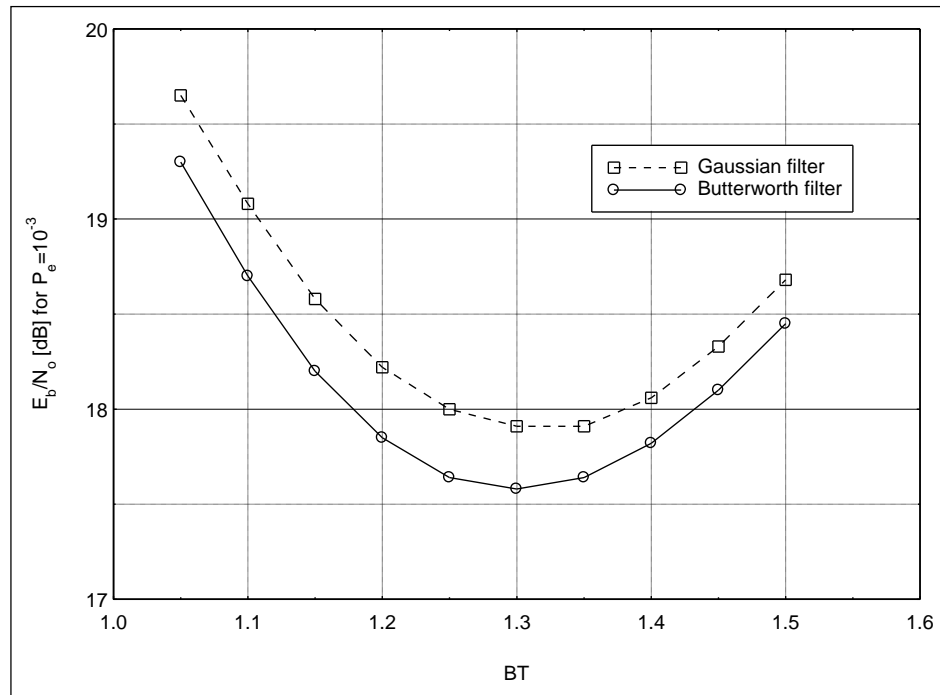


Fig.4.14 Required E_b/N_0 for $P_e = 10^{-3}$ vs. filter bandwidth

Figure 4.15, below, establishes that the BER performance of the system with Gaussian pre-modulation filtering having $BT=0.4$, $h=0.4$, and IF bandwidth normalised to baud rate of $B=1.3$ are found to be the optimum parameter values. It also exhibits that there exists a degradation in the BER performance of about 7 dB compared to the binary case presented in chapter 3 due to ISI domination.

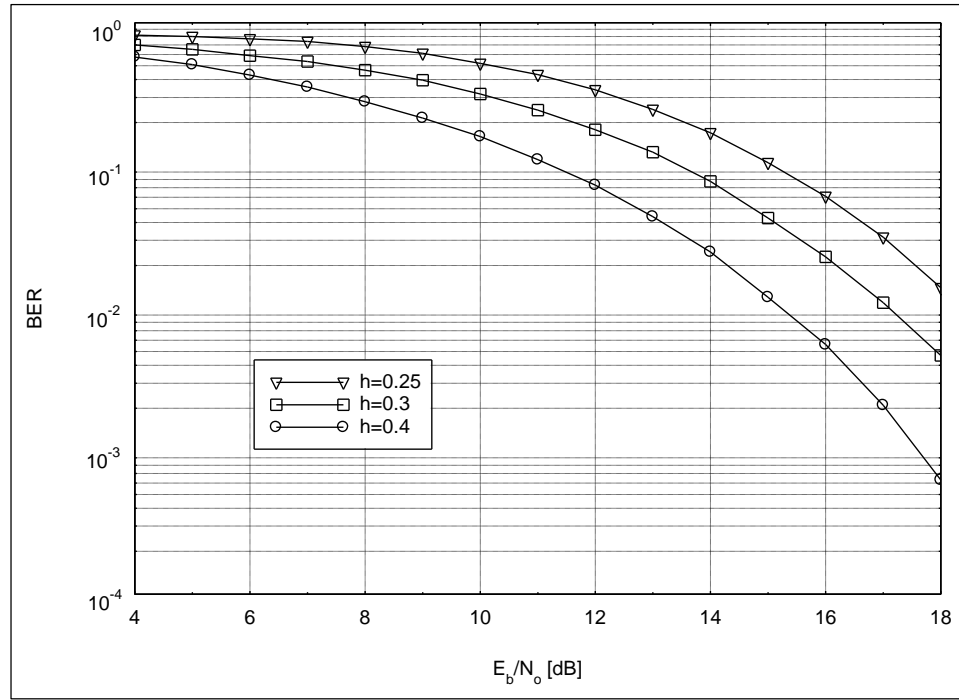


Fig.4.15 CP-QFSK performance with Gaussian-type modulation.

4.4.2 Spectrally Raised Cosine Pulse Shaping (SRC)

Proceeding in a similar manner to that of the Gaussian filter case, the LSRC filter was modelled using the frequency pulse function $g(t)$ below, and the required LSRC filters with different Roll off factors (β) have been created

$$g(t) = \frac{1}{LT} \cdot \frac{\sin\left(\frac{2\pi t}{LT}\right)}{\frac{2\pi t}{LT}} \cdot \frac{\cos\left(\beta \frac{2\pi t}{LT}\right)}{1 - \left(\frac{4\beta}{LT} \cdot t\right)^2}; \quad 0 \leq \beta \leq 1 \quad (4.23)$$

Figure 4.16 below shows the generated power spectrum of the modulated signal having filter roll off factor $\beta = 0.4$.

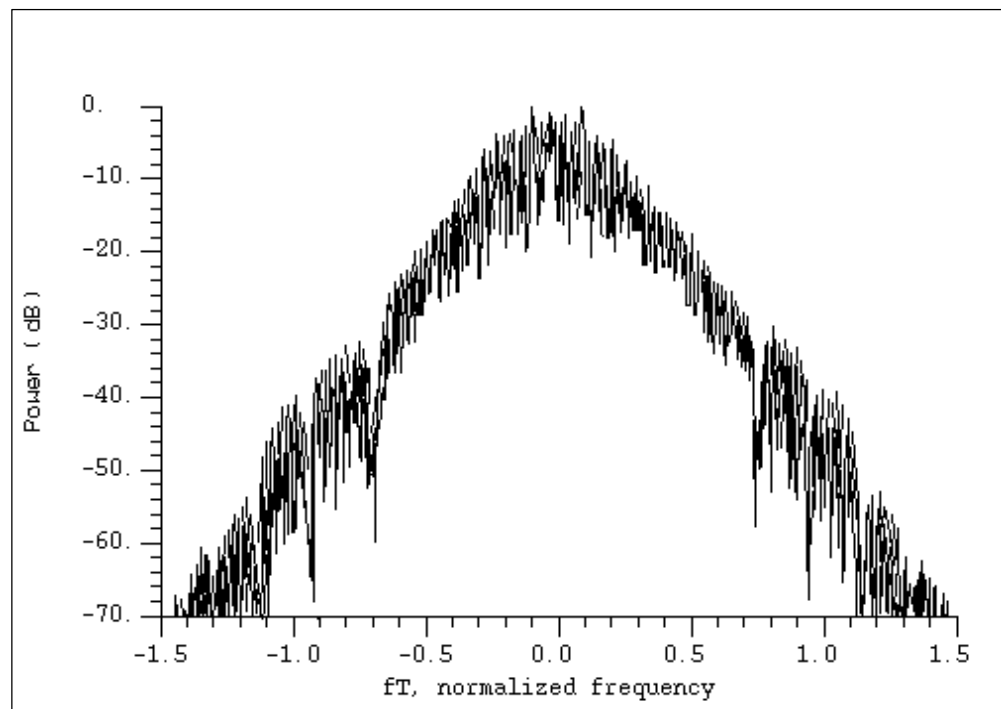


Fig.4.16 Power spectrum of SRC-shaped CP-QFSK signal

From the above power spectrum, it is noticed that the first side lobe is at only 30 dB below the main lobe, and the other side lobes fall off gradually slowly and that in turn results in larger spectral occupancy and hence considerable Adjacent Channel Interference (ACI) being created.

Figure 4.17 below shows the generated eye diagram of SRC-shaped quaternary data having $\beta = 0.4$, indicating the ISI-free characteristics of such filter.

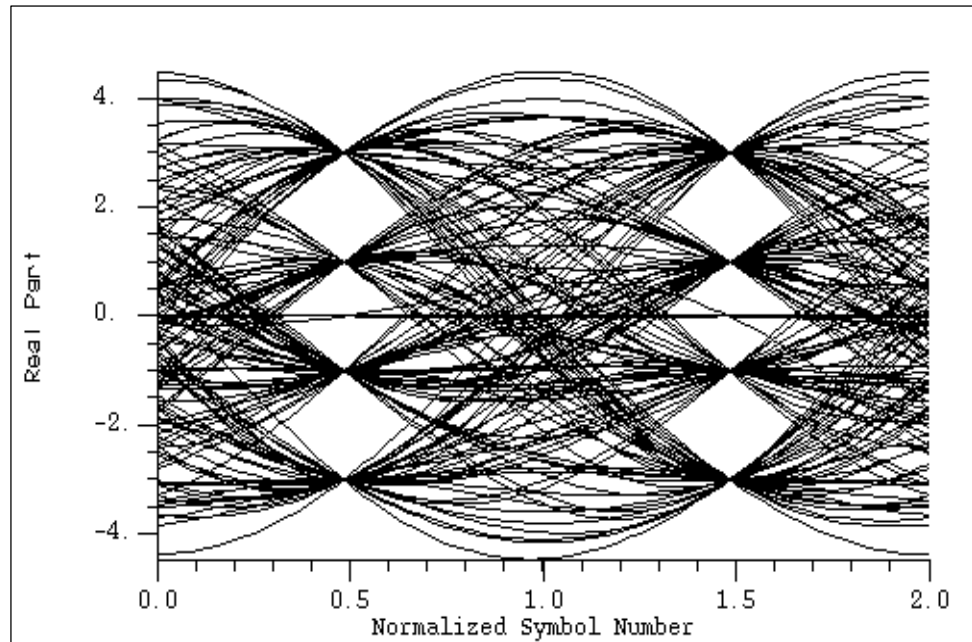


Fig.4.17 Eye diagram of SRC-shaped quaternary data

The measured BER performance in this case, SRC $\beta=0.4$ and $B=1.5$, with h as a parameter is plotted in Fig.4.18 below:

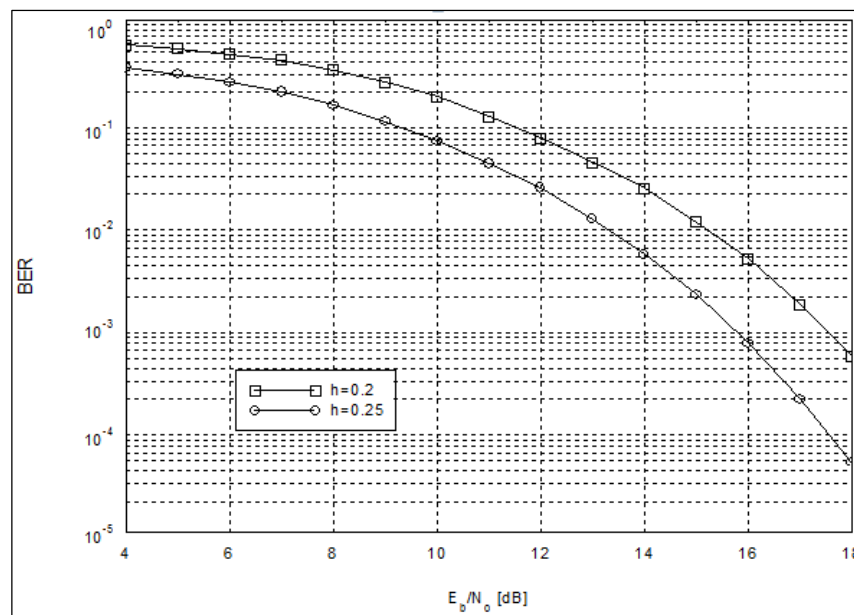


Fig.4.18. Measured BER performance for SRC-shaped CP-QFSK

From the above graph, it is obvious that $h=0.25$ is the optimum modulation index when Spectrally Raised Cosine filter is used to shape the quaternary data before applied to the modulator, also, it outperforms the Gaussian case (Fig. 4.15) by 2dB.

4.4.3 Raised Cosine Pulse Shaping (LRC)

Likewise, the LRC filter was created in the same way as the previous two filter types. The frequency pulse function $g(t)$, from which the impulse response of the required LRC filters with various modulation pulse time widths (LT) have been created, is

$$g(t) = \begin{cases} \frac{1}{2LT} \left[1 - \cos\left(\frac{2\pi t}{LT}\right) \right] \\ 0 \end{cases} \quad (4.24)$$

$$0 \leq t \leq LT \quad ; \text{ otherwise}$$

Where L is the pulse length, e.g., 3RC has $L=3$. 1RC, 2RC, and 3RC have been modelled and examined in relation to the energy percentage bandwidth criterion and BER performance. Consequently, 2RC has been found to be the optimum pulse in this case. Fig. 4.19 shows the generated spectrum of the CP-QFSK when 2RC was used.

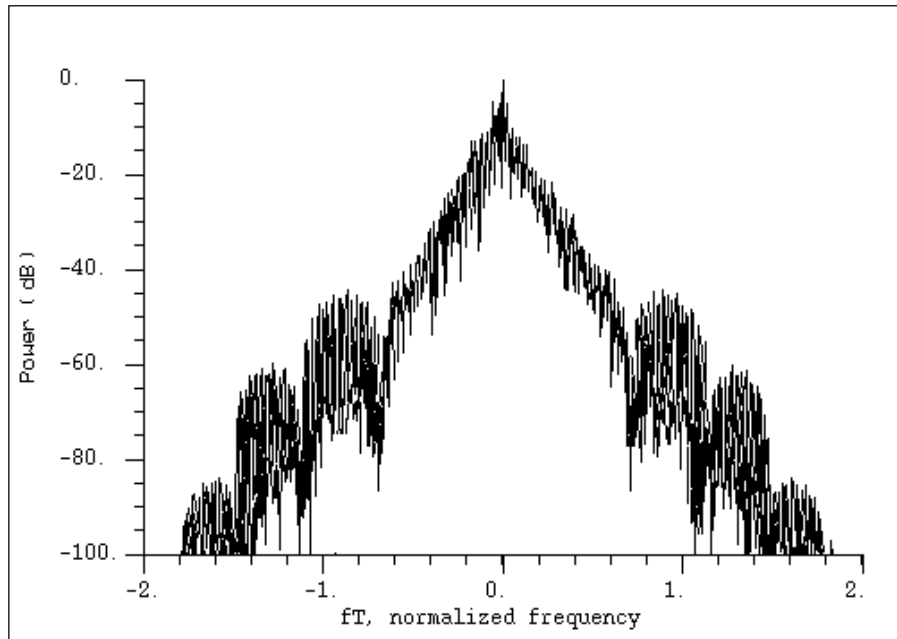


Fig.4.19 Power spectrum of 2RC modulation type

The above power spectrum demonstrates the 2RC supremacy over others presented so far, as the first side lobe is at 40 dB below the main lobe and the remaining side lobes containing insignificant energy diminish off in fairly fast rate, hence the LRC case outweighs LSRC and Gaussian cases in spectral containment, thus out of band radiation power. Also, the 2RC spectral occupancy matches that of the DECT case presented in chapter 3 (Fig. 3.5).

Fig.4.20. shows the eye diagram of 2RC shaped received quaternary data.

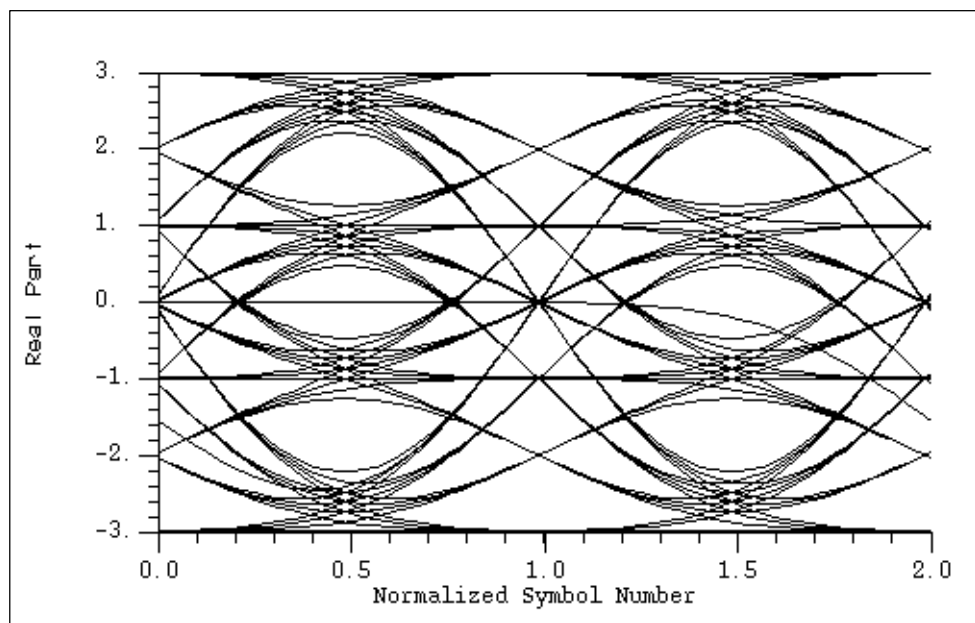


Fig.4.20 Eye diagram of the received signal

The simulation was run to evaluate the BER performance for this case having set the simulation parameters to the values of L from 1 to 3, h taking the values of 0.2, 0.25, 0.3 at a time, and IF filter bandwidth $BT=1.5$. In order to obtain reasonable BER measures, accurately evaluate the channel effects, and to simulate an average call duration of 2 minutes the simulation was carried out for 12000 DECT's frame time each simulation test run. For each frame duration (10ms), one of the 24 time slots was simulated to assess the quality of the link for a single user. Table 4.3 summarizes the main simulation parameter values.

Parameter	Value
Pre-modulation filter	2RC
Modulation index	0.3
IF BT product	1.5
Post-detection BT product	1.1
Simulation run time	12000 frames

Fig 4.3 Simulation parameters values

The simulation output shown in Fig.4.21 reveals that $h=0.3$ is the optimum value of modulation index when Raised Cosine filter with pulse length, $L=2$ is used as pre-modulation filter.

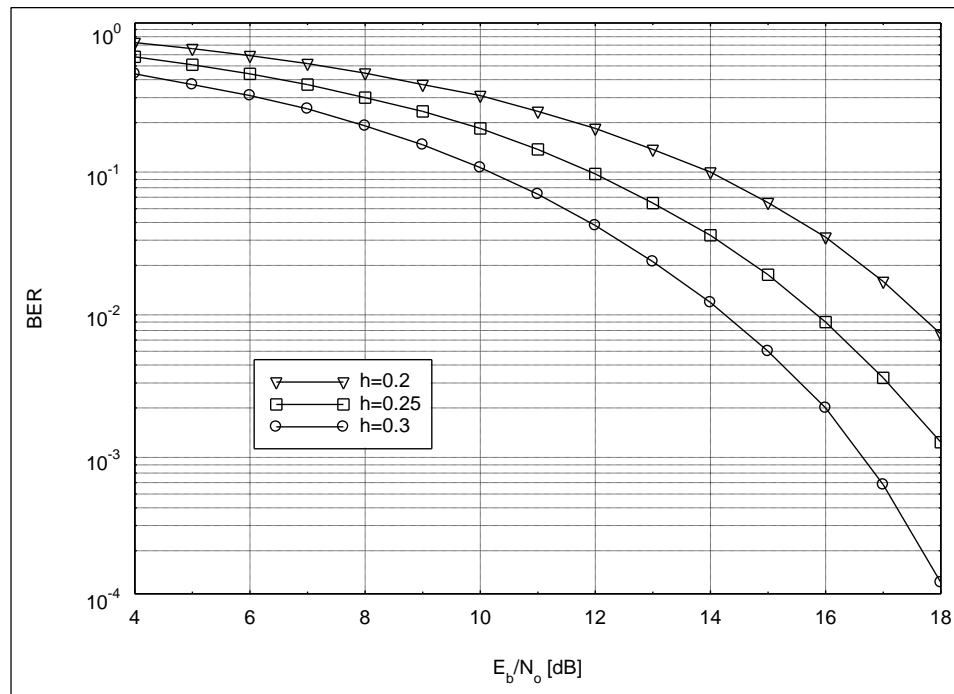


Fig.4.21. Measured BER performance for 2RC-shaped CP-QFSK

Fig. 4.21. above demonstrates an improvement of 1.5 dB over the Gaussian case and a slight degradation of 1 dB in performance compared to LSRC. However, considering

the partial response spectral compactness and ACI supremacy of LRC over others studied so far, it is concluded that 2RC is the optimum filter for shaping the quaternary data prior to modulation in the proposed CP-QFSK system. Comparing this measured performance to that of the conventional binary GMSK system reported in chapter 3 Fig.3.11, an average degradation of about 7 dB has been noticed.

Using a closed form expression for the probability of error of digital FM perturbed by AWGN with discriminator detection [1, 25], a theoretical bit error rate was computed by means of a program [appendix A], output of which was called into a MATLAB subroutine to plot the BER against E_b/N_o as shown in figure 4.22 below. This calculated results agree well with the results obtained by computer simulation presented in Fig.4.21.

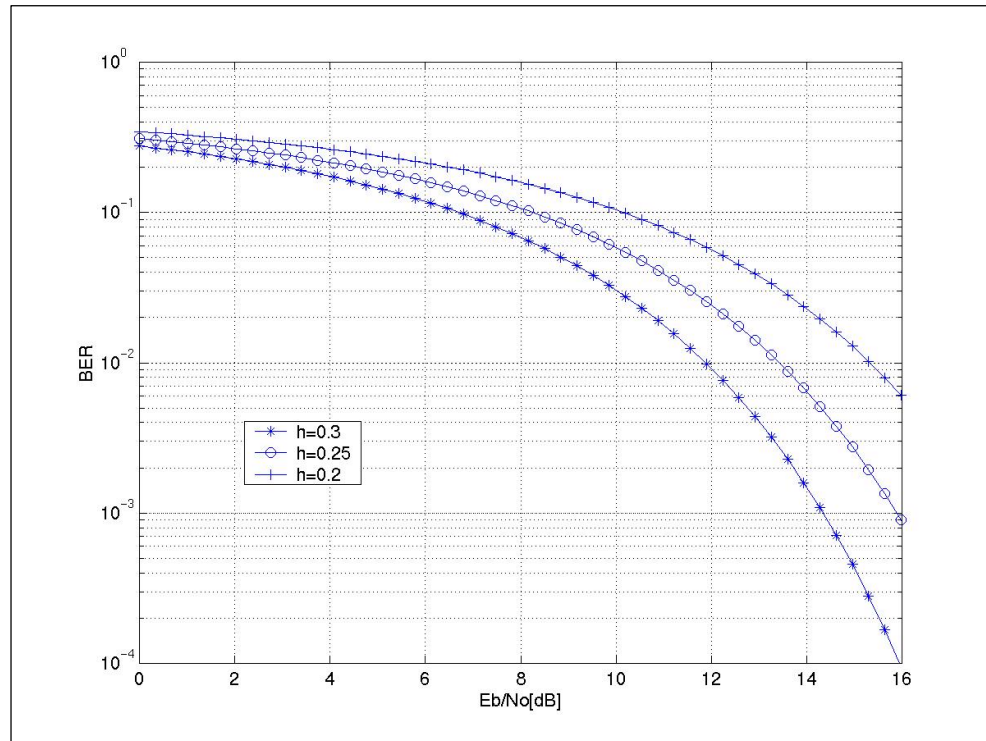


Fig.4.22. Theoretical BER performance for CP-QFSK

SUMMARY:

In this chapter, an overview of the CP-QFSK modulation scheme including theoretical background and rationale for proposing it as a dual data rate alternative system for the

current binary GMSK modulation system was given at the very outset. On those grounds, a system model was designed. Simulation tests were carried out in order to assess system performance in the presence of noise when varying the RF spectrum through baseband shaping, and also to define the role of channel filtering in the obtainable performance and determine optimum system parameter values that are necessary to maintain a power spectrum that fits within the DECT spectral mask. To that end a simulation investigation into a range of pulse shaping functions, channel filtering has led to 2RC pre-modulation pulse shaping with $h=0.3$, pre-detection filter normalized equivalent noise bandwidth $B=1.5$ were found to be the optimum system parameter values. These obtained simulation results have been verified by theoretical computations result of which are presented in fig. 4.22.

BER performance results presented in this chapter revealed that the proposed CP-QFSK system quality is inferior to the binary GMSK system by almost 7dB on average. This degradation in system quality was shown to be primarily due to the domination of the ISI.

So far the system performance evaluation has been carried out under static channel conditions i.e. in the presence of AWGN conditions only. Thus, the system performance under the indoor propagation channel conditions would have to be investigated in the following chapter.

REFERENCES

- [1] PROAKIS J. G. ; "Digital Communications". Fourth Edition, McGraw Hill, New York, 2001.
- [2] STEEL R.; "Deploying Personal Communications Networks". IEEE Communications Magazine, Vol. 28, No. 9, pp. 12-15, September 1990.
- [3] BURR A. G. ; "Application of High Rate Coded Modulation Systems to Radio LANs". IEE Colloquium on Radio LANs, London, pp. 5/1-5/6, 7th May 1992.
- [4] AGHVAMI, A. H.; "Digital Modulation Techniques for Mobile and Personal Communication Systems". Electronics and Communication Engineering Journal, June 1993.
- [5] JOSEPH BOCCUZZI; "Signal Processing for Wireless Communications". The McGraw-Hill Companies, Inc., 2008.
- [6] OETTING, J. "A Comparison of Modulation Techniques for Digital Radio". IEEE Transactions on Communications, Vol.Com-27, No.12, December 1979.
- [7] MASAHIKO, H., TOSHIO M., and KAZUAKI M.; "Multilevel Decision Method for Band-Limited Digital FM with Limiter-Discriminator Detection". IEEE Journal on Selected Areas in Communications, Vol. SAC-2, No. 4, July 1984.
- [8] ZIEMER R. E. and PETERSON R. L.; "Introduction to Digital Communication". Macmillan Publishing Company, Inc. 1992.
- [9] WEBB W. T.; "QAM : The Modulation Scheme for Future Mobile Radio Communications?". IEE Electronics & Communication Engineering Journal, pp. 167-176, August 1992.

-
- [10] IBNKAHLA M.; "Signal Processing for Mobile Communications". CRC Press LLC, 2005.
- [11] PARK H. C., LEE K and FEHER K.; "Continuous Phase Modulation for F-QPSK-B Signals". IEEE Transactions on Vehicular Technology, Vol. 56, No. 1, pp. 157-172, January 2007.
- [12] ANDERSON J. B. and SUNDBERG C. E.; "Advances in Constant Envelop Coded Modulation". IEEE Communications Magazine, Vol. 29, No. 12, pp. 36-45, December 1991.
- [13] SUN J. and REED I. S. "Performance of MDPSK, MPSK, and Noncoherent MFSK in Wireless Rician Fading Channels". IEEE Transactions on Communications, Vol. 47, No. 6, pp. 813-816, June 1999.
- [14] ANDRISANO O., CORAZZA G., and IMMOVILLI G. "Effects of the Interferences in Cellular Digital Mobile Radio Systems using Full Response CPM with Limiter-Discriminator Detection.". Alta Frequenza, Focus on Mobile Radio Systems, No. 2, pp. 109-117, 1988.
- [15] PHOEL W. G., "Improved Performance of Multiple-Symbol Differential Detection of Offset QPSK". IEEE Wireless Communications and Networking Conference, pp. 548-553, 2004.
- [16] HYUNDONG S. and HONG L.; "On the Error Probability of Binary and M-ary Signals in Nakagami-m Fading Channels". IEEE Transactions on Communications, Vol. 52, No. 4, April 2004.
- [17] ANDERSON R. R., and SALZ J.; "Spectra of Digital FM.". Bell Systems Technical Journal, Vol. 44, pp. 1165-1189, July/August 1965.

-
- [18] OSBORNE and LUNTZ M. B.; "Coherent and Non-coherent Detection of CPFSK". IEEE Transactions on Communications, Vol. COM-22, pp. 1023-1036, August 1974.
- [19] SUNDBERG C. E.; "Continuous Phase Modulation : A Class of Jointly Power and Bandwidth Efficient Digital Modulation Schemes with Constant Amplitude.". IEEE Communications Magazine, Vol. 24, No. 4, April 1986.
- [20] GARRISON G. J.; "A Power Spectral Density Analysis for Digital FM.". IEEE Transactions on Communications, Vol. COM-23, No. 11, November 1975.
- [21] RABZEL M., and PASUPATHY S; "Spectral Shaping in Minimum Shift Keying.". IEEE Transactions on Communications, Vol. Com-26, No.1, January 1978.
- [22] TOMMY OBERG, "Modulation, Detection and Coding". John Wiley & Sons, Ltd, 2001.
- [23] EKANAYAKE N.; "M-Ary Continuous Phase Frequency Shift Keying with Modulation index $1/M$ ". IEE Proceedings, Vol.131, Part F, No. 2, April 1984.
- [24] YOSHIHIKO AKAIWA, ICHIRO TAKASE, SUSUMU KOJIMA, MASAO IKOMA, and NOBORU SAEGUSA.; "Performance of Baseband-Bandlimited Multilevel FM with Discriminator Detection for Digital Mobile Telephony.". The Transactions of the IECE of Japan, Vol. E64, No. 7, July 1981.
- [25] RICE, S. O.; "Noise in FM Receivers", Time Series Analysis, John Wiley & Sons, pp. 395-421, 1963.

CHAPTER 5

Performance of CP-QFSK System under different channel conditions

5.1 CP-QFSK System Performance in non-fading environments

There are many sources of interference to mobile communications systems. The effect of multipath-free i.e. Gaussian noise channel only has already been investigated so far which serves as an optimum media. In mobile radio communications systems where a frequency re-use strategy is employed, the receiver in any cell operating on any channel is subjected to Co-Channel Interference (CCI) from the equivalent cells in surrounding clusters, and to Adjacent Channel Interference (ACI) from utilization of the adjacent channels within its own cluster and the adverse effects of the multipath channel will all be the focus of this chapter.

5.1.1 Adjacent Channel Interference (ACI)

This type of interference is characterised by unwanted signals from other frequency channels “spilling over” or injecting energy into the channel of interest. The proximity with which channels can be located in frequency is determined by the modulation spectral roll-off and the width and shape of the main spectral lobe [1]. In multicarrier systems such as the cellular mobile/personal communications networks, channel spacing (and in turn spectral efficiency) is determined by the maximum level of adjacent channel interference that can be tolerated by the modulation scheme. In DECT, the adjacent channel requirements are dictated by the adjacent channel re-use. With the spectrum currently available (120 duplex timeslots) and the geographical re-

use of physical channels, there should be no need for a given RFP to use an adjacent channel in the same timeslot, and hence, no requirement for high isolation between adjacent channels. The isolation need only be sufficient to cover the use of adjacent channels in adjacent cells [2].

With a limiter discriminator detector receiver, an isolation of only 25-30 dB would therefore be required yielding a moderate constraints on out-of-band radiation, and modest IF filter requirements [3, 4]. Moreover, while operating on different carriers, each call connected to the same base station always uses different time slots. This greatly reduces the in-system interference risk due to intermodulation or poor adjacent channel attenuation [5].

In simulating the ACI, as regards the propagation media, it has been assumed, in order to emphasize the interference effects, an ideal multipath-free situation, as regards both the useful channel and the interfering ones. Besides, the interfering signal characteristics are assumed to be of the same kind as the useful one, and also the adjacent channels are symmetrically placed around the useful channel having the same amplitudes. The relative ACI as shown in Fig. 5.1 below is the ratio between the Signal to Interference (S/I) power values before and after the IF filter for an adjacent channel interferer.

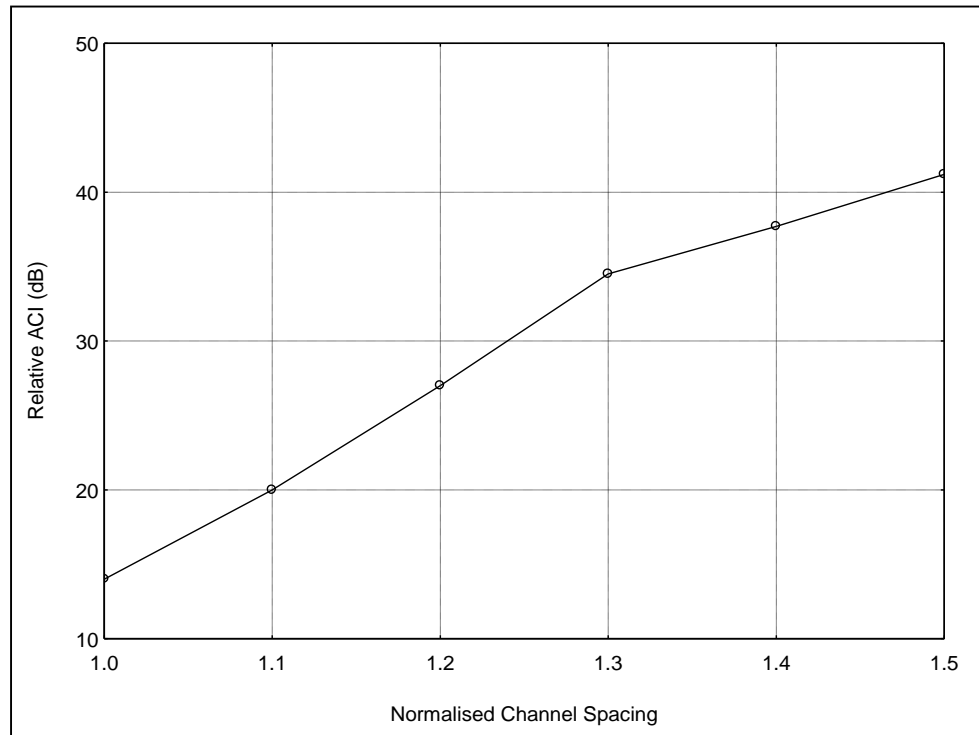


Fig. 5.1 Relative ACI vs channel spacing

With a receiver IF filter having BW=1.5, an adjacent rejection factor of around 40 dB has been achieved at a channel spacing of 1.5 times the symbol rate. The results shown in Fig.5.1 above confirm that the proposed CP-QFSK modulation causes significantly less ACI than the conventional (binary) GMSK, and hence is more spectrally efficient in a multichannel system.

5.1.2 Co-Channel Interference (CCI)

Another common source of distortion is that of co-channel interference from mobile systems using the same frequencies. This interference is caused by an interfering waveform appearing within the signal bandwidth. It can be introduced by a variety of ways, such as accidental transmissions, insufficient vertical and horizontal polarization discrimination, or by radiation spill over from an antenna sidelobe (low-energy beam

surrounding the main antenna beam). It can be brought about by other authorised users of the same spectrum [1]. It is quite important to attempt to quantify and assess the effects of such interference as this is potentially destructive source of distortion in a mobile system. A cellular system is the most sophisticated technique currently in use for area coverage. It is as mentioned in the first chapter based upon the principle of frequency re-use, whereby if a fixed number of radio channels are available for use for a given mobile communications system, they are divided into a number of sets. Each set being allocated for use in a small area called cell which is usually served by a single base station. For planning purposes, the service area is divided into cells in a regular fashion, often the hexagon is used. The distance between the centres of the nearest two cells which have the same frequency assignment is known as the re-use distance. The larger the re-use distance, the lower the interference due to common use of the same channel (CCI) [6].

It should be noted at this point, that a protection ratio can be defined. This is the minimum ratio of wanted to interfering signal power at which acceptable reception can be obtained. Digital schemes require less protection, since they are inherently binary by nature and errors are correctable. Cell size is determined by the coverage which is in turn decided upon by the signal strength in each cell, and if all cells are approximately the same size and each base station transmits the same power, then the co-channel interference is independent of the transmitter power. Co-channel interference can be experienced by both the base station and the mobile receivers in the centre cell. The interference is the sum of the interference from the individual cells surrounding the centre cell.

In the simulation , six interfering sources were combined with a transmission in the centre cell. The interference to the centre cell transmission was then measured by the

use of bit error rates. It was assumed that the transmission was from a base station at the centre of the cell to a mobile on the cell boundary. This effectively meant that the main transmission levels were minimised, whilst the co-channel interference was maximised, i.e., a worst case scenario was being considered.

The first step towards simulating this scenario was to use the CP-QFSK modem that has already been designed and used in the measurement of BER under AWGN channel in the previous chapter, as the system which transmits the desired useful signal. Blocks were then designed to simulate the interfering transmitters themselves. These were essentially based on the transmitting parts of the aforementioned CP-QFSK system from which the wanted useful signal is generated. To simulate the propagation path loss, an attenuator was introduced at the output of each interfering transmitter to account for the propagation loss between the transmitter and the receiving mobile handset. This configuration is shown below in the top-level block diagram of Fig.5.2.

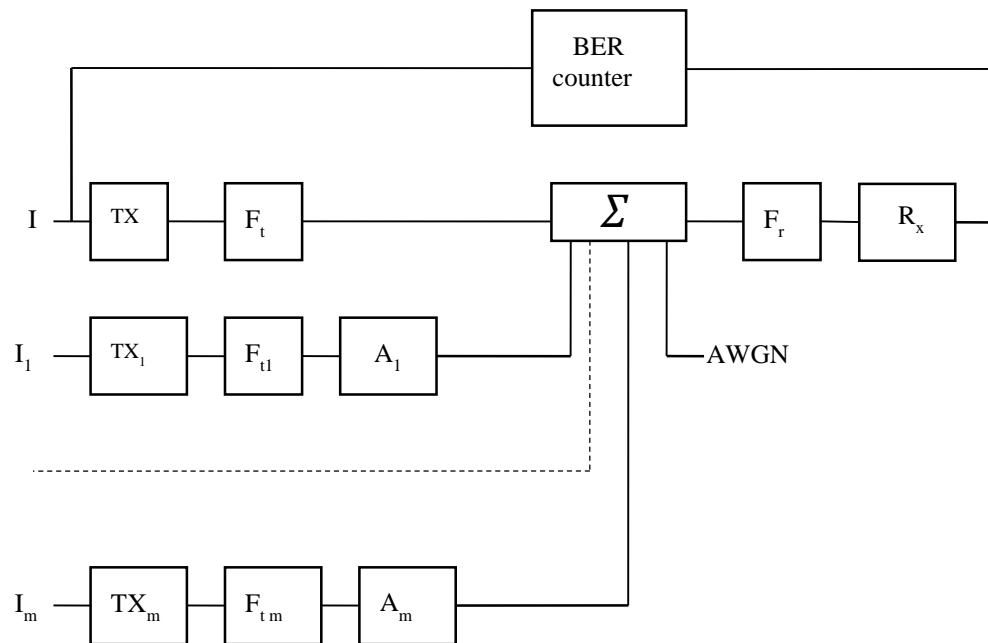


Fig. 5.2 Block diagram of the simulated CCI

In the above diagram, $I, I_1, I_2 \dots, I_m$ = digital signal inputs of the interfered and interfering transmitters, $TX, TX_1, TX_2, \dots, TX_m$ = interfered and interfering CP-QFSK transmitters, $F_t, F_{t1}, F_{t2} \dots, F_{tm}$ = transmit filters, A_1, A_2, \dots, A_m = attenuators, F_r = receive filter of the interfered system, RX = interfered CP-QFSK receiver.

All blocks were thoroughly tested prior to implementation in the main system. In this simulation scenario the attenuated interfering signals were then added to the wanted signal and AWGN by a process of simple addition. The combined signal was then demodulated and the regenerated data signal was input to the BER counter together with the source user data to have a measure of BER.

It is worth mentioning here that the integer seed of the user data of the wanted and interfering signals (I, I_1, \dots, I_m) were set to different large odd numbers to represent the variability in the data pattern being sent, and the parameters of all the modulators and the demodulator are the same as those which have been optimised in the last chapter.

BER against S/I has been plotted in Fig.5.3 where at each E_b/N_0 level, the S/I was varied in the range of 0-40 dB, and in each case the error rate was measured. This has been experimented having E_b/N_0 as a parameter in each case.

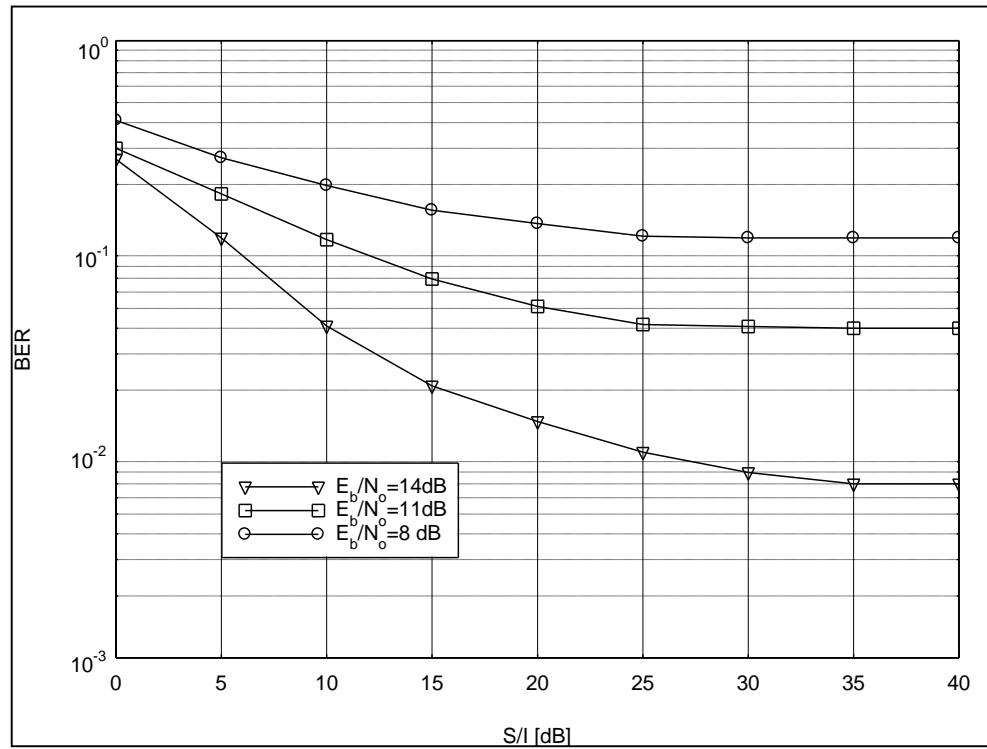


Fig.5.3 CP-QFSK system Performance under co-channel interference

The first point to note here is that the received signal suffers from significant level of interference i.e., the curves level off at high values of S/I, causing BER to rise over the tolerable value. Comparing these results with those obtained from the AWGN case reported in Fig.4.21 of the last chapter, it is obvious that to achieve a certain level of BER, a higher S/I ratio is required than the equivalent level of E_b/N .

5.2 CP-QFSK system performance in fading environments

Determination of the optimum system requires knowledge and modelling of the propagation environment as the mobile radio propagation channel places fundamental limitations on the performance of radio communications systems. So far we have examined the performance of the system under investigation in non-fading environments. The system performance under fading conditions is investigated next.

5.2.1 The Multipath Fading Channel

An inherent characteristic of a radio system is that it is difficult to restrict the radio signal to a single route. Often, significant signals are received by reflection and scattering from buildings, etc.: there are multiple paths from transmitter to receiver. Indeed in many systems, and especially in personal and mobile radio systems, it is rare for there to exist one strong line-of-sight path between transmitter and receiver. Usually all signals on these paths are subject to different delays, phase shifts and Doppler shifts, and arrive at the receiver in random phase relation to one another. The interference between these signals gives rise to a number of deleterious effects which are the most serious problems of the mobile and many other radio channels, and which are collectively known as multipath. The most important of these problems are fading and dispersion.

Fading is due to the interference of multiple signals with random relative phase. Constructive and destructive interference between them cause random variations in the amplitude of the received signal. This will in turn increase the error rate in digital systems, since errors will occur when the signal-to-noise-ratio drops below a certain threshold. If the transmitter or receiver is in motion, as is the case of a mobile radio system, then the relative phase shifts of the different paths will change with time, potentially quite rapidly.

The in-building environment is subject to an extremely harsh multipath conditions that may sometimes exceed the symbol length. A multipath propagation medium contains several paths by which energy travels from the transmitter to the receiver. There is a propagation delay and an attenuation factor associated with each path. In the invariant environment, the multipath components are static and arrive sequentially at the receiver,

where there are constructive or destructive interferences depending on the differential time delays, and on the differential phase. However, in real life we have a dynamic phenomenon in which both attenuation factors and propagation delays are continuously changing as a result of variations in the structure of the medium, giving rise to a highly complex time-varying transmission channel. When a signal with a finite bandwidth is radiated, the effects of multipath propagation will be different for each frequency component. If two frequencies are close, then the different propagation paths have approximately the same electrical length for both components, and their amplitude and phase variations will be very similar. As the frequency separation increases, the differential phase shifts along various paths are quite different at the two frequencies. Signals with a bandwidth greater than that over which the spectral components are affected in a similar way will consequently become distorted. The phenomenon is known as frequency-selective fading [7], and the bandwidth over which the spectral components are affected in a similar manner is known as the coherence bandwidth.

Since the wavelength is very short in the microwave frequencies, small variations in path length results in significant changes in the RF phase. These phases may be considered to be uniformly distributed between $(0, 2\pi)$. Hence, the movement of the receiver antenna can cause rapid fluctuations in the signal level. These rapid fluctuations in the signal level of the received signal are termed signal fading. The short term variation in the signal level, referred to as rapid fading, is due to the obstacles in close proximity to the receiver [8-11]. On the other hand, the long term variation, referred to as slow fading are due to movements over large distances that produce large variations in the overall path length between the mobile terminal and the base station. Multipath propagation creates some of the most difficult problems associated with the mobile radio environments [12, 13], namely:

- delay spread

- phase and amplitude variations

5.2.1.1 Delay Spread

In a digital system the delay spread due to reflections and scattering of electromagnetic waves causes each symbol to overlap with preceding and following symbols, producing ISI. The degree of ISI due to delay spread is dependent upon the bit rate, modulation level and transmission frequency. The bit rate and modulation levels set the symbol duration while transmission frequency sets the amount reflected power and the shape of the impulse response of the channel. The square of the impulse response of the channel is referred to as power delay profile (PDP). At high bit rates where the symbol duration is similar to delay spread in magnitude, the ISI due to multipath can be quite severe. Hence, delay spread sets the limit on the symbol rate in mobile radio channel. An estimation of the delay spread for wireless communication systems is provided in [14].

5.2.1.2 Rayleigh Fading

In indoor environments, because of the surrounding obstacles there is often no line-of-sight between the transmitter and the receiver. Communication is, therefore, mainly by means of multipath reflections and scattering of the electromagnetic waves from the surrounding obstacles. In the absence of the line-of-sight, the receiving signal is made up of a large number of component waves arriving at the receiver. Assuming that the reflections components and scattering consist of independent, randomly phased vectors with a random angle of arrival, then the probability density function of the envelope, from the central limit theorem [15] is

$$P_r(r) = \frac{r}{\sigma^2} e^{-\frac{r^2}{2\sigma^2}} \quad (5.1)$$

Which is a Rayleigh distributed with a mean power σ and $r^2/2$ is the short term fading power.

5.2.1.3 Rician Fading

When there are fixed scatters or signal reflectors in the medium or a direct line-of-sight in addition to the randomly moving scatters, the received signal no longer has a zero mean. The envelope of such a signal is Rician distributed and the channel is said to be Rician fading channel. The steady, non-random component alter the nature of the fading envelope and its statistics [16], and such envelopes can be represented as

$$P_R(r) = e^{-(r^2+s^2)/(2\sigma^2)} I_0\left(\frac{rs}{\sigma^2}\right); \quad r \geq 0 \quad (5.2)$$

The probability of a deep fade in Rician fading channels with a relatively large K-factor (the ratio of line-of-sight power to the echo power oftenly quoted in dB) i.e. mild multipath conditions, is extremely small, virtually non-existent [17].

5.3 Characterisation of the Multipath Fading Channel

Several studies have been reported on propagation channels, some based on propagation simulations [18, 19] and others reporting measurements [9, 20]. In modelling the channel, the propagation medium is assumed to act as a linear filter [21, 22] such that if $s(t)$ is the transmitted signal, the received signal $x(t)$ is equal to

$$x(t) = \sum_{i=1}^m \alpha_i(t) s(t - \tau_i(t)) \quad (5.3)$$

Where, $\tau_i(t)$ is a time-varying propagation delay, and $\alpha_i(t)$ is the attenuation factor.

If Δx_i is the path length difference between the shortest path and the i^{th} path at time instant t , we get $\tau_i(t) = \Delta x_i / c$, where c is the velocity of light. The path length spread X_s is the largest value of Δx of paths with non-negligible responses.

Assuming that $s(t)$ is a carrier signal with frequency f_c without any information signal modulated on it. If E_s is the average symbol energy, then

$$s(t) = \sqrt{E_s} \cdot e^{j2\pi f_c t} \quad (5.4)$$

so, $x(t)$ can be written as

$$x(t) = \sqrt{E_s} \left[\sum_{i=1}^m \alpha_i(t) e^{-j2\pi f_c \tau_i(t)} \right] e^{j2\pi f_c t} \quad (5.5)$$

Now the equivalent low-pass received signal $r(t)$ after demodulation is

$$r(t) = \sqrt{E_s} \sum_{i=1}^m \alpha_i(t) e^{-j2\pi f_c \tau_i(t)} \quad (5.6)$$

The argument of $r(t)$ can be considered to be uniformly distributed over $[0, 2\pi]$.

Because $\alpha_i(t)$ is identically distributed for all i and does not depend on $e^{-j2\pi f_c \tau_i(t)}$, the mean value of the complex signal $r(t)$ is 0.

The central limit theorem states that if m approaches ∞ , then $r(t)$ is a complex-valued variable with Gaussian probability distribution function. More specifically, both the imaginary and the real component of $r(t)$ are independent zero-mean Gaussian distributed variables, so, at any instant t , the envelope

$$|r(t)| = \sqrt{R\{r(t)\}^2 + I\{r(t)\}^2} \quad (5.7)$$

is Rayleigh-distributed. In this model, $s(t)$ is transmitted and a complex AWGN component $n(t)$ is added, so the received signal can be described as

$$r(t) = \alpha(t)e^{-j\varphi(t)}s(t) + n(t) \quad (5.8)$$

The functions $\alpha(t)$ and $\varphi(t)$ are called the Rayleigh fading envelope and the random phase fluctuation respectively and they form together the channel state of a Rayleigh fading channel at which the signal component is multiplied with a Rayleigh distributed variable $\alpha(t)$ with variance $E\{|\alpha(t)|^2\} = 1$, with white Gaussian noise with variance $\sigma^2 = N_0/2$ is added. Typical parameters of the multipath propagation are, the multipath intensity profile $\phi_c(\tau)$ and the multipath spread T_m (the maximum delay τ over which $\phi_c(\tau)$ is essentially non-zero). The reciprocal of multipath spread T_m is the coherence bandwidth [8].

$$(\Delta f)_c = \frac{1}{T_m} \quad (5.9)$$

The coherence bandwidth is a measure for the frequency selectivity of the channel. Since $(\Delta f)_c$ is directly related to T_m , the frequency selectivity is closely connected to the multipath propagation phenomenon. A frequency selective channel is a channel for which $(\Delta f)_c$ is small in comparison to the bandwidth B of the transmitting channel. Conversely, a flat fading channel (or frequency non-selective channel) is a channel for which $(\Delta f)_c$ is large compared to B .

5.4 The Multipath Fading channel Modelling and Simulation

The indoor propagation measurements and results at and around 1.8 GHz performed in indoor environments, particularly in typical DECT environments such as an office type have indicated that delay spreads in the range of 100ns to 200ns (0.2 of the symbol duration) are likely to be encountered in such environments [22-25] yielding the channel coherence bandwidth being larger than that of the transmission bandwidth of the designed CP-QFSK system, and consequently the received signal envelopes for different frequency components would vary similarly due to the frequency separation being smaller than the coherence bandwidth of the propagation channel giving rise to the channel being frequency non-selective channel i.e. flat fading channel. Another aspect of such narrowband channel concerns the phase rotation introduced as a result of the very close arrivals (almost instantly) of the multipath components and in turn the resultant phasor is having almost a constant phase. However, a small phase rotation will appear in practice, but it varies very slowly. This slow varying characteristics of

the phase in the narrowband channel permits the assumption that the phase remains constant during the signal transmission (or at least for a very large part of it). Hence in modelling the narrowband channel only the magnitude variations are considered.

5.4.1 Rayleigh Fading Simulator

The fading simulator employed here is based on the principle presented in [1, 26]. The multipath channel is simulated by 6-tapped-delay-line FIR filter as shown in Fig. 5.4. The excess delays and magnitudes of echoes are defined relative to the line of sight (LOS). The amount of multipath interference in total is adjusted by choosing the maximum echo amplitude.

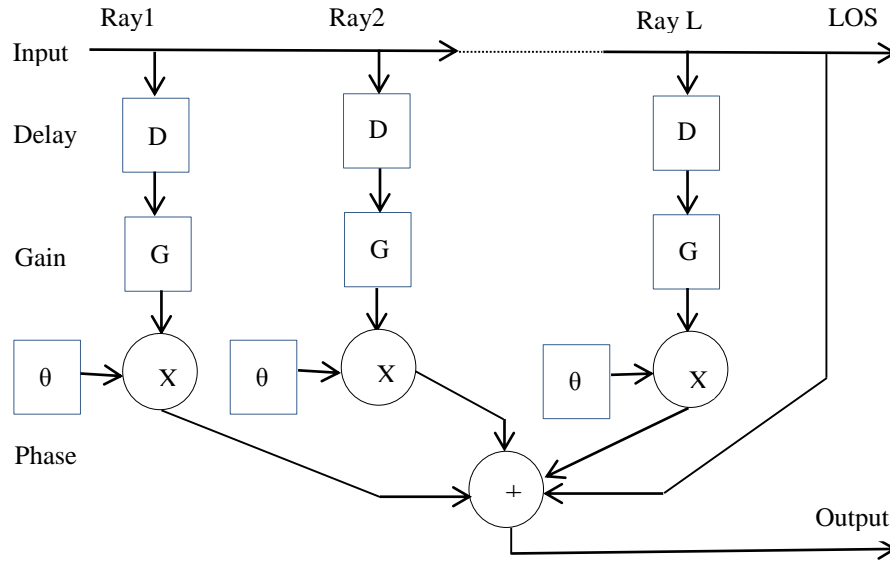


Fig. 5.4 PDP model

The minimum echo amplitude is set to -40dB. The phases of all components are normalized, hence, the amplitudes of echoes are kept constant in the simulation and the resultant phasor varies in magnitude and phase according to a Rayleigh or Rician distribution. The echo phases are defined by random numbers drawn from a uniform random number generator between 0 and 1 and multiplied by 2π . The channel consists

of multipath components combining at the receiver and resulting in fading. The signal strength at the receiver obeys Rayleigh or Rician statistics since the sum of Rayleigh variants is another Rayleigh variant (central limit theorem).

The generated output of the fading simulator is shown in figure 5.6 and it closely follows a Rayleigh probability density function.

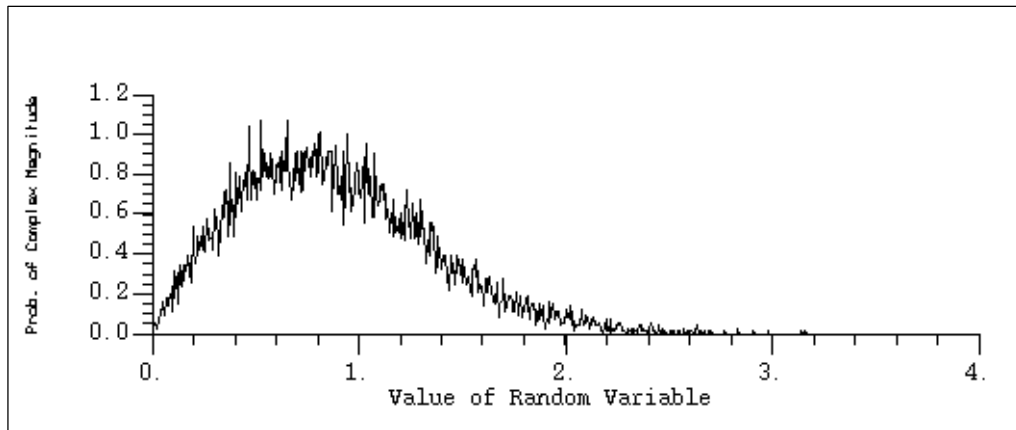


Fig.5.5 Measured Rayleigh PDF

5.4.2 Performance of CP-QFSK in Rayleigh Fading Channel

In order to obtain reasonable BER measures, accurately evaluate the channel effects, and to simulate an average call duration of 2 minutes the simulation was carried out for 12000 DECT's frame time each simulation test run. For each frame duration, i.e. 10 ms, one of the 24 time slots was simulated to assess the quality of the link for a single user. The BER was recorded for various E_b/N_o and plotted as shown in fig.5.7 for a channel with single and two Rayleigh fading path models. A high irreducible error rate caused by the Rayleigh fading conditions especially in the case of 2-path Rayleigh fading case can be seen from Fig.5.7. It is apparent from these simulation results that at typical delay spreads, between 100ns to 200ns, the introduction of some adaptive scheme such as diversity reception would be inevitable.

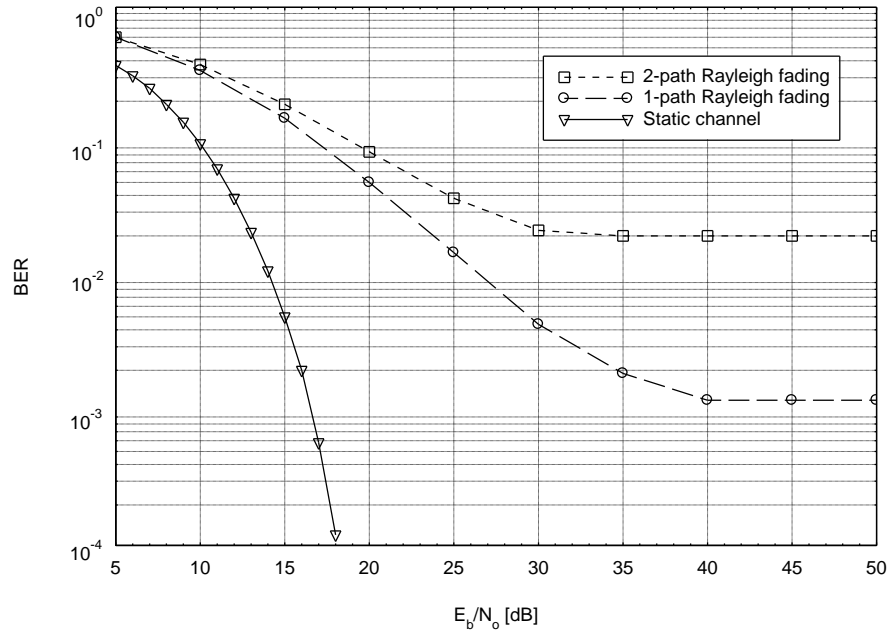


Fig.5.7 Q-CP-FSK performance in static and Rayleigh fading channels

Summary

This chapter has evaluated the CP-QFSK system performance in the portable communications channel. It started by assessing the adverse effects of non-fading conditions, such as adjacent channel interference and co-channel interference, and then the fading effects. Simulation output results demonstrated that an adjacent channel rejection factor of around 40 dB has been achieved at channel spacing of 1.5 times the symbol rate when the DECT system standards stipulate far less rejection limit criterion (25-30 dB), yielding, CP-QFSK modulation system outperforms the conventional GMSK system as it causes less ACI and hence is more spectrally efficient in a multi-channel system. However, this system has proved to be not co-existing well with other interferers when it was tested under CCI conditions, as can be seen from Fig. 5.3.

When the system was put to test under fading conditions, the simulation output results showed that there has been a severe degradation in system performance caused by

Rayleigh fading particularly in the case of 2-path compared to the static case, leading to a high irreducible error rate. This could be perceived from Fig. 5.7 as it reveals that there exists a noise floor of about 40 dB, i.e. irreducible error rate of less than 6.10^{-3} when more than 1-path fading exist.

Thus far, it is concluded that the CP-QFSK system is rather an interference limited than noise limited. Hence, some measures have to be undertaken in order to alleviate these impairing effects and improve the system performance quality. Such measures would be looked at in the next chapter.

REFERENCES

- [1] BERNARD SKLAR.; "Digital Communications: Fundamentals and Applications".
Second Edition, Prentice Hall PTR, 2001.
- [2] SWAIN R.S., and HOLMES D.W.J.; "The Digital European Cordless
Telecommunications Common Air Interface"; British Technology Journal, Vol. 8,
NO. 1, January 1990.
- [3] ETR 015; " Digital European Cordless Telecommunications Reference
Document".
- [4] RES 3-R (91) 122; " DECT Spurious Emissions, Philips Research, UK. ".
- [5] ETR 042 Radio Equipment and Systems (RES); A Guide to DECT Features, July
1992.
- [6] MORTEN TOLSTRUB; "Indoor Radio Planning; A Practical Guide for GSM,
DCS, UMTS and HSPA". First Edition, John Wiley & Sons, Ltd, 2008.
- [7] PROAKIS, J. G.; " Digital Communications ", 4th Edition. New York, McGraw
Hill series in Electrical Engineering, 2001.
- [8] PARSONS, J. D.; "The Mobile Radio Propagation Channel", London, Pentech
press publishers, 1992.
- [9] BULTITUDE, R. J. C., MAHMOUD, S. A. and SULLIVAN, W. A.; " A
comparison of indoor radio propagation characteristics at 910 MHz and 17.5
GHz". IEEE Journal in Selected areas in Communications, Vol. SAC-7, pp. 20-
30, 1989.

-
- [10] BURR, A. G.; "The Multipath problem: an overview". IEE Colloquium on Multipath Countermeasures, Colloquium Digest 1996/120, London, 23 May 1996.
- [11] MOHAMED IBNKAHLA; "Signal Processing for Mobile Communications Handbook.". CRC Press LLC, 2005.
- [12] KRASNY L., ARSLAN H., KOILPILLAI D, and CHANNAKESHU S.; "Doppler Spread Estimation in Mobile Radio Systems". Proceedings of IEEE WCNC Conference, Vol. 5, no. 5, pp. 197-199, May 2001.
- [13] LEE, W. C. Y. ; "Mobile Communications Design Fundamentals". Howard W Sams and Co. Macmillan Inc. Indiana USA, 1986.
- [14] ARSLAN H. and Yucek T.; "Delay Spread Estimation for Wireless Communication Systems". Proceedings of the eight IEEE Symposium on Computers and Communications (ISCC 2003), pp. 282-287, Antalya, Turkey, July 2003.
- [15] LATHI, B.P. ; "Modern Digital and Analogue Communication Systems.", New York, London, Holt Rinehart and Winston, 1983.
- [16] RICE, S. O. ; "Mathematical Analysis of Random Noise.", Bell Systems Technology Journal, Vol. 23, 24, 1945.
- [17] SALEH, A.; RUSTAKO, A. J. and ROMAN, R.; "Distributed Antennas for Indoor Radio Communications". IEEE Transactions on Communications, Vol. COM-35, pp. 1245-1251, December 1987.
- [18] GENESH, R. and PAHLAVAN, K.; "Statistical Modelling and Computer Simulation of Indoor Radio Channel". IEEE Proceedings-I, Vol.138, N0. 3, pp. 153, June 1991.
- [19] SPAIN (UPC); "Further Simulation Results at 60 GHz". COST 231 TD (90) 96/WG3, September 1990.

- [20] RAPPAPORT, T. S.; "The Wireless Revolution". IEEE Communications Magazine, pp. 52-71, November 1991.
- [21] CHUANG, C. I. J.; "The Effect of Time Delay Spread on Portable Radio Communications Channels with Digital Modulation ". IEEE Journal on Selected areas in Communications, Vol. 5, No. 5, pp. 879-889, June 1987.
- [22] DEVASIRVATHAM, D. M. J.; "Time Delay Spread Measurements at 850MHz and 1.7GHz inside a metropolitan office building.", Electronics Letters, Vol. 25, No. 3, pp. 194-196, 1989.
- [23] Simon M. and Alouini, M-S.; "Digital Communications over Fading Channels: A Unified Approach to performance Analysis". John Wiley, New York, 2000.
- [24] MOLKDAR, D.; "Review on Radio Propagation into and within building. "; IEE Proceedings-H, Vol. 138, No.1, pp. 61-73, February 1991.
- [25] ANDERSEN, P.C., HOUEN, O. J., PETERSEN, K. T., FREDSKILD, H. and ZARNOCZAY, I.; "Delay Spread Measurements at 2 Ghz."; EURO-COST 231 TD (91) 29, LUND, June 4-7 1991..
- [26] TAUB, H., SCHILLING, D. L.; "Principles of Communication Systems."; New York, McGraw-Hill, 1968.

CHAPTER 6

Adaptive and Non-Adaptive Techniques

6.1 The Need for Adaptive Techniques

In a multi-path fading channel such as the DECT indoor channel, delay spread due to the variation of the path lengths of echoes arriving at the receiver causes inter symbol interference and puts an upper limit on the maximum available bit rate. The simulation results presented in the last chapter showed an excessive signal fading and intolerable amount of distortion into the signal-band that led to significant deterioration in the CP-QFSK system performance. This necessitates that these impairments need be mitigated or minimised. Simply increasing the transmitter power does not overcome the channel effects. Simulation and analytical results carried out by Sexton, Chaung, and Hummels [1-3] also have shown that without the use of adaptive techniques, the maximum available bit rate is limited by $R_b \leq 0.1/\sigma$, where σ is the rms delay spread. Also, analysis and simulation presented in [4,5] have shown that applying high bit rate constant envelope modulation schemes to digital land-mobile radio, without the use of adaptive techniques, makes such systems capable of tolerating rms delay spreads only of the order of 100ns, which is equivalent to a delay spread in extremely small rooms.

A particular advantage of multilevel modulation scheme accrues if the TDMA multilevel signal has a symbol rate sufficiently low that the mobile radio channel exhibits flat fading rather than frequency selective fading. Thus by ensuring that the modulation bandwidth is less than the coherence bandwidth delay dispersion of the spectral components in the received signal is avoided and the flat fading can be combated by means of diversity techniques [6].

From previous DECT indoor radio channel investigations, it has been found that antenna diversity not only reduces the fading probability, but it also mitigates the effects of time dispersion for a Quasi-narrow-band radio channel. This is due to the correlation between instantaneous power and instantaneous rms delay spread [7].

Among the most effective and perhaps the simplest adaptive techniques used to combat fading effects and to enhance the system performance up to a required level is the diversity reception. The theoretical diversity gain in terms of signal distribution is thoroughly investigated and analysed in [8]. Antenna diversity is a well-known method used to reduce the short-term fading probability and consequently the required fading margin. Hence, this part of the research work focuses on implementing diversity techniques for the CP-QFSK system and assessing the gain acquired in order to maintain an acceptable system performance.

6.1.1 Diversity Reception Techniques

The salient feature of wireless transmission is the randomness of the communications channel, which leads to random fluctuations in the received signal commonly known as fading. This randomness can be exploited to enhance performance through diversity. Diversity is broadly defined as the method of conveying information through multiple independent instantiations of these random fades. There are several forms of diversity, however, in this chapter we focus our attention on spatial diversity.

The advantages of diversity reception in high bit rate digital communications systems operating over multi path fading channels have been investigated extensively in [9, 10], and a variety of techniques have been reported for a variety of applications. It has been reported in the literature that the performance of FSK can be considerably improved by using diversity technique. The ability of diversity systems to reduce the duration of

fades implies that another advantage to be gained from the use of diversity is a significant reduction in the lengths of error bursts. Rayleigh fading tends to cause a burst of errors when the signal enters a deep fade, and since diversity tends to smooth out these deep fades, it not only reduces the error rate, but also affects the error pattern by causing the errors to be distributed more evenly throughout the data stream. This in turn makes the error easier to cope with, and if error correcting codes are used to improve error rate, much shorter codes can be used in conjunction with diversity than would be necessary without it [11-13].

The envelope of a single-frequency radio wave propagation through a multi path channel fluctuates in time. These random fluctuations in time may result in very low signal power at the receiver, sometimes below the minimum useful level. When the signal power is below a minimum useful level, the channel is said to be in a deep fade, resulting in very large errors at the receiver. The basic idea behind diversity reception is that if two or more radio signals are created sufficiently separated in space, frequency, time or polarisation, then fading in these channels will virtually be uncorrelated, and the diversity technique makes use of such received signals to improve the realised SNR or other performance criterion. If the same information is received redundantly over two or more statistically independent fading channels, then the probability of all of the channels being in fade simultaneously is much smaller than the probability of a single channel being in fade. With intelligent processing each symbol decision can be based primarily on the version received at high SNR, thereby greatly reducing the overall error rate. For L^{th} order diversity with equal mean SNR in each branch, the probability of error is the L^{th} power of the probability of error for a single non-diversity fading channel [14,15].

Diversity techniques can be categorised by at least six methods: Angle diversity, Time diversity, Frequency diversity, Polarisation diversity, Space diversity and Multipath diversity. Frequency diversity uses the fact that the fading signals associated with different frequencies are uncorrelated. However, frequency diversity is not a viable proposition for conventional mobile radio, since the coherence bandwidth is quite large (several MHz in some circumstances), and the frequency spectrum can not be used efficiently.

Other such possibilities are polarisation diversity which rely on the scatterer to polarise the transmitted signal, and Field diversity which use the fact that the electrical and magnetic components of the field at any receiving location are uncorrelated. Both these methods have their difficulties with the antenna design. Space diversity methods are relatively simple to implement and most convenient to use with mobile radio systems, and do not require additional frequency spectrum. The basic requirement is that the spacing of the receiving antennas is chosen so as to individual signals are uncorrelated at any time [16]. This can take place at the base station or at the mobile unit as with isotropic scattering, the autocorrelation coefficient of the signal envelope falls to a low value at distances greater than about a quarter wavelength, and so almost independent samples can be obtained at a mobile from antennas sited this far. At VHF and UHF the spatial separation is less than a meter. At 900 MHz and above, it may be feasible even on hand held equipment [17].

The received signal at a portable terminal moving through a scattered field fluctuates both in amplitude and phase. For a receiver using an FM limiter-discriminator detector, the amplitude fluctuations cause fluctuations in the noisy output from the discriminator which can be reduced by implementing diversity scheme [8].

6.1.2 Diversity Combining Methods

The method of combining the n received signals is important and has an effect on the performance improvement. The most often used diversity combining techniques which can be applied to indoor portable radio communications systems are scanning combining, Selection Combining, Equal Gain Combining (EGC) and Maximum Ratio Combining (MRC). These methods are listed in increasing order of performance improvements. Among these different combining schemes, there is a trade-off between performance and complexity.

Selection diversity is the simplest of all diversity systems. It works by selecting the strongest incoming signal (the best available diversity path) among n diversity branches. This nevertheless requires the estimation and comparison of the quality indicators of all available ones, and in ideal system, the signal with the highest instantaneous SNR is selected. However, practical systems usually select the branch with the highest signal plus noise.

The EGC and MRC methods use all the outputs of the receiver then combining them to produce an overall output [18-20]. However, the EGC weighs all the channels equally prior to combining them, whereas MRC weighs each channel in terms of its SNR before combining. This process of combining may be implemented at different points at the receiver producing different levels of complexity and requiring different amounts of circuitry repetition in the channel. If combining takes place after detection, the system is known as “post-detection combiner”, otherwise it is known as “pre-detection combiner”. For the former method, more hardware repetition is required but it is simpler as co-phasing of the receiver input signals is not necessary, since after demodulation all the baseband signals are in phase. For the latter, there is less hardware

repetition of circuitry. However, the complexity is greater as signals must be co-phased before combining [17]. Hence, post-detection MRC diversity technique will be employed in the CP-QFSK system to mitigate the effects of fading and time dispersion as it provides the largest improvement in signal to noise ratio and BER reduction over the other diversity schemes.

6.1.2.1 Maximal Ratio Diversity Receiver

The MRC diversity reception technique simulated here is performed using post-detection combining. Figure 6.1 below shows a block diagram of post-detection MRC combiner:

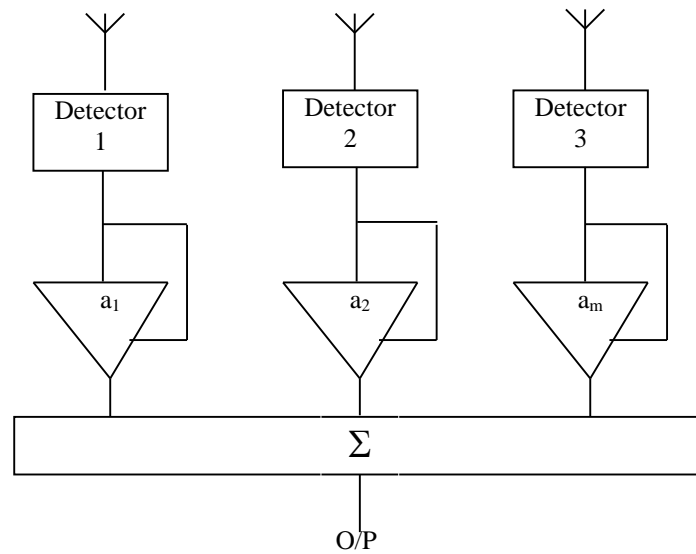


Fig.6.1 Block diagram of post detection MRC combiner

The simplest diversity receiver is a system with two branches, and further improvements in system performance can be achieved by increasing the number of branches. However, the largest improvement in performance is achieved by increasing the number of branches from 1 (no diversity) to 2. With more than 2 branches, the complexity of receiver design increases significantly with a diminishing return in

receiver performance improvement. For this reason only 2-branch system is simulated here.

A maximal ratio combining receiver has been constructed using the basic CP-QFSK receiver previously designed and the maximal ratio combiner. The MRC receiver consists of 2 receiving branches with the combining being performed after the limiter discriminator detection as shown in fig.6.2. In the simulation, The SNR is measured directly after the receiver filter by switching on and off the noise generator and switching on and off the transmitter output and hence the signal. It is also necessary to set up the test system for 0dB SNR as a reference level for all other measurements, this is achieved as follows :

The average signal power is

$$\bar{P}_s = \frac{1}{K} \cdot \sum_{m=1}^K S_m^2 \quad (6.1)$$

Where K is the total number of discrete samples, and S is the discrete signal sample level. The noise power is found out similarly but the noise only is passed to the receiver filter. The average noise power is

$$\bar{P}_n = \frac{1}{K} \cdot \sum_{m=1}^K N_m^2 \quad (6.2)$$

N is the discrete noise sample level. Therefore, the SNR in dB of the system is

$$SNR = 10 \log_{10} \frac{\bar{P}_s}{\bar{P}_n} \quad (6.3)$$

In order to relate the value of E_b/N_0 in dB to that of the measured SNR as measured in the simulation the following equation is used

$$10 \log_{10} \frac{E_b}{N_0} = 10 \log_{10} \frac{\bar{P}_s}{\bar{P}_n} + 10 \log_{10} B_N \cdot T_b \quad (6.4)$$

Where B_N is the equivalent noise bandwidth of the receiver filter and T_b is the bit period. The Rayleigh fading channel previously designed, where the time variant fading nature of the channel is realised by uniformly distributed random phases, has been used by employing two versions of this channel with different seed values of the random number generators that update the set of random phases in each channel.

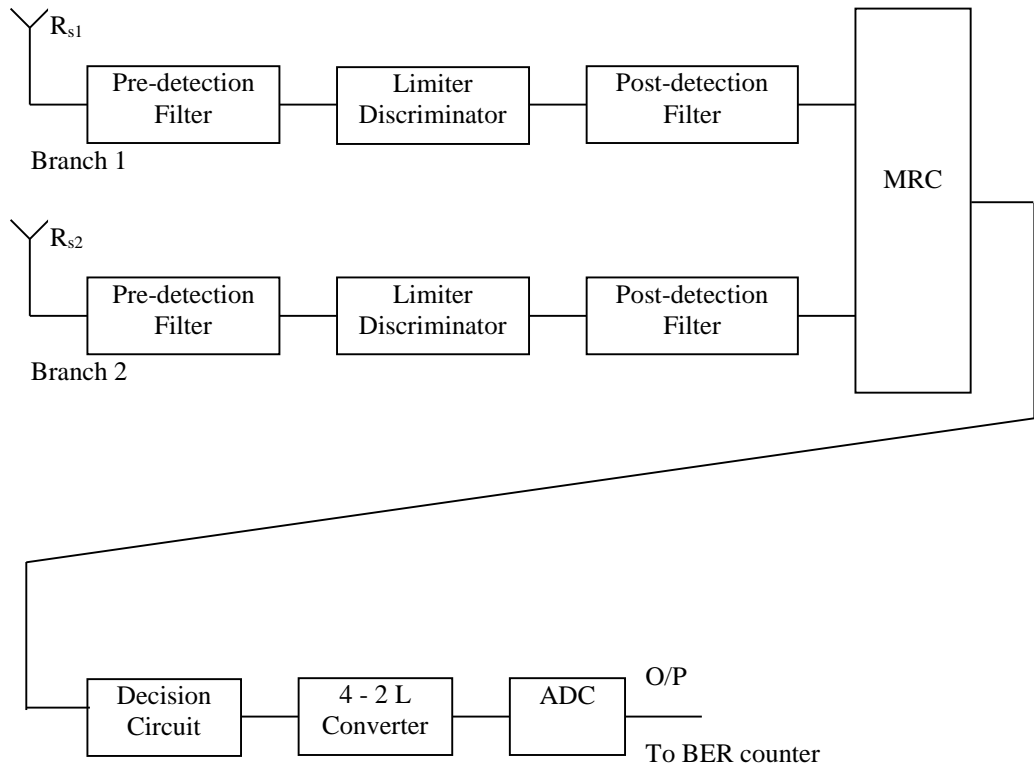


Fig.6.2 Block diagram of post-detection MRC receiver

With maximal ratio combining each receiver signal is weighed in proportion to its own signal voltage to noise power ratio before summation. Figure 6.3 shows the block diagram of the 2-branch MRC implementation:

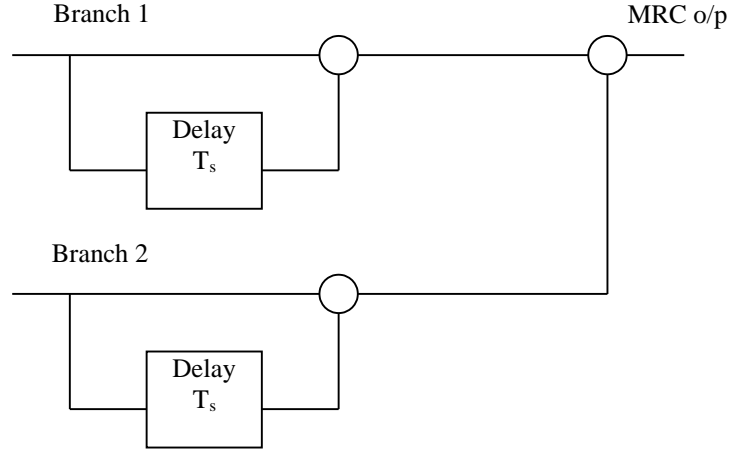


Fig. 6.3 Block diagram of the 2-branch MRC implementation

The combined MRC output signal envelope is equal to:

$$r_{mrc} = \sum_{k=1}^m a_k \cdot r_k \quad (6.5)$$

Where a_k , is the branch weighting factor, r_k is the branch signal envelope and r_{mrc} is the output of the combiner. The total output noise can be written as:

$$N_{tot} = N \sum_{k=1}^m a_k^2 \quad (6.6)$$

Where N is the noise power of an individual branch. The resulting SNR is:

$$\gamma_{mrc} = \frac{r_{tot}^2}{2N_{tot}} \quad (6.7)$$

The weighting factor $a_k = r_k / N$.

The output SNR is equal to the sum of the SNR's of the branch signals and is the best that can be achieved by any linear combiner. The simulation of the above 2-branch post-detection MRC system was run for quite sufficient length of time to ensure enough number of errors was accumulated to obtain at least a BER of 10^{-5} . The output of the simulation is exhibited graphically in Fig. 6.4 below

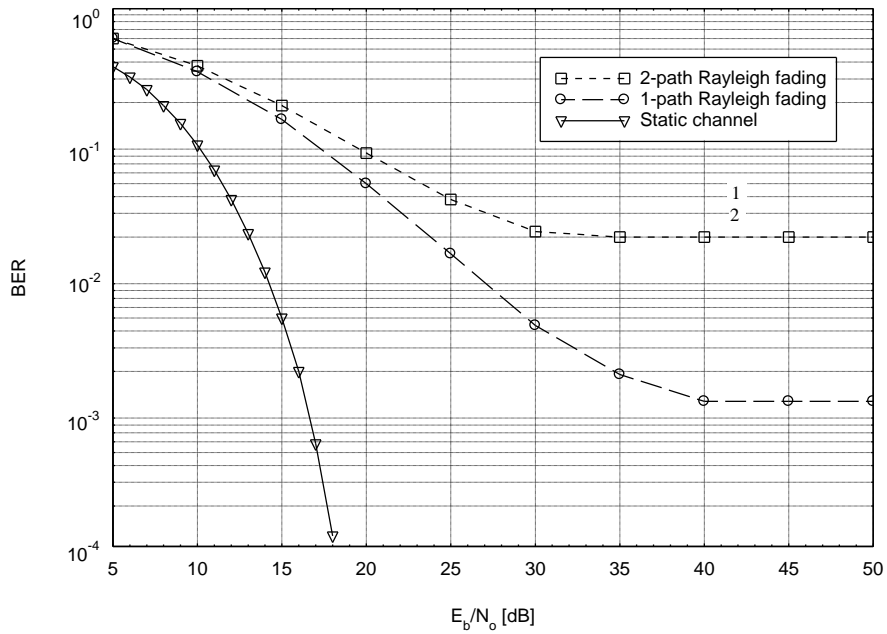


Fig 6.4. Performance of MRC diversity CP-QFSK receiver

Fig. 6.4 reveals that there is a significant performance improvement obtained when a 2 branch maximal ratio diversity CP-QFSK receiver was employed. This system provides a diversity gain of about 5 dB on average.

6.2 The Need for Non-adaptive Techniques

When digital data is transmitted over a noisy channel, there is always a chance that the received data will contain errors due to mobile terminals having small antennas and are usually not provided with adequate RF sensitivity, and the power is limited because of the use of handheld terminals it is difficult to achieve the desired carrier to noise ratio. Clearly an extra gain must be provided. The user generally establishes an error rate above which the received data are not usable. If the received data will not meet such requirement, one solution is the use of error-correction coding to overcome signal degradation due to channel characteristics and hence reduce errors to a level at which they can be tolerated. In mobile applications, coding is often used.

The use of coding will introduce a gain, which is essential to achieve a link margin that will provide good quality links. This coding gain can be expressed in decibels in the required E_b/N_0 to achieve a specified error performance of an error correcting coded system over an un-encoded one with the same modulation scheme [21].

6.2.1 Error Control Coding in Communications Systems

Error Control coding is concerned with methods of delivering information from a source to a destination with a minimum of errors. A coding technique in general is of two types: source coding and channel coding. The source coding technique refers to the encoding procedure of the source information signal into digital form. On the other hand, channel coding is applied to ensure adequate transmission quality of the signals. Channel coding is a systematic approach for the replacement of the original information symbol sequence by a sequence of code symbols in such a way as to permit its reconstruction. Here, attention is focused on the channel encoding technique. Channel

coding can be classified into two major areas: waveform coding and structured sequences. The objective of waveform coding such as M-ary signalling, antipodal, orthogonal, bi-orthogonal, and trans-orthogonal signalling is to provide an improved waveform set so that the detection process is less subject to errors. Structured sequence coding, such as the block and convolutional coding schemes, deal with transforming data sequences into better sequences having ordered redundancy in bits. The redundant bits can then be used for the detection and correction of errors. Here our focus would only be on the structured sequences coding [6].

The early theoretical work demonstrated in a landmark paper of Shannon stated that by proper encoding of the information, errors induced by a noisy channel or storage medium can be reduced to any desired level without sacrificing the rate of information transmission or storage [22]. Essentially, he proved that if the data source rate (R_m) is less than the channel capacity (C), communication over a noisy channel with an error probability as small as desired is possible with proper encoding and decoding. The price paid for reducing the error rate is increased complexity and bandwidth (B). In the AWGN channel the channel capacity is

$$C = B \cdot \log_2 \left(1 + \frac{P}{N_0 B} \right) \quad (6.8)$$

Where P is the received signal power and N_0 is the single-sided noise power spectral density. Substituting $P = E_b \cdot R_m$ and normalizing by the bandwidth B in the above formula results in

$$\frac{C}{B} = \log_2 \left[1 + \frac{E_b}{N_0} \left(\frac{R_m}{B} \right) \right] \quad (6.9)$$

Since Shannon's work, a great deal of effort has been expended on the problem of devising efficient encoding and decoding methods for error control in a noisy environment. The entire field of error control is devoted to the development of techniques to achieve the performance that Shannon proved possible [23].

Recent developments have contributed toward achieving the reliability required by today's high-speed digital systems, and the use of coding for error control has become an integral part in the design of modern communication systems and digital computers [24].

Error control can be provided by introducing redundancy into transmissions. This means that more symbols are included in the message than are strictly needed just to convey the information, with the result that only certain patterns at the receiver correspond to valid transmissions. Once an adequate degree of error control has been introduced, the error rates can be made as low as required by extending the length of the code, thus averaging the effects of noise over a long period. Experience has shown that to find good long codes is more easily said than done. Present-day practice is not to use codes as a way of obtaining the theoretical channel capacity but to concentrate on the improvements that can be obtained compared with uncoded communications. Thus the use of coding may increase the operational range of a communications system, reduce the error rates, reduce the transmitted power requirements or obtain a blend of all these benefits [25]. Apart from the variety of codes that are available, there are several general techniques for the control of errors and the choice will depend on the nature of the data and the user's requirements for error-free reception.

The most complex techniques fall into the category of forward error correction, where it is assumed that errors will occur and a code capable of correcting the assumed errors is applied to the messages. Alternatives are to detect errors and request retransmission,

which is known as retransmission error control, or to use inherent redundancy to process the erroneous data in a way that will make the errors subjectively unimportant. The latter technique is not considered here, rather, this chapter focuses on forward error correction, and in particular, the BCH codes, which are among the most important block codes available, since they can achieve significant coding gain and also the complexity of their decoders is such that they are implementable even at high speeds [23].

The subjects of information and coding theory are extensively treated in literature. The discussion here is brief and is intended to be introductory. References [26] through [30] provide excellent exposition of the subject.

Error-correction coding is essentially a signal processing technique that is used to improve the reliability of communication on digital channels. There exists many different forms of coding schemes, but they all share the following two common features :

1. Use of redundancy. Coded digital messages always contain extra or redundant symbols. These symbols are used to accentuate the uniqueness of each message. They are always chosen so as to make it very unlikely that the channel disturbance will corrupt enough of the symbols in a message to destroy its uniqueness. In order to correct errors in a message represented by sequence of n binary symbols, then it is absolutely essential not to allow the use of 2^n possible sequences as being legitimate messages. Thus, to correct all patterns of t or fewer errors, it is necessary for every legitimate message sequence to differ from every other legitimate message sequence in at least $2t + 1$ positions. The number of positions in which any two sequences differ from each other is referred to as Hamming distance, d , between the two sequences. The smallest

value of d for all pairs of code sequences is called the minimum distance of the code and is designated as d_{min} .

2. Noise averaging. This averaging effect is obtained by making the redundant symbols depend on a span of several information symbols. It has been proven in [19] that for a fixed block error rate, the fraction of errors that must be corrected decrease with increasing block length, which indicates the potential for performance improvement that is obtained through noise averaging.

The function of the two new elements i.e. the encoder and the decoder will be discussed in the succeeding sections:

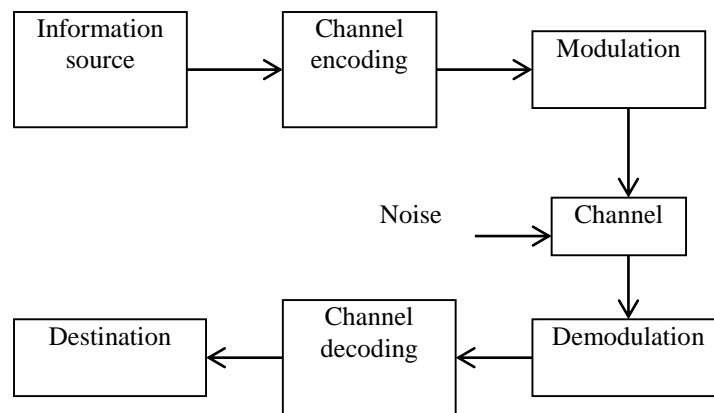


Figure 6.5 Block diagram of a coding system

There are two different types of codes in common use today, block codes and convolutional codes. The distinguishing difference between the encoders of these two codes is the presence or absence of memory. Conceptually, the encoder for a block code is a memoryless device which maps a k -symbol input sequence into an n -symbol output sequence that contain more symbols than the input, i.e. redundancy has been added. The term “memoryless” indicates that each n -symbol block depends only upon a specific k -symbol block and on no others. It does not mean that the encoder does not contain memory elements. This type of encoder can be implemented with a

combinational logic circuit. A commonly used description of a code is the code rate

(R), which is the ratio of input to output symbols in one frame ($R = k/n$). A low code rate indicates a high degree of redundancy, which is likely to provide more effective error control than a higher rate at the expense of reducing the information throughput.

The encoder for a convolution code is a device with memory that accepts binary symbols in sets of k_0 and outputs binary symbols in sets of n_0 . Each set of n_0 output symbols is determined by the current input set and a span of v of the proceeding input symbols. The memory span of the encoder is, therefore, $v + k_0$ input symbols. The parameter $v + k_0$ is often referred to as the constraint length of the code. A general block diagram of an encoder is presented in figure 6.6 below:

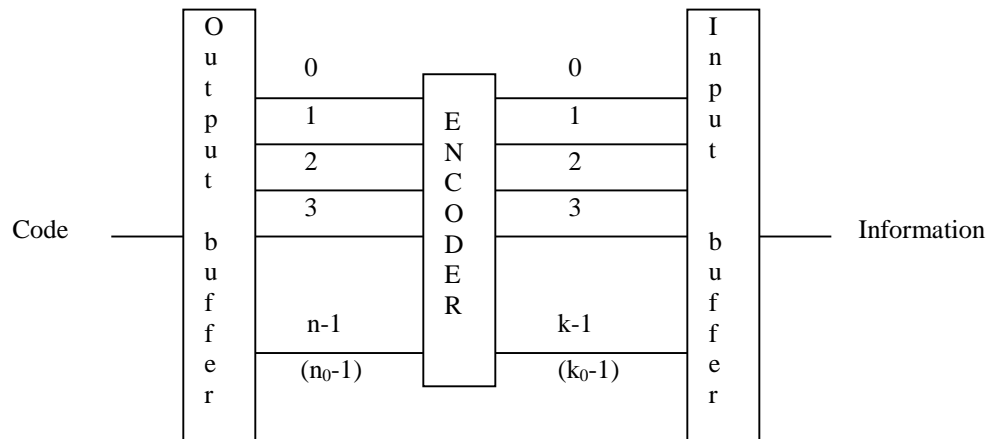


Fig.6.6 Block diagram of an Encoder

The decoder is a device that inverts the operation of the encoder, and its job is to decide what the transmitted information was. It is able to do this because only certain transmitted sequences (codewords) are possible and any errors are likely to result in reception of a noncode sequence. On a memoryless channel, the best strategy for the decoder is to compare the received sequence with all the codewords, taking into account the confidence in the received symbols, and select the codeword that is closest to the

received sequence. The measure of difference between sequences is known as distance, and this method is called minimum distance decoding.

Regardless of the code and the decoding method, there are a number of common characteristics of coding systems. The first is that they aim to correct the most likely errors, but have to accept that less likely errors will not be handled correctly. The other main point is that when error correction is being carried out, if the decoder does not get it completely right, then it will make several errors and may well make things worse. For a thorough mathematical treatment of these issues of coding, see references [30-33].

6.2.2 Simulation of BCH-Encoded CP-QFSK System

Bose-Chaudhuri-Hocquengham (BCH) codes form a large class of powerful random error-correction cyclic codes and are among the most important block codes available since they exist for a wide range of rates, they can achieve significant coding gain, and the complexity of their decoders is such that they are implementable even at high speeds, and they also are widely applied in a variety of modern communications systems particularly in cellular mobile telephony. The BCH codes are linear cyclic codes which are always defined by their code generator polynomial. This class of binary codes provides the communications system designer with a large selection of block lengths and code rates. Specific values for t and k can be found using algebraic techniques for determining code polynomials, however, there exists tables like the one presented in [23] which gives all of the known values for n , k , and t for BCH codes with block lengths up to $n = 1023$, see [appendix B]. It is noted that the code rate $R = k/n$ varies over a wide range and that the number of errors which can be corrected increases as the code rate decreases. The code polynomials which generate such codes can be found in reference [28].

The coding gain achievable using BCH codes varies as the code parameters n and k vary, but in all cases the performance improves as the block length n increases. The function of the BCH decoder, on the other hand, is to produce an estimate of the error polynomial which was most likely to have occurred given the received polynomial. BCH decoders are commercially available and are widely used.

Scanning through the table of the possible BCH code parameters given in appendix B, several standard BCH code values were examined and the (63, 36) BCH code was found to be quite adequate as this code yields a reasonable degree of redundancy for effective error correction at the expense of minimum reduction in the information throughput. This code length and ability to correct large number of errors in code block does not allow an expansion of the bandwidth beyond the channel bandwidth.

The BCH encoder was introduced in the CP-QFSK system after the random binary data source i.e. before the DAC (Digital to Analogue Converter) circuit and the BCH decoder was introduced after the ADC (Analogue to Digital Converter) circuit and before the BER meter. The internal structure of the modelled BCH coder and decoder circuits are presented in appendix [C]. The simulation was carried out with the same CP-QFSK system parameters defined in chapter 4. Figure 6.7 shows the input data applied to the encoder

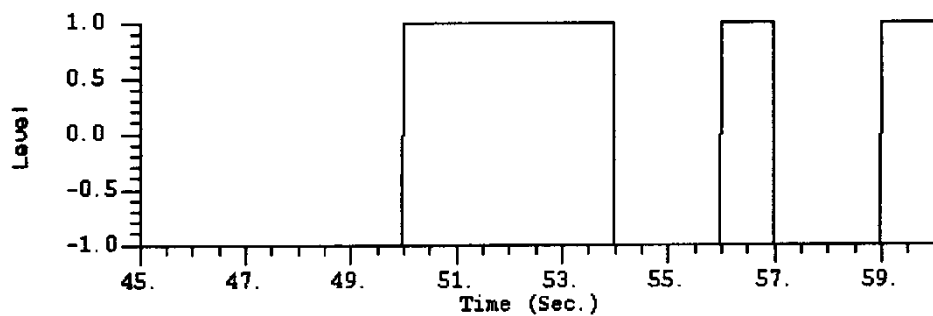


Fig. 6.7 BCH encoder input data stream

The encoded data coming out of the BCH encoder is shown in Fig. 6.8.

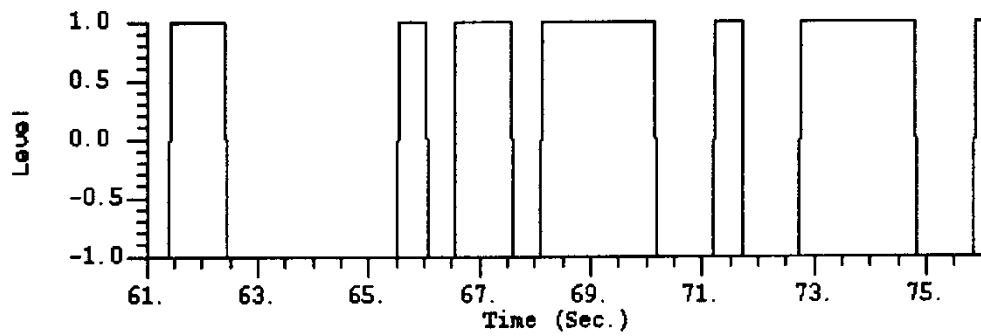


Fig. 6.8 BCH encoder output data stream

Fig.6.9 displays the detected data input to the decoder with 5 errors encountered compared to fig. 6.8.

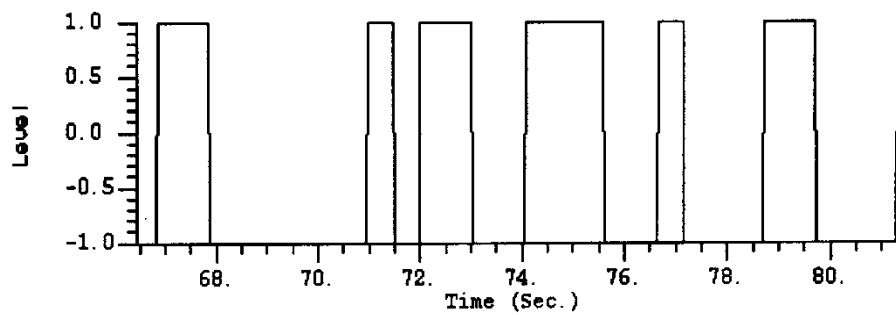


Fig.6.9. Detected data

When the above detected data was input to the BCH decoder, these 5 errors were corrected as shown in figure 6.10 below. Clearly system delay has been created and this is evident from the above figures.

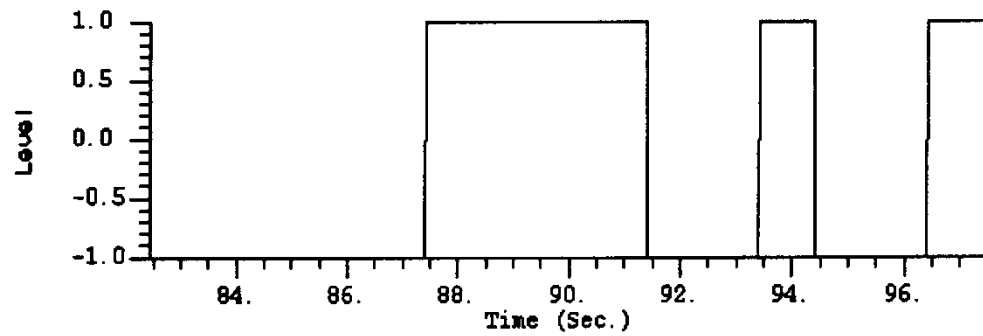


Fig. 6.10. Decoded data

To assess the coding gain achieved using coding, a simulation test was carried out output of which is graphically displayed in Fig. 6.11. For reference the un-coded CP-QFSK and the binary GMSK results are included.

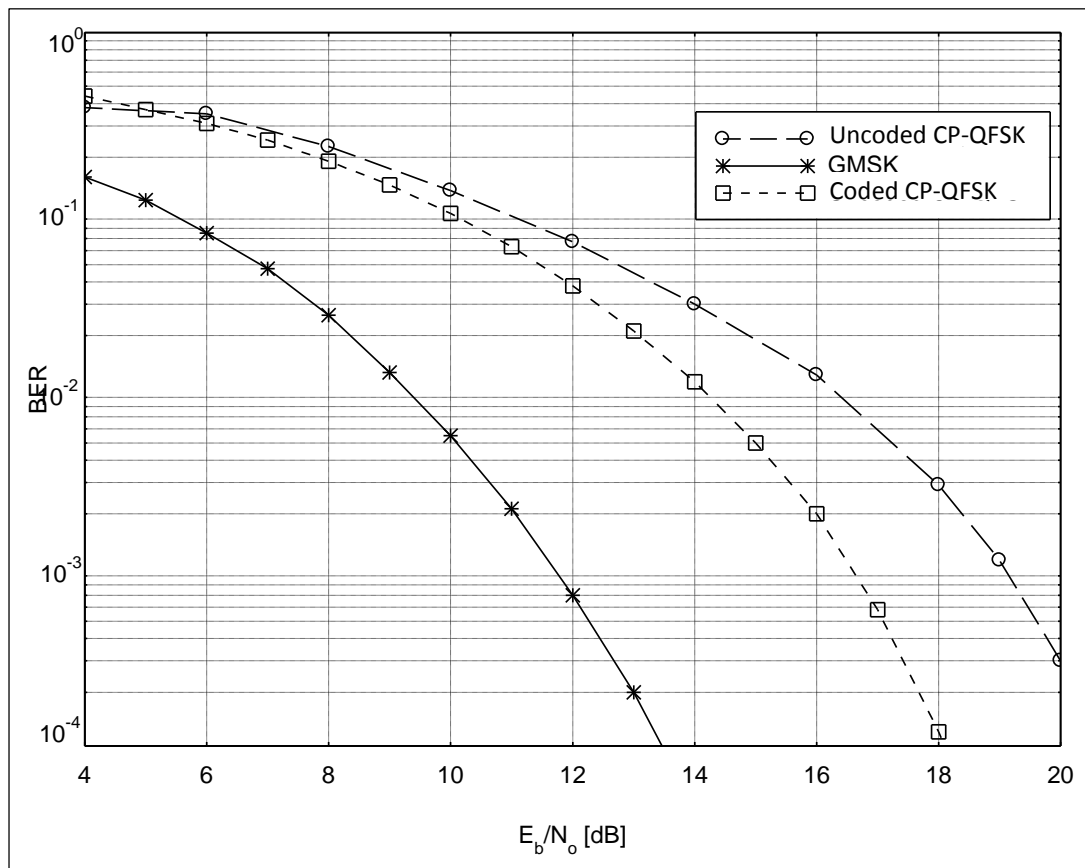


Fig. 6.11. BCH-encoded-CP-QFSK performance.

Fig. 6.11 demonstrates that the overall system performance in terms of BER is still insufficient for the data link quality specified by the DECT system standard. It is inferior to that of un-coded system by about 3dB margin due to substantial effects of channel interference.

SUMMARY:

In this chapter, a number of adaptive and non-adaptive techniques were explored and from the theoretical background presented at the outset, two of such techniques were chosen and implemented to mitigate the adverse in-door portable channel effects.

Adaptive technique, namely, Maximum Ratio combiner diversity has first been examined and found to provide a gain of about 5 dB on average.

On implementing non-adaptive technique, BCH coding, the reported results showed that the overall performance results incorporating both techniques depicted in Fig.6.11 signify that the studied CP-QFSK requires high signal-to-interference ratios at the receiver to achieve an acceptable performance. It can support voice call services but is still below the data link quality criteria specified by the majority of cellular mobile communications systems standards such as the DECT system standard for the support of data communication services.

It is concluded that the quality of the signal is severely affected and degraded more by the effects of channel filtering, hence other techniques such as equalization or employing coherent detection are suggested in order to significantly improve the data link quality. Due to time limitation, the research and implementation of such techniques are beyond the scope of this work and open for research by others working in the same research field.

REFERENCES

- [1] SEXTON, T. A. and PAHLAVAN, K.; " Channel Modelling and Adaptive Equalisation of Indoor Radio Channels."; IEEE Journal , Vol. SAC-7, No. 1, pp. 114, January 1989.
- [2] CHAUNG C. I. J.; " The Effect of Time Delay Spread on Portable Radio Communications Channels with Digital Modulation."; IEEE Journal on Selected Areas in Communications, Vol. 5, No. 5, pp. 879-889, June 1987.
- [3] HUMMELS, D. R. and RATCLIFFE, D. R.; "Calculation of Error Probabilities for MSK and OQPSK Systems Operating in a Fading Multipath Environment.", IEEE Transactions, Vehicular Technology, Vol.VT-30, No.3, pp.112-120, August 1981.
- [4] SPAIN (UPC); "Further Simulation Results at 60GHz."; COST 231, TD(90) WG3 96, September 1990.
- [5] LAHTENMAKI, J.; "More Wideband Measurements At 1.7GHz.", COST 231 TD(91) 34, Lund, 4-7 June 1991.
- [6] IBNKAHLA M.; "Signal Processing for Mobile Communications Handbook.". CRC Press LLC, 2005.
- [7] MOGENSEN, P. E.; "Wideband Polarisation Diversity Measurements For Wireless Personal Radio Communications."; Proceedings of Nordic Radio Symposium, pp. 49-53, Aalborg, 1992.
- [8] JAKES, W. C. ; "Microwave Mobile Communications."; John Wiley & Sons, Inc, 1974.

-
- [9] PIERCE, J. N. ; “Theoretical Diversity Improvement in Frequency Shift Keying.”; Proceedings of IRE, Vol. 46, pp. 903-910, May 1958.
- [10] AL-DHAIR N. and DIGGAVI S. N.; “On the Achievable Rates of Time-Varying Frequency-Selective Channels”; Conference on Information Science and Systems, pp. 860-865, Princeton, NJ, March 2002.
- [11] MIKI, T. and HATA, M. ; “Performance of 16Kbits/s GMSK Transmission with Postdetection Selection Diversity in Inland Mobile Radio.”; IEEE Journal on Selected Areas in Communications, Vol. SAC-2, No. 4, pp. 512, Jul 1984.
- [12] ADACHI, F. and PARSONS, J. D. ; “Error Rate Performance of Digital FM Mobile Radio with Postdetection Diversity.”; IEEE Transactions on Communications, Vol. 37, No. 3, pp.200, March 1989.
- [13] BEAULIEU, N. C. and ABU-DAYYA, A.; “Analysis of Equal Gain Diversity on Nakagami Fading Channels.”; IEEE Transactions on Communications, Vol. COM-39, No. 2, pp. 225, February 1991.
- [14] STEIN, S. ; “Fading Channel Issues in System Engineering.”; IEEE Journal, Vol. SAC-5, No. 2, pp. 68-89, February 1987.
- [15] PROAKIS, J. G.; " Digital Communications ", 4th Edition. New York, McGraw Hill series in Electrical Engineering, 2001.
- [16] TOMMY OBERG, “Modulation, Detection and Coding”, John Wiley & Sons, Ltd, 2001.
- [17] PARSONS, J. D. and GARDINER, J. G. ; “Mobile Communication Systems.”; Blackie, Halsted Press USA, 1989.
- [18] TOMIUK B. R., BEAULIEU N. C. and ABU-DAYYA A. A., “Maximal Ratio Combining with Channel Estimation Errors”. IEEE Conference on Communications, Computers and Signal Processing, pp. 363-366, 1995.

-
- [19] YANG H. C. and Alouini M. S.; "Performance analysis of multibranch switched diversity systems". IEEE Transactions on Communications, COM-51 (5), pp. 782-794, 2003.
- [20] ALTMAN F. J. and SICHAK W.; "A simplified diversity system for beyond the horizon link". IRE Transactions on Communications, Vol. CS-4, pp. 50-55, March 1956.
- [21] GEORGE C. CLARK and BIBB CAIN J. "Error-Correction Coding for Digital Communications"; Plenum Press, New York, 1981.
- [22] SHANNON C. E., "A Mathematical Theory of Communication", Bell Systems Technical Journal, 27, pp. 379-423 (Part 1), 623-656 (Part 2), July 1948.
- [23] BERNARD SKLAR.; "Digital Communications: Fundamentals and Applications". Second Edition, Prentice Hall PTR, 2001.
- [24] SHU LIN and DANIEL J. COSTELLO, JR. "Error Control Coding, Fundamentals and Applications"; Prentice-Hall, Inc, New Jersey, 1983.
- [25] PETER SWEENEY, "Error Control Coding An Introduction"; Prentice Hall International (UK) Ltd, 1991.
- [26] Gallager R. G., "Information Theory and Reliable Communication Engineering"; New York; John Wiley, 1968.
- [27] Wozencraft J. M. and JACOBS I. M., "Principles of Communication Engineering"; New York; John Wiley, 1965.
- [28] Lin S. and Costello D. J., "Error Control Coding: Fundamentals and Applications"; Englewood Cliffs, NJ: Printice-Hall, 1983.
- [29] Berlekamp E. R., "Algebraic Coding Theory"; New York: McGraw-Hill, 1968.
- [30] Bluhut R., "Theory and Practice of Error Control Codes"; Reading, Mass: Addisson-Wesley, 1983.

- [31] Berger T., “Rate Distribution theory”; Prentice-Hall, Englewood Cliffs, N. J., 1971.
- [32] Davisson L. and Gray R., eds, “Data Compression”; Dowden, Hutchinson, and Ross, Stroudsburg, Pa., 1976.
- [33] Blahut, R. E. ; “Principles and Practice of Information Theory”. Addison Wesley, Dowden, Reading Mass, 1987.

CHAPTER 7

Conclusions and Further Work

7.1 Conclusions

7.1.1 Rationale

In the introductory chapter of this thesis the case was argued for a return to continuous phase modulation schemes to consider the viability of such schemes to contribute to the changing personal communications environment. Now that cellular telephones and Wi Fi technology are virtually universal not only in the traditional innovator territories of North America, Europe and Scandinavia, Japan and Korea but also in the rapidly emerging markets of India, China and Africa, and this means that pressures on spectrum and on technological innovation are now intense.

In this context it has been appropriate to review the history of personal communications from the early analogue cellular radio system (1G), through the emergence of digital cellular systems of which GSM has been particularly successful to the subsequent development of UMTS using wideband CDMA. More recently OFDMA has attracted major development effort. It is of interest to note that the co-ordinated European effort in the Group Special Mobile (GSM) was appropriate in its time but that such a process is not repeated in current co-operative ventures which are now much more international. A principal feature of all current developments has been the dependence in innovation on simulation. And this has been the basis of the research set out in the present thesis.

7.1.2 Methodology

Having established that this research is simulation based it has then been necessary to select appropriate tools. The most general approach remains the Monte Carlo method. This involves expressing each variable in terms of its PDF and then selecting values at random to compute the outcomes. Generality, however, comes at the cost of huge computation demands which plainly are unacceptable when the number of variables is large. A number of alternative strategies have been adopted, particularly when an optimum is the target of the computation. These rely on creating analogues of other physical processes. Genetic algorithm is a case in point in which each generation of parameter values represents an improvement towards the optimum over the previous generation [1, 2]. An alternative is “Simulated Annealing” which follows the physical process of achieving a homogenous alloy from a variety of input components [3-6].

In this thesis a further technique is employed. This recognises that personal communications systems are consigned to narrow bands of frequencies in much higher parts of spectrum. This involves representing the band-pass signal as an equivalent complex low-pass signal. In classical network theory it is commonplace to design band-pass filters by transforming a low-pass design to a band-pass equivalent so it is clearly advantageous to perform similar processes in signal representation and so reduce the computational burden.

Over several decades a number of software simulation packages have been developed to embody these principals and used in various applications. Of these MATLAB (Matrix Laboratory) is the best known and widely used in simulating linear systems. “Simulink” provides support for signal simulation in a MATLAB environment.

However, in the present research, the Block Oriented System Simulator (BOSS) has proved to be the most appropriate. The reasons for this choice have been set out and the related problem of simulation accuracy discussed at some length in Chapter 3.

In order to demonstrate the performance of BOSS in a practical application, the Digital European Telecommunication (DECT) has been chosen and simulated. Whilst the DECT system has been in use for a number of years and most domestic cordless telephones use it, it is nevertheless a significant element in the personal communications environment.

Having demonstrated the efficacy of simulation in the DECT system, attention returned to consideration of the specific opportunities represented by CP-QFSK. Here, the issues of significance are first, practical aspects in particular amplification, detection and system complexity and second, bandwidth occupancy. In the latter case, modulation index is a major factor but this is also related to pre-modulation pulse shaping and this relationship has been explored in detail in Chapter 4. In particular it has been shown that CP-QFSK is spectrally more compact than MSK as used in GSM. The remaining aspect relating to pulse shaping has concentrated on the rival merits of Gaussian and raised cosine filtering. The outcome has been choice of parameters and the consequences shown in appropriate graphs.

The effectiveness of any communications system is its robustness in the presence of interference. This issue has been explored for the case of CP-QFSK by considering the most significant interferences namely adjacent channel interference, co-channel interference and delay spread. Encouraging results have been obtained and have been reported in Chapter 5 while in Chapter 6 attention has been focused both adaptive and non-adaptive strategies for maximising system performance.

7.2 Further Observations

One of the key areas in the design and implementation of an efficient and reliable communications system is the field of modulation particularly in cellular mobile radio communications systems. This research work has undertaken the design, analysis and evaluation of a non-coherent transceiver based on a sub-class of continuous phase signaling, namely, CP-QFSK modulation scheme. The system has the prominent merits of high spectral efficiency, hardware simplicity and high ACI rejection capability. It has been found that this system offers an adjacent channel rejection factor of around 40 dB, while the DECT system standards stipulated far less rejection limit criterion (25-30dB), yielding the CP-QFSK modulation scheme outperforms the conventional GMSK as it causes significantly less ACI, hence it is more spectrally efficient in multi-channel systems. However, simulation output results have indicated that the system is not co-existing well with other interferers when it was tested under CCI conditions. At simulated delay spreads between 100 ns to 200ns, which are commonly encountered in the indoor portable communication channel, results showed that there has been a severe degradation in the system performance, apparently, due to multi-path fading conditions, yielding a high irreducible error rate as there exists a noise floor of about 40 dB for BER of 6.10^{-3} when more than 1-path fading exist, consequently, to achieve a certain level of BER, a higher S/I ratio is required than the equivalent level of E_b/N_0 . This suggests that this system renders itself to be interference limited rather than noise limited.

On implementing adaptive and non-adaptive techniques, namely, MRC diversity combiner and BCH codec systems to alleviate the above mentioned adverse affects of the mobile radio channel which offered a good gain in performance, however, when

assessing the performance achieved by these techniques, the overall system performance is still inferior to that of un-coded system by about 3dB margin due to channel interference.

In conclusion, the studied CP-QFSK system could support voice call services as they could tolerate such BER performance whereas for data services it is still below the data link quality criteria specified by the majority of cellular mobile radio systems such as the DECT system. It requires higher signal-to-interference ratio at the receiver to achieve acceptable performance.

7.3 Further Work

As it has been established that the CP-QFSK system performance quality is greatly affected by the channel filtering interference, thus this necessitates the recourse to much more sophisticated techniques such as coherent detection or Maximum-Likelihood Sequence Estimation (MLSE) equalization in order to improve the data link quality significantly. Due to time limitation, the research and implementation of such techniques are beyond the scope of this work and open for research by others working in the same research field.

Nevertheless, with growing emphasis on “software-Defined Radio”, it is apparent that research is now progressing to self-adapting technology in which radio systems will respond to environmental circumstances by selecting the optimum system parameters to deliver the services which users require [7-10].

Looking further into the future, the theme of this research has been to position current work in the context of ever increasing demand by users and increasing need to exploit hitherto untapped spectrum resources. Whereas progress from one generation to the next has been based on innovation within the confines of existing spectrum allocations,

the time has come to look to the untapped resource of the mmWave spectrum. Of particular significance in the 60GHz band which offers massive enhancement of user density since this band is the oxygen absorption frequency so that co-channel interference is virtually eliminated. This is already declared to be the 5G World [11-14].

REFERENCES

- [1] Zhao Xin; Xiu Chunbo, "New genetic algorithm improved and its applications," Electronics, Communications and Control (ICECC), 2011 International Conference on, vol., no., pp.926, 928, 9-11 Sept. 2011.
- [2] Hancheng Liao, "An SDA-Aided Genetic Algorithm Detector for CDMA System," Communications and Mobile Computing (CMC), 2010 International Conference on, vol.2, no., pp.316, 319, 12-14 April 2010.
- [3] R. Kwan, C. Leung, and M. E. Aydin; "Simulated Annealing and Multiuser Scheduling in Mobile Communication Networks". INTECH Open Access Publisher, 2012.
- [4] Mirhosseini, S.H.; Yarmohamadi, H.; Kabudian, J., "MiGSA: A new simulated annealing algorithm with mixture distribution as generating function," Computer and Knowledge Engineering (ICCKE), 2014 4th International Conference on , vol., no., pp.455,461, 29-30 Oct. 2014.
- [5] Luokai Hu; Jin Liu; Chao Liang; Fuchuan Ni, "A Map Reduce Enabled Simulated Annealing Genetic Algorithm," Identification, Information and Knowledge in the Internet of Things (IIKI), 2014 International Conference on , vol., no., pp.252,255, 17-18 Oct. 2014.
- [6] Guangming Lv; Xiaomeng Sun; Jian Wang, "A simulated annealing- new genetic algorithm and its application," Electronics and Optoelectronics (ICEOE), 2011 International Conference on, vol.3, no., pp.V3-246,V3-249, 29-31 July 2011.

-
- [7] H. Harada, "A Software Defined Cognitive Radio Prototype," IEEE 18th International Symposium on Personal, Indoor and Mobile Radio Communications, 2007. PIMRC 2007, vol., no., pp.1-5, 3-7 Sept. 2007.
- [8] Luiz Garcia Reis, A.; Barros, A.F.; Gusso Lenzi, K.; Pedroso Meloni, L.G.; Barbin, S.E., "Introduction to the Software-defined Radio Approach," *Latin America Transactions, IEEE (Revista IEEE America Latina)*, vol.10, no.1, pp.1156,1161, Jan. 2012.
- [9] Kelley, Brian, "Software defined radio for broadband OFDM protocols," *Systems, Man and Cybernetics, 2009. SMC 2009. IEEE International Conference on*, vol., no., pp. 2309-2314, 11-14 Oct. 2009.
- [10] Mueck, M.; Piipponen, A.; Kalliojärvi, K.; Dimitrakopoulos, G.; Tsagkaris, K.; Demestichas, P.; Casadevall, F.; Pérez-Romero, J.; Sallent, O.; Baldini, G.; Filin, S.; Harada, H.; Debbah, M.; Haustein, T.; Gebert, J.; Deschamps, B.; Bender, P.; Street, M.; Kandeepan, S.; Lota, J.; Hayar, A., "ETSI reconfigurable radio systems: status and future directions on software defined radio and cognitive radio standards," *Communications Magazine, IEEE*, vol.48, no.9, pp.78,86, Sept. 2010.
- [11] B. Bangerter, S. Talwar, R. Arefi and K. Stewart; "Networks and devices for the 5G era," *IEEE Communications Magazine*, vol.52, no.2, pp.90-96, February 2014.
- [12] Shimojo, Takuya; Takano, Yusuke; Khan, Ashiq; Kaptchouang, Stephane; Tamura, Motoshi; Iwashina, Shigeru, "Future mobile core network for efficient service operation," *Network Softwarization (NetSoft), 2015 1st IEEE Conference on*, vol., no., pp.1,6, 13-17 April 2015.
- [13] Lili Wei; Hu, R.; Yi Qian; Geng Wu, "Key elements to enable millimeter wave communications for 5G wireless systems," *Wireless Communications, IEEE*, vol.21, no.6, pp.136,143, December 2014.

-
- [14] Akoum, S.; El Ayach, O.; Heath, R.W., "Coverage and capacity in mmWave cellular systems," *Signals, Systems and Computers (ASILOMAR), 2012 Conference Record of the Forty Sixth Asilomar Conference on*, vol., no., pp.688,692, 4-7 Nov. 2012.

Appendix A: BER computations program of CP-QFSK

```

c   This program generates and writes BER points of CP-QFSK to an output file
c   called LRC.out
c
c   Type a.out to run this program after compilation
c
C   Call the output data file in MATLAB software and plot the curves
c
C   PROGRAM START
C
COMMON/DATA/PI,NT
C
REAL*8 AS,AF,WX(32),AX(32),PI,G1,G0,G2,A0,A1,A2,
&      ERF,T,BIN(2),AK,AM,S1,SUM,MIN,DMIN2,
&      SD,SNR,SND,XVALUE,BER,DF,G0FUN,G1FUN,G2FUN
C
INTEGER IT,IFAIL,I,NTX,NT,KA,I1,I0,I2,KAM,NPP
C
EXTERNAL D01BBF,D01BAZ,G0FUN,G1FUN,G2FUN,ERF
c
OPEN(10,FILE='riscos42.out')
C
SD=0.0D0
NT=16
MIN=20.0D0
c
WRITE(*,*)'INSERT THE MODULATION INDEX -->'
READ(*,*)H
PI=4.0D0*DATAN(1.0D0)
BIN(1)=-1.0D0
BIN(2)=1.0D0

```

```
      AM=4.0D0
      KAM=AM
C
      DO 3 KA=1,KAM-1
      AK=KA
C
      DO 4 I1=1,2
      A1=BIN(I1)
C
      DO 5 I0=1,2
      A0=BIN(I0)
C
      DO 6 I2=1,2
      A2=BIN(I2)
C
      NTX=16
C
      AS=1.5D0
      AF=2.5D0
      IT=1
      IFAIL=1
      CALL D01BBF(D01BAZ,AS,AF,IT,NTX,WX,AX,IFAIL)
C
      S1=0.0D0
      DO 1 I=1,NTX
      T=AX(I)
C
      G0=G0FUN(T)
C
      G1=G1FUN(T)
C
      G2=G2FUN(T)
C
```

```

SUM=2.0D0*PI*H*AK*(A1*G1+A0*G0+A2*G2)
C
    S1=S1+DCOS(SUM)*WX(I)
C
1 CONTINUE
C
    DMIN2=DLOG(AM)/DLOG(2.0D0)*(1.0d0-S1)
C
    SD=SD+DMIN2
    WRITE(*,*)'DMIN=',DMIN2
    IF(DMIN2.LE.MIN) THEN
        MIN=DMIN2
    END IF
c
6 CONTINUE
C
5 CONTINUE
C
4 CONTINUE
C
3 CONTINUE
    WRITE(*,*)'MINIMUM VALUE =',MIN,'AVERAGE MIN=',SD/24.d0
    SNR=17.0D0
    NPP=50
    S1=NPP
    DF=SNR/S1
    DO 7 I=1,NPP+1
        SNR=0.0D0+(I-1.0D0)*DF
        SND=10.d0**(SNR/10.0D0)
        XVALUE=DSQRT(SND*MIN)
        BER=0.5D0*(1.0D0-ERF(XVALUE))
        WRITE(10,*)SNR,BER
7 CONTINUE

```

```
C
    close(10)

    STOP
    END
C
    REAL*8 FUNCTION ERF(X)
C
    COMMON/DATA/PI,NT
C
    REAL*8 PI,X,S,AX(32),WX(32),AS,AF
C
    INTEGER I,IT,NT,IFAIL
C
    EXTERNAL D01BBF,D01BAZ
C
    AS=0.0D0
    AF=X
    IT=1
    IFAIL=1
    CALL D01BBF(D01BAZ,AS,AF,IT,NT,WX,AX,IFAIL)
C
    S=0.0D0
    DO 1 I=1,NT
        S=S+2.0D0/SQRT(PI)*DEXP(-AX(I)**2)*WX(I)
1 CONTINUE
    ERF=S
    RETURN
    END
C
    REAL*8 FUNCTION G0FUN(X)
C
    COMMON/DATA/PI,NT
```

```
C
    REAL*8 PI,X
C
    INTEGER NT
C
    G0FUN=0.0D0
C
    IF(X.GE.1.5D0.AND.X.LE.2.0D0) THEN
        G0FUN=0.5D0-(PI*X-DSIN(PI*X))/(4.0D0*PI)
    END IF
C
    RETURN
END
C
    REAL*8 FUNCTION G1FUN(X)
C
    COMMON/DATA/PI,NT
C
    REAL*8 PI,X
C
    INTEGER NT
C
    G1FUN=0.0D0
C
    IF(X.GE.1.5D0.AND.X.LE.2.5D0) THEN
        G1FUN=0.7045774D0-(PI*X+DSIN(PI*X))/(4.0D0*PI)
    END IF
C
    RETURN
END
C
```

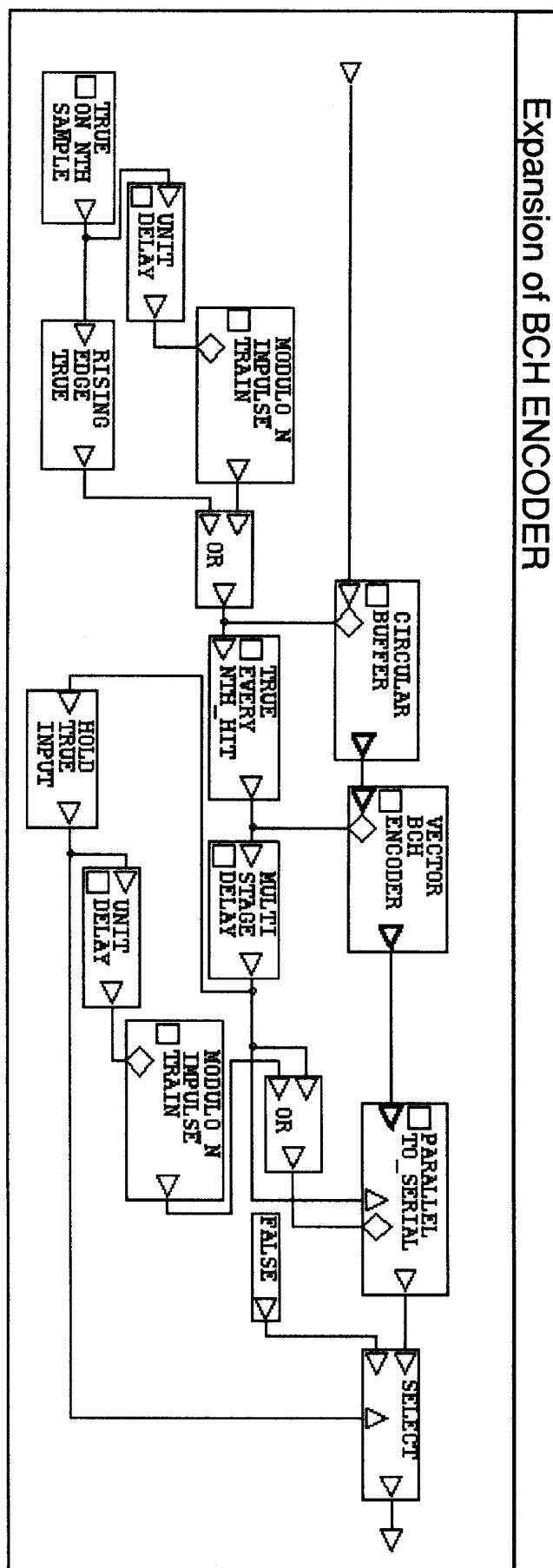
```
      REAL*8 FUNCTION G2FUN(X)
C
      COMMON/DATA/PI,NT
C
      REAL*8 PI,X
C
      INTEGER NT
C
      G2FUN=0.0D0
C
      IF(X.GE.2.D0.AND.X.LE.2.5D0) THEN
      G2FUN=0.5454225D0-(PI*X-DSIN(PI*X))/(4.0D0*PI)
      END IF
C
      RETURN
      END
```

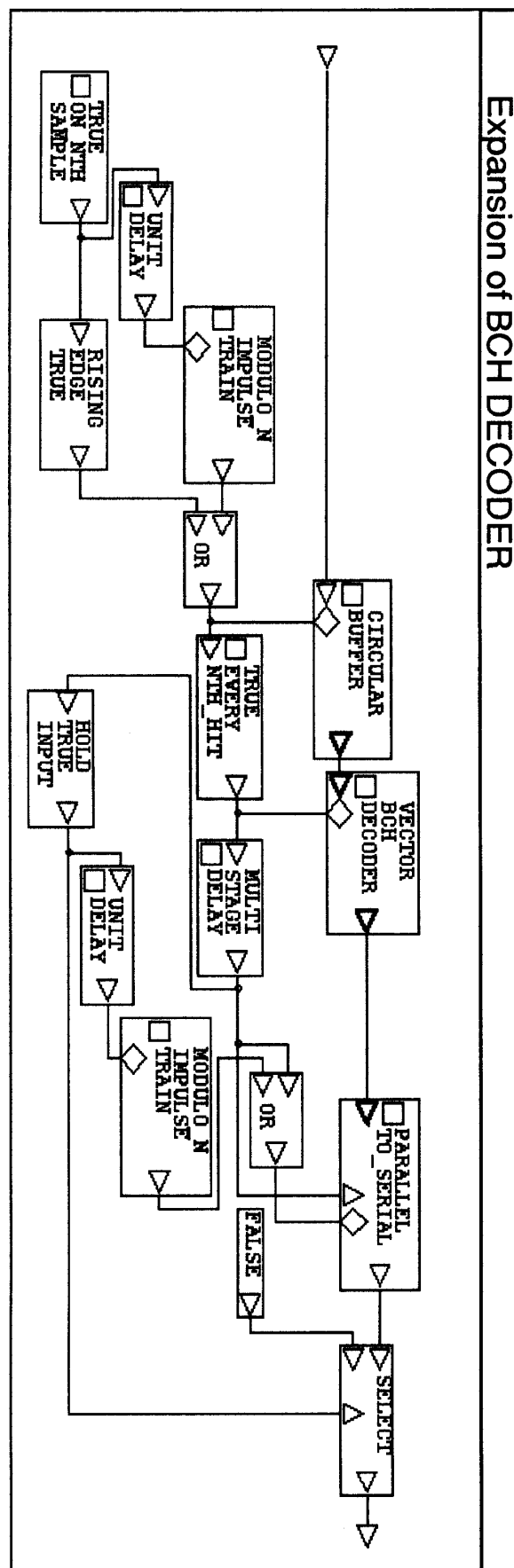

Appendix B: List of possible BCH Code Parameters

n	k	t	n	k	t	n	k	t
7	4	1	255	163	12	511	268	29
15	11	1		155	13		259	30
	7	2		147	14		250	31
	5	3		139	15		241	36
31	26	1		131	18		238	37
	21	2		123	19		229	38
	16	3		115	21		220	39
	11	5		107	22		221	41
	6	7		99	23		202	42
63	57	1		91	25		193	43
	51	2		87	26		184	45
	45	3		79	27		175	46
	39	4		71	29		166	47
	36	5		63	30		157	51
	30	6		55	31		148	53
	24	7		47	42		139	54
	18	10		45	43		130	55
	16	11		37	45		121	58
	10	13		29	47		112	59
	7	15		21	55		103	61
127	120	1		13	59		94	62
	113	2		9	63		85	63
	106	3	511	502	1		76	85
	99	4		593	2		67	87
	92	5		484	3		58	91
	85	6		475	4		49	93
	78	7		466	5		40	95
	71	9		457	6		31	109
	64	10		448	7		28	111
	57	11		439	8		19	119
	50	13		430	9		10	121
	43	14		421	10	1023	1013	1
	36	15		412	11		1003	2
	29	21		403	12		993	3
	22	23		394	13		983	4
	15	27		385	14		973	5
	8	31		376	15		963	6
255	247	1		367	16		953	7
	239	2		358	18		943	8
	231	3		349	19		933	9
	223	4		340	20		923	10
	215	5		331	21		913	11

Table continued

n	k	t	n	k	t	n	k	t
	207	6		322	22		903	12
	199	7		313	23		893	13
	191	8		304	25		883	14
	187	9		295	26		873	15
	179	10		286	27		863	16
	171	11		277	28		858	17
1023	848	18	1023	553	52	1023	268	103
	838	19		543	53		258	106
	828	20		533	54		248	107
	818	21		523	55		238	109
	808	22		513	57		228	110
	798	23		503	58		218	111
	788	24		493	59		208	115
	778	25		483	60		203	117
	768	26		473	61		193	118
	758	27		463	62		183	119
	748	28		453	63		173	122
	738	29		443	73		163	123
	728	30		433	74		153	125
	718	31		423	75		143	126
	708	34		413	77		133	127
	698	35		403	78		123	170
	688	36		393	79		121	171
	678	37		383	82		111	173
	668	38		378	83		101	175
	658	39		368	85		91	181
	648	41		358	86		86	183
	638	42		348	87		76	187
	628	43		338	89		66	189
	618	44		328	90		56	191
	608	45		318	91		46	219
	598	46		308	93		36	223
	588	47		298	94		26	239
	578	49		288	95		16	147
	573	50		278	102		11	255
	563	51						





Author's list of publications

Journal Publication:

1. M.A. Bomhara, J.G. Gardiner, R.A. Abd-Alhameed, Adaptiv and Non-adaptive Techniques for enhancing link quality of CP-QFSK transeiver in indoor environments, Journal of Telecommunications, submitted and under review since 10th June 2015; ISSN: 2042-8839.

Referred Conference papers:

1. M.A. Bomhara, J.G. Gardiner, H.A. Obeidat, R.A. Abd-Alhameed, CP-QFSK Modem for TDMA Short range Communications Systems, Fourth International Workshop on Energy Efficient and Reconfigurable Transceivers (EERT): Towards a Green Wireless Internet, Proceedings of the sixth International conference on Internet Technologies and Applications (ITA 15), Glyndŵr University, Wrexham, Wales, UK, 8th – 11th September 2015, accepted for publication.
2. M.A. Bomhara, J.G. Gardiner, H.A. Obeidat, R.A. Abd-Alhameed, On the Eligibility grounds of CP-QFSK for Mobile Radio Systems, Fourth International Workshop on Energy Efficient and Reconfigurable Transceivers (EERT): Towards a Green Wireless Internet, Proceedings of the sixth International conference on Internet Technologies and Applications (ITA 15), Glyndŵr University, Wrexham, Wales, UK, 8th – 11th September 2015, accepted for publication.

CP-QFSK Modem for TDMA Short Range Communications Systems

M.A. Bomhara¹, J.G. Gardiner¹, H.A. Obeidat¹ and R.A. Abd-Alhameed¹

¹Electrical Engineering and Computer Science, University of Bradford, Bradford, BD7 1DP, United Kingdom
mohamedbomhara@hotmail.co.uk, H.A.Obeida@student.bradford.ac.uk, r.a.abd@bradford.ac.uk

Abstract— Work presented in this paper investigates the feasibility of Continuous-Phase Quaternary Frequency Shift Keying (CP-QFSK) with limiter-discriminator detection modem as a viable dual data rate system that can be employed in TDMA short range communications systems. It offers a great deal of spectral efficiency in multi-channel systems, hardware simplicity and robustness to adjacent Channel Interference (ACI). The interrelated system design parameters are defined and optimized and the system performance in different propagation media is evaluated. Simulation results have demonstrated that adjacent channel rejection factor of 40 dB has been achieved and that the CP-QFSK system outperforms the GMSK modulation scheme as it causes far less ACI, and hence coexists well in a multi-channel system. Error correction coding has been applied to enhance the system quality.

Keywords: Modulation, TDMA, CP-QFSK, coding, ACI, Noncoherent detection.

I. INTRODUCTION

One of the major driving elements behind the explosive boom in wireless revolution is the advances in the field of modulation which plays a fundamental role in any communications system and especially in cellular radio systems and other recent technologies such as the development of Wireless Fidelity (Wi-Fi) hot spots and the commercialization of low-cost wireless local area networks (LANs) for business and residential applications [1]. In any communication system, the two primary resources that of paramount significance; are the transmission power and channel bandwidth and communication channels are classified as power-limited or band-limited accordingly, and a general system design objective priority would be to use these two resources as efficiently as possible. As far as band-limited channels are concerned, spectrally efficient modulation techniques would be used to maximize the spectrum efficiency in these channels. Thus, the choice of spectrally efficient modulation scheme has not only a direct impact on the capacity of a digital communications system in terms of the number of bits per second per Hertz (b/s/H), but also on the degree of immunity to ACI, as ACI has become a critical issue in some systems whose radio interfaces are based on the IEEE 802.11a, after it has been proven in [2], contrary to what was widely believed, that such systems suffer from throughput degradation due to ACI, the magnitude of which depends mainly on the interfering data rates among other factors. Hence, the elaborate choice of an efficient modulation scheme is of paramount importance in the design and employment of any communications system.

Over the past two decades or so, there has been a large amount of research conducted on continuous phase-constant

envelop digital modulation schemes (CPM) on account of their promising merits if employed in applications where efficient spectrum utilization is required and its immunity to nonlinearity distortion produced by the power amplifiers in transmitters overweighs the use of constant envelop modulation, and fading conditions, random phase and center frequency drift leads to employing non-coherent detection methods such as limiter discriminator (the severe fading conditions make carrier recovery quite difficult), and its applicability to arbitrary values of modulation index which impacts positively on complexity and cost [3-5]. From the aforementioned qualities, a sub-class of the CPM signaling scheme, namely, CP-QFSK has been chosen as a viable and modulation scheme for the employment in a dual rate short range system. In this type of modulation, the instantaneous frequency is constant over each symbol interval and the phase is constrained to be continuous. This phase continuity results in reducing the transient effects of the signal at the symbol transitions, thereby offering spectral bandwidth advantages. Moreover, memory imposed upon the waveform by continuous phase transitions improves performance by providing for the use of several symbols to make a decision [6, 7].

II. SIMULATION MODEL

In order to model a CPFSK signal, we first represent the baseband data signal as

$$d(t) = \sum_n I_n g(t - nT) \quad (1)$$

Where $g(t)$ is a rectangular pulse of amplitude $1/2T$ and duration T . This signal used to frequency-modulate the carrier. Consequently, the equivalent complex low-pass waveform $v(t)$ is expressed as:

$$v(t) = A \exp \left\{ j \left[4\pi T f_d \int_{-\infty}^t d(\tau) d\tau + \Phi_0 \right] \right\} \quad (2)$$

A is a real amplitude and f_d is the peak frequency deviation which relates frequency displacement to baseband signal voltage, and Φ_0 is an initial phase of the carrier. The carrier modulated signal corresponding to (2) may be expressed as

$$s(t) = A \cos[2\pi f_c t + \Phi(t, I) + \Phi_0] \quad (3)$$

Where ϕ_0 is an arbitrary starting phase, and (t, I) represents the time-varying phase of the carrier, which is defined as

$$\Phi(t, I) = 4\pi T f_d \int_{-\infty}^t d(\tau) d\tau \quad (4)$$

Which by means of equation (1) becomes

$$\Phi(t, I) = 4\pi T f_d \int_{-\infty}^t \left[\sum_{k=-\infty}^{n-1} I_k g(\tau - nT) \right] d\tau \quad (5)$$

Although the signal $d(t)$ contains discontinuities, the integral of $d(t)$ is continuous which implies continuous-phase signal $s(t)$. The phase of the carrier in the interval $nT \leq t \leq (n+1)T$ is determined by integrating (4), thus

$$\begin{aligned} \Phi(t, I) &= 2\pi f_d T \sum_{k=-\infty}^{n-1} I_k + 2\pi f_d (t - nT) I_n \\ &= \theta_n + 2\pi h I_n q(t - nT) \end{aligned} \quad (6)$$

Where h , θ_n , and $q(t)$ are defined respectively as

$$h = 2f_d T \quad (7)$$

$$\theta_n = \pi h \sum_{k=-\infty}^{n-1} I_k \quad (8)$$

$$q(t) = \begin{cases} 0 & t < 0 \\ \frac{t}{2T} & 0 \leq t \leq T \\ \frac{1}{2} & t > T \end{cases} \quad (9)$$

θ_n represents the accumulation (memory) of all symbols up to time $(n-1)T$ and the deviation ratio parameter h is the modulation index. Equation 8 represents a full response CPFSK modulation scheme which corresponds to linear phase trajectories over each symbol interval [8]. When expressed in the form of (5), CP-FSK becomes a special case of a general class of continuous-phase modulated (CPM) signaling scheme in which the carrier phase is given by

$$\Phi(t, I) = 2\pi \sum_{k=-\infty}^n I_k h q(t - kT); \quad nT \leq t \leq (n+1)T \quad (10)$$

Where $q(t)$ is some normalized waveform shape (phase response function) that may be represented in general as the integral of some frequency pulse $g(t)$, i.e.

$$q(t) = \int_0^t g(\tau) d\tau \quad (11)$$

If $g(t) = 0$ for $t > T$, the CPM signal is called full response CPM. Otherwise, if $g(t) \neq 0$ for $t > T$, the modulated signal is called partial response CPM, and in this case the pulse shape $g(t)$ is smoother and the corresponding spectral occupancy of the signal is reduced [9].

Based on the above theoretical background, a CP-QFSK system model has been designed. The transmitter configuration consists of a PRBS data source which generates a serial NRZ binary data stream at a rate twice that of the DECT bit rate. This unipolar binary bit stream is then fed into the 2-4 level converter which maps each consecutive dibits of the TDMA signal into symbols having four possible levels $\{\pm 1, \pm 3\}$, resulting in a baud rate equivalent that of the DECT symbol rate. The generated quaternary signal was then applied to a pre-modulation filter with pulse shape $g(t)$ to smooth out the sudden variations in the baseband signal, and consequently control the shape of the signal power spectrum. The smoothed data is then applied to an FM modulator, the output of which is a constant amplitude signal. The global functional block diagram of the baseband equivalent model of the CP-QFSK is shown in Fig.1.

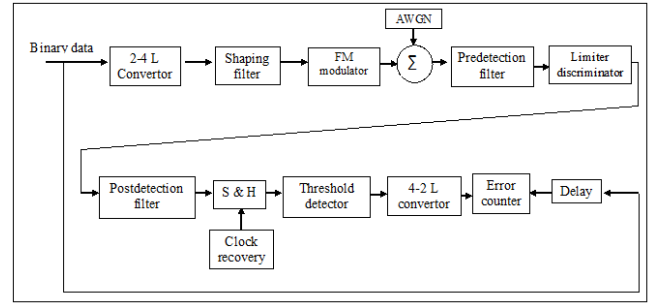


Fig. 1. Simulated CP-QFSK system.

The input to the receiver consists of the transmitted signal plus additive white Gaussian noise with single sided spectral density N_0 . The pre-detection low-pass filter at the front end of the receiver suppresses noise and interference power from adjacent channels in the signal band. The output of the pre-detection filter is then limited before being passed on to the discriminator which converts the frequency variations, i.e., the derivative of the phase of the incoming signal, into voltage variations to yield the quaternary signal plus noise. After passing through a post-detection filter (LPF), the noise and unwanted components are removed. The output of the post-detection filter is then fed to a threshold detector which converts the recovered baseband modulation signal into a

sequence of di-bit symbols. The threshold comparator is gated by the recovery clock that is generated by the symbol timing-recovery block at the baud rate enabling to sample the demodulated signal right in the middle of each symbol duration time. The threshold comparator having three decision levels, corresponding to angular frequency deviations, set at the center of the eye openings regenerates the symbols, and the binary data is recovered back in the 4-2 level converter. Finally, the regenerated output is fed into the error counter for BER measurement.

In optimizing the system parameters, as there is a trade-off between the modulation index and the baseband filtering (pulse shaping) necessary to get a power spectrum that fits within the spectral mask. Thus, it follows from the above qualitative considerations that an optimum pulse shape which has good characteristics in both the time and frequency domain and a modulation index which will serve as system simulation parameters or system design criteria need to be found, i.e. there are three issues of concern: How does the system performance degrade in the presence of noise when varying the RF spectrum through baseband modulation pulse shaping? What is the role of channel filtering in the obtainable performance? What are the optimum values of the system parameters with different baseband shaping? Three pulse functions were investigated through simulation; i.e., the Gaussian pulse shaping, the Raised cosine pulse, and the Spectral raised cosine pulse shaping. Extensive simulation tests were carried out to evaluate BER performance for different pulse shapes, pre-demodulation bandwidth, modulation index, and receiver pre-detection filter normalized-noise bandwidth (B). The simulation results revealed that 2RC pre-modulation pulse shaping with $h=0.3$ and pre-detection filter normalized equivalent noise bandwidth=1.5 were found to be the optimum system parameter values. The generated spectrum of the 2RC shaped CP-QFSK signal is shown in Fig. 2.

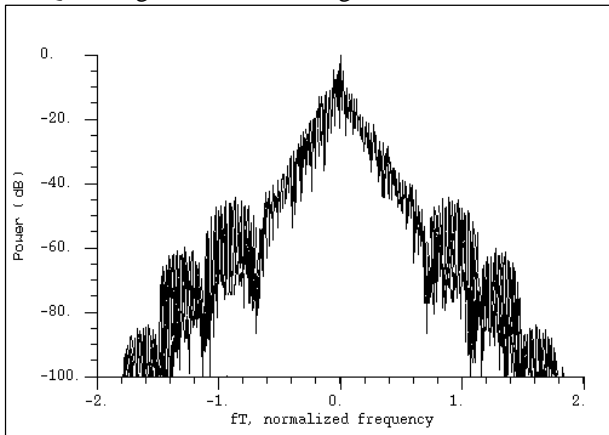


Fig. 2. CP-FSK Power spectrum.

It can be seen from the Fig. 2 that the first side lobe is at 40 dB below the main lobe and the remaining side lobes

containing insignificant energy diminish off fairly fast, thus it has a good spectral containment and out of band radiation power. Fig. 3 depicts the eye diagram of the received quaternary data.

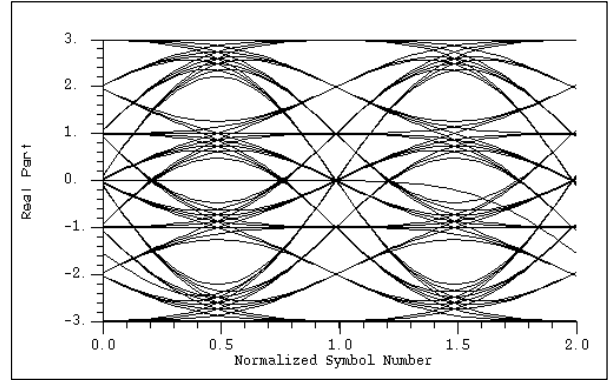


Fig. 3. Eye diagram of the received CP-QFSK signal

III. SIMULATION RESULTS

In order to obtain reasonable BER measures, the simulation was carried out for 12000 frame time each simulation test run. The measured BER performance is shown in Fig. 4.

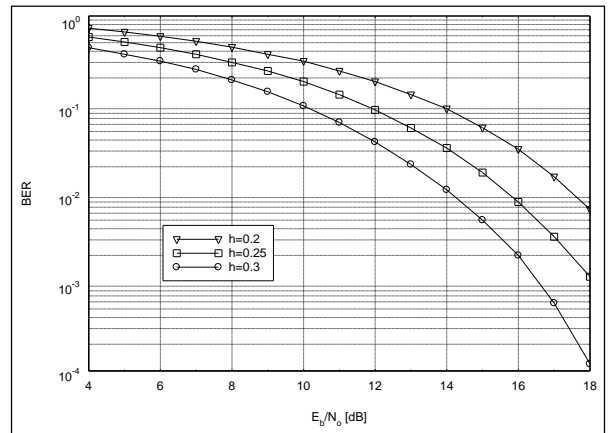


Fig.4. Measured BER performance of CP-QFSK.

These results have been validated using a closed form expression for the probability of error derived in [10], whereby a theoretical bit error rate was computed and the BER is plotted against E_b/N_o as shown in Fig. 5. These results agree with that obtained through simulation presented in Fig. 4, particularly at low E_b/N_o instances. However, comparing these results with those of the binary GMSK (DECT signalling) reported in [11], a difference of almost 7 dB on average has been noticed. This degradation in system quality is primarily due to the domination of the ISI.

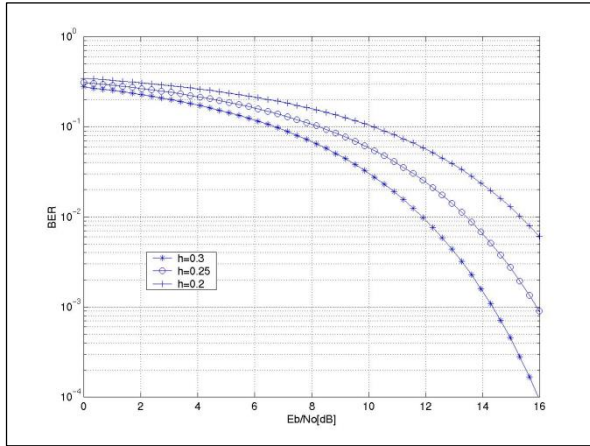


Fig. 5. Theoretical BER performance of CP-QFSK.

In simulating, as regards the propagation media, it has been assumed, in order to emphasize the interference effects, an ideal multipath-free situation, for both the useful channel and the interfering ones. The relative ACI as shown in Fig. 6, is the ratio between the Signal to Interference (S/I) power values before and after the IF filter for an adjacent channel interferer. With a receiver IF filter having BW=1.5, an adjacent rejection factor of around 40 dB has been achieved at a channel spacing of 1.5 times the symbol rate which signifies that the proposed CP-QFSK modulation causes significantly less ACI than the GMSK signaling, hence is more spectrally efficient in a multichannel system.

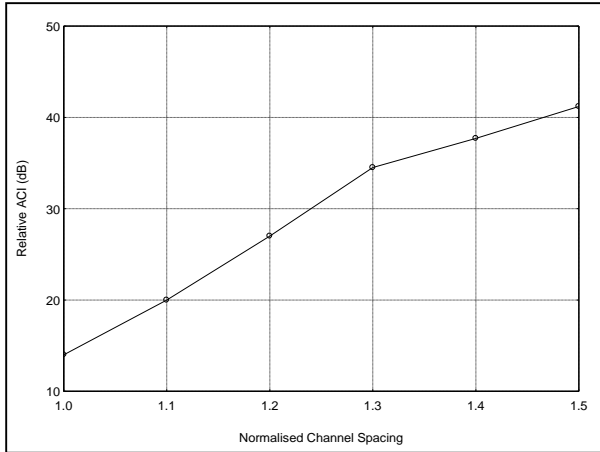


Fig. 6. Relative ACI vs channel spacing.

The effects of Co-channel interference has been modelled and quantified by exposing the system to six interfering sources and their interference to the desired signal of the CP-QFSK system. To simulate the propagation path loss, an attenuator was introduced at the output of each interfering transmitter to account for the propagation loss between the transmitter and the receiving mobile handset, and the attenuated interfering signals were then added to the wanted

signal and AWGN. The combined signal was then demodulated and the BER performance was measured as shown in Fig. 7.

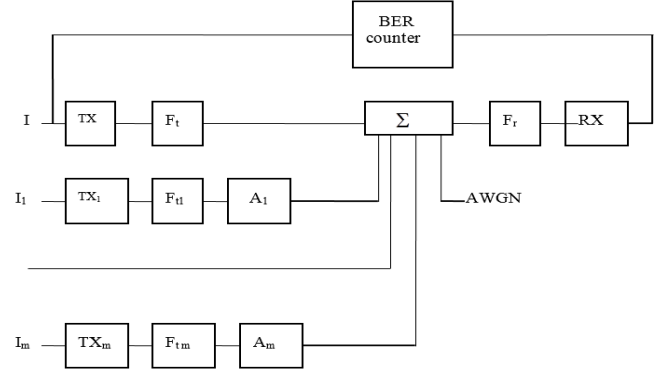


Fig. 7. Block diagram of the simulated CCI.

In Fig. 7, $I, I_1, I_2 \dots, I_m$ = digital signal inputs of the interfered and interfering transmitters, TX, TX1, TX2, \dots , TXm = interfered and interfering CP-QFSK transmitters, $F_t, F_{t1}, F_{t2} \dots, F_{tm}$ = transmit filters, A_1, A_2, \dots, A_m = attenuators, F_r = receive filter of the interfered system, RX = interfered CP-QFSK receiver. The integer seed of the user data of the wanted and interfering signals were set to different large odd numbers to represent the variability in the data pattern being sent, and the parameters of all the modulators and the demodulator are the same. BER against S/I is shown in Fig. 8.

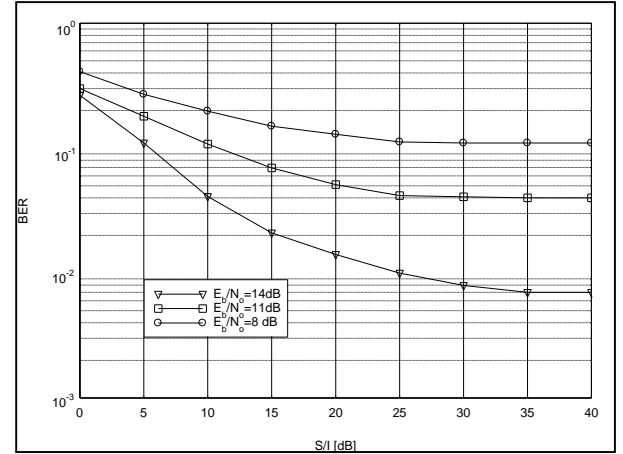


Fig. 8. CP-QFSK system Performance under co-channel interference.

As it can be seen from Fig. 8, the received signal suffers a significant level of CCI, as the curves level off at high values of S/I, causing BER to rise over the tolerable value. Comparing these results with those in Fig. 4, it is obvious that to achieve a certain level of BER, a higher S/I ratio is required than the equivalent level of E_b/N_0 . This suggests that CCI more dominates the channel link than the noise does, and consequently, this system renders itself to be an interference limited rather than noise limited. This difference is fairly

substantial and is more apparent at higher ratios of S/I. This necessitates that this impairment needs to be mitigated. To this end, a corrective measure such as error correction coding which is often used in mobile radio systems should be applied. There exist many different forms of coding schemes, but they all share the two common features: redundancy and noise averaging. It has been proven in [12, 13] that for a fixed block error rate, the fraction of errors that must be corrected decrease with increasing block length, which indicates the potential for performance improvement that is gained through noise averaging.

Bose-Chaudhuri-Hocquengham (BCH) codes form a large class of powerful random linear cyclic codes and are among the most important block codes available since they can achieve significant coding gain. The coding gain achievable using BCH codes varies with the code rate $R_c = k/n$ (k is the information bits and n is the code word length). In our simulation we have chosen the block code parameters (63, 36) BCH code as it yields a reasonable degree of redundancy for effective error correction at the expense of minimum reduction in the information throughput. This code length and ability to correct large number of errors in code block does not allow an expansion of the bandwidth beyond the channel bandwidth.

The BCH encoder was introduced in the CP-QFSK system after the random binary data source and the decoder was introduced before the BER meter. To assess the coding gain, the simulation was carried out with the same system parameters defined above, and the results are graphically displayed in Fig. 9. which demonstrate that coding has brought about 3dB in average improvement.

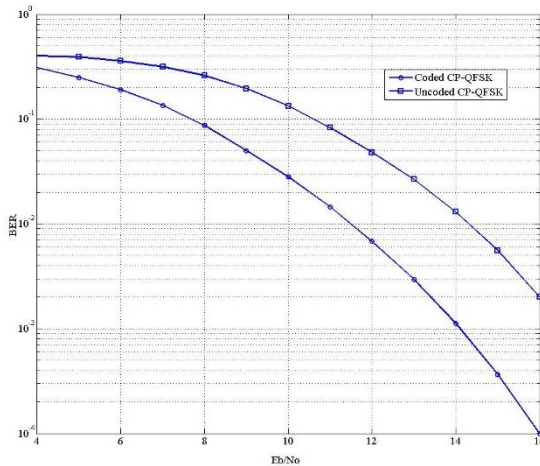


Fig. 9. BCH-encoded-CP-QFSK performance.

IV. CONCLUSION

A spectrally efficient dual data rate modem has been designed, its parameters have been optimized and its performance has been measured. Obtained results showed that an adjacent rejection factor of around 40 dB has been

achieved at a channel spacing of 1.5 times the symbol rate yielding that the proposed CP-QFSK modulation causes far less ACI than the GMSK signaling, hence is more spectrally efficient in a multichannel systems. However, CCI more dominates the channel link than the noise and this degrading effect is more apparent at higher ratios of S/I. Consequently, this system renders itself to be an interference limited rather than noise limited. On implementing error correction coding, an improvement of 3dB has been attained. The system performance has been assessed in non-fading environment. Evaluating the performance under other adverse mobile channel conditions such as multipath fading, and adaptive techniques such as equalization employed to enhance the system's quality and robustness are areas for further work to be conducted.

REFERENCES

- [1] M. Ibnkahila "Signal Processing for Mobile Communications Handbook", CRC Press LLC, 2005.
- [2] V. Angelakis, S. Papadakis, V. A. Siris and A. Traganitis "Adjacent Channel Interference in 802.11a is harmful: Testbed Validation of a simple Quantification Model", IEEE Communications Magazine, pp.106-166, March 2001.
- [3] J. Boccuzzi "Signal Processing for Wireless Communications", The McGraw-Hill Companies, Inc., 2008.
- [4] S. Hyundong and L. Hong "On the Error Probability of Binary and M-ary Signals in Nakagami-m channels", IEEE Transactions on Communications, Vol. 52, No. 4, April 2004.
- [5] G. J.; Campeanu, A.; Nafornita, I., "Noncoherent demodulation of continuous phase modulated signals using Extended Kalman Filtering," Optimization of Electrical and Electronic Equipment (OPTIM), 2010 12th International Conference on , vol., no., pp.724,727, 20-22 May 2010.
- [6] O. Anderisano, G. Corraza and G. Immovilli "Effects of the Interference in Cellular Digital Mobile Radio Systems using Full Response CPM with Limiter-Discriminator Detection", Alta Frequenza, Focus on Mobile Radio Systems, No. 2, pp. 109-117, 1988.
- [7] Park, H.C., "Power and bandwidth efficient constant-envelope BPSK signals and its continuous phase modulation interpretation," Communications, IEE Proceedings- , vol.152, no.3, pp.288,294, 3 June 2005.
- [8] J. G. Proakis, "Digital Communications" Fourth Edition, McGraw Hill, New York, 2001.
- [9] T. Oberg, "Modulation, Detection and Coding" John Wiley & Sons Ltd 2001..
- [10] R. Steel, "Mobile Radio Communications", Pentech Press Limited, 1992.
- [11] RES 3-R (91) 122; "DECT Spurious Emissions", Philips Research, UK.
- [12] B. Sklar, "Digital Communications; Fundamentals and Applications," Second Edition, Prentice Hall PTR, 2001.
- [13] Teng, C.-C.; Fonseca, J.P.; Dowling, E.M., "Non-coherent detectors for quadrature-multiplexed continuous phase modulation signals," Communications, IET, vol.3, no.4, pp.610,619, April 2009

On The Elegibility Grounds Of CP-QFSK for Mobile Radio Systems

M.A. Bomhara¹, J.G. Gardiner¹, H.A. Obeidat¹ and R.A. Abd-Alhameed¹

¹Electrical Engineering and Computer Science, University of Bradford, Bradford, BD7 1DP, United Kingdom
mohamedbomhara@hotmail.co.uk, H.A.Obeida@student.bradford.ac.uk, r.a.a.abd@bradford.ac.uk

Abstract— In this paper we review a class of the Continuous Phase modulation (CPM), namely, the Quaternary Frequency Shift Keying (CP-QFSK) signaling and investigate its suitability for the application in mobile radio systems. This type of modulation renders its self as a spectrally efficient scheme that is currently used in a wide variety of applications ranging from communications systems to sonar, geophysics, and biomedicine, etc. It is exhibited herein that this scheme outperforms its MSK and QPSK counterparts in terms of bandwidth occupancy due to its spectral containment. An extensive survey of research material is provided and some of the CP-QFSK system applications in various realms are highlighted. It is concluded that this signaling scheme due to its spectral efficiency is a viable and promising modulation scheme particularly in the multichannel systems of communications.

Keywords: Modulation, PM, Spectral Efficiency, CP-QFSK, systems, Detection.

I. INTRODUCTION

One of the major driving elements behind the explosive boom in wireless communications revolution is the advances in the field of modulation which plays a fundamental role in any communication system, and especially in mobile radio systems. Hence, the elaborate choice of an efficient modulation scheme is of paramount importance in the design and employment of any communications system. Phase Modulation (PM) has gained substantial attention and widely studied since it was developed in 1970s, owing to its appealing properties that it offers near-capacity performance both in single user and multiuser systems [1-4]. A sub-class of PM signaling scheme called Continuous Phase Quaternary Frequency Shift Keying (CP-QFSK) in which the instantaneous frequency is constant over each symbol interval and the phase is constrained to be continuous has found its way in a variety of applications such as communications systems, sonar, geophysics, and biomedicine [11], to name just few, due to their relatively low spectral sidelobes, and because its envelope is constant, the power amplifier can be operated in the saturation (nonlinear) region without causing much signal distortion, yielding better power efficiency [5-16].

Conceptually, the two primary communication resources in any communication system are the transmitted power and channel bandwidth [17]. A general system-design objective priority would be to use these two resources as efficiently as possible. Generally, Communications channels are either of two types; power limited or band limited [18-20]. Different

strategies are taken to optimize the use of the resources in each case:

1- Power-limited channels: Such channels are often characterized by the power efficiency which is a measure of how much received power is required to achieve a specified BER performance. This efficiency is also defined in terms of the required average received bit energy-to-noise density ratio E_b/N_0 for a given f_d . Coding schemes are often used in such systems to save power. The typical example is a satellite mobile channel.

2- Band-limited channels: In order to maximize the spectrum efficiency in such channels, spectrally efficient modulation schemes are adopted. A common example is the urban cellular radio channel.

Apart from spectrally efficient modulation techniques, other approaches or strategies are used to reduce the required bandwidth such as: Low-bit-rate speech and channel coding, multiple access techniques, deployment of microcells and increase in network intelligence.

The choice of modulation technique has a direct impact on the capacity of a digital mobile communication system, as it defines the bandwidth efficiency of the channel [21, 22]. Multilevel modulation techniques are further divided into three classes, these are: M-ary Phase Shift Keying (MPSK) in which the phase variations contain the transmitted information, M-ary Frequency Shift Keying (MFSK) where the information modulated in the frequency variations of the carrier and M-ary Quadrature Amplitude modulation (MQAM) where the transmitted information is contained in both the amplitude and phase variations.

In selecting a suitable modulation scheme for a mobile radio system, consideration must be given to achieving the following: Minimal out-of-bandwidth emissions, high efficiency in power and/or spectrum, low carrier-to-cochannel interference ratio of power, constant envelope signaling, implementation easiness and cost, and robustness against channel impairments such as multipath fading.

Optimizing all these features at the same time is not possible as each has its practical limitation and also is related to others. For instance, to achieve high bandwidth efficiency one may choose to use high-level modulation. However, the power efficiency of the system would be reduced consequently. Moreover, the bandlimited high-level modulated signal will have a large envelope variation which results in a large out-of-band radiation accordingly if this signal is to be passed through a power efficient nonlinear

amplifier that in turn introduces interference to adjacent channels, and although this can be circumvented by using linear power amplifiers, but these have poor power efficiency. Hence, it is necessary to look for a good compromise among these criteria, depending on the precise nature of the anticipated utilization of the system in question [23].

II. MODULATION SCHEME SUITABILITY

Digital modulation techniques can also be broadly classified in two groups, each one being thought to be more appropriate for the two kinds of the aforementioned channels. The modulation techniques more used in the present systems belong to the group of continuous phase modulations or, equivalently, constant envelope modulations, which are inherently power efficient. However, further improvements in related systems, like amplification devices, permit the increasing use of linear modulations, leading to a more bandwidth efficient systems. Moreover, the following issues need to be considered:

1) *Amplification problem:*

Obviously, a highly efficient method of amplification should be searched for. In a mobile environment, the power supply problem is quite important and a maximum duration of battery use without recharging is desired. Also, the power amplifier in the handset is constrained to operate in its saturated nonlinear region in order to maximize the dc efficiency of the battery powered handset. Owing to this imposed nonlinearity, linear modulation schemes such as QAM and QPSK would be unsuitable for mobile radio telephony [24].

The high power amplifiers (HPA) used in many systems, for example, in mobile radio handsets, are usually highly nonlinear, because of the requirement for power efficiency. These amplifiers give rise to amplitude modulation-amplitude modulation (AM-AM) and amplitude modulation-phase modulation (AM-PM) conversion, which may result in an irreducible BER floor. This can be overcome through the use of a modulation scheme that has constant envelope and continuous phase properties such as multilevel CP-FSK. This is not the case for a modulation system with any kind of amplitude modulation or even for a system which in principle has a constant envelope but a non-continuous phase. This is due to the fact that this discontinuity introduces a high level of side lobes which need be suppressed. By doing this with the appropriate filtering, envelope variations are introduced. If these variations are suppressed by hard limiting, the side lobes are introduced again resulting in severe adjacent channel interference, and in digital systems, the bandwidth of the signal relative to the carrier is usually narrow, and filter implementation would be extremely difficult. It has been found that the amplification of linear signals with high power non-linear amplifiers introduces a penalty of 2 to 3 dB, in terms of power efficiency [25].

2) *Detection problem:*

Essentially, an optimum receiver detects the signal coherently which necessitates the carrier frequency and phase recovery. However, non-coherent receivers such as the differential (when possible) or the limiter-discriminator type are suboptimum in the sense that they require an increase in the E_b/N_0 to achieve a given BER with respect to the optimum (typical values range from 1 to 3 dB), leading to not very power efficient systems. This is true in an AWGN channel, but things are quite different in a phase-noisy channel, with multipath (fast Rayleigh fading), Doppler effect, and random FM, are all phenomena quite commonly encountered in mobile radio environment, hence, using non-coherent modulation schemes such as discriminator detection would be advantageous owing to its resistance to center frequency drift and fast fading, and the possibility of using broad range of modulation index values [26]. It has been established in [27] that a small price is paid in using noncoherent FSK instead of coherent FSK for the decidedly large advantage of not having to establish M-coherent references at the receiver.

3) *System Complexity:*

Modulation schemes as mentioned earlier can be classified as either linear or nonlinear. Linear schemes are generally non-constant envelope after bandlimiting and the information is carried in both the amplitude and phase of the carrier, whereas nonlinear modulation has a constant envelope property and the information is solely contained in the excess phase function of the carrier. However, when linear schemes are coherently demodulated, recovering of the carrier signal through phase locked loop methods becomes a must, resulting in additional demodulator complexity. Nonlinear schemes can be realized as direct modulation of a voltage controlled oscillator (VCO), where the data sequence is applied directly to the tuning port. Besides, nonlinear schemes can be demodulated noncoherently with limiter discriminator detection in which case the carrier reference required in a coherent system need not be generated at the demodulator. With mobile telephony, where the requirement of a light handheld radio, imposed by the personal communication scenario in which everybody has fast access to all services through a personal handheld mobile unit, would mean a great decrease in size and weight of the handset and associated circuitry and this in turn reduces dramatically the cost. Therefore, modulation schemes that can be detected non-coherently offer a great deal of hardware simplicity and hence are much more desirable.

4) *Binary versus Multilevel schemes:*

The use of multilevel modulation schemes instead of binary ones produces an increase of the bit transmission rate for a given bandwidth. So, for a given bit rate, they imply a reduction of the required channel bandwidth and an increase in the spectrum efficiency, thus achieving a significant increase in the number of the accommodated users. However, a consequence of transmitting more than one bit per symbol is that the signal power must be commensurately increased for the same channel noise if the symbol error is not to increase. This gives rise to a reduction in the number

of channels/cell due to the ensued increase in cluster size. The result is that the tele traffic throughput is not modified, but the complexity is significantly increased. This situation is very frequently encountered in conventional cellular systems, but if we consider microcells, e.g. in an indoor environment the situation is completely different due to the close proximity of the base station and the mobile, a high values of SNR can be achieved within the coverage area with considerably lower power, thus increasing the power efficiency of the unit. Moreover, the signal to interference ratio (SIR) is considerably higher due to the severe fast fall in signal level. Based on these principles, a research study performed in such minimum cluster sizes showed that multilevel modulation schemes can be introduced without cluster size penalties [27, 28].

III. CONTINUOUS PHASE QUATERNARY FREQUENCY SHIFT KEYING

A sub-class of the Constant Envelope, Continuous Phase (CECP) continuous phase PM signaling scheme known for its spectral efficiency superiority is the Continuous Phase Quaternary FSK (CP-QFSK) in which the instantaneous frequency is constant over each symbol interval and the phase is constrained to be continuous will be discussed in what follows. This constraint of phase continuity results in affecting the signal in two important ways: Firstly, sharp transitions at the symbol boundaries are reduced, and that in turn lowers the signal spectral spillage, and hence increasing the spectral efficiency. Secondly, the introduced memory to the signal through the continuous phase transitions property allows for making use of several symbols to make a decision over several symbols when recovering the signal [29-35]. An FSK signal can be generated by shifting the carrier signal by an amount equal to:

$$A_n(f) = \frac{\sin\pi[fT - (2n - 1 - M)h/2]}{n[fT - (2n - 1 - M)h/2]} \quad (1)$$

Where $A_n = \pm 1, \pm 3, \dots, \pm(M - 1)$ denotes the resulted symbol sequence from mapping k -bit blocks $= \log_2 M$ of binary digits from the information sequence $\{a_n\}$ into $M = 2^k$ that ensues from mapping k -bit blocks of binary data sequence into $M=2^k$ possible levels to form the information signal which modulates the carrier [20]. The resulting frequency-modulated signal is phase continuous, i.e. the phase is a continuous function of time, and hence it is called Continuous-Phase Frequency Shift Keying (CP-FSK). The baseband data signal may be represented as:

$$d(t) = \sum_n I_n g(t - nT) \quad (2)$$

Where $g(t)$ is a square pulse whose amplitude is $1/2T$ and duration of T seconds. The carrier is frequency modulated by

the $d(t)$ signal. The complex low pass waveform $v(t)$ is represented as:

$$v(t) = A \exp \left\{ j \left[4\pi T f_d \int_{-\infty}^t d(\tau) d\tau + \Phi_0 \right] \right\} \quad (3)$$

A is a real amplitude and f_d is the peak frequency deviation which relates frequency displacement to baseband signal voltage, and Φ_0 is an initial phase of the carrier. The carrier modulated signal corresponding to (3) may be expressed as:

$$s(t) = A \cos[2\pi f_c t + \Phi(t, I) + \Phi_0] \quad (4)$$

Where Φ_0 an arbitrary starting phase, and (t, I) represents the time-varying phase of the carrier, which is defined as

$$\Phi(t, I) = 4\pi T f_d \int_{-\infty}^t d(\tau) d\tau \quad (5)$$

Which by means of equation (1) becomes

$$\Phi(t, I) = 4\pi T f_d \int_{-\infty}^t \left[\sum I_n g(\tau - nT) \right] d\tau \quad (6)$$

Although the signal $d(t)$ contains discontinuities, the integral of $d(t)$ is continuous which implies continuous-phase signal $s(t)$. The phase of the carrier in the interval $nT \leq t \leq (n+1)T$ is determined by integrating (6), thus

$$\begin{aligned} \Phi(t, I) &= 2\pi f_d T \sum_{k=-\infty}^{n-1} I_k + 2\pi f_d (t - nT) I_n \\ &= \theta_n + 2\pi h I_n q(t - nT) \end{aligned} \quad (7)$$

Where h , θ_n , and $q(t)$ are defined respectively as:

$$h = 2f_d T \quad (8)$$

$$\theta_n = \pi h \sum_{k=-\infty}^{n-1} I_k \quad (9)$$

$$q(t) = \begin{cases} 0 & t < 0 \\ \frac{t}{2T} & 0 \leq t \leq T \\ \frac{1}{2} & t > T \end{cases} \quad (10)$$

θ_n denotes memory (accumulation) of all symbols up to $(n-1)T$, and h denotes the modulation index. Equation 10 represents a full response CPFSK modulation scheme which *corresponds* to linear phase trajectories over each symbol interval. The set of phase trajectories $\varphi(t, I)$ generated by the information sequence $\{I_n\}$ for the CP-QFSK with $\varphi_0 = 0$ is sketched in Fig.1 for two symbol intervals. The phase trajectories reflect the linear phase trajectories over the symbol period due to $g(t)$ is a square pulse [36].

There exist other types of more smooth pulses that do not have discontinuities such as raised cosine pulses. It is worth

noting that when h is a rational number, the phase trajectories, shown in Fig. 1, would fold up on its self-modulo 2π [36].

Using equation (7), the CP-FSK signal becomes a subclass of CPM whose carries is:

$$\Phi(t, I) = 2\pi \sum_{k=-\infty}^n I_k h q(t - kT); \quad nT \leq t \leq (n+1)T \quad (11)$$

Where $q(t)$ is the phase response function that can be expressed as:

$$q(t) = \int_0^t g(\tau) d\tau \quad (12)$$

If $g(t)=0$ for $t > T$, then the CPM signal is termed full response CPM. Conversely, if $g(t) \neq 0$ for $t > T$, it is a partial response CPM, and consequently, the pulse shape $g(t)$ is smoother and the spectral occupancy of the signal is lessened. Varying h , the pulse shape $g(t)$ and the alphabet size M , an infinite variety of CPM signals can be attained [36, 37].

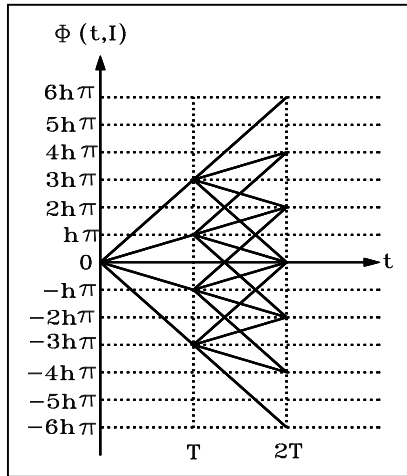


Fig. 1. CP-QFSK Phase trajectories

Unlike the case with PAM, PSK, and QAM, CPM signals cannot be described by discrete points in signal space due to the time-variance of the carrier phase. Alternatively, they are represented by the different paths or trajectories. A constant amplitude CP signal trajectories form a circle. As an example, the signal space diagram for CP-FSK signals with $h = 1/2$ and $h = 1/4$ is illustrated in Fig. 2. The start and end instances of the phase trajectories are indicated by a dot. It is noted that the length of the phase trajectory increases with an increase in h and this in turn increases the signal bandwidth accordingly.

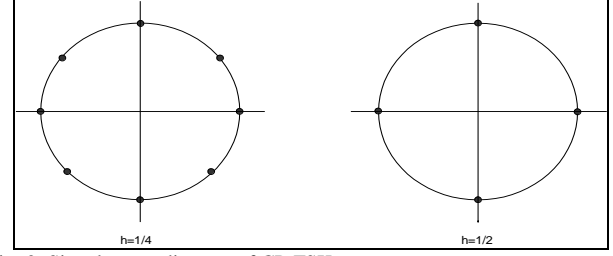


Fig. 2. Signal-space diagram of CP-FSK

An important descriptive feature of any information-carrying system is the power spectral density function (psdf) that results from the combination of the characteristics of the information signal and the technique of modulation. Estimates of bandwidth occupancy, interference to or from flanking carrier channels, and relative comparisons of different modulation techniques all exemplify situations where a knowledge of the psdf is imperative.

In most digital communications systems, the available channel bandwidth is limited. It is of great importance to consider the constraints imposed by the channel bandwidth limitation in the selection of the modulation technique to be used to transmit the information.

The power density spectra of CP-QFSK along with its counterparts; MSK and QPSK are sketched in Fig. 3. MSK and QPSK have been included to allow for easiness of comparison. To accurately compare the three spectral characteristics, the frequency variable was normalized by the bit interval T_b . From Fig. 3, it is clearly seen that the CP-QFSK signal has the narrowest main lobe among the three spectra and its side lobes fall off considerably faster than the MSK and QPSK do. Consequently, CP-QFSK has the narrowest spectral occupancy and hence is more bandwidth efficient than QPSK and MSK allowing more channels to be accommodated in a given bandwidth. Thus, in bandlimited situations, CP-QFSK is superior to MSK and PSK.

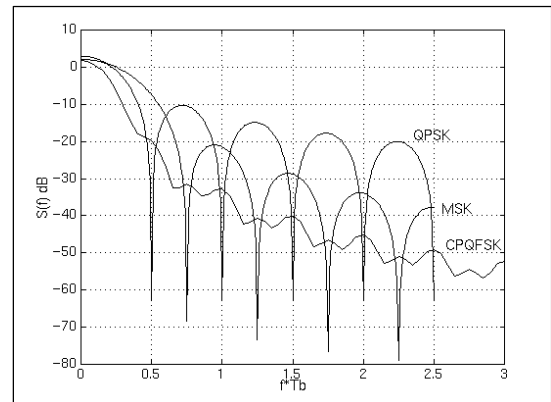


Fig. 3. CP-QFSK, MSK and QFSK power density spectra

The performance of any CPM modulation scheme can be improved by increasing the minimum Euclidean distance [38]. In [39, 40], different forms of CPM modulation combined with block encoding were used to increase the

minimum distance of CPM signals in order to avoid the merging events of low Euclidean distances taking place, as opposed to standard codes that cause the Hamming distance increase.

It is illustrated by considering full response CPFSK, partial response CPM and trellis coded CPFSK, that the proposed block encoding method can be applied to many forms of CPM signaling techniques. Reported numerical results indicated that the minimum distance of CPM signals can be significantly increased by using block coding at commonly used values of h . Nonlinear block codes were also considered.

A comparative study in terms of BER performance between duobinary-encoded CPFSK and a 4-level CPFSK (4FSK) in static, as well as narrowband land-mobile channel environment has been presented in [41-43]. BER performance of partial-response duobinary CPFSK, and full-response 4-level CPFSK were compared under the same RF spectral occupancy, data rate and non-coherently detected by limiter discriminator under nonfading (Gaussian) and fading channels. It was found that CP-QFSK system has significantly outperforms the 3-level duobinary CPFSK over a narrowband FM radio link. This is attributed to the receiver bandwidth is lowered for 4FSK which results in higher frequency.

IV. SYSTEM APPLICATIONS

In this sub-section, among the numerous applications where CP-QFSK modulation has been adopted, a number of examples are quoted. The field of Digital Network Coding (DNC) is witnessing ongoing development where CP-QFSK is applied. In two-way relay networks, the throughput can be enhanced using the relaying technique DNC. At the relay, the digital code word are generated by means of demodulation, channel decoding, and re-encoding [43-49]. In [43], a comparison between the network performance of binary FSK and multilevel CP-FSK using two matrix; the simulated BER and the information rate between the sources and the relay was presented. Reported results showed that the quaternary FSK energy-efficiency merit on point-to-point link was improved when it was implemented in digital network coding. The throughput improvement gained by the use of DNC over Link Layer Network coding (LNC) was quantified in a typical application, and found to increase from 37.1% for $M = 2$ to 41% for $M = 4$. The technique is well-suited for FSK systems, and it is known that the capacity of FSK increases with the number of levels.

CP-QFSK has also attracted attention in the synchronous and asynchronous frequency-hop spread-spectrum multiple-access (FHSS-MA) networks to maximize their throughput. In [44], system parameter values were optimized and used to evaluate the performance of FHMA system with multilevel FSK. More detailed information can be sited in [44-49].

Another active area where Multilevel FSK is applied is the power line transmission systems, where it is employed in a spread spectrum to double the transmission rate [50]. A detailed account of such systems description and design can be cited in [51] through [56].

V. CONCLUSION

In this paper we investigated the suitability of a sub-class of continuous phase modulation, namely, CP-QFSK for the application in mobile radio systems. It is concluded that this signaling scheme is a viable and promising modulation scheme particularly in the multichannel systems of communications as it has the narrowest spectral occupancy compared to NSK and QPSK signals, hence, is more spectrally efficient than its two counterparts, thus allowing more channels to be accommodated in a given bandwidth. The investigative material presented in this paper explores the concepts and principles underlying this technology and sheds the light on some of their appealing properties and uses in various realms. The resources list of material serves an expansion on the subject for the reader.

REFERENCES

- [1] T. Aulin, N. Rydbeck and C.-E. Sundberg, "Continuous phase modulation, Part I and Part II," IEEE Trans. Commun., vol. COM-29, pp. 196-225, Mar. 1981.
- [2] P. Moqvist and T. M. Aulin, "Serially concatenated continuous phase modulation with iterative decoding," IEEE Trans. Commun., vol. 49, pp. 1901-1915, Nov. 2001.
- [3] M. Xiao and T. M. Aulin, "Serially concatenated continuous phase modulation with convolutional codes over rings," IEEE Trans. Commun., vol. 54, pp. 1385-1396, Nov. 2006.
- [4] A. Graell i Amat, C. A. Nour, and C. Douillard, "Serially concatenated continuous phase modulation for satellite communications," IEEE Trans. Wireless Commun., vol. 8, no. 6, pp. 3260-3269, Jun. 2009.
- [5] A. Perotti, A. Tarable, S. Benedetto, G. Montorsi, "Capacity-achieving CPM schemes," IEEE Trans. FT., vol. 56, no. 4, pp. 1521-1541, Apr. 2010.
- [6] L. Bing, T. Aulin and B. Baoming, "Continuous Phase Modulation Orthogonal Multiple Access Scheme," Global Communications Conference (GlobeCOM), 214 IEEE, Page(s): 3886-3891, 2014.
- [7] Park H. C., Lee K And Feher K.; "Continuous Phase Modulation for F-QPSK-B Signals". IEEE Transactions on Vehicular Technology, Vol. 56, No. 1, pp. 157-172, January 2007.
- [8] P. Moqvist, "Multiuser serially concatenated continuous phase modulation," Ph.D. thesis, Chalmers University of Technology, Goteborg, Sweden, 2002. Available: <http://www.chalmers.se/JcseJEN/research/researchgroups/publications-fromlphd-theses>.
- [9] P. Moqvist and T. Aulin, "Multiuser serially concatenated continuous phase modulation," in Proc. International Symposium on Turbo Codes, Brest, France, 2003, pp. 211-214.
- [10] P. A. Murphy, M. Golanbari, G. E. Ford, and M. J. Ready, "Optimum and reduced complexity multiuser detectors for asynchronous CPM signaling," IEEE Trans. Wireless Commun., vol. 5, pp. 1959-1965, Aug. 2006.
- [11] D. Bokolamulla and T. Aulin, "Serially concatenated space-time coded continuous phase modulated signals," IEEE Trans. Wireless Commun., vol. 6, no. 10, pp. 3487-3492, 2007.
- [12] A. Barbieri, D. Fertonani, and G. Colavolpe, "Spectrally-efficient continuous phase modulations," IEEE Trans. Wireless Commun., vol. 8, pp. 1564-1572, Mar. 2009.

- [13] A. Perotti, S. Benedetto and P. Remlein, "Spectrally efficient multiuser continuous-phase modulation systems," in Proceedings of IEEE International Conference on Communications (ICC), Cape Town, South Africa, pp. 1-5, May 2010.
- [14] N. Noels and M. Moeneclaey, "Iterative multiuser detection of spectrally efficient FDMA-CPM," IEEE Trans. Signal. Process., vol. 60, no. 10, pp. 5254-5267, Oct. 2012.
- [15] L. Bing, T. Aulin and B. Bai, "Efficient algorithms for calculating Euclidean distance spectra of multi-user continuous phase modulation systems," in Proc. IEEE International Symposium on Information Theory, ISIT 2012, Cambridge, MA, pp. 2391-2395, July. 2012.
- [16] L. Bing, B. Bai and J. F. Dou, "The Power Spectral Density of Multiuser Continuous Phase Modulation Systems," in Proc. IEEE International Conference on Wireless Communications and Signal Processing, WCSP 2013, October. 2013, Hangzhou.
- [17] L. Bing, T. Aulin and B. Bai, "Spectrally efficient FDMA-CPM systems," in Proc. IEEE International Conference on Communications, ICC 2014, Sydney, June. 2014.
- [18] L. Bing, T. Aulin and B. Bai, "A Simplified detector for spectrally efficient multiuser CPM systems," in Proc. IEEE Wireless Communications and Networking Conference, WCNC 2014, April. 2014, Istanbul.
- [19] M. Wylie-Green, E. Perrins, and T. Svensson, "Introduction to CPM-SC-FDMA: A novel multiple-access power-efficient transmission scheme," IEEE Trans. Commun., vol. 59, no. 7, pp. 1904-1915, July 2011.
- [20] J. Proakis; "Digital Communications". Fourth Edition, McGraw Hill, New York, 2001.
- [21] R. Steele; "Deploying Personal Communications Networks". IEEE Communications Magazine, Vol. 28, No. 9, pp. 12-15, September 1990.
- [22] A. Burr; "Application of High Rate Coded Modulation Systems to Radio LANs". IEEE Colloquium on Radio LANs, London, pp. 5/1-5/6, 7th May 1992.
- [23] A. Aghvami "Digital Modulation Techniques for Mobile and Personal Communication Systems". Electronics and Communication Engineering Journal, June 1993.
- [24] J. Bocuzzi; "Signal Processing for Wireless Communications". The McGraw-Hill Companies, Inc., 2008.
- [25] J. Oetting; "A Comparison of Modulation Techniques for Digital Radio". IEEE Transactions on Communications, Vol. Com-27, No. 12, December 1979.
- [26] H. Masahiko, M. TOSHIO, And M. KAZUAKI; "Multilevel Decision Method for Band-Limited Digital FM with Limiter-Discriminator Detection". IEEE Journal on Selected Areas in Communications, Vol. SAC-2, No. 4, July 1984.
- [27] R. Ziemer And R. Peterson; "Introduction to Digital Communication". Macmillan Publishing Company, Inc. 1992.
- [28] W. Webb; "QAM : The Modulation Scheme for Future Mobile Radio Communications?". IEEE Electronics & Communication Engineering Journal, pp. 167-176, August 1992.
- [29] M. Ibnkahla; "Signal Processing for Mobile Communications". CRC Press LLC, 2005.
- [30] H. Park, K. Lee and K. Feher; "Continuous Phase Modulation for F-QPSK-B Signals". IEEE Transactions on Vehicular Technology, Vol. 56, No. 1, pp. 157-172, January 2007.
- [31] J. Anderson and C. Sundberg; "Advances in Constant Envelope Coded Modulation". IEEE Communications Magazine, Vol. 29, No. 12, pp. 36-45, December 1991.
- [32] J. Sun J. and I. Reed; "Performance of MDPSK, MPSK, and Noncoherent MFSK in Wireless Rician Fading Channels". IEEE Transactions on Communications, Vol. 47, No. 6, pp. 813-816, June 1999.
- [33] O. Andrisano, G. Corazza, and G. Immovali; "Effects of the Interferences in Cellular Digital Mobile Radio Systems using Full Response CPM with Limiter-Discriminator Detection". Alta Frequenza, Focus on Mobile Radio Systems, No. 2, pp. 109-117, 1988.
- [34] W. Phoe; "Improved Performance of Multiple-Symbol Differential Detection of Offset QPSK". IEEE Wireless Communications and Networking Conference, pp. 548-553, 2004.
- [35] S. Hyundong and L. HONG; "On the Error Probability of Binary and M-ary Signals in Nakagami-m Fading Channels". IEEE Transactions on Communications, Vol. 52, No. 4, April 2004.
- [36] Osborne and M. Luntz; "Coherent and Non-coherent Detection of CPFSK". IEEE Transactions on Communications, Vol. COM-22, pp. 1023-1036, August 1974.
- [37] C. Sundberg; "Continuous Phase Modulation : A Class of Jointly Power and Bandwidth Efficient Digital Modulation Schemes with Constant Amplitude.". IEEE Communications Magazine, Vol. 24, No. 4, April 1986.
- [38] J. B. Anderson, T. Aulin, and C. E. Sundberg, "Digital Phase Modulation". New York Plenum, 1986.
- [39] J. P. Fonseka; "Block Encoding with Continuous Phase Modulation". IEEE Transactions on Communications, Vol. 42, No. 12, December 1994.
- [40] C. Jinguang; L. Sheng, "Error probability of coherent PSK and FSK systems with multiple cochannel interferences," Electronics Letters, vol. 27, no. 8, pp. 640, 642, 11 April 1991.
- [41] A. Bruce, and J. R. Butcher and K. Behnam; "Comparison of Duobinary and 4-Level Continuous Phase Frequency Shift Keying Signals for Narrowband Land Mobile Radio Applications", IEEE Transactions on Broadcasting, Vol 45, NO. 2, June 1999.
- [42] B. Butcher, "Comparison of Duobinary Encoded and 4-Level CPFSK for Narrowband Land Mobile Radio," Master's Project Report, Mercer University, May 1997.
- [43] T. Ferrett, C. Matthew, and D. Torrieri; "Noncoherent Digital Network Coding Using Multi-tone CPFSK Modulation", The 2011 Military Communications Conference - Track 1 - Waveforms and Signal Processing, Page(s): 299 - 304, 2011.
- [44] S. Fu, K. Lu, Y. Qian, and H.-H. Chen, "Cooperative wireless networks based on physical layer network coding," IEEE Wireless Commun. Mag., pp. 86-95, Dec. 2010.
- [45] S. Katti, S. Gollakota, and D. Katabi, "Embracing wireless interference: analog network coding," Proc. ACM SIGCOMM, pp. 397-408, 2007.
- [46] S. Zhang, S. C. Liew, and P. P. Lam, "Hot topic: physical-layer network coding," Proc. 12th Annu. Int. Conf. Mobile Comput. and Netw., pp. 358-365, 2006.
- [47] J. Sørensen, R. Krigslund, P. Popovski, T. Akino, and T. Larsen, "Physical layer network coding for FSK systems," IEEE Commun. Lett., vol. 13, no. 8, pp. 597-599, Aug. 2009.
- [48] M. C. Valenti, D. Torrieri, and T. Ferrett, "Noncoherent physical-layer network coding using binary CPFSK modulation," Proc. IEEE Military Commun. Conf., Oct. 2009.
- [49] K. Cheun and K. Choi, "Performance of FHSS multiple-access networks using MFSK modulation", IEEE Trans. Commun., vol. 44, no. 11, pp. 1514-1526, Nov. 1996.
- [50] A. Oshinomi, G. Marubayashi, S. Tachikawa, and M. Hamamura, "Trial model of the M-ary multilevel FSK power-line transmission modem," in Proc. 7th Int. Symp. on power-line communications and its applications, pp. 298-303, Kyoto, Japan, March 2003.
- [51] B. Adebisi, S. Ali, B. Honary, "Multi-emitting/multi-receiving points MMFSK for power-line communications," Power Line Communications and Its Applications, 2009. ISPLC 2009. IEEE International Symposium on, vol., no., pp. 239, 243, March 29 2009-April 1 2009.
- [52] G. Marubayashi, and M. Hamamura "Extended even-odd discrimination method of hopping pattern synthesis for MMFSK power-line transmission system," Power Line Communications and Its Applications, 2005 International Symposium on, vol., no., pp. 186, 190, 6-8 April 2005.
- [53] F. Nishijyo, K. Hozumi, S. Tachikawa, M. Hamamura, and G. Marubayashi, "Performance of several MMFSK systems using limiters for high frequency power-line communications," in Proc. 7th Int. Symp. on power-line communications and its applications, pp. 85-90, Kyoto, Japan. March 2003.
- [54] V. Tarokh, N. Seshadri, and A. R. Calderbank, "Space-time codes for high data rate wireless communication: performance criterion and code construction," IEEE Trans. Inform. Theory, vol. 44, no. 2, pp. 744-765, Mar 1998.

- [55] C. L. Giovaneli, P. Farrell, and B. Honary, "Application of space-time block codes for power line channels," in Communications Systems, Networks and Signal Processing CSNDSP 2002 Conference. Stafford, United Kingdom. July 2002.
- [56] C. L. Giovaneli, P. G. Farrell, and B. Honary, "Space-Frequency coded OFDM System for Multi-Wire Power Communications," in Proc. ISPLC 2005, pp. 50-55, Vancouver, Canada, 2005.

